ibvt
Institut für Bioverfahrenstechnik

Technische Universität Braunschweig

Band 58
ibvt-Schriftenreihe

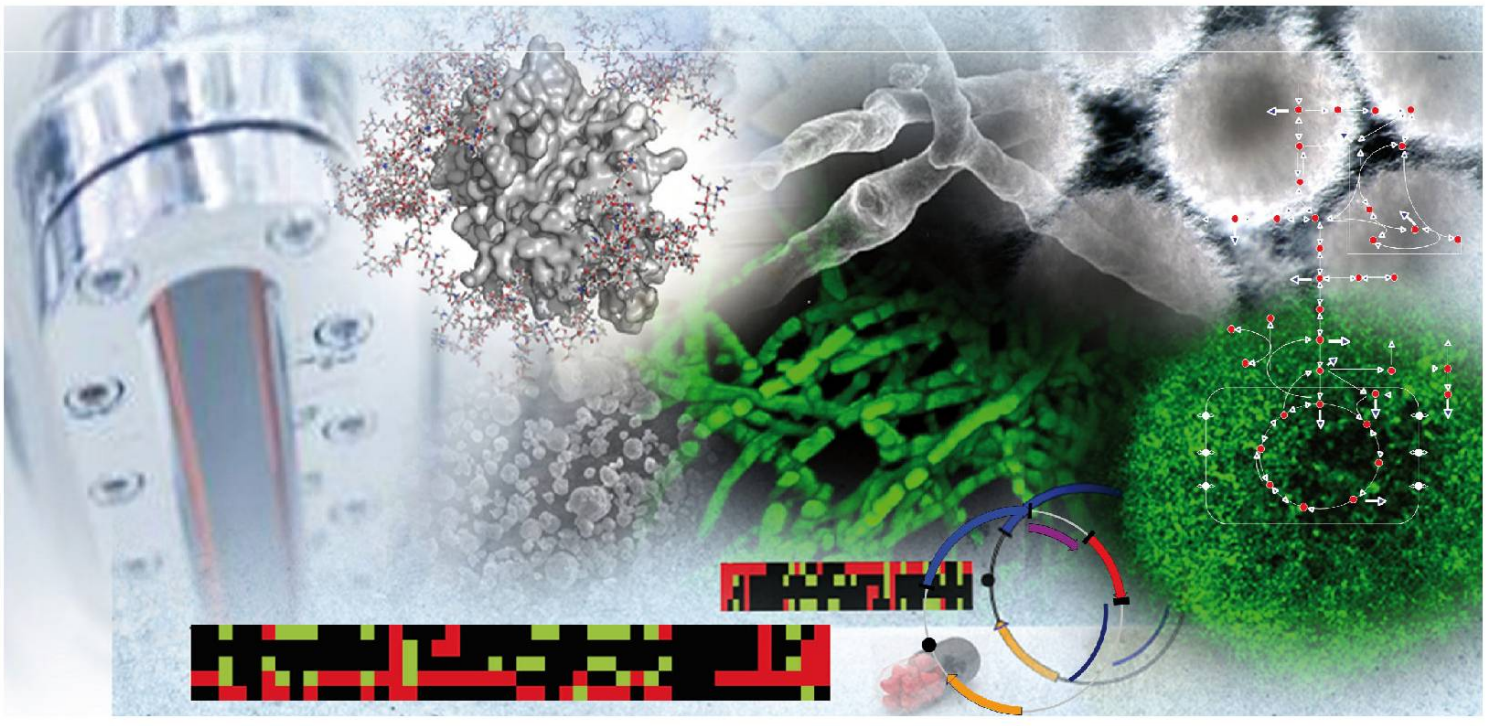

Systems Biotechnology of Recombinant Protein Production in *Aspergillus niger*

Cuvillier-Verlag

ibvt-Schriftenreihe

Schriftenreihe des Instituts für Bioverfahrenstechnik
der Technischen Universität Braunschweig

Herausgegeben von Prof. Dr. Christoph Wittmann

Band 58

Cuvillier-Verlag
Göttingen, Deutschland

Herausgeber
Prof. Dr. Christoph Wittmann
Institut für Bioverfahrenstechnik
TU Braunschweig
Gaußstraße 17, 38106 Braunschweig
www.ibvt.de

Bibliographische Informationen der Deutschen Nationalbibliothek
Die Deutsche Nationalbibliothek verzeichnet diese Publikation in der Deutschen Nationalbibliographie; detaillierte bibliographische Daten sind im Internet über *http://dnb.d-nb.de* abrufbar.
1. Aufl. – Göttingen: Cuvillier, 2011

Nonnenstieg 8, 37075 Göttingen
Telefon: 0551-54724-0
Telefax: 0551-54724-21
www.cuvillier.de

1. Auflage, 2011
Gedruckt auf säurefreiem Papier

ISBN 978-3-86955-808-0
ISSN 1431-7230

Systems Biotechnology of Recombinant Protein Production in *Aspergillus niger*

Von der Fakultät für Maschinenbau
der Technischen Universität Carolo-Wilhelmina zu Braunschweig

zur Erlangung der Würde
eines Doktor-Ingenieurs (Dr.-Ing.)

genehmigte Dissertation

von Dipl.- Biotechnol. Habib Driouch
aus Boujad - Marokko

eingereicht am: 21.04.2011
mündliche Prüfung am: 17.06.2011

Prüfungsvorsitzender:	**Prof. Dr. Rainer Krull**
1. Referent:	**Prof. Dr. Christoph Wittmann**
2. Referent:	**Prof. Dr.-Ing. Arno Kwade**

2011

**Wissenschaft ist eine wunderbare Sache,
wenn man nicht davon leben muss. Albert Einstein**

Für meine Familie

Vorwort

Die vorliegende Arbeit wurde im Rahmen meiner Tätigkeit als wissenschaftlicher Mitarbeiter am Institut für Bioverfahrenstechnik der Technischen Universität Carolo-Wilhelmina zu Braunschweig im Teilprojekt B11 „Dynamik metabolischer Netzwerke zur Produktion rekombinanter Glycosyltransferasen“ des Sonderforschungsbereiches SFB 578 „Integration gen- und verfahrenstechnischer Methoden zur Entwicklung biotechnologischer Prozesse - Vom Gen zum Produkt -“ unter Leitung von Herrn Prof. Dr. Christoph Wittmann angefertigt.

Ein besonderes erstes Wort des Dankes möchte ich an meinen Doktorvater und ersten Gutachter Herrn Prof. Dr. Christoph Wittmann richten. Mit seiner Erfahrung, Unterstützung, wertvollen Anregungen, fachspezifischen Fragen, und den vielen Ideen konnte diese Arbeit in die richtige Bahn gelenkt werden.

Mein dank gilt Herrn Prof. Dr. Rainer Krull und Herrn Prof. Dr.-Ing. Arno Kwade für die Bereitschaft zur Übernahme des Prüfungsvorsitz bzw. des Koreferats.

Mein Dank gilt Herrn Dr. Robert Hänsch aus Institut für Pflanzenbiologie, Abteilung für Molekular- und Zellbiologie der Pflanzen für die Unterstützung bei den CLSM Aufnahmen, sowie Herrn Dr.-Ing. Ingo Kampen aus Institut für Partikeltechnik für die Unterstützung bei der Partikelgrössenanalyse. Frau Simone Schulze aus dem Institut für Chemische und Thermische Verfahrenstechnik danke ich für die Unterstützung bei der Elktronenmikroskopie, und Herrn Dr. Manfred Nimtz aus der Abteilung für Zelluläre Proteomforschung aus Helmholtz-Zentrum für Infektionsforschung danke ich für die Unterstützung bei der Durchführung von MALDI-TOF-MS-Analysen. Dr. Nicola Zamboni von ETH-IMSB Zurich danke ich für die Bereitstellung der software FiatFLUX 1.67 zur Berechnung der Stoffflüsse.

Besonders Dank gilt auch Herrn Dr.-Ing. Guido Melzer und Herrn Dr. Bernd Nörtemann.

Allen Mitarbeitern des Institutes für Bioverfahrenstechnik möchte ich für die allseits angenehme Arbeitsatmosphäre danken.

Mein großer und besonderer Dank gilt gemeinsam meinen Eltern, meinen Geschwistern und meiner Frau, ohne die mein Studium und diese Doktorarbeit niemals möglich geworden wären.

Peer-reviewed Publications

Partial results of this thesis have been published in advance in the following papers, manuscripts and book chapter. This was authorized by the Department of Mechanical Engineering of the Technical University of Braunschweig, Institute of Biochemical Engineering represented by Prof. Dr. Christoph Wittmann:

I*:* Driouch. H., Sommer. B., Wittmann. C. (2010) Morphology Engineering of *Aspergillus niger* for Improved Enzyme Production. Biotechnol. Bioeng. 105: 1058-1068.

II*:* Driouch. H., Roth. A., Dersch. P., Wittmann. C. (2010) Optimized Bioprocess for Production of Fructofuranosidase by Recombinant *Aspergillus niger*. Appl. Microbiol. Biotechnol. 87: 2011-2024.

III (BOOK CHAPTER I): Wucherpfennig. T., Kiep. K. A., **Driouch. H**., Wittmann. C., Krull. R. (2010) Morphology and Rheology in Filamentous Cultivations*.* Adv. Appl. Mircobiol. 72: 89-136, Academic Press, ISBN: 978-0-12-380989-6.

IV: Driouch. H., Roth. A., Dersch. P., Wittmann. C. (2011) Filamentous Fungi in Good Shape: Microparticles for Tailor-Made Fungal Morphology and Enhanced Enzyme Production. Bioeng. Bugs. 2:100-104.

Submitted Publications

V: Driouch. H., Hänsch. R., Wittmann. C. (2011) Improved enzyme production in *Aspergillus niger* - Targeted morphology engineering of hyper-productive bio-pellets using titanate micro particles*.* Biotechnol. Bioeng.

IV: Driouch. H., Melzer. G., Wittmann. C. (2011) Pathway flux analysis and design- Impact of recombinant protein production on in vivo and in silico fluxes in *Aspergillus niger.* Metab. Eng.

Lectures

Driouch. H., Wittmann. C. (2010) Design and Engineering of Cellular Morphology in *Aspergillus niger* for Superior Enzyme Production. ,,DECHEMA Vortrags- und Diskussionstagung: Bioprozessorientiertes Anlagendesign''. 10. - 12. Mai 2010, Nürnberg- Germany.

Melzer, G., **Driouch, H**., Wittmann, C. (2011) Systems-Level Design of Filamentous Fungi - Integration of in silico Flux Modes and in vivo Pathway Fluxes Towards Desired Production Properties. ,,26th Fungal Genetics Conference at Asilomar'' 15. - 20 March 2011. California- U.S.A.

Driouch. H., Roth. A., Dersch. P., Wittmann. C. (2011) Systems Biotechnology for Production of Recombinant Proteins by *Aspergillus niger.* ,,1st European Congress of Applied Biotechnology-Together with DECHEMA's Biotechnology Annual Meeting''. 25. -29. September 2011. Berlin- Germany.

Conference contributions

Driouch. H., Dalpiaz. A., Bohle. K., Göcke. Y., Jonas. R., Kucklick. M., Melzer, G., Nörtemann. B., Jänsch. L., Jahn. D., Franco-Lara. E., Dersch. P., Wittmann, C., Hempel. D. (2008) Influence of Process Conditions on Glucoamylase Production in Continuous Cultures of *A. niger* AB 1.13. ,,DECHEMA's Congress European BioPerspectives''. 7.-9. October 2008, Hannover- Germany.

Driouch. H., Sommer. B., Wittmann. C. (2009) Morphology Engineering of *Apsergillus niger* for Improved Enzyme Production using Microparticles of Talc. ,,14th European Congress on Biotechnology: SYMBIOSIS-Science, Industry and Society''. 13.-16. September 2009, Barcelona- Spain.

Driouch. H., Sommer. B., Roth. A.., Dersch. P., Wittmann. C. (2010) Targeted Morphology Engineering of *Aspergillus niger* for Improved Enzyme Production. ,,10th European Conference on fungal genetics ECFG''. 29-.März 01-.April 2010, Amsterdam- Holland.

Driouch. H and Wittmann. C. (2010) Design and Engineering of Cellular Morphology in *Aspergillus niger* for Superior Enzyme Production. ,,DECHEMA Vortrags- und Diskussionstagung „Bioprozessorien Anlagendesign''. 10. -12. Mai 2010, Nürnberg- Germany (prized with a poster award and oral presentation)

Driouch. H., Wittmann. C. (2011) Systems biotechnology towards superior production of recombinant proteins in *Aspergillus niger.* ,,Annual Conference of the Association for General and applied Microbiology''. 3. -6. April 2011. Karlsruhe- Germany.

Driouch. H., Roth. A., Dersch. P., Wittmann. C. (2011) In Bioproduktion an Oberflächen: Optimierung der Morphologie filamentöser Mikroorganismen zur Produktion rekombinanter Proteine. ,,DECHEMA Vortrags- und Diskussionstagung-Bioverfahrenstechnik an Grenzflächen''. 30. Mai.-01. Juni. Postdam- Germany.

TABLE OF CONTENTS

1 ABSTRACT

The filamentous fungus *Aspergillus niger* is an important efficient microbial cell factory for industrial production of enzymes as well as organic acids or antibiotics. In submerged cultivation, *A. niger* exhibits a rather complex morphology which typically has a strong influence on production performance. Although difficult to control so far, the morphological shape is obviously linked to key production characteristics of fungal cell factories.

In this regard, comprehensive approaches, combining systems-wide analysis and optimization at the cellular level with process-driven engineering of the bioreactor environment, seem most useful in order to achieve superior production processes. This was applied to recombinant proteins production in *A. niger.* The optimization included the use of talc or alumina micro particles, added to the culture, which allowed to the precise controlling the morphological shape of *A. niger* and increase enzyme production in different recombinant strains. Additionally, the targeted engineering of the morphology of *A. niger* into high-producing bio-pellet forms of various sizes by the addition of titanate micro particles was demonstrated. This strategy was combined with model-based medium design and development of efficient fed-batch strategies to optimize the production of the high-value enzyme fructofuranosidase, an important biocatalyst for neo-sugar in food or pharmaceutical industry, in the recombinant strain *A. niger* SKAn1015. As a result, the achieved enzyme titre could be increased to 2,800 U/mL, more than tenfold as compared to previously described processes. The enzyme, obtained by this micro particle enhanced process, could be applied as biocatalyst with minimal pre-treatment for the biosynthesis of 450 g/L of neo-sugar of the inulin type, such as 1-kestose and 1-nystose, which all display pre-biotics with substantial commercial interest.

These studies were complementary by systems biotechnology analysis of *A. niger* as it is expected that this may lead to increased understanding of the context of cellular metabolism, regulation and thus further improvement of strains and processes. Fluxome analyses by ^{13}C-isotope studies and in silico design are applied to quantify the underlying carbon core metabolism of *A. niger* under different conditions. This yielding valuable insights towards the tailor-made design of *A. niger* as a cell factory for recombinant protein production.

2 ZUSAMMENFASSUNG

Filamentöse Pilze wie *Aspergillus niger* sind wichtige Zellfabriken in der industriellen Biotechnologie, besonders für die Produktion von hochwertigen Feinchemikalien, Antibiotika, Enzymen und organische Säuren. In submersen Kulturen weisen filamentöse Pilze eine komplexe Morphologie auf und wachsen als Pellets oder feine Myzelien. Obwohl schwer zu kontrollieren, existiert ein enger Zusammenhang zwischen der morphologischen Struktur und wichtigen Produktionseigenschaften.
Im Rahmen der vorliegenden Arbeit wird ein systembiotechnologischer Ansatz vorgestellt, der auf das maßgeschneiderte Design der Morphologie von *A. niger* abzielt, um optimale Syntheseeigenschaften einzustellen. In systematischen Untersuchungen wurde dabei zunächst gezeigt, dass sich durch Zugabe von Mikropartikeln aus Talk, Aluminiumoxid oder Titanat in einem neuartigen Verfahren die Morphologie von *A. niger* gezielt steuern lässt und man Pellets gewünschten Durchmessers bis hin zu Mycelstrukturen reproduzierbar durch Wahl von Partikelmaterial, -größe und -menge einstellen kann. Diese ermöglichen eine signifikant verbesserte Produktion rekombinanter Proteine, wie für verschiedene Stämme gezeigt, der eine durch den Einfluss der Partikel hochproduktive Biomasse zugrunde liegt. Gekoppelt an modellgestützte Medienoptimierung und die Entwicklung effizienter Prozessführungsstrategien konnte durch Einsatz von Talkmikropartikeln die Produktion von ß-Fructofuranosidase in einem rekombinanten *A. niger* optimiert werden. Dabei stellt der erreichte Enzymtiter von (2800 U/mL) eine zehnfache Steigerung gegenüber allen bisher beschriebenen Verfahren dar. Das auf diese Weise hergestellte, in den Überstand sekretierte Enzym kann effizient für die Synthese von hochwertigen präbiotischen Oligosacchariden mit Anwendungen in der Lebensmittel- oder Pharmaindustrie eingesetzt werden. Bei minimaler Behandlung lassen sich aus Saccharose innerhalb von 10 min etwa 450 g/L an Oligozucker wie Nystose oder Kestose synthetisieren. Die Möglichkeit der maßgeschneiderten Einstellung von Morphologie erlaubt nun auch erstmals deren gezielte Untersuchung. Ergänzend wurde *A. niger* auf der Ebene des metabolischen Netzwerks, ^{13}C-Fluxomics analysen und *in silico* Pathway-Analysen charakterisiert. Dies ergab faszinierende Einblicke in den zugrunde liegenden Metabolismus und neue Ansatzpunkte für die weitere Entwicklung filamentöser Mikroorganismen als Zellfabrik für die Produktion rekombinanter Proteine.

3 INTRODUCTION

3.1 *Aspergillus niger* as Cell Factory and Model Organism

Industrial biotechnology as platform for sustainable growth uses microorganisms or enzymes, to make products in a wide range of industrial sectors including chemicals that can be used as fuels or building blocks for the production of solvents and materials. Industrial biotechnology offers opportunities for the production of highly specialised metabolites or enzymes for bioconversions and for sustainable and economic process alternatives.

The filamentous fungus *A. niger* (black mould) has been used for centuries as industrial versatile microbial cell factory for production of organic acids as well as various extracellular enzymes, native or heterologous proteins and antibiotics. *A. niger* shows an amazing nutritional flexibility and metabolic capacity, and produces high levels of secreted primary and secondary metabolites. Nowadays, it is difficult to think of filamentous fungus where the metabolic capabilities are of greater interest than *A. niger* (Andersen et al. 2008). As a eukaryotic organism, *A. niger* offers valuable advantages for enzyme secretion, such as facilitated proteolytic processing and protein folding as well as posttranslational modifications (Lubertozzi and Keasling 2009; Nevalainen et al. 2005). This has made this microorganism a potentially attractive host for the biotechnological industry. Especially the genus *Aspergillus*, frequently applied in enzyme production due to the GRAS status (generally regarded as save), has received particular attention. Due to enormous development of genetic engineering and efficient expression systems, *Aspergillus* species have also achieved increased attention as host for industrial production of homologues and heterologous proteins (Wang et al. 2005).

Industrial strains can secrete large quantities of many economically desired products, e.g. 25 g/L cephalosporin, 30 g/L glucoamylase, 40 g/L cellulase, 50 g/L penicillin, 140 g/L citric acid (Gordon et al. 2000a; Grimm et al. 2005; Papagianni 2004). It is estimated that there are many enzymes that have industrial relevance (see http://www.report2008.novozymes.com). A fraction of these is currently produced as mono-component enzymes (Novozymes A/S or see list of commercial enzymes of the Association of Manufacturers and Formulators of Enzyme Products: http://www.ampep.org/list/html or the Enzyme Technical Association:

http://enzymetechnicalassoc). Recently, according to an updated technical market research report, enzymes for industrial applications from BCC Research, the global market for industrial enzymes increased from $2.2 billion in 2005 to an estimated $3.3 billion by the end of 2010. The market is expected to increase to over $4.4 billion by 2015 based on three main application sectors including technical, food and animal feed enzymes (Figure 1).

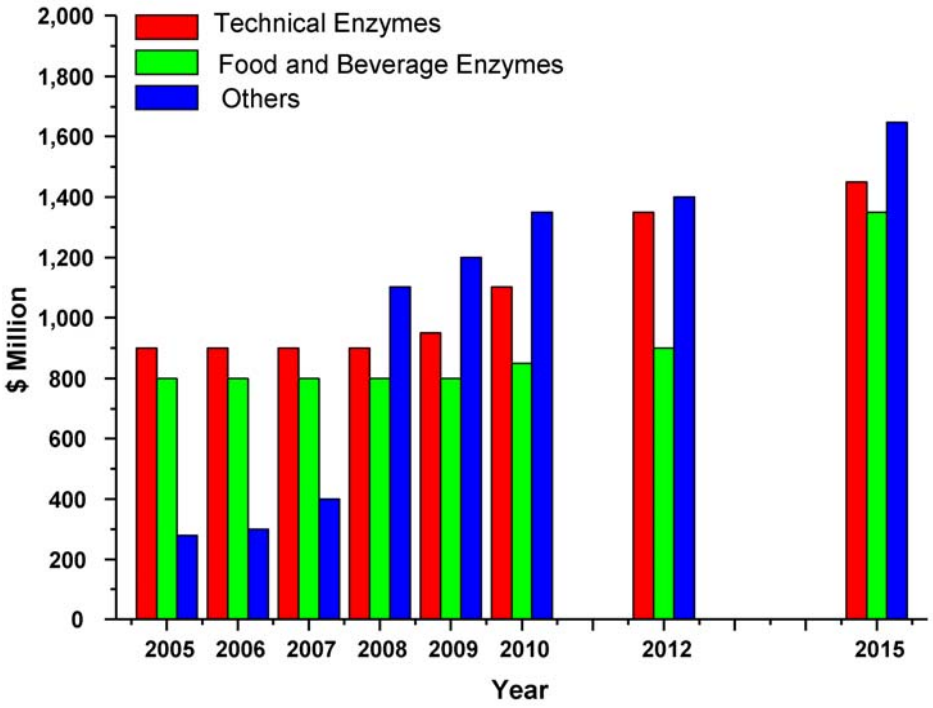

Figure 1. Global market of industrial enzymes based on three application sectors from 2005 to 2015 in $Millions - BCC Research.

Furthermore, *Aspergillus* species are capable to produce eukaryotic gene products such as tissue plasminogen activator (t-PA), Lactoferrin, and hen eggs lysozyme (HEWL) (Archer et al. 1990; Gheshlaghi et al. 2007; Ward et al. 1992; Wiebe et al. 2001).

Supplementary to the improvement of productivity by genetically modified strains (metabolic engineering), much research is focussed on the development of bioprocessing strategies resulting in an increased, controlled and tailored formation of a desired morphology and products while avoiding by-products. Still, the ability of *Aspergillus* to secrete the targeted metabolites is gaining ever increasing attention from the scientific community and industry. The bioprocessing strategies can be

applied to increase the production yield, titre and productivity in recombinant filamentous fungi in submerged culture, although is known that fungal cultivation system is recognized as a complicated multi-phase, multi-component process. For example the improvements in the cultivation and the productivity of the producer organisms have led to high recovery yields of penicillin (Nielsen et al. 1995a). However, *A. niger* has been widely applied as a model organism in studies of general cell physiology as a eukaryotic model or as a systems biotechnology workhorse. The idea of systems biotechnology is the understanding of the function of a cellular system as a whole towards improvement of desired product. As shown in various works there exists a close link between the bioprocess, the morphology and the underlying metabolism of the cell factory *A. niger* (Wucherpfennig et al. 2010). The scientific community is far from understanding of the underlying metabolic and regulatory mechanisms. Newly arising omic's (wet experimental) including genome, trancriptome, proteome, metabolome and fluxome and in silico design (dry experiments) in systems biotechnology, however, now provide a powerful toolbox to step towards understanding of this complex link between biological and engineering aspects of fungal cultures (Andersen and Nielsen 2009; Krull et al. 2010). Since the complexity of fungal systems is beyond intuitive comprehension, the core of systems biotechnology involves mathematical modelling of biological processes. Additionally, the significant similarity of the cell function among eukaryotic microorganisms offers promising prospects for *A. niger* models. In this thesis, different recombinant *A. niger* mutants as well as morphological forms such as pellet and free dispersed mycelia are investigated at various levels.

3.2 Aims of this Thesis

This thesis aims at studying fungal morphology and productivity towards superior biosynthesis of recombinant proteins in the cell factory *A. niger*, which cover the production of a large important commercially products, in the sense of quality as well as the diversity of intermediate metabolites. Classical genetic modification such as mutation or selection without consideration of its consequences to the entire system might cause unexpected changes in central core metabolism. Therefore, a systems-level approach was presented.

Among filamentous fungi, *A. niger* is important as the major world source of citric acid and higher-value enzyme products including pectinases, proteases, amyloglucosidases, cellulases, hemicellulases, and lipases. For *Aspergillus* species, dispersed mycelial suspensions often lead to higher product yield and are thus preferred over the pelleted form. In a pioneering study, the use of inorganic microparticles added to the culture was recently introduced to influence fungal morphology (Kaup et al. 2007). In this regard the use of micro particles for the control of morphology in different strains of *A. niger* (SKAn1015 and AB 1.13) producing different recombinant enzymes was applied. Using co-expression of glucoamylase with green fluorescent protein in the model strain of *A. niger* ARAn701, the origin of the enhanced enzyme production could be investigated in more detail.

Pelleted growth, however, also displays an important industrial morphology. As example, it is beneficial for production of organic acid such as itaconic acid or citric acid, glucoamylase or penicillin. Beyond direct production characteristics pellets provide a reduced viscosity of the culture fluid and thus improve mixing and oxygen transfer within the broth as well as a simplified separation of biomass. A severe disadvantage, however, is the low mass transfer within the pellet itself. Accordingly, the supply of oxygen and other nutrients to the cells especially in the pellet interior is typically limited. In this regard, design of superior bio-pellets of *A. niger* using selected micro particles added to the culture medium to manipulate fungal biopellet and enhance enzyme production was investigated.

One of the recently emerging enzymes available through recombinant *A. niger* strains is ß-fructofuranosidase, an important biocatalyst for the synthesis of rare neo-sugars

as functional food ingredients. The high industrial relevance of ß-fructofuranosidases and the still suboptimal production, lead to the demand for strong efforts in metabolic and biochemical engineering focusing on superior strains, as well as the design of appropriate media and process conditions towards improved production. In this regard, ß-fructofuranosidase production by *A. niger* SKAn1015 was systematically optimized. Moreover, the obtained enzyme suspension can be efficiently used for the biosynthesis of neo-sugars, prebiotics with substantial commercial interest. In particular, these compounds are highly attractive for human consumption, since they have been shown to reduce the risk of colon cancer.

The creation of an *A. niger* strain with high expression of the recombinant product encoding gene, medium design and bioprocess optimization have enabled an efficient production process for fructofuranosidase. This promising situation now drives increasing interest on the underlying metabolism of *A. niger* towards further optimization. Hereby, metabolic flux analysis has proven as powerful method to unravel key production characteristics and metabolic engineering targets due to the close correlation of the metabolic fluxes to the cellular phenotype. Concerning *A. niger,* metabolic flux analysis, which is evolved from pioneering studies on small stoichiometric models, has revealed that fluxes in *A. niger* are flexible depending on the nutrient status, genetic background or the type of product formed. Obviously, the filamentous fungus re-distributes the flux of carbon to adjust its metabolism to the environmental conditions or the actual requirement for product biosynthesis. This appears particularly important in recombinant protein production requesting for additional targets in central metabolism complementing the over-expression of the recombinant gene itself.

The knowledge accumulated in this systems-level approach can be further applied in targeted metabolic engineering to rationally enhance product formation. An overview of the systems biotechnology approach applied in this thesis is presented in Figure 2.

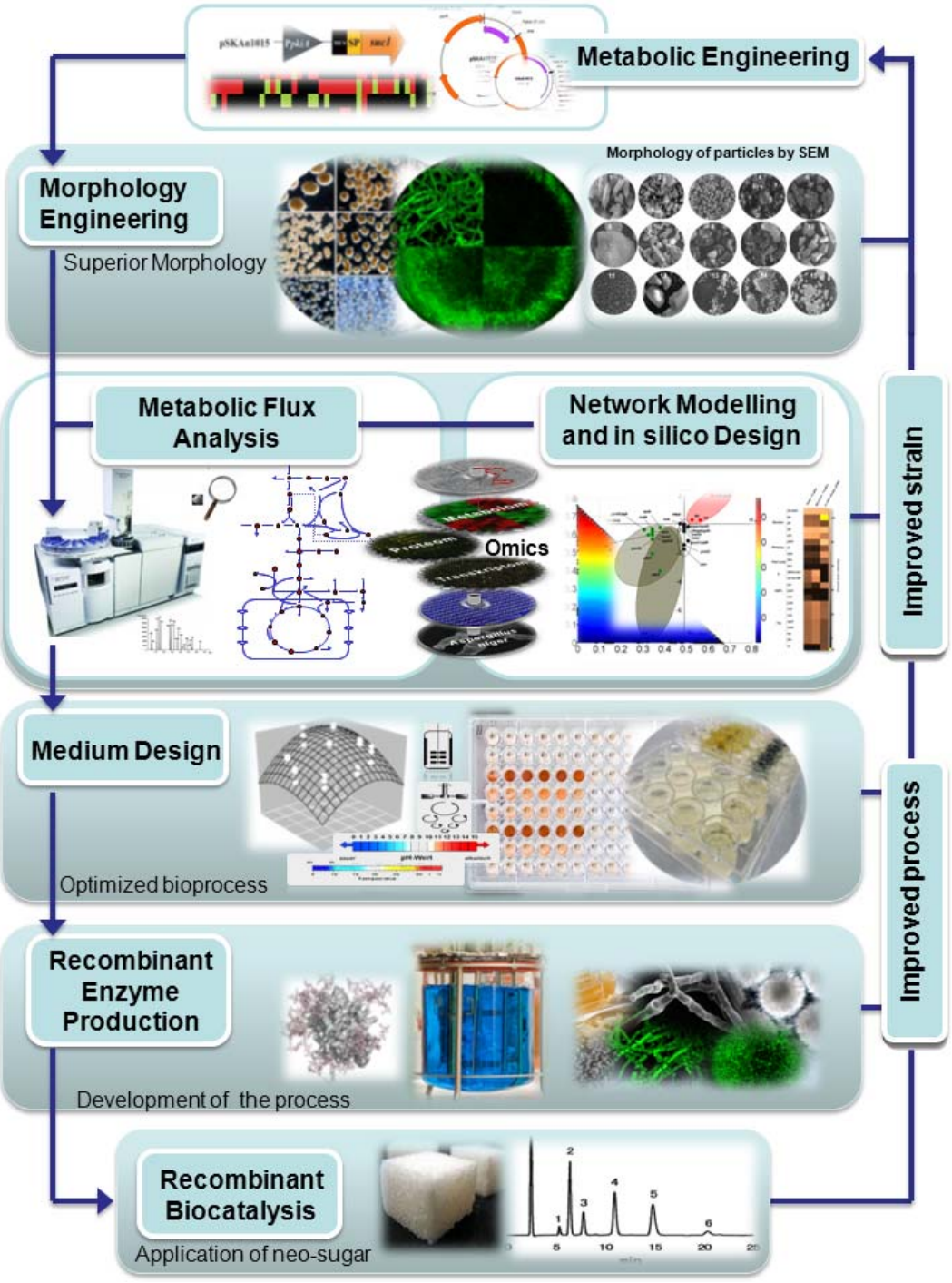

Figure 2: Systems biotechnology approach improved recombinant protein production by *Aspergillus niger.*

4 THEORETICAL BACKGROUND

4.1 Fungal Morphology

The filamentous fungus *A. niger* (black mold) has a long history as industrially attractive producer of organic acids as well as of various extracellular enzymes, native or heterologous proteins and antibiotics. A close link between fungal morphology and productivity has early been identified in important industrial processes yielding e.g. citric acid, enzymes or antibiotics (Papagianni 2004). Pioneered approaches aimed at modelling this morphological development suggested structured models and described important morphological steps inclunding a very fast spore aggregation, followed by a second slower aggregation step promoted by germination and hyphal tip growth, and the growth of pellets as the last process (Grimm et al. 2005; Kelly et al. 2004; Nielsen 1996). A model of morphogenesis describes the early phase of cultivation of filamentous microorganisms is perviously published (Grimm et al. 2005; Kelly et al. 2004; Nielsen 1996). Filamentous growth in a bioreactor consists of a complex microscopical differentiation process from spores (Figure 3) to hyphae resulting in various macroscopically visible appearances, whereas two extreme formations can be described, mycelial (Figure 4A) and pelleted form (Figure 4B). Additionally, in submerged cultivation an intermediate aggregated termed clump is generally known.

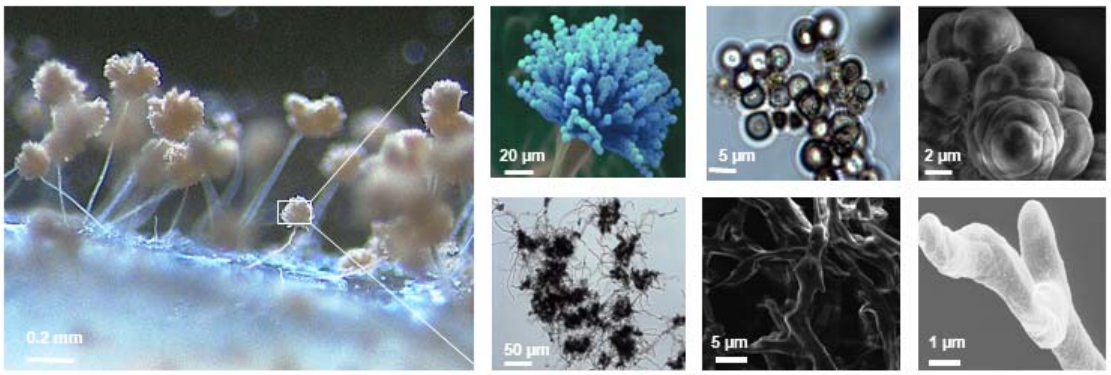

Figure 3: An aggregate of spores and hyphae of *Aspergillus niger* resulting from spores germination.

Generally, the morphogenesis of filamentous fungi like *A. niger* already starts after the inoculation of the bioreactor with a spore suspension. The spores used for inoculation are able to aggregate before hyphal growth takes place. The interaction between spores in culture medium leads to spores-spores packages and a first aggregation. Due to the very fast second aggregation processes, spore concentration is decreased by germination and hyphal length growth after 6 - 8 hours cultivation time (Kelly et al. 2006a). During further process time, branching and clump occur and lead to mycelial (Figure 4A) or biopellets (Figure 4B) form depending on the process conditions.

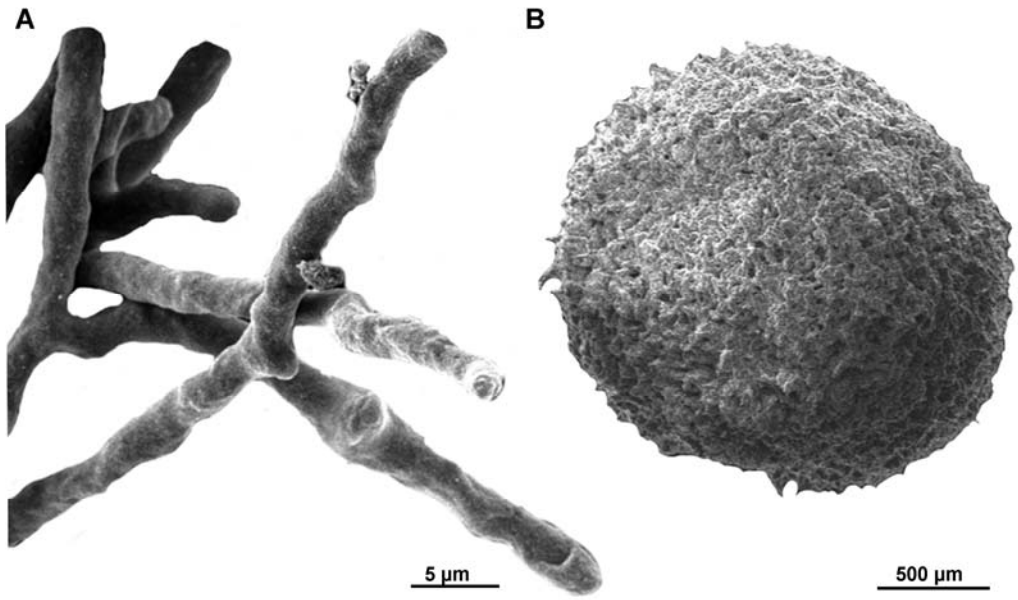

Figure 4: Morphogenesis of *Aspergillus niger* in submerged cultivation. Free dispersed mycelium form (A) and Pellet form (B).

The type of morphology depends on operating parameters and the genotype of the applied strain (Cronenberg et al. 1994; Hille et al. 2005; Wucherpfennig et al. 2010). Concerning the process parameters, the formation of morphology can be controlled chiefly by the initial pH-value of the cultivation medium (Kaup et al. 2007; Papagianni 2004), the dimension of shear forces by the impeller speed (Kelly et al. 2004) and the initial spore concentration (Papagianni and Mattey 2006). However, pellets are characterized by an inhomogenous distribution over the biomass radius with respect to the formation of nutrient gradients directed to the pellet centre. The result of the

substrate limitation at the core of a pellet affects biomass growth and production. Since the gradient formation lead to zones with mass transfer limitations along the pellet radius, and turnover within the pellets, they are unsuitable for the application of steady state experiments (Cronenberg et al. 1994; Hille et al. 2009; Hille et al. 2005).

4.2 Impact of Morphology on Bioproduction in Filamentous Fungi

One of the outstanding and, unfortunately often problematic, characteristics of filamentous fungi is their complex morphology in submerged culture. Hereby, the productivity in biotechnological processes is often correlated with the morphological form (Kaup et al. 2007; Petzoldt 1971; Zhang et al. 2007; Znidarsic and Pavko 2001). As example, pellet growth (Figure 5A) is found optimal for production of itaconic acid (Metz 1976), or citric acid (Gomez et al. 1988). In other cases freely dispersed mycelium (Figure 5B) seems favorable and regarded as prerequisite to ensure high productivity (Papagianni and Mattey 2006). This holds for the production of enzymes such as amylase, neo-fructosyltransferase, or phytase (Teng et al. 2009) or the production of penicillin (Vecht-Lifshitz et al. 1990). Here, the mycelial form allows an increased oxygen supply of the cells stimulating growth and production (Wittler et al. 1986), compared to pelleted growth (Figure 5C-F).

The high importance of the correct morphology for good performance has stimulated attempts to manipulate the growth characteristics of filamentous fungi. Selected studies have included the variation of operating parameters such as inoculum level, stirring rate, or pH value (McIntyre et al. 2001a; McIntyre et al. 2001b; Nielsen 1996; Papagianni and Mattey 2006). In many cases these attempts, however, require conditions incompatible with effective production such as extreme pH value causing enzyme instability or high stirring rate resulting in increased energy costs. Distinct environmental conditions result in different morphological forms and thereby affecting the production yields of native as well as heterologous proteins. Apart from these parameters, the inoculum level, pH-value and power input are generally recognized as the most important operating parameters on morphology formation and productivity in submerged processes (see Appendix E).

Alternatively, desired morphological characteristics were also achieved by random mutagenesis and selection for mutants with affected morphology which revealed

enhanced hemicellulolytic enzyme production (De Nicolas-Santiago et al. 2006; Wang et al. 2005).

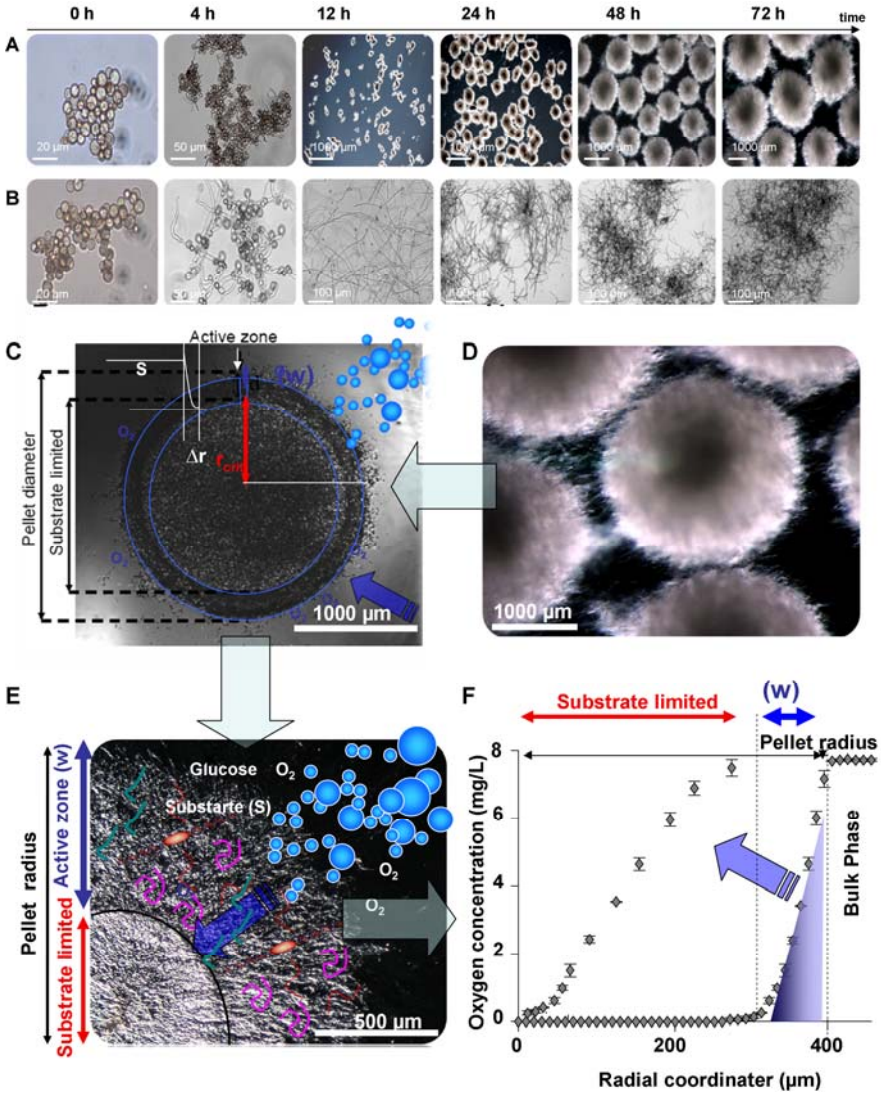

Figure 5: Morphogenesis of *Aspergillus niger* in submerged cultivation in stirred bioreactor depending on the initial pH-value of culture, pelleted growth at pH 5 (A-E), free dispersed mycelium at pH 3 (B), intersection in a large compact pellet with limited zones (C), schematic representation of oxygen concentration profiles in pellet (E-F).

Inoculum level

Morphology and productivity are correlated with the spore concentration of the inoculum (Bizukojc and Ledakowicz 2010; Carlsen et al. 1996; Carmichael and Pickard 1989; Domingues et al. 2000; Hemmersdorfer et al. 1987; Kelly et al. 2004; L'Hocine et al. 2000; Liu et al. 2008; Nielsen et al. 1995a; Papagianni 2004; Papagianni and Mattey 2006; Tucker and Thomas 1992; Vecht-Lifshitz et al. 1990). Generally, different levels of inoculum were used for the development of distinctive

morphological forms in shake flask and bioreactor cultures. Morphology can be manipulated by means of inoculum levels (concentration of spores) or inoculum type (vegetative or spores) and was also shown to affect protease levels (Papagianni et al. 2002 ; Xu et al. 2000). Growth in the form of large pellets was associated with lower specific protease activities and increased specific glucoamylase activities compared with filamentous morphologies. The morphology clearly affects protease secretion as well as protein production, but the exact mechanism needs further investigation (Grimm et al. 2005). Grimm et al. investigated the influence of spore concentration on the aggregation velocity (Grimm et al. 2005). As result, the aggregation velocity increases with increasing inoculum spores until a maximum at a concentration of $3\ 10^6\ mL^{-1}$ is reached. Besides, spore germination and hyphal growth rate are slowed down at higher conidia concentration. Xu et al. showed a decrease in pellet size with increasing conidia concentration (L'Hocine et al. 2000). At values above $10^7\ mL^{-1}$ freely dispersed mycelium occurs. A maximum yield of heterologous proteins in *A. niger* was observed with a spore concentration of $4\ 10^6\ mL^{-1}$, and therefore in pelleted growth (L'Hocine et al. 2000).

pH of the medium

The pH of the medium can affect the morphology and productivity (Bizukojc and Ledakowicz 2010; Carlsen et al. 1996; Jimenez-Tobon et al. 1997 ; Mainwaring et al. 1999; O'Donnell et al. 2001; Papagianni 2004; Rowley and Pirt 1972; Vats et al. 2004; Vecht-Lifshitz et al. 1990). Especially, in the beginning of the submerged cultivation the chosen pH impacts aggregation of spores and therefore dictates the final morphology within submerged cultivations (Carlsen et al. 1996; Galbraith and Smith 1969; Grimm et al. 2005). Freely dispersed mycelium is linked to an acidic pH compared to distinct pellets at higher pH values. Pirt et al. showed, that a rise increase of the pH > 6 during cultivation results in an decrease of the hyphal length (Rowley and Pirt 1972). A further increase above a pH-value of 7 results in swollen hyphae and pellet formation (Rowley and Pirt 1972). In batch cultivations with *A. oryzae*, optimal α-amylase productivity was achieved at pH 6, as described by Carlsen et al (Carlsen et al. 1996). Vats et al. have reported an increase in phytase production of *A. niger* in an acidic environment of pH 1.5 to 1.8 (Vats et al. 2004). It is known that a low pH value during the initial phase of germination can be used to avoid spore aggregation and induce the formation of mycelium instead of pellets

(Figure 5B). However, the adjustment of the morphology by low pH-value leads mostly to product instability (Driouch et al. 2010b).

Power input due to agitation and aeration

The influence of the agitation intensity (Amanullah et al. 2002; Casas López et al. 2005; Cui et al. 1998; El-Enshasy et al. 1999; El-Enshasy et al. 2006; Friedrich et al. 1989; Jimenez-Tobon et al. 1997 ; Kelly et al. 2004; Kelly et al. 2006b; Liu et al. 2008; Mitard and Riba 1988; Nielsen et al. 1995a; O'Donnell et al. 2001; Papagianni et al. 1998; Smith et al. 1990; Vats et al. 2004; Wang et al. 2003; Wongwicharn et al. 1999) as well as aeration (Casas López et al. 2005; Cox et al. 1998; Cui et al. 1998; Friedrich et al. 1989; Li et al. 2008; Wongwicharn et al. 1999), and therefore varying mechanical power input (Lin et al. 2010; Nielsen and Krabben 1995), on morphology and productivity has been an objective in several studies and reviews (Gibbs et al. 2000). Lin et al. described the alteration in pellet micromorphology (internal and surface structure) and macromorphology (pellet size and concentration) under different aeration and agitation intensities, although the total volumetric power input has been kept constant (Lin et al. 2010). As a result of the increased share of aeration in the total power, the glucoamylase production was raised due to a high number of small and loosely structured pellets. Papagianni et al. found an increase in the production of citric acid with higher agitation intensities (Papagianni et al. 1998). Further process parameters investigated were the temperature (Carlsen et al. 1996), the medium composition (Domingues et al. 2000; Liu et al. 2008) and the cultivation conditions (Haack et al. 2006). In other studies, the effect of biodegradable polymers added to the medium (Liu et al. 2008), or different carriers for immobilization was tested (Mussatto et al. 2009).

Solid material addition

In a pioneering study, the use of inorganic microparticles added to the culture was recently introduced to influence fungal morphology (Kaup et al. 2007). As shown for *Caldariomyces fumago*, the addition of microparticles consisting of aluminum oxide or hydrous magnesium silicate caused a dispersion of the cells up to the level of single hyphae and enhanced chloroperoxidase production. The authors observed that micro particles influence the morphology also of other filamentous fungi suggesting that intentional supplementation to the culture might generally stimulate growth of these

organisms. This appears must attractive as novel approach to control the morphological development of *A. niger* in submerged culture and could be open new possibilities to use micro particles for tailor-made morphology design in biotechnological processes (Table 1).

Table 1. Impact of talc or alumina microparticles on different filamentous microorganisms (Kaup et al. 2007).

Organism	DSMZ number/ division	Pellet size[a] -particles (mm)	Pellet size[a] +particles (mm) (mm)	Single hyphae/cells[b]	Exemplary products
Penicillium digitatum	62840, ascomycota	5–60	0.2–1.2	+	Enzymes
Penicillium chrysogenum	848, ascomycota	2–60	0.1–3	++	Penicillium
Emericella nidulans	820, ascomycota	1–3	0.05–0.2	++	Cholic acid, Conversion of steroids
Aspergillus niger	821, ascomycota	3–8	0.1–1.5	+	Citric acid, oxalic acid, enzymes
Acremonium chrysogenum	880, ascomycota	1–10	0.1–0.7	+	Proteases, chephalosporins C, N, P
Pleurotus sapidus	8266, basidiomycota	-30	0.1–6, 0.1–0.3	+	Enzymes
Rhizopus oryzae	907, zygomycota	-80	1–5	+	Steroids
Chaetomium globosum	1962, ascomycota	1–5	0.2–3.5	+	Cellulase
Streptomyces aureofaciens	40127, eubacteria	0.9–2.1	0.06–0.5	+	Chlor-tetracycline

[a] The pellet size was estimated by microscopy. [b] Single hyphae/cells: ++ formed predominantly, + formed significantly.

4.3 Metabolic Pathways in *Aspergillus niger*

The metabolic pathway network of *A. niger* is summarized in Figure 6 (Melzer 2010; Melzer et al. 2009). The underlging metabolic reaction network was constructed based on large-scale and genome models recently described in the literature (Andersen et al. 2008; Gheshlaghi et al. 2007; Meijer et al. 2009; Melzer et al. 2009). Essential reactions in compartmentalized metabolism for growth of *A. niger* on glucose as carbon source comprise major catabolic pathways, namely glycolysis (EMP, Embden Meyerhof Parnas Pathway), pentose phosphate pathway (PPP), tricarboxylic acid (TCA) cycle, glyoxylate pathway (GLP), anaplerotic reactions (ANAPL) as well as biosynthetic routs towords polyols or organic acids. As main function carbon core metabolism serves the purpose of converting glucose to precursor metabolites and energy that are required for biomass synthesis as well as

building blocks needed for recombinant protein synthesis which directly branch of the central carbon pathways.

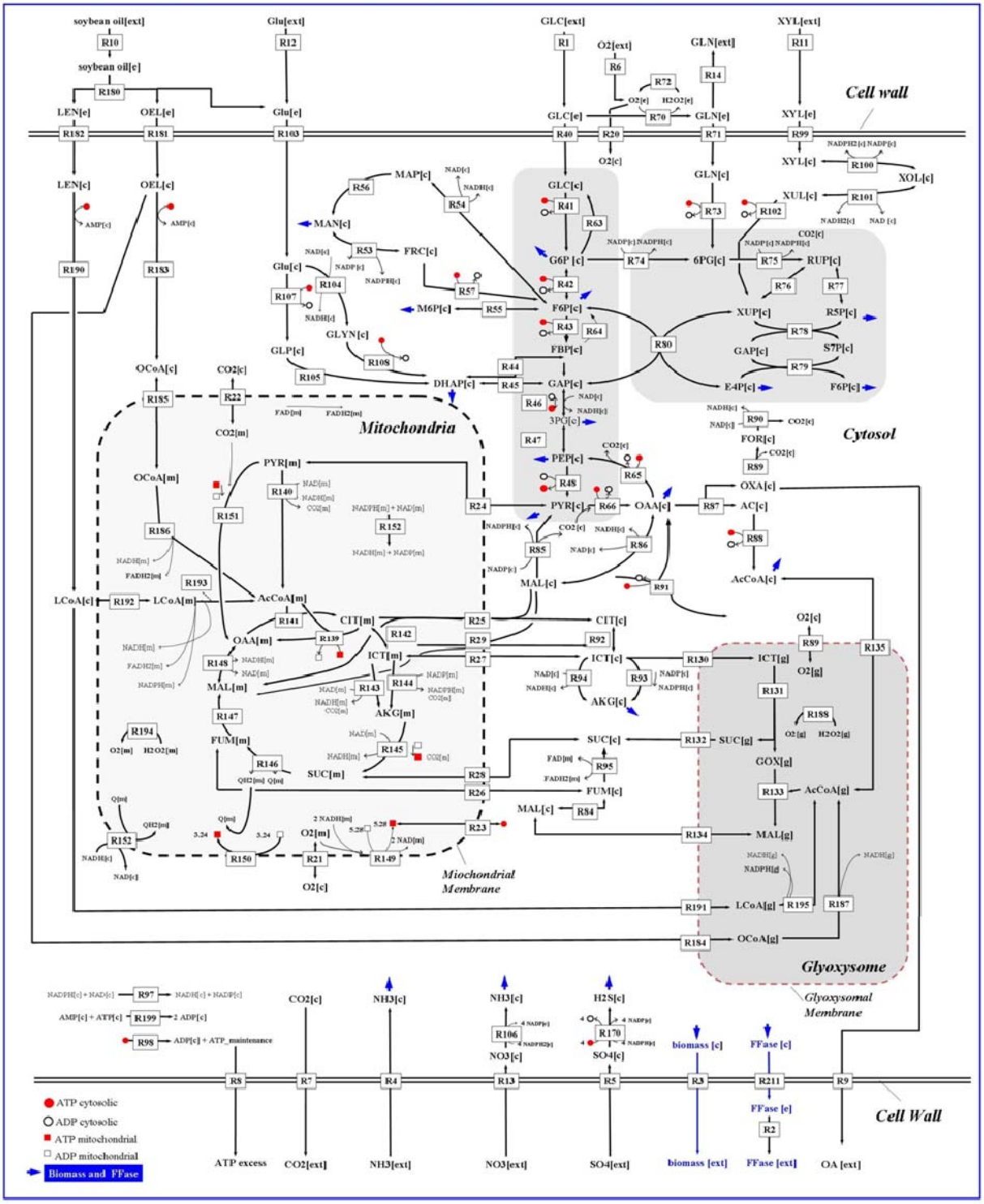

Figure 6: Large-scale metabolic network of *Aspergillus niger*. Reactions and metabolites are compartmentalized in extracellular (ex), cytosolic (c), mitochondrial (m) and glyoxysomal (g) compartments. Reaction numbers refer to a detailed model description in the supplement (Melzer 2010; Melzer et al. 2009).

An overview of the amino acids and their corresponding precursor metabolites stemming from the glycolysis, the PPP and the TCA cycle in fungi is schematically given in Figure 7 (Michal 1999; Nielsen 1997).

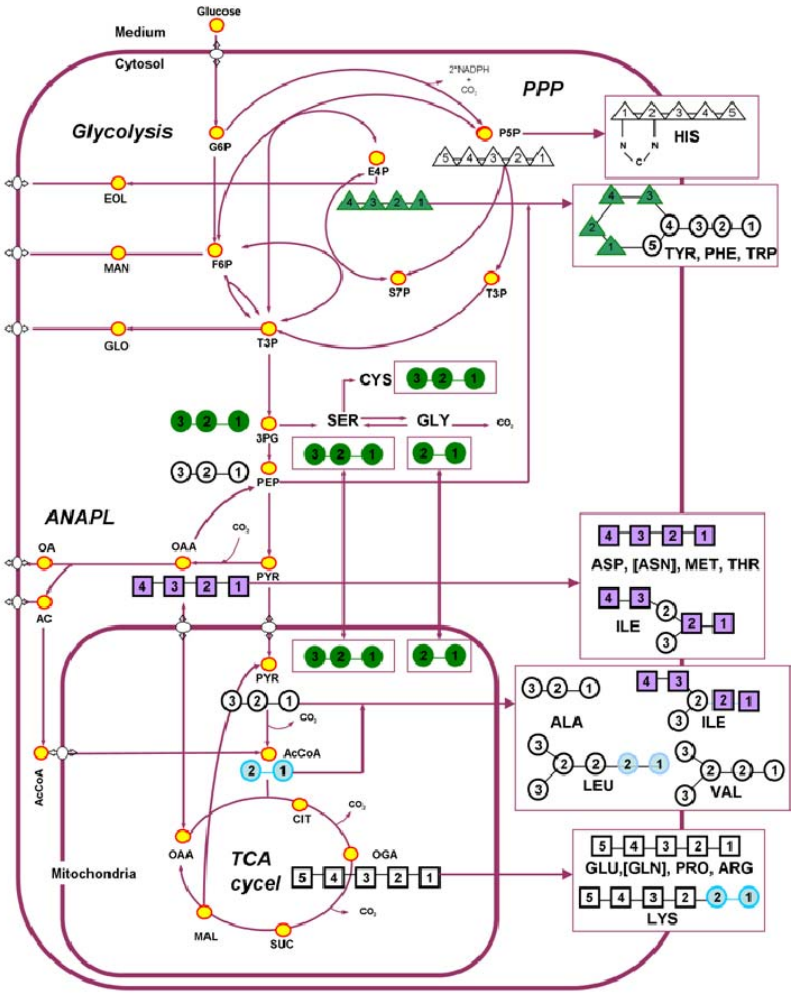

Figure 7: Eukaryotic central carbon metabolism network model of amino acids biosynthesis using glucose as a carbon source Amino acids and carbon fragments originating from a single intermediate of the central carbon metabolism are represented in rectangular boxes (Jouhten et al. 2009; Maaheimo et al. 2001; Sola et al. 2004).

Cells need a large amount of building blocks for the synthesis of proteins. The biosynthetic pathways for all 20 proteinogenic amino acids are elucidated for eukaryotes and prokaryotes and can be categorized into five families with respect to the specific precursor that serves as the starting point (Michal 1999). The pathways of amino acid biosynthesis reconstructed in Figure 7 corresponded to the pathways utilized by yeasts and fungi (Jouhten et al. 2009; Maaheimo et al. 2001; Sola et al. 2004). Serine, glyine, cysteine, aspartate, asparagine methionine, threonine, tyrptophane, and phenylalainine are exclusively derived from metabolite pools

located in the cytosol (cyt). The histidine biosynthesis in cytosol is fairly complicated and cannot be easily grouped with the others (Brock and Madigan 1994). Serine, as known as the major one-carbon (C1) donor, is reversibly cleaved into cysteine, glycine and a C1 unit. Mitochondrial (mit) and cytoplasmic (cyt) serine hydroxymethyl transferase isozymes exist, and their action is complemented by the mitochondrial glycine cleavage pathway which interconverts glycine into a C1 unit and CO_2 (Jouhten et al. 2009; Maaheimo et al. 2001; Sola et al. 2004). Alaine, valine, leucine and isoleucine synthesis requires mitochondrial pyruvate. For alaine, the first step is the amination of pyruvate catalysed by alanine aminotransferase. For valine and leucine, the condensation of two molecules of pyruvate to 2-acetolactate catalysed by acetolactate synthase, and for Ile, the condensation of pyruvate and 2-oxobutyrate (arising from threonine) to 2-aceto-2-hydroxybutyrate (isoleucine) catalysed by acetolactate synthase, serve as the first steps. While the subcellular localization of the alanine aminotransferase has not yet been identified, acetolactate synthase is located in the mitochondria. Moreover, the incorporation of AcCoA-mit into leucine is catalysed by mitochondrial a-isopropylmalate synthase. Glutamate, glutamine, proline and arginine are synthesized from a-ketoglutarate, which is exclusively generated in the mitochondria. Lys is synthesized from a-ketoglutarate and AcCoA-cyt via the cytosolic homocitrate synthase. Lysine is synthesized via the a-aminoadipate pathway from a-ketoglutarate and AcCoA-cyt while glyine is generated through both serine cleavage via serine hydroxymethyl transferase and threonine cleavage via threonine aldolase, as well as the mitochondrial glycine cleavage pathway. In bacteria, yeasts and plants, lysine is synthesized from pyruvate and b-aspartic-semialdehyde via diaminopimelic acid an important building block for bacteria cell wall, whereas in fungi it is synthesized from α-ketoglutarate and AcCoA-cyt.

Stoichiometric formulation of a metabolic pathway of an organism is the basis for any quantitative approach of central core metabolism. This requires some basic information about different major pathways normally present in living cells. The proposed model for *A. niger* consists of three compartments. The cytosolic compartment contains the reactions comprising glycolysis, gluconeogenesis, the PP pathway, and the majority of ANAPL pathways. The mitochondrial compartment includes the TCA cycle, the biosynthesis pathways of the amino acids such as alanine, leucine, valine, glutamine, glutamate, proline, arginine and a part of the

biosynthesis of isoleucine and lysine. The glyoxylate pathway (GLP) is considered to operate in glyoxysome (Melzer 2010; Melzer et al. 2009).

4.4 Recombinant Protein Production in *Aspergillus niger*

The filamentous fungus *A. niger* is an important host in industrial protein production, since it is able to synthesize, glycosylate, and secrete high levels of proteins into the culture medium (Papagianni 2004). Especially the genus *Aspergillus*, frequently applied in enzyme production due to the GRAS status, has received particular attention. The products of interest in the present thesis, ß-fructofuranosidase and glucoamylase, which belong to the enzyme class of hydrolases with high glycosylation structure, and the green fluorescent protein (GFP) modell are all provided by different strains of *A. niger*. They are attractive due to their adaptable biotechnological applications, which will be discussed in the following chapters.

4.4.1 Fructofuranosidase

The extracellular ß-fructofuranosidase (FFase, EC 3.2.1.26) is an important enzyme used in the food- and pharmaceutical industry. This highly glycosylated enzyme (Figure 6) exhibits two different activities, the hydrolase and fructosyltransferase activity, the hydrolysis of the substrate sucrose into fructose and glucose (i), and the transfer of fructose from a donor sucrose molecule units onto acceptor sucrose molecules (ii) leading to the formation of neo-sugars, such as kestose, nystose and 1F-ß-fructofuranosylnystose (Figure 8), which are promising products for the food- and pharmaceutical industry (Fernandez et al. 2004; Maiorano et al. 2008; Rubio and Maldonado 1995; Zuccaro et al. 2008).

Furthermore, it was reported that fructofuranosidase has been used as a sensor for continuous sucrose determination (Balasubramaniem et al. 2001). Generally, three extracellular ß-fructofuranosidase variants from different *A. niger* strains are known and have been characterized (Boddy et al. 1993; Yanai et al. 2001; Yuan et al. 2006). The amino acid sequences of all the three enzymes are similar, but the ratio of the fructosyltransfer/hydrolytic activity appears to be different for each enzyme (Zuccaro et al. 2008). Amino acid sequence and sugar composition of this enzyme

required for in silico pathway and ^{13}C-metabolic flux analysis are presented in Table 20 (see Appendix A).

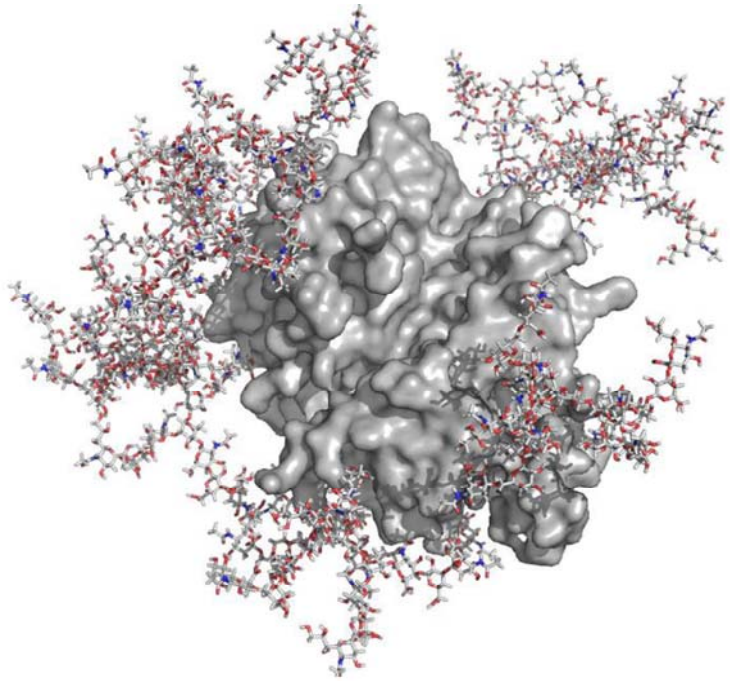

Figure 8: In silico structure of fructofuranosidase. Glycosylation was performed by GlyProt (http://www.glycosciences.de/modeling/glyprot).

Application of neo-sugars

Neo-sugars, also known as short chain-fructooligosaccharides or fructans are polymeric complex carbohydrates classified as important group of oligosaccharides in distinguished classes differing in the degree of fructose units polymerization included inulin, levans, neoseries, and lastly neo-sugar with a degree of polimerization ranging from 1 to 5 fructose units such as 1-kestose (GF_2), nystose (GF_3) and 1F-ß-fructofuranosylnystose (GF_4) as the biggest neo-sugar molecule (Figure 9). Many workers have proposed a network of the reaction mechanism model for the neo-sugars synthesis from sucrose catalyzed by the fructofuranosidase or fructosyltransferase (Beine et al. 2009; Gutierrez-Alonsto et al. 2009; Jung et al. 1989; Yun 1996).

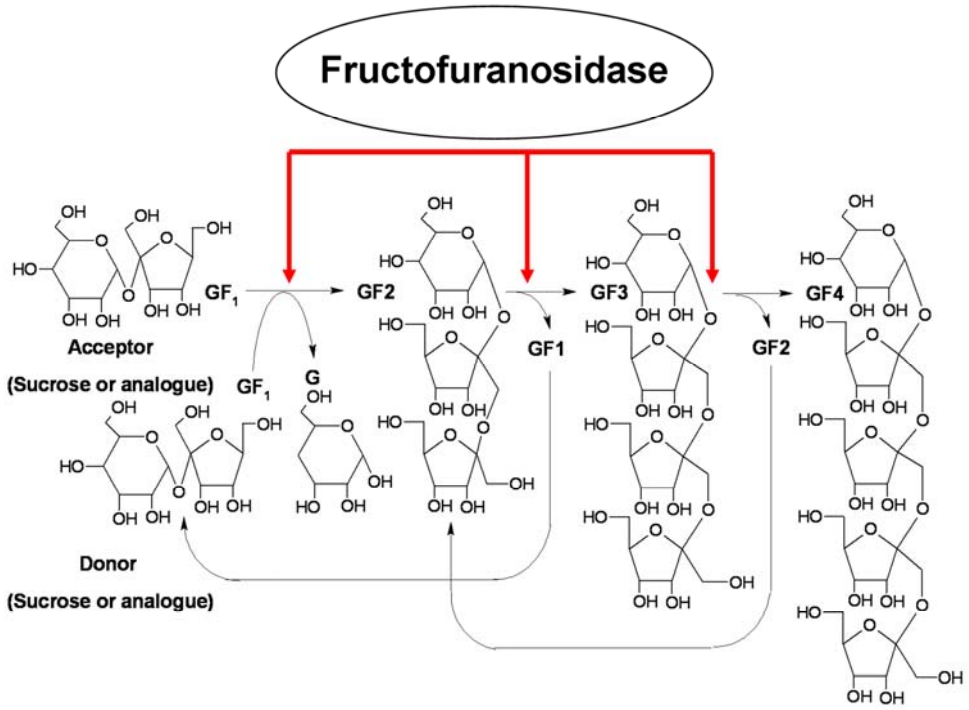

Figure 9: Biosynthesis of neo-sugars of the inulin type by recombinant fructofuranosidase from *Aspergillus niger.* Enzymatic reaction including transfructorylation towards GF_1: Sucrose; GF_2: 1-kestose, GF_3: 1-nystose and GF_4: 1F-ß-fructofuranosylnystose.

Neo-sugars are functional food ingredients that have a great potential to improve the quality of many foods and are known as pre-biotic agents with physiologically functional properties. Neo-sugars are able to stimulate the dietary modulations of intestinal flora (Figure 10) by enhanced numbers of activities of bifidobacteria and consequently, improve the growth of beneficial bacteria (probiotic).

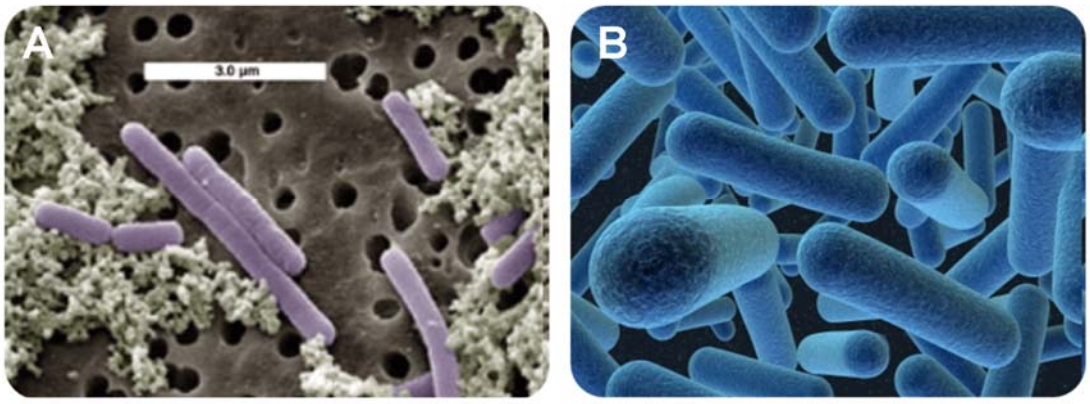

Figure 10: Micro-aerophile, rod-shaped cells of *Lactobacilli* in pairs or short chains (A). Anaerobic intestinal rod-shaped *Bifidobacteria* (B).

Due to all this health benefits, neo-sugars application in food processing industry as artificial sweeteners and in pharmaceutical or the diagnostic sector has increased rapidly essentially by industrial enzymatic biotechno (Fernandez et al. 2004; Maiorano et al. 2008; Rubio and Maldonado 1995; Zuccaro et al. 2008). Neo-sugars with low polymeric grade have better therapeutic properties than those with a high polymeric degree. The global market of functional foods is estimated up to 33 billion US $ in 2000. Prebiotics is a very small part but important concern of the global functional food market (6.5% of the global market) and this market grown substantial and continues to expand gradually at 15% per year (Sangeetha et al. 2005b). Japan is an important market for functional foods with a specific health related food category called Foods of Specified Health Use (FSHU) and the demand for prebiotics in Japan was 69,000 tons/year in 2000 (Nakakuki 2002). Neo-sugars are mainly products of filamentous fungi including *Aspergillus, Penicillium, or Aureobasidium*, whereby only a few species are considered for industrial production (Sangeetha et al. 2005a). Especially the genus *Aspergillus*, frequently applied in enzyme production due to the GRAS status, has received particular attention. Neo-sugar are widely distributed in servel plant products (Yun 1996), however, the concentration of neo-sugar is low and mass production is limited by seasonal conditions or from inulin by controlled chemical synthesis with enzymatic hydrolysis.

They are also mainly produced either from sucrose in different industrial microorganisms such as fungi, yeast and bacteria by means acting of specific extracellular or intracellular enzymes with transfructosylating activity, which transfer fructose units from sucrose as donor into neo-sugar in the presence of high concentrations of the substrate sucrose (Hidaka et al. 1988). Fructofuranosidases (E.C. 3.2.1.26) or fructosyltransferases (E.C. 2.4.1.9) are members of the family of glycoside hydrolases. They are produced by most of filamentous fungi such as *Aspergillus* (Guimaraes et al. 2009; Hidaka et al. 1988; Shin et al. 2004; Wang and Zhou 2006; Yoshikawa et al. 2006; Yoshikawa et al. 2007; Zuccaro et al. 2008), *Aureobasidium* (Yoshikawa et al. 2007) and *Penicillium* (Dhake and Patil 2007; Sanchez et al. 2008; Sheu et al. 2002), in different large-scale cultivation process strategies.

4.4.2 Glucoamylase

Glucoamylase, also known as amyloglucosidase or amylase (GA, EC 3.2.1.3), is a microbial extracellular inducible glycoprotein that hydrolyzes saccharides such as starch by attacking both alpha (1-4) and alpha (1-6) glucosidic linkages from the non-reducing end of the molecule (Figure 11). Glucoamylase of *A. niger* contained 10-20% carbohydrate and have a molecular weight of 48-90 kDa (Boel et al. 1984; Venkataraman et al. 1975). The glycolysation enhances the glucoamylase enzyme stability. Glucoamylase is produced by many fungal species such as *A. niger* for decades reaching yields of over 20 g/L in fed-batch cultivations using traditional strain improvement and process optimization (Finkelstein 1987; Pedersen et al. 2000a; van Brunt 1986). Glucoamylase can be produced by submerged, solid state and semi-solid state cultivation using stirred tank vessels, airlift rectors or stacked trays. Glucoamylase finds many applications in industry. It is an important industrial enzyme used in saccharification steps in both starch enzymatic conversion and alcohol production. It is used in dextrose production, in the baking industry, in the brewing of low calorie beer and in whole grain hydrolysis for the alcohol industry. The most important application of glucoamylase is the production of high glucose syrups from starch with an annual output of over 8 million tons (Lee 1991). Glucoamylase has two domains, namely a catalytic domain and a starch binding domain.

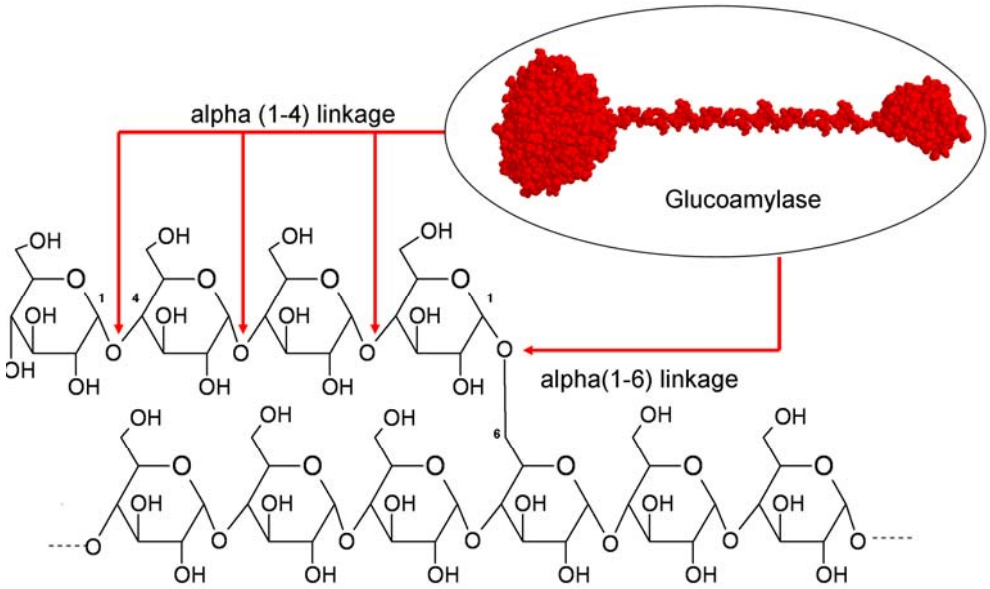

Figure 11: alpha-(1-4) and alpha (1-6) linked glucose units in starch hydrolysis by glucoamylase.

The two domains are connected by an O-glycosylated polypeptide linker located at the N-terminus. The starch binding domain of glucoamylase plays an active role in hydrolyzing raw starch and supports the enzyme adsorption to the cell wall where local increase of enzyme concentration may result in enhanced glucose flow to the cell. The expression of the gene for glucoamylase is efficiently controlled by the induction ot the *glaA* promoter, which is widely used for heterologous protein production (Nevalainen et al. 2005; Punt et al. 2002). This promotor is active, if starch, maltose or glucose are present in the cultivation medium. Xylose is known to strongly repress *glaA* expression, while maltose is a potent inducer of *glaA* promoter controlled genes. For some strains maltose has been found to be superior to glucose and starch for production of glucoamylase, whereas for other strains there seems no difference between the three carbon sources (Fowler et al. 1990; Schrickx et al. 1993).

4.4.3 Green fluorescent protein

Green fluorescent protein (GFP) is a 27 kDa protein with 238 amino acids from the Pacific Northwest jellyfish *Aequorea victoria* commonly used as a molecular marker for gene expression because it is easy to detect using a fluorescence detector, which exhibits bright green fluorescence when exposed to blue or ultraviolet light. Its absorbance and/or excitation peak is at 395 nm with a minor peak at 475 nm, and the emission peak is at 508 nm. The GFP has been expressed in various organisms, where it has been used as a reporter for gene expression, a tracer of cell lineage and a fluorescent tag for monitoring the sub-cellular localization in living cells. The first use of GFP as a vital reporter for gene expression was in bacteria and *Caenorhabditis elegans* (Cubitt et al. 1995). Subsequently, GFP has been used to monitor the sub-cellular distribution of a protein in the cells, as a vital marker of gene expression in a variety of living cell types at various developmental stages, and as an expression marker in pathogenic mycobacteria (Cubitt et al. 1995; Yang et al. 1996).

4.5 Bioprocess Optimization Using Design-of-Experiments

In order to obtain suitable process conditions for cell growth and/or product yield, a series of traditionally and statistically designed studies were conducted to investigate the effect of various factors on target response. The application of classical-based methods such as one-factor-at-a-time (OFAT) experiment, statistically-based optimization methods of design-of-experiments (DoE), factorial design (FD) or response surface methodology (RSM) provide powerful and efficient ways to systematically optimize cultivations and other unit operations and procedures using a reduced number of experiments (Mandenius and Brundin 2008). Generally, classical and statistical experimental planning, factorial design, and DoE, are more or less synonymous concepts for investigating the mathematical relationships between input and output variables of a system (Figure 12). DoE investigates defined input factors such as medium components and other process parameters components to a converting biosystem from which mostly common and well-defined output factors or responses are generated, such as biomass and/ or product yield (Mandenius and Brundin 2008).

Figure 12: Principle of input factors and output responses of a bioprocess or system as a basis for design-of-experiments (Montgomerty 2001)

One-factor-at-a-time experiment (OFAT)

At the beginning of a study there may be many potentially important factors. It is reasonable to assume that only a few of them will turn out to be important, but their identities are not known. Thus factor screening is needed. Many screening designs are available for this purpose, including the OFAT designs. This approach is a classical simple strategy of experimentation that extensively used in practice for

process optimization. Many engineers and scientists perform OFAT experiments, which vary only one factor at a time while keeping others unchanged under a specific set of conditions. It is useful only when one or a small number of factors are applied (Montgomery 2001). With a small number of factors, this strategy is convenient and simple to handle and allows for the interpretation of results without statistical analysis. However, the method becomes more complex when a large number of factors need to be optimized. In addition, this often requires a considerable amount of experimental work and may be costly. OFAT experimentation is generally discouraged in the literature about experimental design. Reasons cited for this include that it requires more runs for the same precision in effect estimation (i), it fails to consider any possible interaction between the factors (ii); the conclusions from its analysis are not general (iii), it can miss optimal settings of factors (iv), OFAT can be susceptible to bias due to time trends (v). Nevertheless, preliminary optimizations can be conducted using the classical OFAT method. This method identifies the input variables that can have a significant effect on the response. Thus the classical or empirical method can reduce the number of experiments to be carried out later when using a statistically-based method.

Design-of-experiments

The purpose of classical OFAT method is to identify which factors of the medium or cultivation parameters were the most important for the response. Statistically-based optimizations also know as design-of-experiments (DoE) is a proven tool for overcoming the limitations of the OFAT method. Moreover, it is valuable for measuring interactions among factors and for the prediction of optimal process conditions (i) and another strong point of using statistically-based optimization is that no complex calculations are required to analyze the resulting data (ii). Within one class of statistically-based optimization, two design types were used: the so-called factorial design and central composite design. Optimization through DoE is a general method used in biotechnology and several researchers have employed this for the bioprocess optimization (Montgomery 2001).

Central composite design

The central composite design (CCD) based response surface methodology (RSM) is an efficient mathematical approach widely applied in the optimization of cultivation processes. CCD is a collection of mathematical and statistical techniques useful for the modelling and analysis of problems in which a response of interest is influenced by servel factors and objectives is to optimize this response (Montgomery 2001). It is perhaps the most popular class of second order designs. Since introduced by Box and Wilson, the CCD has been studied and used by many researchers (Box and Wilson 1951). Often a researcher is interested in a process response, which is influenced by several factors, and the goal is to optimize this response. The design of choice to establish a quadratic model is the CCD. Each design consists of a standard first order design with 2^k factorial points and centre points CP, augmented by axial points (±α). Axial points are also commonly referred to as star points and this are points located at a specified distance α from the design centre in each direction on each axis defined by the coded factor levels. Hence, for a design consists of *k* factor, there will be 2^k distinct axial points. The distance of the axial runs from the design centre CCD α and the number of centre points CP must be specified regarding the properties required of the design (Montgomery 2001).

4.6 Systems Biotechnology for Strain Improvement

The improvement of the productivity of industrial relevant strains is one of the primary aims in biotechnology-based processes. Traditionally, many industrial strains have been developed via multiple cycles of classical methods such as random mutagenesis and selection, which might cause unwanted alterations in the strains (Park et al. 2008). Number of systems biotechnology approaches toward strain improvement and process development have been significantly increase in the recent years as elegant methods (Lee et al. 2005). There exist many definitions of systems biotechnology. It can be defined, as the application of science and technology at systems-level to living organism as well as part, products and models thereof, for the production of knowledge, goods and services (Lee et al. 2005). In most case the objective of any systems biotechnology approaches is the elucidation of cell function and physiology through the integrated use of board based genomic and physiological data (Kim et al. 2006). Therefore, systems biotechnology is a dynamic interaction and

combination of datasets for gene expression such as genomics, transcriptomics and proteomics with metabolite profiles (metabolomics) and flux distributions (fluxomics) (Deckwer et al. 2006).

4.6.1 Systems-level analysis of *Aspergillus* using omics approach

Within a few years systems-level studies have added much knowledge on strains and processes in this important family of filamentous fungi and lead to improved understanding on key targets for strains and processes (Andersen and Nielsen 2009). However, the complexity of *Aspergillus* is a challenge for scientific community and industry. In these days, this complexity within the cell can be understood by the omic's study including genomics, transcriptomics, proteomics, metabolomics and fluxomics (Figure 13), and a more holistic view of the system under study than a traditional reductionist approach is therefore often required. Omic's is everything describes methodological approaches targeting at the capture and analysis of all molecules of a specific type (Deckwer et al. 2006).

For this reason, the use of a multi-level analysis becomes more important. In recent years, several studies have been published using systems-wide tools. Many genomes have been sequenced and they applications have been published. The available genome makes the system wide approach even more appealing for the future. Currently, different platforms of transcription studies for *Aspergillus* have been published (Andersen and Nielsen 2009). Additionally, the fields of proteomics and metabolomics have produced fascinating results and novel applications. Finally, multiple levels of *Aspergillus* metabolism have been reconstructed and modelled (Andersen and Nielsen 2009). The results of omic's, and those of in silico design can be integrated at the systems-level within the global context of the systems metabolic engineering (Figure 14). This leads to the generation of new knowledge that can be used for biotechnological processes and strain development with the maximum performance and productivities (Lee et al. 2005). This shows the possibilities and potential of systems biotechnology, and the perspectives of developing new platforms and tools (Andersen and Nielsen 2009).

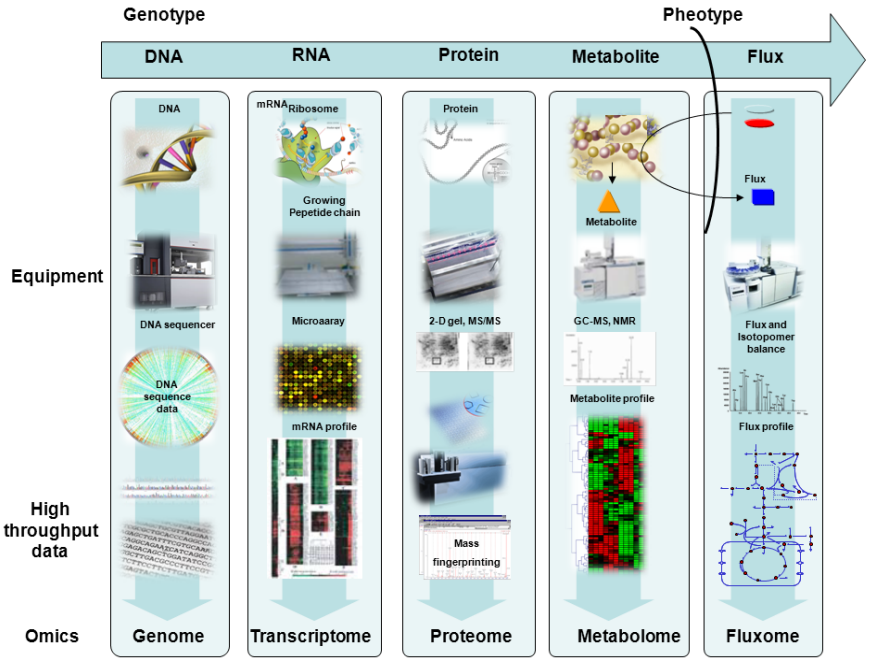

Figure 13: Omics research adapted from Lee et al. (2005) - Genomics advanced by the development of high-speed DNA sequencing is now accompanied by transcriptome studies using DNA microarrays such as complementary DNA and affymetrix. Proteomics is joining the high-throughput race as using 1(2)-D-SDS-PAGE or chromatography coupled with various MS methods is advancing. Metabolome profiling is also rapidly advancing with the development of gas chromatography-time-of-flight mass spectrometry, liquid chromatography–mass spectrometry and nuclear magnetic resonance technologies. Fluxome followed by challenging with isotopically labelled substrate allows determination of flux profiles in the cell (Lee et al. 2005).

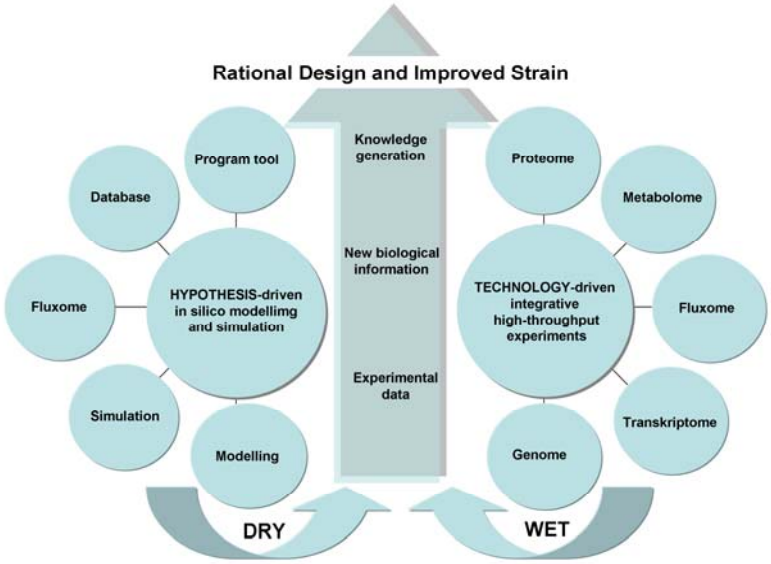

Figure 14: Integration of wet and dry experiments adapted from Lee et al. (2005). Omic's (wet experiments) lead to the accumulation of large amounts of data, which can be analyzed in conjunction with *in silico* design results (dry experiments) (Lee et al. 2005).

In this chapter, omic's approach for strains developments in *Aspergillus* is presented in the context of systems biotechnology.

Genomics and transcriptomics

Today the genome sequencing and the bioinformatics is *Aspergillus* have been established (Andersen et al. 2008; Coutinho et al. 2009; Galagan et al. 2003). As DNA sequencing has become faster and cheaper the genome sequences from many microorganisms have been sequenced and many more are in progress. However, the determination and structure of genome sequences of more complex microorganisms with large genome sizes and complexities are still a considerable challenge. The first sequenced fungus was the yeast *S. cervisiae* (Goffeau 1998). The genome sequencing projects for the *A. nidulans* started as early as 1997 using the whole-genome shotgun approaches with a 3x converge (Hamer 1997). In December 2003, the Whitehead Institute Centre for Genome Research released a draft version of the genome sequence of *A. nidulans* and the finished version of the genome sequence was published (Galagan et al. 2003). Later, this sequence was re-released by the Whitehead Institute/MIT Center for Genome Research with the addition of a 10x coverage sequence. Similarly, DSM/The Netherlands announced the genome sequencing of a recombinant protein-producing strain of *A. niger* CBS 513.88. The genome size of this strain is 33.9 Mb and consists of 8 chromosomes (Pel et al. 2007). Table 2 summarizes some genome sequence projects for *Aspergillus* from the recent overviews (Andersen and Nielsen 2009; Jones 2007).

The genomic era of *Aspergillus* has only just started (Andersen and Nielsen 2009). The future genome studies of more sequences as well as more thorough comparative genomics studies in the near future holds promises for unravelling many different and new mechanisms and the identification of key that define the individual species as well as are conserved through-out the genus. Furthermore, possibilities for studying *Aspergillus* on a systematic level are open for further research. Especially for research in biotechnology, future genome studies may have a substantial impact. The sequencing of *Aspergillus* genomes, both the currently available and the ones to be released in the future will continue to drive the progress of the other levels of systems-wide studies (Andersen and Nielsen 2009).

Table 2: Overview of some genome sequence projects for *Aspergillus.*

Strain	Institution/ Company, coverage	Genome Size (Mb*)	References
A. clavatus NRRL 181	TIGR, complete (11.4x)	28	(Fedorova et al. 2008)
A. flavus NRRL 3357	TIGR 3388, complete (10x)	36	(Yu et al. 2005)
A. fumigatus Af293	TIGR/Sanger Institute, complete (10.5x)	30	(Nierman et al. 2005)
A. nidulans FGSC A4	Broad Institute, complete (13x)	30	(Galagan et al. 2003)
A. nidulans CBS 513.88	DSM, The Netherlands, complete (7.5x)	34	(Pel et al. 2007)
A. niger ATCC 9029	IntegGenomics, complete (4x)	nd	(Pel et al. 2007)
A. niger ATCC 1015	DOE Joint Genome Institute, complete (8.9x)	35	(Baker 2006)
A. oryzae RIB40	NITE, Japan, complete (9x)	37	(Machida et al. 2005)
A. parasiticus	Unknowna University of Oklahoma, incomplete	nd	(Machida et al. 2005)
A. terreus ATCC 20542	Microbia, incomplete	nd	(Machida et al. 2005)
A. terreus NIH 2624	Broad Institute, complete (11x)	30	(Machida et al. 2005)

Data was gathered from the reviews (Andersen and Nielsen 2009; Jones 2007) and the Broad Institute database at see the website http://www.broad.mit.edu/annotation/genome/ aspergillus_group/MultiHome.html. *Mb .: megabases, nd .: not available

Table 3: List of DNA microarray studies in *Aspergillus*

Species	Gene models (%)	Focus	Type of DNA Microarray	References
A. nidulans	19.4	Comparison of gene expression signatures	cDNA	(Pocsi et al. 2005)
	26.0	Exposing to camptothecin-induced DNA damage	cDNA	(Malavazi et al. 2006)
	79.0	Ataxia-Telangiectasia mutated/ null mutant	Oligo	(Malavazi et al. 2007)
	89.2	Secondary metabolic gene cluster silencing	Nimblegen	(Bok et al. 2006)
	30.6	Comparison of wild type and creA mutant during growth on glucose or ethanol	Febit	(Mogensen et al. 2006)
		Recombinant protein secretion and the unfolded-protein response in vivo	cDNA	(Sims et al. 2005)
	99.6	Comparative transcriptomics of three *Aspergillus* species	Affymetrix	(Andersen et al. 2008)
A. niger	100	Genome sequencing and analysis	Affymetrix	(Pel et al. 2007)
	99.3	Comparative transcriptomics of three Aspergillus species	Affymetrix	(Andersen et al. 2008)
A. fumigatus	96.2	Comparison of the genomic sequence of the pathogenic and allergenic	Oligo	(Nierman et al. 2005)
A. oryzae	16.8	Analysis of genes for energy catabolism and hydrolytic enzymes	cDNA	(Maeda et al. 2004)
	99.7	Comparative transcriptomics of three Aspergillus species	Affymetrix	(Andersen et al. 2008)
	89.1	Regulation of genes on the non-syntenic blocks and its functional relationship to solid-state cultivation	Oligo	(Tamano et al. 2008)

Transcriptomics allow the parallel analysis of expression level of mRNA by using high-throughput techniques based on DNA-microarrays such as cDNA, oilgo,

nimblegen and affymetrix. This become an increasingly important tool over the last decade to examine the expression level at the genome level as it allows for identification of which genes are active and to what extent. Different transcriptome platforms have been made available in the *Aspergillus* species (Table 3), illustrating the possibilities of transcriptomics to elucidate complex biological processes in *Aspergillus*. The accessibility of the genome sequences has resulted in several transcriptome studies (Andersen et al. 2008). Since DNA-microarrays for expression analysis of *Aspergillus* have not yet been designed by industry, the research is mainly driven by the efforts of scientific community that have designed arrays and often have made the technology available to other researchers. This tool may be a powerful aid in unravelling the role of the hundreds of transcriptional regulators present in the *Aspergillus* species.

Proteomics

Recently few reviews of proteomics in filamentous fungi uses a definition of the proteome to be the ''*global set of proteins expressed in a cell at a given time and biological state*'' with the aim to obtain quantitative data of differential protein expression in response to process parameters (Carberry and Doyle 2007; Kim et al. 2007; Lu et al. 2010). While the presence of a genome sequence allows the identification of a protein from information on the amino acid sequence, the limitation in proteomics is often the purification, separation, detection and quantification of the individual proteins (Andersen and Nielsen 2009). Proteomics allows analysis of the protein complement of the cell or its parts by using 1(2)-D-SDS-PAGE or chromatography coupled with various MS methods, protein arrays, isotope-coded Affinity Tagging and Techniques for investigation of protein interactions. Method development in proteomics of Aspergilli is being actively pursued, and the review refers to four studies presenting methods for sample preparation in relation to *Aspergillus* (Kim et al. 2007; Lu et al. 2010). While proteomics is in still its infancy, the perspectives and potentials of the method are evident. Recently, the potential of systems-level proteomics in filamentous fungus are showing using novel statistical methods and an LC-MS methodology to perform high-throughput analysis of the proteome of *T. reesei* and the identification of more as 1500 proteins (Daly et al. 2008).

Metabolomics

The full set of metabolites found in a biological organism enables quantitative profiling of metabolites and metabolic intermediates using gas or liquid chromatography coupled with MS or NMR. The study of the metabolome is, compared to genomics, transcriptomics, and proteomics, a more complex task due to the large variation in the physical and chemical properties of the metabolites. This has lead to the development of a number of high-throughput tandem methods for quantitative analysis including GC-TOF-MS and LC-MS (Bolten et al. 2007). While the potential is thus present (Fernie et al. 2004), however, only very few research papers have been published doing large-scale quantitative studies in *Aspergillus* (Askenazi et al. 2003; Frisvad et al. 2009; Kouskoumvekaki et al. 2008).

Fluxomics

Metabolic flux distributions are process streams in a cell. Quantification of intracellular fluxes is called metabolic flux analysis (MFA), which applies mass balances around metabolites according to the stoichiometric model. MFA has become one of the major and popular tools in metabolic engineering in recent years. It allows the detailed quantification of all in vivo fluxes in the central metabolism of a cell (Wiechert 2002; Wiechert et al. 2001). The basic idea of MFA is that with the help of a stoichiometric model and with some extracellular flux measurements, it is possible to find the values of the rates at which each reaction operates. A flux distribution is a vector which entries are these rate values and that gives some insight on the mechanism of the organisms. Based on the results in a flux map that shows the distribution of anabolic fluxes over the metabolic network, possible targets for genetic modifications might be identified and the results of an already genetic manipulation can be judged or conclusions about the cellular energy metabolism can be drawn (Haverkorn van Rijsewijk et al. 2011; Kohlstedt et al. 2010; Wittmann 2007; Zamboni et al. 2009; Zamboni and Sauer 2009).

Metabolic flux ratio (METAFoR) analysis

A particular method to investigate the metabolism of organism at a local level is the metabolic flux ratio (METAFoR) analysis, which quantifies the relative contribution of two or more converging pathways to a given metabolite (Nanchen et al. 2006; Sauer 2004). METAFoR analysis utilises directly the ^{13}C-labelling data to deduce ratios of converging fluxes in the metabolic network. Thus the inaccuracies in the data or in the assumptions or errors in the network model affect the results only locally in contrast to the global methods (Zamboni et al. 2009). METAFoR analysis was initially developed to rely on uniform ^{13}C-labelling approach by the biosynthetically directed ^{13}C-labelling of the proteinogenic amino acids and following analysis of ^{13}C-labelling patterns by two-dimensional NMR spectroscopy (Szyperski 1995; Szyperski et al. 1999). Since the carbon backbones of metabolic intermediates of central carbon metabolism are conserved in synthesis of proteinogenic amino acids and the amino acid synthesis pathways were well known for *E. coli*, Szyperski back propagated the ^{13}C-labelling patterns from the amino acids to metabolites and derived equations for ratios of converging fluxes in central carbon metabolism (Szyperski 1995; Szyperski et al. 1999). Later Maaheimo *et al.* extended the method and derived flux ratio equations for compartmental metabolism of eukaryotic *Sachromyces cerevisiae* (Maaheimo et al. 2001). It is based on ^{13}C-labeling experiments, ^{13}C-NMR multiples (Szyperski 1995; Szyperski et al. 1999) or GC-MS analysis (Fischer and Sauer 2003), and probabilities equations that relate mass distribution in proteinogenic amino acids to pathway activity (Nanchen et al). The labelling pattern can then be related to their precursor molecules that are key components of central metabolism. The method provides a comprehensive perspective on central carbon metabolism by quantifying 12 independent ratios of converging pathway and reaction fluxes for [1-^{13}C] and [U-^{13}C]glucose experiments (Fischer and Sauer 2003).

In recent years, METAFoR analysis has proven to be a valuable tool to characterize various organisms such as yeast *S. cerevisiae* (Blank et al. 2005; Blank and Sauer 2004; Fiaux et al. 2003), *Pichia anomola* (Fredlund et al. 2004), *P. stipitis* (Fiaux et al. 2003*), P. pastoris* (Sola et al. 2004) and fungi such as *T. reesei* (Jouhten et al. 2009) and knockout mutants to answer biologically important questions (Fischer and Sauer 2003). The equations derived for eukaryotic metabolism have then been utilised in analysis of metabolic states of at least the following other yeasts and a fungus

P. pastoris (Sola et al. 2004), *P. stipitis* (Fiaux et al. 2003), *P. anomala* (Fredlund et al. 2004) and *T. reesei* (Jouhten et al. 2009). The METAFoR analysis can also be used as constraints in a stoichiometic reaction model for the estimation of intracellular carbon fluxes (Zamboni et al. 2005). Local flux ratios determined from ^{13}C-labelling experiments are experimental information that can be utilised as additional constraints in a conventional MFA system. Although of this goes beyond the scope of this chapter, the publicly available software tool FiatFLUX was used in this work to determine both METAFoR and intracellular net fluxes from ^{13}C-labeling experiments. In FiatFLUX, all the steps necessary for METAFoR calculation are implemented and the software directly calculates ratios from GC-MS raw data. The principle of this methodology and an example is illustrated in the following.

Calculation of METAFoR by GC-MS

The ratio of an intracellular pool of a given metabolite can be derived from other metabolite pools through biochemicals pathways. For each amino acid fragment (*aa)*, a mass isotopomer distribution vector (*MDV*) (Eq. 1) was assigned.

$$MDV_{aa} = \begin{bmatrix} (M_0) \\ (M_1) \\ (M_{2)}) \\ . \\ . \\ (M_n) \end{bmatrix} \quad \text{with} \quad \sum M_i = 1 \qquad (1)$$

where M_0 is the fractional abundance of fragments with the lowest mass and $M_{i>0}$ is the abundances of molecules with higher masses.

If a target metabolite T (MDV_T, *here* MDV_{PEP}) can be derived through two alternative pathways, from metabolite 1 (MDV_1, MDV_{3PG}) using pathway *A* or through metabolite 2 (MDV_2, MDV_{OAA}) and metabolite 3 (MDV_3, MDV_{PYR}) using an alternative pathway *B and C*, the contribution of each pathway can be determined (Figure 15 and Eq. 2).

The fractional contribution f , know as metabolic flux ratio, of a pathway to a target metabolite pool with MDV_T was determined as (Eq. 2):

$$MDV_{T(PEP)} = f * MDV_{1(3PG)} + MDV_{2(OAA)} * f_1 + MDV_{3(PYR)} * f_2 \qquad (2)$$

Where f is the fractional contribution of pathway *A* and 1- f_1 - f_2 is he contribution of the alternative pathway *B*, MDV_2 and C, MDV_3 are the mass distributions of the source metabolites degraded through the examined and the alternative pathway, respectively.

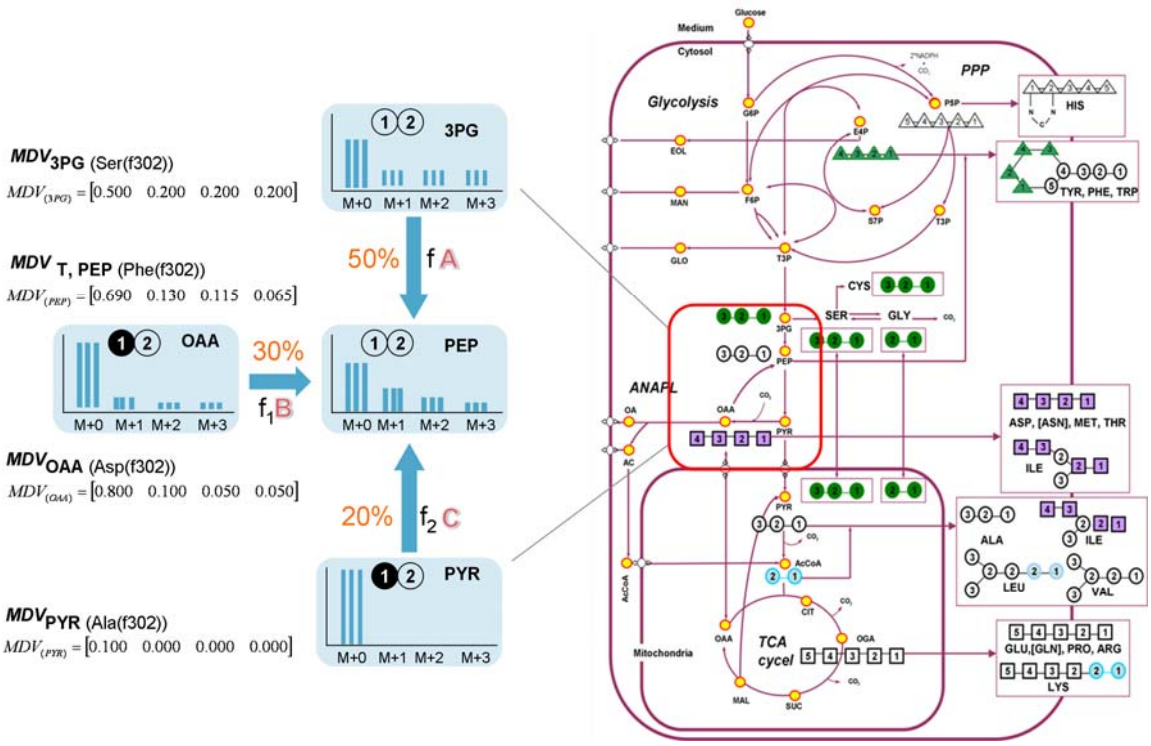

Figure 15: Mass distribution of alternative pathway leading to target metabolite pools (Fürch et al. 2007).

Because MDV are vectors and not single data points. Eq. 2 represents a linear system of algebraic equations and is usually over-determined. Rearrangement of Eq. 2 leads to Eq. 3 -4.

$$\begin{bmatrix} f_1 \\ f_2 \end{bmatrix} = \frac{MDV_{T(PEP)} - MDV_{3(PYR)}}{\begin{bmatrix} MDV_{2(3PG)} - MDV_{3(PYR)} \\ MDV_{3(OAA)} - MDV_{3(PYR)} \end{bmatrix}} \qquad (3)$$

$$\begin{bmatrix} f_1 \\ f_2 \end{bmatrix} = \frac{[0.069 \quad 0.130 \quad 0.115 \quad 0.065] - [0.5 \quad 0.2 \quad 0.2 \quad 0.1]}{\begin{bmatrix} [0.800 \quad 0.100 \quad 0.050 \quad 0.050] - [0.5 \quad 0.2 \quad 0.2 \quad 0.1] \\ [1.000 \quad 0.000 \quad 0.000 \quad 0.000] - [0.5 \quad 0.2 \quad 0.2 \quad 0.1] \end{bmatrix}} = \begin{bmatrix} 0.3 \\ 0.2 \end{bmatrix} \qquad (4)$$

$$f = 1 - f_1 - f_2 = 1 - 0.3 - 0.2 = 0.5$$

Where f represents the least squares solution to Eq. 8 and the division is a right-hand matrix division. Accordingly, using *MDV* with n+1 element (M_0 to M_n) up to alternative pathways can be distinguished.

Table 3 summarizes the calculable ratios and gives the type of ^{13}C-labeling experiment needed to calculate then. For explanations on the different ratios see paper (Fischer and Sauer 2003; Nanchen et al. 2006).

Table 4: Calculable ratios and gives the type of ^{13}C-labeling experiment.

Ratios	^{13}C-labeling experiment
SER through Glycolysis	**1***
E4P from P5P	**U***
P5P from E4P	**U**
P5P from G6P	**U**
SER from GLY	**U**
GLY from SER	**U**
PEP from PP Pathway (ub)	**U**
OAA from PEP	**U**
OAA from GLP	**U**
PYRm from MAL (Malic enzyme, ub or lb)	**U**
PEP from OAAc (PEP caboxykinase)	**U**

*U: mixture of [U-^{13}C]glucose and natural glucose, *1: 100% of [1-^{13}C]glucose, lb: lower bound, up: upper bound.

An overview of the ^{13}C-based metabolic flux ratio including ^{13}C-Labeling experiment, the measurement of isotopomer distribution, the flux determination, metabolic network identification and, overall scheme for metabolic flux analysis to uncover metabolic regulation is presented in Figure 16.

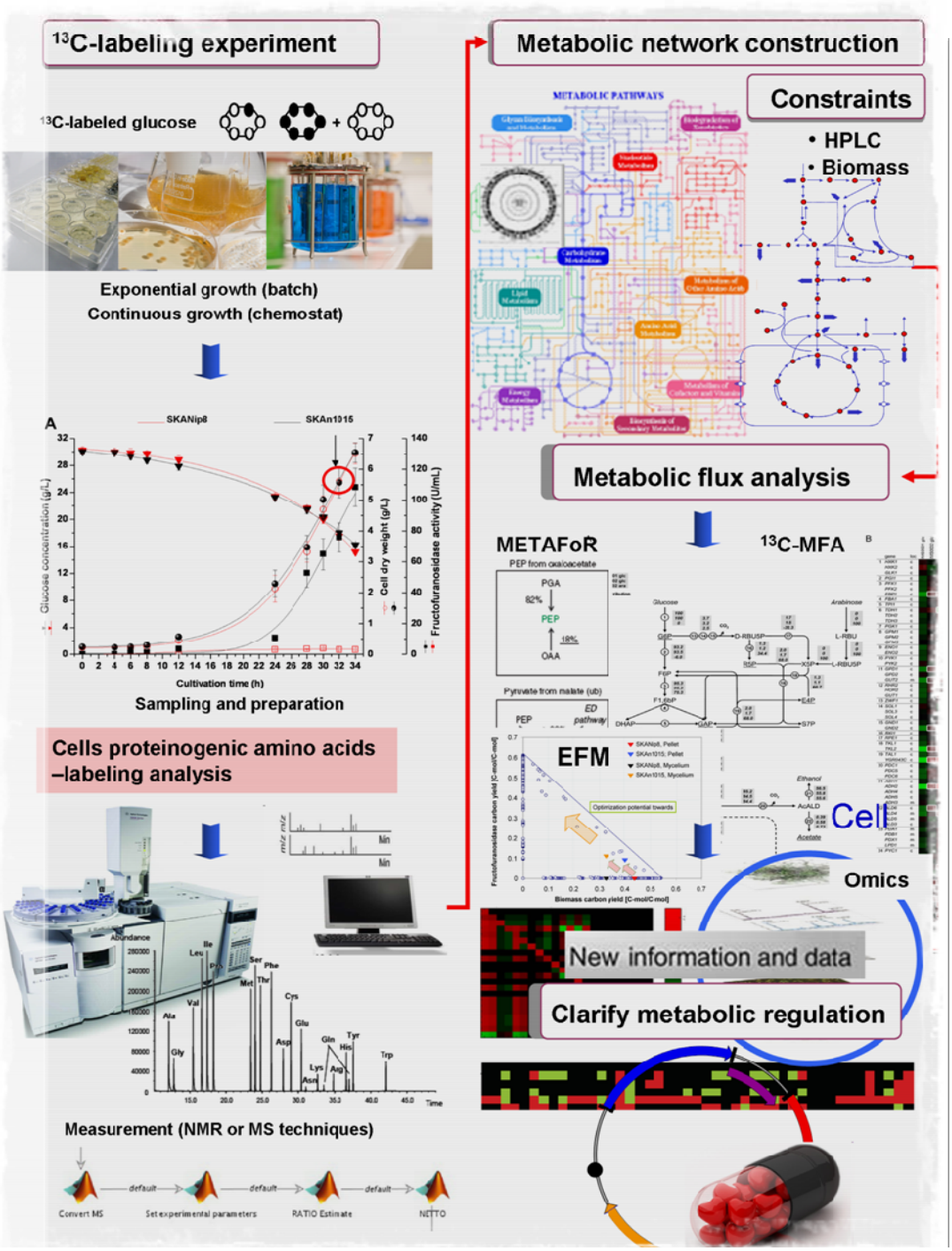

Figure 16: ^{13}C-based metabolic flux ratio including ^{13}C-Labeling experiment, the measurement of isotopomer distribution, and the flux determination, metabolic network identification and, overall scheme for metabolic flux analysis to uncover metabolic regulation.

4.6.2 Systems-level design of filamentous fungi

In addition to omic's analysis, in silico design pathways analysis is an important aspect of systems biotechnology. Many effects such as genetic perturbations as well as environmental perturbations on cellular metabolism can be predicted by in silico design.

In the last two decades two main modelling studies including kinetic modelling and metabolic flux analysis using several of stoichiometric models particularly for *Aspergillus* species of different complexity have been applied. The metabolic reconstruction aims at depicting a detailed description of the central core metabolism of different *Aspergillus* species, namely of the metabolism of carbohydrates, organic acids, polyols, and amino-sugars, as well as the oxidative phosphorylation in the electron transport chain. Major control steps of citrate production in *A. niger* using kinetic modelling approaches based on the biochemical system theory have been presented in a number of studies (Alvarez-Vasquez et al. 2000; Torres et al. 1993 ; Torres et al. 1998; Torres 1994). Metabolic flux analysis in a small stoichiometric model of *A. niger* was firstly introduced (Pedersen et al. 2000b; Schmidt et al. 1999). Afterwards, a stoichiometric model has been published for optimization of succinate production by the use of flux balance analysis and metabolic control analysis of xylose catabolism (David et al. 2003; Prathumpai et al. 2003), respectively. A smaller model of *A. niger* metabolism based on late model and other literature information, have been presented (Melzer et al. 2007), this model was used to investigated the metabolic flux distribution as function of pH of cultures. A most comprehensive model of *A. niger* metabolism based on the genome data, the validation and analysis was presented (Andersen et al. 2008; Meijer et al. 2009). For *A. nidulans* stoichiometric models have been published (David et al. 2006; David et al. 2005; David et al. 2008).

The recent efforts in genome sequencing and genome-scale modelling are major drivers for the prediction of genetic targets and optimal pathways towards superior cell factories. On basis of this rich set of information, computational and experimental strategies now aim at systems-wide optimization of tailor-made filamentous fungi (Melzer et al. 2009). Melzer reported on a novel approach recruiting computationally and experimentally derived flux information for metabolic design of superior production properties. On basis of a large-scale metabolic model of *A. niger*, functionally condensed from genome-scale, elementary flux modes were determined

for different scenarios of interest. Hereby, a novel approach screened the large set of elementary modes, each representing a unique flux distribution for flux correlations between metabolic reactions (Melzer et al. 2009). This, identified reactions coupled to desired properties such as production fluxes and thus, for the first time allowed the simultaneous prediction of deletion and amplification targets. Exemplified for different industrially relevant cell factories, products such as recombinant enzymes or chemicals and raw materials such as sugars, hemicelluloses or oils, the simulations revealed that the success of identification of most of the genetic targets depends on the differentiation of biological states, i.e. growth-associated or non-growth-associated formation of the target product. In addition, selected targets, such as the pathways of protein synthesis seem independent of the biological state. The simulation results nicely match with experimental data, comprising in vitro enzyme assay and experimental flux data. The integrated strategy of combining computational and experimental systems biology seems of high relevance for future metabolic engineering of fungal cell factories.

The wide diversity of fungal metabolites identified to date is strong motivation to develop *Aspergillus* as a cell factory for expression of novel filamentous fungal genes, further successes in their improvement as cell factory for non-fungal genes can help pay for more exploration into secondary metabolite engineering (Andersen and Nielsen 2009). Besides producing unique proteins, it should soon be possible to engineer recombinant fungi with complex interacting pathways, performing multiple reactions in a consolidated bioprocess, e.g. a single strain to convert cellulosic waste or recycled plastics directly into liquid fuels. *Aspergillus* could become a multi-purpose biotechnological cell factory, producing food, fuel, fibre and industrial chemicals as well as medicine. Integrating the powerful methods of metabolic engineering with the omics and in silico design tools for strain and process improvement will be a great multi-disciplinary challenge for biotechnology research and development in the near future (Lee et al. 2005; Lubertozzi and Keasling 2009; Stephanopoulos 2007). The growing knowledge of fungal metabolism and the unique capabilities assure it a continued place among the most biotechnologically useful strains.

5 MATERIALS AND METHODS

5.1 Strains, Plasmids and Maintenance

The recombinant strains of *Aspergillus niger* used in this work have been all derived from the mutant strain *A. niger* AB 1.13 which had been originally obtained from the wild type NRRL 3 (ATCC 9029) after three UV-mutagenesis (Blom et al. 1952; Debets et al. 1956; Mattern et al. 1992; Van Hartingsveldt et al. 1987). The genesis of the strains is given in Table 5.

Table 5: Genesis of *Aspergillus niger* AB 1.13.

Strains	Method of modification	New properties	Reference
AB 1.13	UV-mutagenesis of AB 4.1 (*pyr*G-)	Protease aspergillopepsin A and B deficient	(Mattern et al. 1992)
SKANip8	AB 1.13 without integrated Plasmid *pyrG+, suc1*-gene (wild type for SKAn1015)	Control of endogenous *Suc1* (fructofuranosidase, FFase)	(Zuccaro et al. 2008)
SKAn 1015	AB 1.13 with integrated *suc1*+gene plasmid with constitutive *pki*-promotor	Fructofuranosidase over-production	(Zuccaro et al. 2008)
pARAn 701	AB 1.13 with integrated pARAn701 + P*gal*A promoter	Co-expressing of glucoamylase and green fluorescent protein under the control of the P*gal*A	(Driouch et al. 2010b)

A. niger AB1. 13 is an uridine auxotrophic, protease deficient, and glucoamylase-producing strain (Mattern et al. 1992) derived by UV irradiation from *A. niger* AB 4.1 (Van Hartingsveldt et al. 1987). Additionally, three *A. niger* mutants, the wild type strain SKANip8, the recombinant strain SKAn1015 and the green fluorescent protein (GFP2) ARAn701, were used in this work. *A. niger* SKANip8 was used as control to study the endogenous *Suc1* (fructofuranosidase, FFase) activity of the host strain. The fructofuranosidase overproducing strain of *A. niger* SKAn1015 carrying the *suc1* gene to produce fructofuranosidase under the control of the constitutive *pki*A (pyruvate kinase) promoter was obtained from *A. niger* AB1.13 by transformation (Zuccaro et al. 2008). Similarly, *A. niger* ARAn701 which co-expresses the genes for

glucoamylase and green fluorescent protein (GFP2) under the control of the *p*galA promoter was derived from the mutant strain AB1.13. The *pgal*A promoter is repressed by xylose and inducible by carbon sources such as glucose or maltose.

Suc1 (ß-fructofuranosidase gene, FFase) was amplified by PCR from chromosomal DNA of *A. niger* AB1.13. The generated PCR fragment was purified, digested and cloned into SKANip8 (without *Suc-1* gene) plasmid under control of the constitutive *pki*A (pyruvate kinase) promoter. This generated *Suc+1* SKANip8 plasmid was named pSKAn1015 and was used for the transformation into the pyrG-protease deficient *A. niger* AB1.13 strain, and integrated into the *A. niger* chromosom (Zuccaro et al. 2008). For construction of ARAn701 (P*gla*A-*gfp*) plasmid, expressing *gfp* under control of the *glaA* promoter, the plasmid was integrated into the protease-deficient strain AB1.13 by protoblast transformation as described previously (Driouch et al. 2010a; Roth and Dersch 2010).

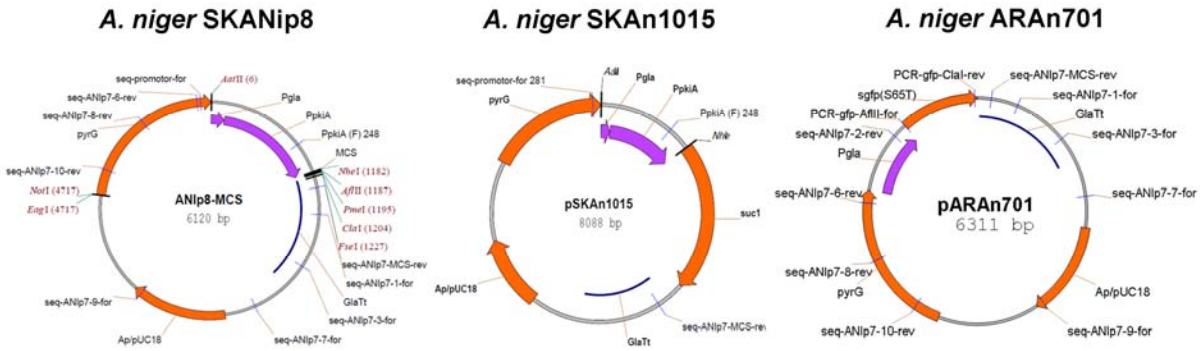

Figure 17: Plasmids used in this work to express recombinant proteins (fructofuranosidase, FFase and green fluorescent protein, GFP2) in *Aspergillus niger*

All organisms were maintained as frozen spore suspension in 50% glycerol at -80 °C.

5.2 Seed Culture

A spore inoculum of *A. niger* was prepared by growing thawn spores from the maintenance culture at 30 °C for 3 days on solid medium with 30 g/L potato dextrose and 10 g/L agar (Sigma-Aldrich, Seelze, Germany). For the strain AB 1.13, 1 g/L

uridine was added to the plates. Spores were then harvested as spore suspension from the plate into 20 mL 0.9 % (w/v) NaCl solution, which was spreaded onto the plate (Figure 18). After filtration (Miracloth, 25 µm pore size, CalBioChem, Darmstadt, Germany) the spore concentration was determined photometrically at 600 nm. Cultivations were inoculated to an initial spore concentration of 10^6/mL.

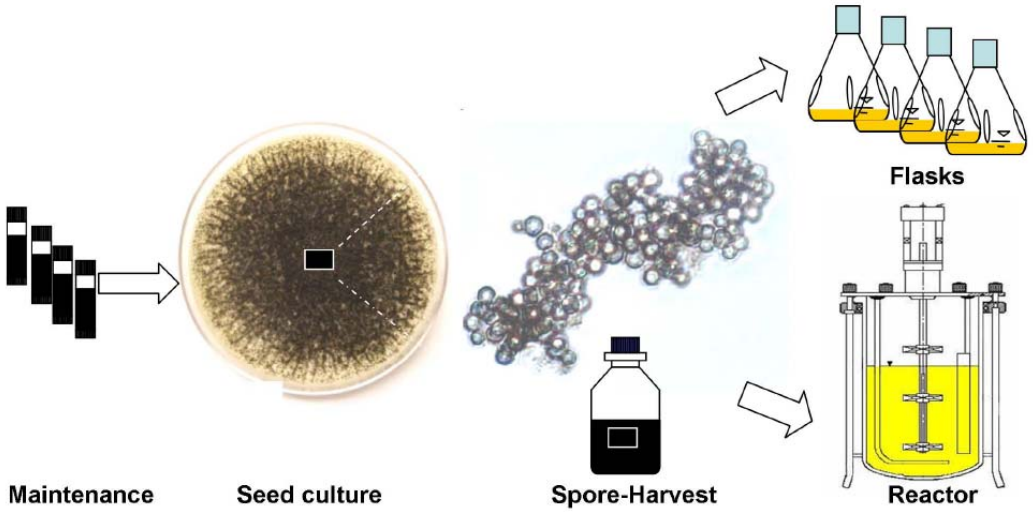

Figure 18: Overview of the *Aspergillus niger* seed culture preparation

5.3 Chemicals

Micro particles in different size diameter and chemical composition (such as particles of hydrous magnesium silicate ($3MgO\ 4SiO_2 \cdot H_2O$, talc powder) in different size fractions (<10 µm, 325 mesh, 350 mesh) as well as alumina micro particles (aluminum oxide hydrate, Al_2O_3, >64% as Al_2O_3) were obtained as dry powder from Sigma-Aldrich (Seelze, Germany) and MP Biomedicals (Eschwege, Germany), respectively (Table 6). Prior to use, micro particles were resuspended in 50 mM sodium-acetate buffer (pH 6.5) and subsequently separate autoclaved at 121 °C for 20 min. After autoclaving, micro particles were added to sterile minimal growth medium. In control cultures the micro particle suspension was replaced by 50 mM sodium-acetate buffer (pH 6.5). They greatly differed with respect to chemical composition and average particle size diameter and size distribution as estimated by experimental measurement by particle size analysis (Table 7).

Table 6: Tested inorganic micro particles with chemical composition, average particle size and density.

Material, chemical composition	Average diameter (µm)	Density at 20-25 °C (g cm^{-3})
Talc (hydrous magnesium silicate, $3Mg\ 4SiO_2 \cdot H_2O$)	6	2.8
Kaolin (Aluminum silicate hydroxide, $Al_2Si_2O_5\ OH$)	24	1.3
CalSil (Calcium silicate, $CaSiO_4$)	8	1.2
Nanoclay (Hydrophilic bentonite, $Al_2O_{34}SiO_2 \cdot H_2O$)	3	2.1
Florisil (Magnesium silicate, $MgSiO_3$)	280	3.2
Alumina (Aluminum oxide, Al_2O_3)	14	4.1
Aluminum silicate ($3Al_2O_{32}SiO_2$)	24	2.8
Zirconium (VI) silicate ($ZrSiO_4$)	50	6.5
Silica (SiO_2)	9	2.0
Alumium titanate oxide ($Al_2O_3TiO_2$)	27	4.3
Titanium silicate oxide ($TiSiO_4$)	8	4.2
SingmaCell ($(C_6H_{10}O_5)_n$)	48	1.3
Iron (II) oxide (Fe_2O_3)	5	5.8
Iron (III) oxide (Fe_3O_4)	4	5.2
Nickel oxide (NiO/Fe_2O_3)	6	6.8

Table 7: Volume-related specific surface of particle, mass-related specific surface of particle and size diameter of tested micro particles

Material	S_v (m^2 cm^{-3})*	S_m (cm^2 g^{-1})**	Particles size diameter (µm)***		
			X_{10}	**X_{50}**	X_{90}
Talc (-350 mesh)	1.40 ± 0.03	E05 ± 116	2.4 ± 0.1	**6.0** ± 0.0	12.5 ± 0.2
Kaolin (---)	0.62 ± 0.01	E05 ± 111	3.2 ± 0.2	**24.0** ± 0.1	56.6 ± 0.3
Nanoclay (---)	3.47 ± 0.01	E06 ± 125	1.0 ± 0.4	**2.7** ± 0.2	8.5 ± 0.5
Aluminium oxide (---)	0.79 ± 0.04	E03 ± 105	5.1 ± 0.0	**13.7** ± 0.1	30.7 ± 0.2
Calcium silicate (-200 mesh)	1.55 ± 0.03	E05 ± 096	1.7 ± 0.2	**8.0** ± 0.0	26.0 ± 0.1
Titanium silicate oxide (---)	2.13 ± 0.05	E06 ± 106	1.2 ± 0.1	**7.6** ± 0.0	19.0 ± 0.0
Alumium titanate oxide (---)	0.34 ± 0.00	E06 ± 098	15 ± 0.2	**27.4** ± 0.1	45.8 ± 0.4
Aluminum silicate (---)	0.56 ± 0.01	E06 ± 102	10± 0.3	**24.4** ± 0.2	41.6 ± 0.4
Zirconium (VI)silicate	1.40 ± 0.03	E06 ± 116	20 ± 0.4	**50.1** ± 0.0	85.5 ± 0.2
Florisil (30-60 mesh)	1.06 ± 0.01	E05 ± 112	90 ± 0.3	**280** ± 4.0	590.7 ± 0.2
Sigmacell (~50 µm)	0.83 ± 0.02	E06 ± 099	19 ± 0.1	**48.1** ± 0.0	78.4 ± 0.2
Silica (7-12 µm)	0.90 ± 0.01	E06 ± 100	7.0 ± 0.1	**9.5** ± 0.0	12.0 ± 0.2
Iron (II) oxide (-325 mesh)	1.40 ± 0.03	E05 ± 120	2.0 ± 0.2	**5.3** ± 0.1	13.0 ± 0.1
Iron (III) oxide (<5 µm)	1.40 ± 0.03	E06 ± 100	1.6 ± 0.1	**4.1** ± 0.2	9.5 ± 0.1
Iron nickel oxide (---)	1.40 ± 0.03	E06 ± 113	2.0 ± 0.2	**6.0** ± 0.1	15.0 ± 0.4

*S_v: volume-related specific surface of particle, **S_m: mass-related specific surface of particle and ***Particle size diameter were estimated experimentally by particle size analysis. S_v and S_m are measured under the assumption that the particles are spherical.

Labelled glucose was purchased from Campro Scientific (Cambridge Isotope Laboratories, Andover, USA). Complex media such as potato dextrose and agar were obtained from Sigma-Aldrich (Seelze, Germany). All other chemicals used in this work were of analytical grade and obtained from Sigma, Fluka or Merck.

5.4 Cultivation Media

The batch cultivation medium of *A. niger* AB1.13 contained per liter: 20 g glucose, 0.25 g uridine, 50 mL salt solution (6.6 g/L $(NH_4)_2SO_4$, 2.5 g/L KH_2PO_4, 0.2 g/L $MgSO_4 \cdot 7H_2O$, 0.1 g/L $CaCl_2 \cdot H_2O$), and 100 mL trace element solution (5 mg/L citric acid $\cdot H_2O$, 5 mg/L $ZnSO_4 \cdot 7H_2O$, 1 mg/L $Fe(NH_4)_2 (SO_4)_2 \cdot 6H_2O$, 0.16 mg/L $CuSO_4$, 0.05 mg/L H_3BO_3, 0.05 mg/L $Na_2MoO_4 \cdot H_2O$, and 0.037 mg/L $MnSO_4 \cdot H_2O$).

The batch cultivation medium of *A. niger* ARAn701 contained per liter: 10 g xylose, 50 mL salt solution (6.6 g/L $(NH_4)_2SO_4$, 2.5 g/L KH_2PO_4, 0.2 g/L $MgSO_4 \cdot 7H_2O$, and 0.1 g/L $CaCl_2 \cdot H_2O$) and 100 mL trace elements (5 mg/L citric acid $\cdot H_2O$, 5 mg/L $ZnSO_4 \cdot 7H_2O$, 1 mg/L $Fe(NH_4)_2(SO_4)_2 \cdot 6H_2O$, 0.16 mg/L $CuSO_4$, 0.05 mg/L H_3BO_3, 0.05 mg/L $Na_2MoO_4 \cdot H_2O$, and 0.037 mg/L $MnSO_4 \cdot H_2O$). After 40 h of cultivation, 10 g/L maltose was added to induce the glucoamyylase production.

The basic medium for batch cultivation of the fructofuranosidase strain SKAn1015 contained per litre: 20 g glucose, 50 mL salt solution (6 g $NaNO_3$, 0.5 g KCl, 1.5 g KH_2PO_4, 0.5 g $MgSO_4 \cdot 7H_2O$, and 1 mL trace elements (10 mg EDTA, 4.4 mg $ZnSO_4 \cdot 7H_2O$, 1.01 mg $MnCl_2$ $4H_2O$, 0.32 mg $CuSO_4 \cdot 5H_2O$, 1 mg $FeSO_4 \cdot 7H_2O$, 0.32 mg $CoCl_2 \cdot 6H_2O$, 1.47 mg $CaCl_2 \cdot 2H_2O$ and 0.22 mg $(NH_4)_6Mo_7O_{24} \cdot 4H_2O$).

These basic medium formulations were varied as described in the results section to achieve improved production performance. This included the replacement of glucose and nitrate by other carbon and nitrogen sources, respectively. Additionally, the level of nutrients was altered to investigate the effect on production. The optimal medium finally discovered, differed from the basic composition by elevated levels of glucose (30 g/L), $NaNO_3$ (9 g/L), $FeSO_4 \cdot 7H_2O$ (7.5 mg/L) and $MnCl_2 \cdot 4H_2O$ (1.5 mg/L).

In fed-batch processes with *A. niger* SKAn1015 in the bioreactor, the above medium was used for the batch phase. The medium for the feeding phase contained per litre: 200 g glucose, 40 g $NaNO_3$, 0.5 g KCl, 1.5 g KH_2PO_4, 0.5 g $MgSO_4 \cdot 7H_2O$, 10 mg EDTA, 4.4 mg $ZnSO_4 \cdot 7H_2O$, 30 mg $MnCl_2 \cdot 4H_2O$, 0.32 mg $CuSO_4 \cdot 5H_2O$, 2.5 g $FeSO_4 \cdot 7H_2O$, 0.32 mg $CoCl_2 \cdot 6H_2O$, 1.47 mg $CaCl_2 \cdot 2H_2O$ and 0.22 mg $(NH_4)_6Mo_7O_{24} \cdot 4H_2O$).

The batch medium for *A. niger* ARAn701 contained per litre: 10 g xylose, 6.6 g/L $(NH_4)_2SO_4$, 2.5 g/L KH_2PO_4, 0.2 g/L $MgSO_4 \cdot 7H_2O$, 0.1 g/L $CaCl_2 \cdot H_2O$, and 5 mg/L citric acid $\cdot H_2O$, 50 g/L $ZnSO_4 \cdot 7H_2O$, 10 g/L $Fe(NH_4)_2(SO_4) \cdot 6H_2O$, 16 g/L $CuSO_4$, 0.5 g/L H_3BO_3, 0.5 g/L $Na_2MoO_4 \cdot H_2O$, and 0.37 g/L $MnSO_4 \cdot H_2O$. In all cases the

solutions containing the carbon source, the inorganic salts and the trace element were sterilized separately at 121 °C for 20 min and cooled down to room temperature prior to mixing.

5.5 Culture Conditions

5.5.1 Batch cultivation

Cultures of *A. niger* grown in 250 mL baffled shake flasks containing 50 mL medium were incubated for 72 h at 120 min^{-1} on a rotary shaker in triplicate (Certomat BS-1/50 mm, Sartorius, Göttingen, Germany). The growth temperature was 37 ^{o}C (*A. niger* SKAn1015) and 30 ^{o}C (*A. niger* AB1.13 and *A. niger* ARAn701), respectively. Additionally, a 3.0 L stirred tank bioreactor (Applikon, Schiedam, The Netherlands) with a working volume of 2.2 L was employed for cultivation of *A. niger*. All bioreactor cultivations were carried out in duplicate. The aeration rate was maintained constant at 1.00 ± 0.02 L min^{-1} using a mass flow controller (red-y compact, Vögtlin Instruments, Hamburg, Germany). The agitation speed was kept at 200 ± 1 min^{-1} using two six-bladed disk turbine impellers (equal to a volumetric power input of 44 W m^{-3}). The levels of oxygen and carbon dioxide in the exhaust gas were monitored (BC perFerm, BlueSens, Herten, Germany). Antifoam (Ucolub N115, Mühlheim, Germany) was added manually when required. The pH was automatically kept constant by the addition of 2 M NaOH and 2 M HCl.

5.5.2 Fed-batch cultivation

For bioprocess optimization a 3 L stirred tank bioreactor (Applikon, Schiedam, The Netherlands) with two six-bladed disc turbine impellers (equal to a volumetric power input of 44 W m^{-3}) was employed. All bioreactor cultivations were carried out in duplicate. Aeration rate (1.0 L min^{-1}), 37 ^{o}C temperature for *A. niger* SKAn1015, 30 ^{o}C temperature for *A. niger* ARAn701, and pH value (pH 5.0) were automatically kept constant. Antifoam (Ucolub N115) was added manually, when required. The concentration of oxygen and carbon dioxide in the exhaust gas was monitored online (BC perFerm, BlueSens, Germany). Fed-batch processes exhibited an initial batch phase with 1.5 L starting volume. Intermittent feeding was started immediately when

the substrate level had decreased to about 5 g/L using a peristaltic pump (Applikon, Schiedam, The Netherlands). The feed was controlled such that the substrate level remained above 1 g/L, which was monitored by measurement in the broth. The total feed volume added was 1 L. The agitation speed was maintained at 200 min^{-1} during the first 24 hours for *A. niger* SKAn1015 and the first 40 hours for *A. niger* ARAn701. After that, the agitation speed was increased stepwise every 30 min to 300, 400, 500 and 550 min^{-1}, meaning that the latter value was then maintained for the rest of the process. In selected cultivations, micro particle of hydrous magnesium silicate ($3MgO\ 4SiO_2 \cdot H_2O$, 6 µm, 5 g/L, talc powder) were added. Prior to use, the micro particles were re-suspended in 50 mM Na-acetate buffer (pH 6.5), autoclaved at 121 °C for 20 min and added to the sterile growth medium prior to inoculation.

5.5.3 pH-shift cultivation

A. niger SKAn1015 was cultivated under two different pH conditions (pH 3, pH 5). During the first 20 hours of the cultivation the pH was maintained at the initial pH-values of 3 or 5. After 20 h, the pH-value was shifted automatically over a 5 hour period from 3 to 5 or from 5 to 3 by the addition of 2 M NaOH or 2 M HCl, respectively. After that, the final pH was kept constant throughout the experiment, in order to investigate the morphology and the fructofuranosidase production.

5.6 Analytical Methods

5.6.1 Analysis of substrates and products

Concentration of cell dry biomass was determined in triplicate. For this purpose, 5 mL samples were filtered on a pre-weighted cellulose acetate filter (pore size 20 µm, Sartorius, Göttingen, Germany). Subsequently, the filter was rinsed twice with water and then dried at 100 °C until weight constancy. After cooling in a desiccator, the cell dry weight was determined by re-weighing. The quantification of polyols and organic in cultivation supernatant, obtained by filtration (Minisart 0.2 µm, Sartorius, Göttingen, Germany) was carried out using HPLC (Elite Lachrome HITACHI Ltd., Japan) with a Metacarb 67H column (250 mm x 4.6 mm, 5 µm, VWR-Hitachi, Darmstadt, Germany) and 1 mM H_2SO_4 as mobile phase at a flow rate of 0.8 mL min^{-1} and 70 °C. Polyols

(mannitol, erytrithol, and glycerol) and organic acids (formate, oxalate, acetate, butyrate, and gluconate) were detected via refractive index UV absorbance at 210 nm. In addition, Glucose concentration was determined using a glucose analyzer (Biochemistry Analyze, YSI, OH, USA).

5.6.2 Enzymatic in vivo activity

Fructofuranosidase activity

The specific activity of fructofuranosidase was quantified in culture supernatant obtained by filtration of 10 mL culture broth through a cellulose acetate filter (pore size 20 µm, Sartorius). The reaction was started by addition of 200 µL 1.65 M sucrose to a 20 µL sample and incubated at 55 ^{o}C for 20 min. The reaction was stopped by heating at 95 ^{o}C for 10 min. After cooling, the reaction mixture was centrifuged at 13,000x*g* for 10 min at 4 ^{o}C. Glucose formed from cleavage of sucrose by the enzyme was then quantified using a GOD/ POD assay (Sigma–Aldrich) (Miller, 1959). In the present work the assay was modified for high-throughput analysis in 96-well microtiter plates (MaxiSorp, Nunc, Langenselbold, Germany). For this propose an enzyme reagent solution was prepared by re-suspending 10.5 mg glucose oxidase (GOD) and 3 mg of peroxidase (POD) in 90 mL of 0.05 M phosphate buffer (pH 7.0) and 10 mL of 95% ethanol containing 25 mg of o-dianosidine, respectively. Subsequently, the reagent solution was filtered through a cellulose acetate filter (pore size 20 mm, Sartorius) and immediately used for the assay. For this purpose, 1.6 mL sample was mixed with 200 mL of the reagent solution in a microtiter plate well. After 10 min incubation at room temperature, glucose was quantified indirectly through absorption measurement at 450 nm using a 96-well Sunrise microplate reader (TECAN, Crailsheim, Germany) and the XFlour4 data retrieval software. To account for residual glucose in the culture broth, negative controls were carried out by using samples in which fructofuranosidase was inactivated by heating at 95 °C for 10 min prior to incubation. All enzymatic assays were done in triplicate.

The measured enzyme activity was on average 1.8-fold higher as compared to values determined at 40 °C. This ratio, estimated from the analysis of ten different culture samples at both temperatures, was used to compare the obtained results with

previous studies which had employed 40 °C or 55°C for the fructofuranosidase assay.

Glucoamylase activity

Glucoamylase activity was determined in cell extracts. For this purpose cells were harvested from 5 mL of culture broth by filtration (pore size 20 mm, Sartorius) including two washing steps with 10 mM sodium-acetate buffer (pH 4.5). Cells were then suspended in fresh buffer and disrupted by a mill mortar for 6 min (RMO, Retsch, Haan, Germany) and again filtered (0.2 µm pore size, Sartorius). Glucoamylase activity in crude cell extract was measured by the method of (Withers et al., 1978) using p-nitrophenylalphaglucopyranoside (pNPG) as substrate. For this purpose 500 µL of pNPG solution (0.1% w/v, in sodium-acetate buffer, pH 4.8) was added to 250 µL cell extract. After incubating for 20 min at 60 °C, the enzymatic reaction was stopped by addition of 750 µL of 0.1 M sodium borate. After filtration (0.2 µm pore size, Sartorius) the absorption was measured at 400 nm. All enzymatic assays were done in triplicate.

5.7 Microscopy

5.7.1 Image analysis of cellular morphology

The culture morphology of *A. niger* was analyzed throughout the cultivation via 3-D photographs using a stereo-microscope (Stemi 2000-C, ZEISS, Jena, Germany) with an AxioCamMRc5 digital camera (Stemi 2000-C, ZEISS), which was connected to the computer. Pellets were suspended individually in a Petri dish filled with a cultivation medium. Images of the pellets were acquired, improved and binarized. The image analysis was automated so that more than 100 pellets were counted for each sample in duplicate of a certain volume after 72 h of cultivation. The area projected by each pellet was analyzed by the software (KS300, ZEISS) and the average pellet size diameter was derived from the measured projected area.

5.7.2 Spatial resolution of protein production

Confocal laser scanning microscopy (CLSM) was applied to analyze the spatial distribution of GFP fluorescence within cellular aggregates. For this purpose cells were harvested from 5 mL culture by filtration, washed three times with deionized water, re-suspended in 100 µL deionized water and added into the well of a PCR plate with kryo medium (Neg-50, Richard-Allan Scientific, Malamazoo, MI). Subsequently, the filled plate was incubated for 40 min in the dark followed by freezing at -20 °C. Subsequently, the frozen samples were cut into 70 µm slices (HM 550, Microm, Neuss, Germany). The slices were then fixed on an microscope object slide by partial thawing of the cut medium and analyzed by CLSM with a system equipped with an LSM 510 Mata Camera and an argon laser (Carl-ZEISS International Micro Imaging, Jana, Germany) with an excitation wavelength of 488 nm line and an emission wavelength at 550–570 nm band pass (ZEISS). During the preparation, the 70 µm pellet slices were exposed to ambient temperature for more than 30 min prior to CLSM analysis so that all GFP produced could be converted into its fluorescent derivate, requiring oxygen, even for the cases that the original pellet in the culture had been oxygen limited.

5.7.3 Scanning electron microscopy

Scanning electron microscopy (SEM) analysis was used to study the morphological structures of micro particles. Samples of different micro particles were analyzed by SEM (EVO® LS 25, Carl-ZEISS International Micro Imaging, Jena, Germany). Samples of 1 mg were mounted (carbon adhesive Leit-Tabs 12 mm No.: G 3347, Plano, Wetzlar, Germany) and fixed at room temperature on aluminum specimen stubs (0.5 mm SEM-Stubs-G031Z; Plano, Wetzlar, Germany). Analysis was then performed with a Zeiss DSM 962 Digital Scanning Microscope (Zeiss, Aalen, Germany) which is a fully computer-controlled SEM (Software SmartSEM™, VO5.03) with field emission. An accelerating voltage of 10 kV was used to collect SEM images for the composite specimen. A gold coating of a few nanometres in thickness was coated on impact fracture surfaces.

5.8 Experimental Design

5.8.1 Screening of the suited media components

The effect of medium constituents on fructofuranosidase production by *A. niger* SKAn1015 was first investigated in shake flasks by the one-factor-at-a-time (OFAT) approach. Different carbohydrates, nitrogen sources and various essential elements were investigated with regard to fructofuranosidase production. Starting from the formulation of the basic medium, the concentration of each investigated nutrient was decreased to 50 % (low level, -1) or increased to 200 % (high level, +1). The expression media were inoculated with 1.10^6 spores mL^{-1} and cultivated in 250 mL flasks for 60 hours, following by measurement of cell dry weight and fructofuranosidase activity, respectively. From these screening experiments, the key nutrients that affected fructofuranosidase production were identified and optimized further using central composite design.

5.8.2 Central composite design

Based on the results from the screening experiments, k = 4 nutrients that significantly affected the growth and the fructofuranosidase production were identified and optimized further using the central composite design (CCD). From this N = 30 nutrient combinations were designed for further shake flask studies, meaning that this included 16 combinations from a full 2^4 factorial composite rotary design, 6 at the centre point (*CP*) and 8 experiments (axial points), where one factor was set to an extreme level (± α). The star distance was chosen to be ± 2 to make this design rotatable. CCD was used with a 30 total number of treatment combinations (Eq. 5), which were carried out in triplicate.

$$N = 2^k + 2k + CP \tag{6}$$

Here, *N* is the number of experiments, 2 is the level of experiments, *k* is the number of independent variables and *CP* is the number of repetitions of the experiments at the center point. The predictor factors were coded according to the following (Eq. 6).

$$x_i = \frac{X_i - X_0}{\Delta X} \quad (6)$$

Here, x_i is the coded value of independent variables, X_i is the independent variable's real value, X_0 is the independent variable's real value at the centre point (*CP*), and ΔX_i is the step change value. This methodology allows the modelling of the data by a second-order equation. The quadratic model for estimating the concentration of the investigated nutrients for optimum fructofuranosidase activity is given by E. 7.

$$Y = \beta_0 + \sum \beta_i X_i + \sum \beta_{ii} X_i^2 + \sum \beta_{ij} X_i X_j \quad (7)$$

Here, Y is the response variable, i.e. the fructofuranosidase activity, X_i and X_j are the independent input variables, i.e. the nutrient levels. The values for $\beta_0, \beta_{ii}, \beta_{ij}$ are the resulting regression variables for intercept, linear, quadratic, and interaction terms, respectively. The parameter estimation from the data by 2nd-order multiple regression models was carried out using a statistical software (Design-Expert, Version 7.0, Stat-Ease, Minneapolis, Minn., USA). This included thorough statistical treatment of the data, involving a quality check of the fitted polynomial models by the coefficient of determination (R^2) and the correlation coefficient (R), as well as the analysis of variance (ANOVA) combined with an *F*-test to evaluate, if a given term had a significant effect ($p<0.05$).

5.9 Protein Analysis

5.9.1 Protein concentration in the culture supernatant

The protein concentration in the culture supernatants (cell-free filtrate) was determined by the bicinchoninic acid (BCA) method using bovine serum albumin as external standard (BSA protein assay kit, Pierce, Rockford, USA) following the instruction given by the distributor. For this purpose, 5 mL samples were filtered (cellulose acetate filter, pore size 20 µm, Sartorius, Germany) and clarified by centrifugation (13,000*xg*, 10 min, 4 °C) prior to analysis.

5.9.2 Extracellular protein pattern

SDS–PAGE was used to separate the secreted proteins in culture supernatant samples. First, the protein in culture supernatants was concentrated by (1:6) acetone precipitation. A volume of 3 µL of acetone precipitated supernatant was then separated using a 4-12 % Bis-Tris-Mini Gel (Novex Mini-Cell 1 mm, 15 well, Invitrogen, Karlsruhe, Germany) following the instruction given by the distributor. The applied molecular mass marker was the PageRuler Unstained Protein Ladder (SM0661, Fermentas, St. Leon-Rot, Germany). The highly glycosylated fructofuranosidase has a molecular weight of about 110-120 kDa (Zuccaro et al. 2008). For quantification of the relative amount of fructofuranosidase in the supernatant, the gel was scanned using the Molecular Imager ® PharosFX System (BioRad, Munich, Germany). The volume of the corresponding protein bands was determined by the 1-D Analysis Software (Version 4.6.9, BioRad, Munich, Germany).

5.9.3 MALDI-TOF-MS analysis

Extracellular proteins of *A. niger* SKAn1015 were identified by MALDI-TOF-MS analysis. For identification, bands were manually excised from the gel, cut into small pieces and prepared for peptide digestion by trypsin addition. Peptide mass fingerprints and peptide fragmentation data were analysed using an UltrafleXterme™ TOF/TOF mass spectrometer (Bruker Daltonic GmbH, Bremen, Germany) and subsequently processed using FlexAnalysis™ 3.0 and the Biotools™ 3.2 program of the software-package Masslynx™. The Mascot 2.2 search program was used for protein identification with the annotated *A. niger* genome (EMBL: http://www.ebi.ac.uk/genomes/eukaryota.html) serving as database. Annotations were according to the sequenced genome of *A. niger* and the current NCBI Reference Sequence database.

5.10 Fluxomics

5.10.1 Strains and maintenance

Two *Aspergillus niger* strains, the wild type SKANip8 and the recombinant strain *A. niger* SKAn1015, were used in this work (Zuccaro et al. 2008). The recombinant strain expresses the *suc1* gene, encoding fructofuranosidase, under the control of the constitutive *pki*A (pyruvate kinase) promoter (Driouch et al. 2010b; Zuccaro et al. 2008). Both strains were maintained as frozen spore suspension in 50% glycerol at -80 °C.

5.10.2 Medium for ^{13}C-tracer experiments

The cultivation medium for ^{13}C-tracer experiments contained per litre: 30 g glucose, 20 mL salt solution (50x with 180 g/L $NaNO_3$, 10 g/L KCl, 30 g/L KH_2PO_4, 10 g/L $MgSO_4 \cdot 7H_2O$) and 1 mL trace element solution (1000x with 10 g/L EDTA, 4.4 g/L $ZnSO_4 \cdot 7H_2O$, 1.5 g/L $MnCl_2 \cdot 4H_2O$, 0.32 g/L $CuSO_4 \cdot 5H_2O$, 7.5 g/L $FeSO_4 \cdot 7H_2O$, 0.32 g/L $CoCl_2 \cdot 6H_2O$, 1.47 g/L $CaCl_2 \cdot 2H_2O$, and 0.22 g/L $(NH_4)_6Mo_7O_{24} \cdot 4H_2O$). In ^{13}C-labeling experiments, the glucose was replaced by equimolar concentrations of ^{13}C-labelled glucose. In addition, three replicates with non-labeled glucose were performed to quantify kinetics and growth of the examined cells. To resolve the metabolic fluxes of interest two parallel set-ups were chosen for the labelling studies (Wittmann and Heinzle 2002) including (i) [1-^{13}C] glucose (99%, Cambridge Isotope Laboratories, Andover, USA) and (ii) a 1:1 mixture of [$^{13}C_6$] glucose (99%, Cambridge Isotope Laboratories, Andover, USA) and naturally labelled glucose. The basal medium and the stock solutions for salt and trace elements were autoclaved separately for 20 min at 121 °C and cooled down to room temperature prior to mixing.

5.10.3 Cultivation and ^{13}C tracer experiments

A spore inoculum of *A. niger* was prepared by incubating thawn spores from the glycerol stock at 30 °C for 3 days on 30 g/L potato dextrose agar (Sigma-Aldrich, Seelze, Germany). Spores were then harvested as suspension by spreading 20 mL sterile 0.9% NaCl solution over the plate. After filtration of the suspension (Miracloth, 25 µm pore size, CalBioChem, Darmstadt, Germany) the obtained spore concentration was quantified photometrically at 600 nm considering a correlation

factor of 1 OD_{600} = 1.16 10^7 spores/mL which had been determined experimentally. Liquid cultures were then inoculated to an initial spore concentration of < 1 % of final cell dry weight. All cultivations were performed in three independent replicates using 100 mL baffled shake flasks with 30 mL medium on a rotary shaker (Certomat BS-1/50 mm, Sartorius, Göttingen, Germany) at 37 °C at 120 rpm.

5.10.4 Labelling analysis of proteinogenic amino acids by GC-MS

Cells of *A. niger* were harvested during mid-exponential growth by filtration of 5 mL culture broth through a cellulose acetate filter (pore size 20 µm, Sartorius, Göttingen, Germany). After removal of excess medium by two washing steps with sterile 0.9% NaCl solution, the cells were frozen in liquid nitrogen and then lyophilized at -60 °C (Alpha 1-4 LD, Christ GmbH, Osterode, Germany). For protein hydrolysis 10 mg of lyophilized biomass was incubated in 400 µL of 6 M HCl at 100 °C for 24 h. After pH adjustment to 7.0 by 6 M NaOH, the hydrolysate was clarified (0.2 µm, Ultrafree MC, Millipore, Bedford, MA, USA) and again lyophilized. The contained proteinogenic amino acids were then converted into *t*-butyl-di-methyl-silyl derivates (Wittmann et al. 2002). Their labelling pattern was quantified by GC-MS (HP 6890, M 5973, Agilent Technologies, Waldbronn, Germany) as described previously (Kiefer et al. 2004). All samples were measured first in scan mode, therewith excluding isobaric interference (Wittmann 2007). The relative fractions of the mass isotopomers of interest were then determined in duplicate in selective ion monitoring (SIM) mode.

5.10.5 Metabolic reaction network

A compartmented metabolic network model of *A. niger* was constructed on basis of validated models recently described (Andersen et al. 2008; Jouhten et al. 2009; Meijer et al. 2009; Melzer et al. 2009). Briefly, the network included all major central pathways, such as the glycolysis, the pentose phosphate pathway (PPP), the gluconeogenic and the anaplerotic pathways, the tricarboxylic acid (TCA) cycle, and the glyoxylate pathway, the anabolic metabolism, the biosynthetic route towards the recombinant fructofuranosidase as well as reactions involved in substrate uptake and by-product formation (Figure 19). A detailed overview on the model including all reactions is provided in the Appendix A. The cytosol and the mitochondrion were considered as separate compartments. This included separate pools for pyruvate,

oxaloacetate and acetyl-CoA in both compartments. The transport of pyruvate into the mitochondria was considered to be unidirectional. However, the transport of oxaloacetate and acetyl-CoA into the mitochondria was regarded reversible and a priori to be bi-directional. The compartmentation of anabolism, including amino acid biosynthesis, was revised by inspection of metabolic flux studies on different yeasts and fungi. This revealed that the central carbon metabolism of yeast such as *S. cerevisiae* (Blank et al. 2005; Blank and Sauer 2004; Fiaux et al. 2003), *P. anomola* (Fredlund et al. 2004), *P. stipitis* (Fiaux et al. 2003*), P. pastoris* (Sola et al. 2004) and fungi such as *T. reesei* (Jouhten et al. 2009) is rather similar and conserved with respect to pathway reactions and their localization, despite variations with respect to its regulation. The metabolic reaction network consisted of 46 irreversible and 11 reversible reactions and 28 intracellular metabolites (Figure 19).

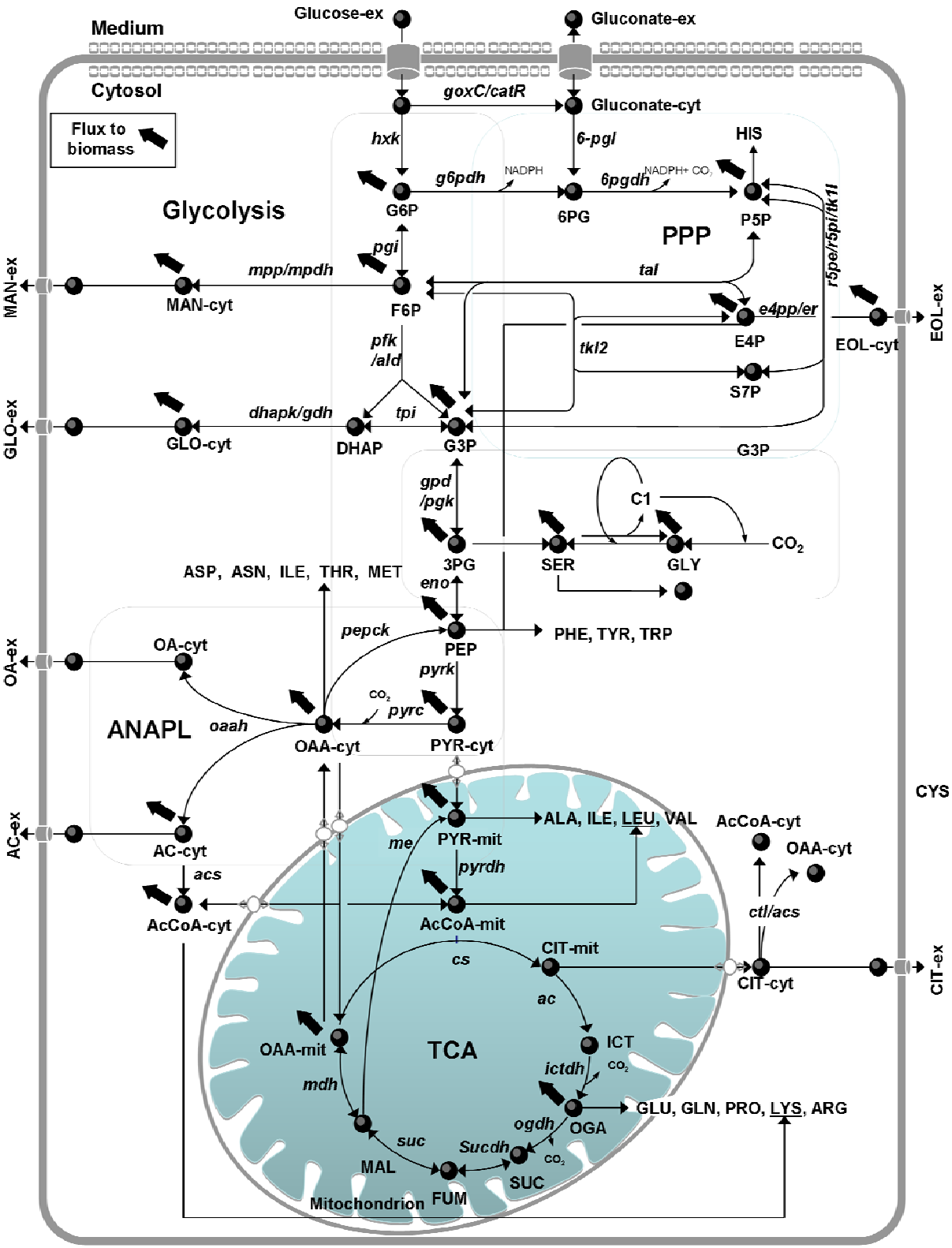

Figure 19: Compartmented metabolic network of *Aspergillus niger*.

5.10.6 Metabolic flux calculation

The estimation of metabolic fluxes was performed with the MATLAB-based program FiatFLUX 1.67 which was kindly provided by the authors (Zamboni et al. 2005). This software package consists of two modules for (i) computation of metabolic flux ratios for ^{13}C-labeling data and (ii) estimation of net carbon fluxes within a comprehensive model of metabolite balances from determined metabolic flux ratios, measured extracellular fluxes, and biomass requirement. Shortly, the proteinogenic amino acids are synthesized from one or more metabolic intermediates. A detailed description of the principle and the evaluation of flux ratios from MDV_M of metabolic intermediates is given elsewhere (Fredlund et al. 2004; Zamboni et al. 2005). For flux calculation in the present work, the obtained mass isotopomer distributions of the derivatized amino acids alanine, glycine, valine, leucine, isoleucine, proline, serine, threonine, phenylalanine, aspartate, glutamate, histidine, lysine and tyrosine were corrected for natural abundance of stable isotopes. Due to the low inoculum level the potential interference of non-labelled carbon from the inoculum could be neglected. For flux calculation, the metabolic flux ratios were first determined by the flux ratio module and then used on basis of the metabolic reaction network with 46 reactions and 28 metabolites to obtain the net fluxes. For this purpose, the metabolic fluxes were calculated using (i) the stoichiometric reaction matrix, (ii) the metabolic flux ratios as additional constraints for the stoichiometric equation system (iii) time-averaged uptake and production rates of external metabolites and (iv) precursor requirements for biomass synthesis as described previously (Andersen et al. 2008; Meijer et al. 2009; Melzer et al. 2009).

5.11 Elementary Flux Mode Analysis

Elementary flux mode calculation was performed on basis of the genome-scale network model of *A. niger* (Andersen et al. 2008) as described recently (Melzer et al. 2009). In addition to the previous calculations, the network model was extended by pathways towards relevant by-products, i.e. gluconate, oxalate, mannitol and glycerol, observed in the cultivation experiments. The corresponding metabolic network reactions are listed in the Appendix A. On basis of the determined elementary modes, a detailed investigation of metabolic network properties was

carried out. This included the estimation of theoretical (maximum) yields, relative fluxes through intracellular metabolic pathways and target prediction for strain engineering. Calculations were partially automated and implemented into Matlab (Mathworks Inc., Natick, MA) and evaluated in Excel (Microsoft Office, Windows, 2007).

6 RESULTS AND DISCUSSION

6.1 Morphology Engineering for Improved Enzyme Production

6.1.1 Evalution of classical strategies based on pH-shift

As described above morphology of *A. niger* is influenced by many parameters, whereby the pH is one of the most important (Wucherpfennig et al. 2010). Therefore, the first investigations focussed on the use of pH-shifting strategies to provide the desired morphology of a freely dispersed mycelium for enhance fructofuranosidase production.

6.1.1.1 Effect of pH-value on morphology and enzyme production

Batch cultivation of *A. niger* SKAn1015 at pH 3 or pH 5 clearly revealed significant differences in the morphology (Figure 20), the maximum biomass concentration and the final activity of fructofuranosidase (Figure 21). *A. niger* SKAn1015 was able to grow at both pH-values tested.

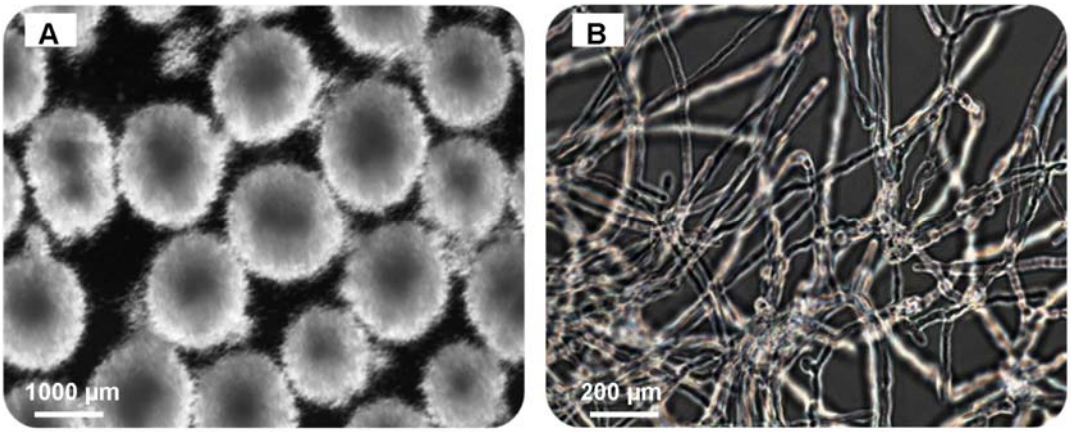

Figure 20: Characteristic morphologies of *Aspergillus niger* SKAn1015 after 72 h in submerged cultures (3 L bioreactor) depending on the pH-value. A : pellets (pH 5) and B : mycelia (pH 3) formed after 72 h.

The cell growth as well as the fructofuranosidase activity were significantly higher at pH-value of 5 compared to pH 3 (Figure 21A). At a pH-value of 5, cells grew as distinct pellets (Figure 20A) and a significant fructofuranosidase activity in the culture fluid could be determined after a lag phase of 18 h. The maximal activity (160 U/mL)

was occurred simultaneously with maximal biomass concentration (7.2 g/L) after a cultivation time of 100 h. In contrast, maximum fructofuranosidase activity with cells growing as mycelium (Figure 20B) (maximum biomass concentration, 5.4 g/L) at pH 3 was observed already at 50 h, but was low (18 U/mL) and, in addition, decreased again subsequently (Figure 21B). This indicated either degradation of the fructofuranosidase by protease activity or denaturation due to the low pH-value (Denison 2000; Mattern et al. 1992; O'Donnell et al. 2001). These results showed that the morphology and the release of fructofuranosidase from the cells were influenced by the pH-value of the culture medium. The pH of 3 provide the desired morphology, but low product titer due to enzyme instability, whereas also at pH 5 suboptimal pelleted forms was obtain probably limiting production.

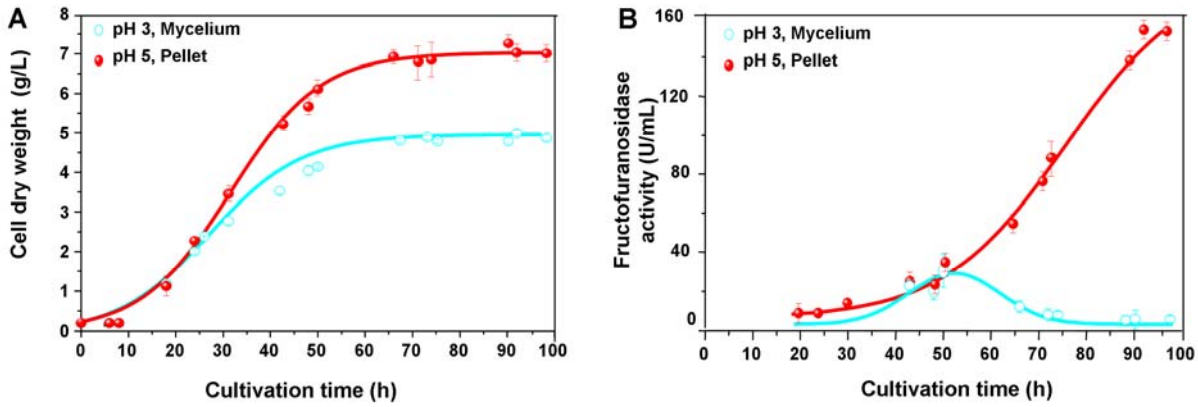

Figure 21: Time course of cell dry mass and fructofuranosidase activity during submerged cultivation of *A. niger* SKAn1015 in a 3 L bioreactor.

6.1.1.2 pH-shifting experiments to increase enzyme production

From the above experiments it seemed that the highest productivity for fructofuranosidase could be achieved with mycelium growing at pH 5. Due to this pH-shifting experiments were carried out. The results shown in Figure 22 clearly indicate that during the cultivation at pH 5 (either before a shift from pH 5 to pH 3 or after a shift from pH 3 to 5) the increase in the biomass concentration was significantly higher than in the respective cultivations of pH 3. When *A. niger* was grown at an initial pH of 5 with shift to 3 after 20 hours of cultivation pellets were formed and remained stable during the cultivation (Figure 20A). After 80 hours, glucose was completely consumed, but the biomass concentration and, in particular, the fructofuranosidase activity remained relatively low compared to cultivation at a

constant pH-value of 3 (Figure 22). In contrast, the pH-shift from 3 to 5 led to a 3.5-fold increase of fructofuranosidase activity (corresponding to 14 U/mL to 61 U/mL).

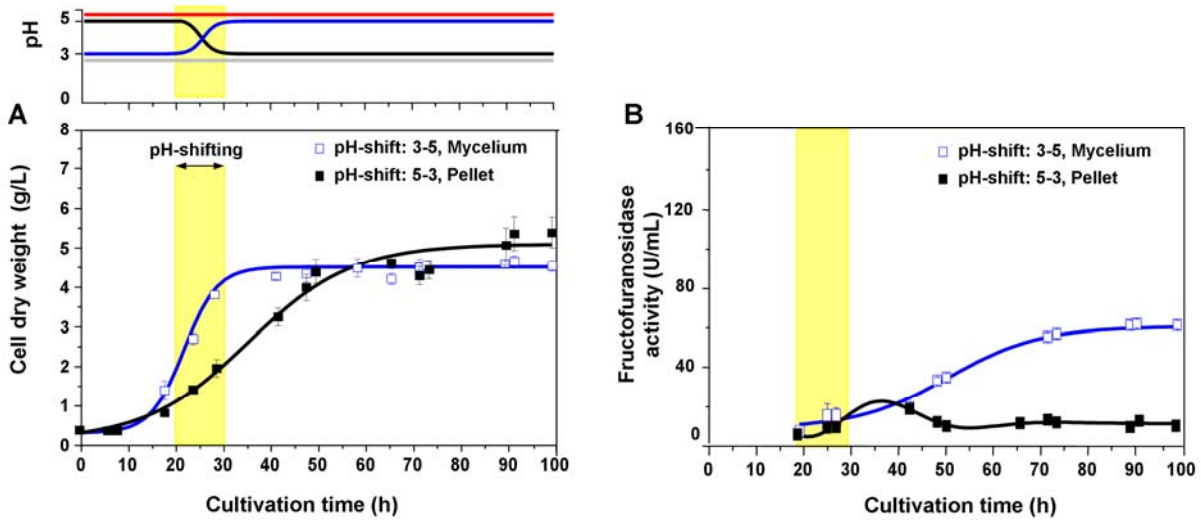

Figure 22: Time course of cell dry mass and fructofuranosidase activity during submerged cultivation of *A. niger* SKAn1015 in a 3 L bioreactor.

This result reveals that during a cultivation process at pH 3 the activity of fructofuranosidase was drastically inhibited even with pellet formation, whereas a high pH of 5 was always accompanied with a high fructofuranosidase activity. However, a shift from pH 3 to pH 5 could not generate the same high fructofuranosidase activity compared to the fructofuranosidase activity at a constant pH-value of 5. Therefore, the results show that the morphology and the fructofuranosidase production basically depend on the initial pH-value during the cultivation of *A. niger* SKAn1015. The fructofuranosidase production at an initial and constant pH-value of 5 was approximately 12-fold that obtained at a constant value of pH 3, and 3.5-fold than that found with an initial pH of 3 and a subsequent pH-shifting from 3 to 5, suggesting the pellet form is more suitable for fructofuranosidase production. The best (or favoured) morphology for fructofuranosidase production was the fluffy and loose pellet form. The final biomass concentration at pH 5 was significantly higher than that in the cultivation at pH 3, although the consumption of the substrate glucose was almost the same in both experiments.

Therefore, the lower biomass yield at the higher pH-value could not be explained by a higher production of undesired by-product such as oxalate (Andersen et al. 2009;

Magnuson and Lasure 2004; Pedersen et al. 2000b; Ruijter et al. 1999). *A. niger* is a well known organism for its ability to accumulate various organic acids, among which oxalate was found at the highest concentration in this work. Other extracellular metabolites such as organic acids (formate, acetate, butyrate, gluconate) and polyols (mannitol, erytrithol, glycerol) were released in the medium only in insignificant amounts at pH-value 5 (data not shown here). The type and amount of acid which is actually formed is mainly controlled by the pH-value of the culture medium (Andersen et al. 2009). For example at a constant pH of 5, oxalate was produced in large amounts (3.2 g/L, see Figure 23), whereas the production of unwanted organic acids as by-product was avoided at a constant pH-value of 3, but also the yield of fructofuranosidasein the culture medium was low due to high protease activity or the denaturation effects (see above).

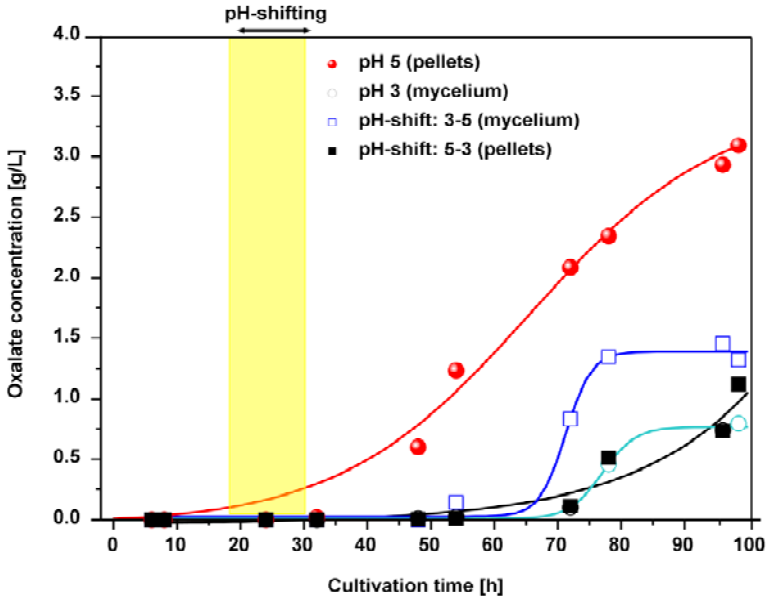

Figure 23: Oxalate as by-product by *Aspergillus niger* SKAn1015

However, as indicated by Figure 23, the highest concentrations of oxalate were found at a continuous pH-value of 5 or at a pH-shift from 3 to 5, both conditions which were also found to be suitable for fructofuranosidase production or activity. The accumulation of oxalate seems to fit the general strategy of *A. niger* to acidify its environment, e.g. to repress competitive microorganisms, to help to degrade plant cell walls, and to (re)-dissolve essential trace metals to make them bioavailable. A variety of fungi including phytopathogenic species produce oxalate (Dutton and Evans 1996), and in particular, *A. niger* is known as a very efficient oxalate producer.

6.1.2 Micro particle material screening

6.1.2.1 Effect on fungal morphology and productivity

Based on the unsatisfying performance of the classically pH-shift experiment, a novel strategy was now investigated; employ inorganic micro particles to influence morphology. Towards a superior morphology for recombinant protein production in *A. niger* a broad micro particle screening was initially performed.

Overall, 15 different materials were tested in amounts up to 50 g/L for their potential to influence growth, morphology and fructofuranosidase production by *A. niger*. This included talc ($3MgO\ 4SiO_2 \cdot H_2O$, hydrous magnesium silicate) and alumina (Al_2O_3, >64% as Al_2O_3, aluminum oxide hydrate) previously described (Driouch et al. 2011; Driouch et al. 2010b; Kaup et al. 2007) to improve production by *A. niger* and a series of so far not considered micro powders. The obtained results are summarized as heat map in Figure 24. The micro particles caused quite diverse effects. Most of the materials enhanced production significantly as compared to the control (Figure 24A). The highest improvement of fructofuranosidase production resulted for titanate (titanium silicate oxide, $TiSiO_4$, 8 µm). Among all materials and conditions tested, the highest enzyme production (150 U/mL) was achieved after addition of 25 g/L titanate (Figure 24A). As compared to the control (41 U/mL) the enzyme level was enhanced more than 3.5 fold. In addition, also alumina and talc and to a lower extent iron oxide, iron nickel oxide and silica improved production.

Other materials even caused negative effects and reduced production. It was interesting to note that the beneficial materials were all found rather effective to create small pellets or even free mycelia in comparison to rather large pellets in the control (Figure 24B). However, such morphology did not automatically lead to high production as observed e.g. for nanoclay, suggesting a rather complex relationship between the micro particles and the metabolic properties of the fungus. Most strikingly, a number of particles increased cell (Figure 24C).

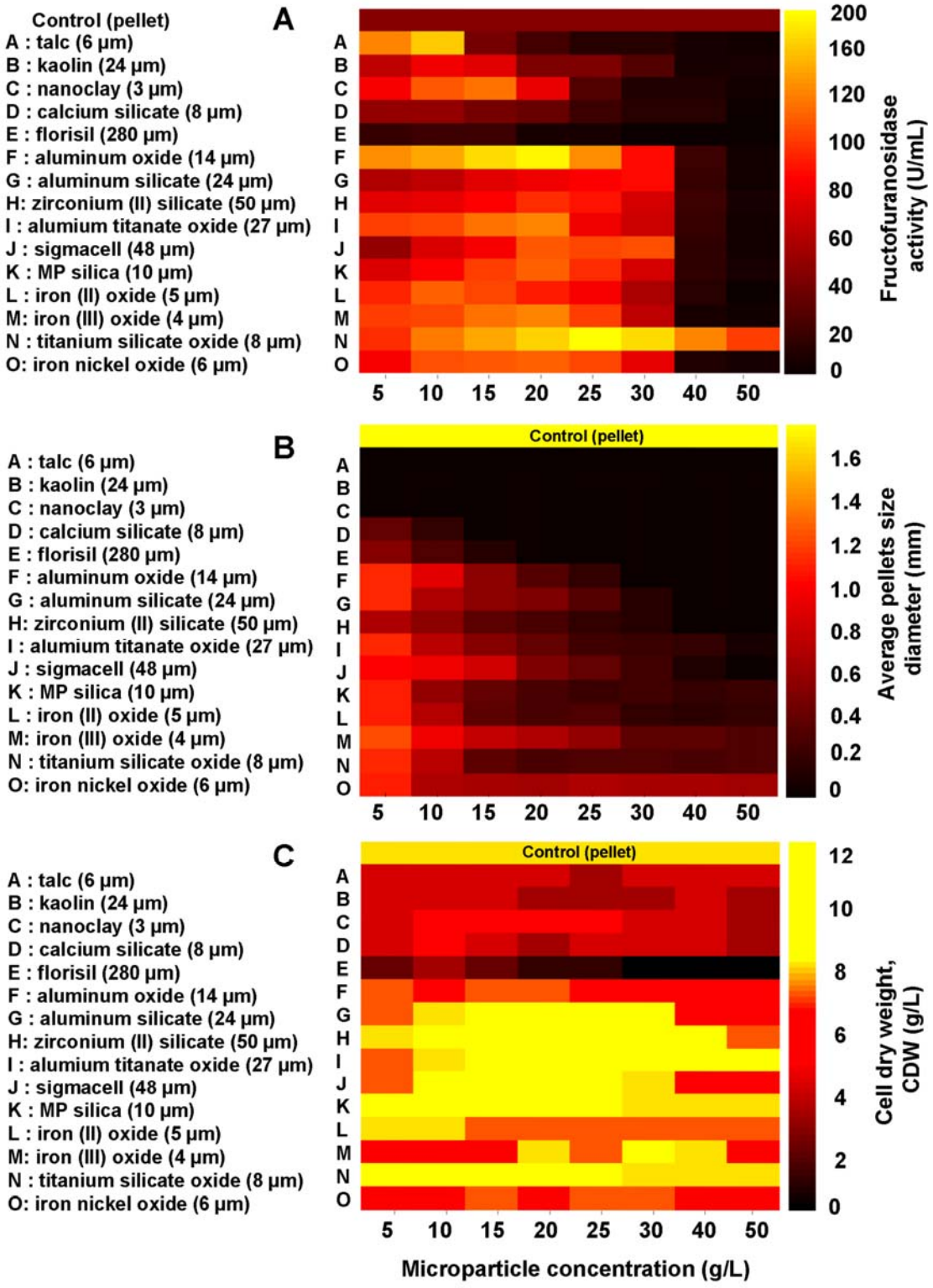

Figure 24: Micro particle screening of *Aspergillus niger* SKAn1015 cultures for fructofuranosidase activity (A), pellet diameter (B) and growth (C) comparing various materials. The data given comprise the average of three replicates each for the time point after 72 h of cultivation. All cultures were carried out in 250 mL shake flask cultures. The impact of each micro material is visualized by a heat map.

Obviously, for each material a specific optimum concentration resulted. Further increase obviously exposed the fungus to stress resulting in lower biomass and enzyme yield. All micro particles used in this work are obtained as commercial dry powder (diameter has been given in mesh-unit) from Sigma-Aldrich (Seelze, Germany) and MP Biomedicals (Eschwege, Germany). The morphology structure of micro particles is a landscape not clearly visualized by light microscopy. Many micro particles elaborate protrusive structures such lamellipodia, and surface ruffles that play important roles in the interaction between the microparticles and the cells (Figure 25).

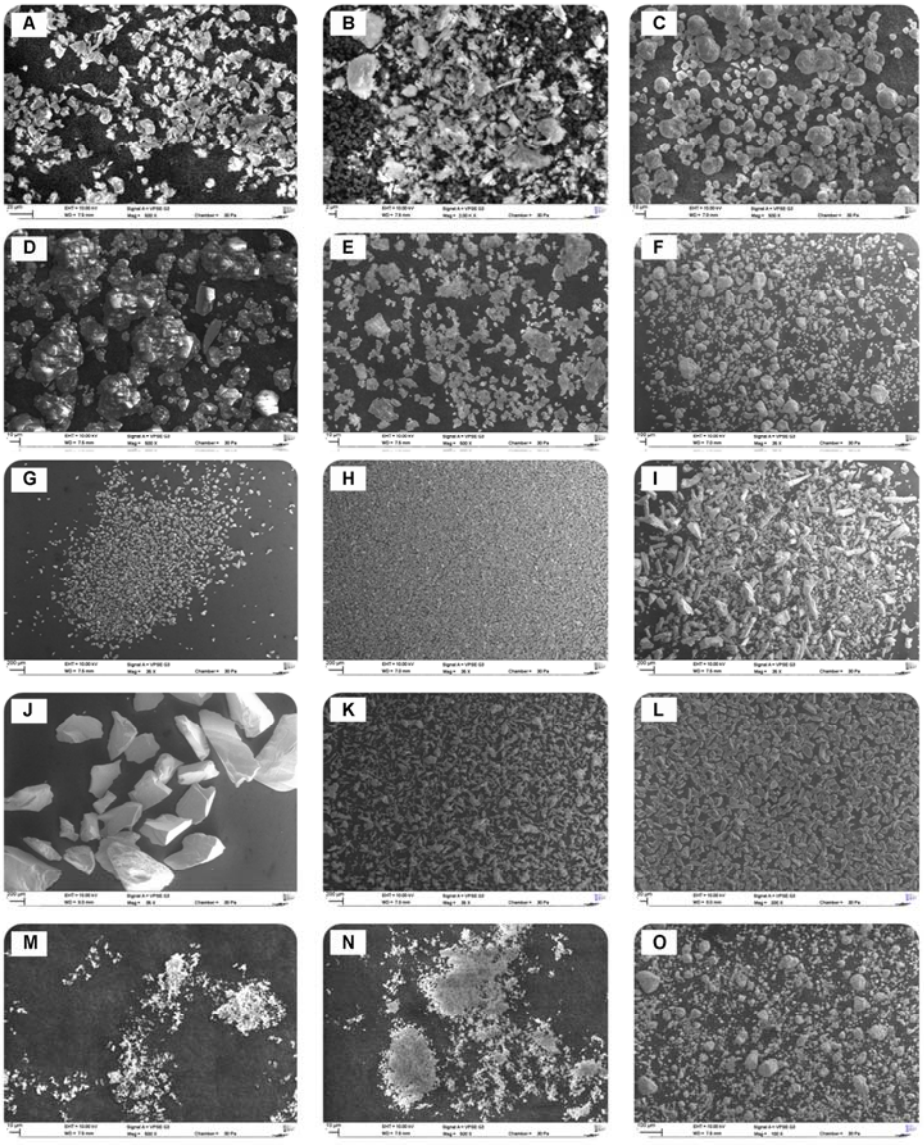

Figure 25: Microphotographs of surface morphology of different micro particles used in this work by SEM. (A : talc (6 µm), B : kaolin (24 µm), C : nanoclay (3 µm), D : aluminum oxide (14 µm), E : calcium silicate (8 µm), F : aluminum silicate (8 µm), G : alumium titanate oxide (27 µm), H : titanium silicate oxide (24 µm), I : zirconium (II) silicate (50 µm), J : florisil (280 µm), K : sigmacell (48 µm), L : MP silica (10 µm), M : iron (II) oxide (5 µm), N: iron (III) oxide (4 µm), O : iron nickel oxide (6 µm).

The high resolution of SEM makes it an ideal technique for studies of the particles surface; however, preservation of fine surface structure can be problematic. The results are summarized in Table 5. Figure 25 show the micrographs of surface morphology by scanning electron microscopy (SEM) taken from the samples of various particles investigated in this work and confirmed additionally the size diameter distribution of micro particles determined by particle size analysis.

The most promising micro material, i.e. talc, alumina and titanate (Figure 26) were now selected for further investigation towards optimization protein production in different strains of *A. niger.*

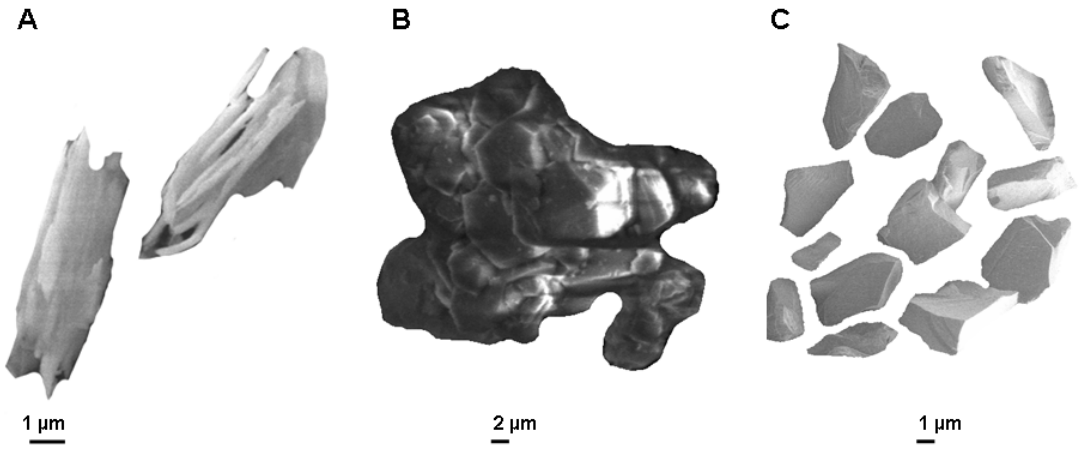

Figure 26: Surface morphology of the selected micro particles for further investigation (A : Talc, 6 µm, B : alumina, 14 µm and C : titanate, 8 µm).

6.1.3 Tailor-made fungal morphology

In a pioneering study, the use of inorganic micro particles added to the culture was recently introduced to influence fungal morphology (Kaup et al. 2007). As shown for *Caldariomyces fumago*, the addition of micro particles consisting of aluminum oxide or hydrous magnesium silicate caused a dispersion of the cells up to the level of single hyphae and enhanced chloroperoxidase production.

The authors observed that micro particles influence the morphology also of other filamentous fungi suggesting that intentional supplementation to the culture might generally stimulate growth of these organisms. Among filamentous fungi, *A. niger* is important as the major world source of citric acid and higher-value enzyme products including pectinases, proteases, amyloglucosidases, cellulases, hemicellulases, and lipases (Jones 2007). For *Aspergillus* species, dispersed mycelial suspensions often lead to higher product yield and are thus preferred over the pelleted form (Gibbs et al. 2000). In this regard the present work now focussed on the use of micro particles for the control of morphology in different strains of *A. niger* producing the recombinant enzymes ß-fructofuranosidase (EC 3.2.1.26) and glucoamylase (GA) (EC 3.2.1.3).

In the presence of silicate-based microparticles the resulting morphology of *A. niger* was studied at different particle diameter and concentration using image analysis. This screening allowed identifying optimum conditions with respect to production performance which could then be utilized to significantly optimize protein production. Using a mutant, co-expressing glucoamylase and GFP (green fluorescent protein) under control of the same promoter, the effects of micro particles on the spatial distribution of protein production in the cellular aggregates formed could be visualized for the first time providing a detailed picture of the strongly altered underlying metabolism in *A. niger*.

6.1.3.1 Influence of talc micro particles on morphology

In an initial study, the impact of talc micro particles (6 µm) on the morphology was studied in shake flask culture. Without addition of the talc powder, *A. niger* formed mycelial clumps growing to an average diameter of 1.7 ± 0.1 mm (Figure 27A).

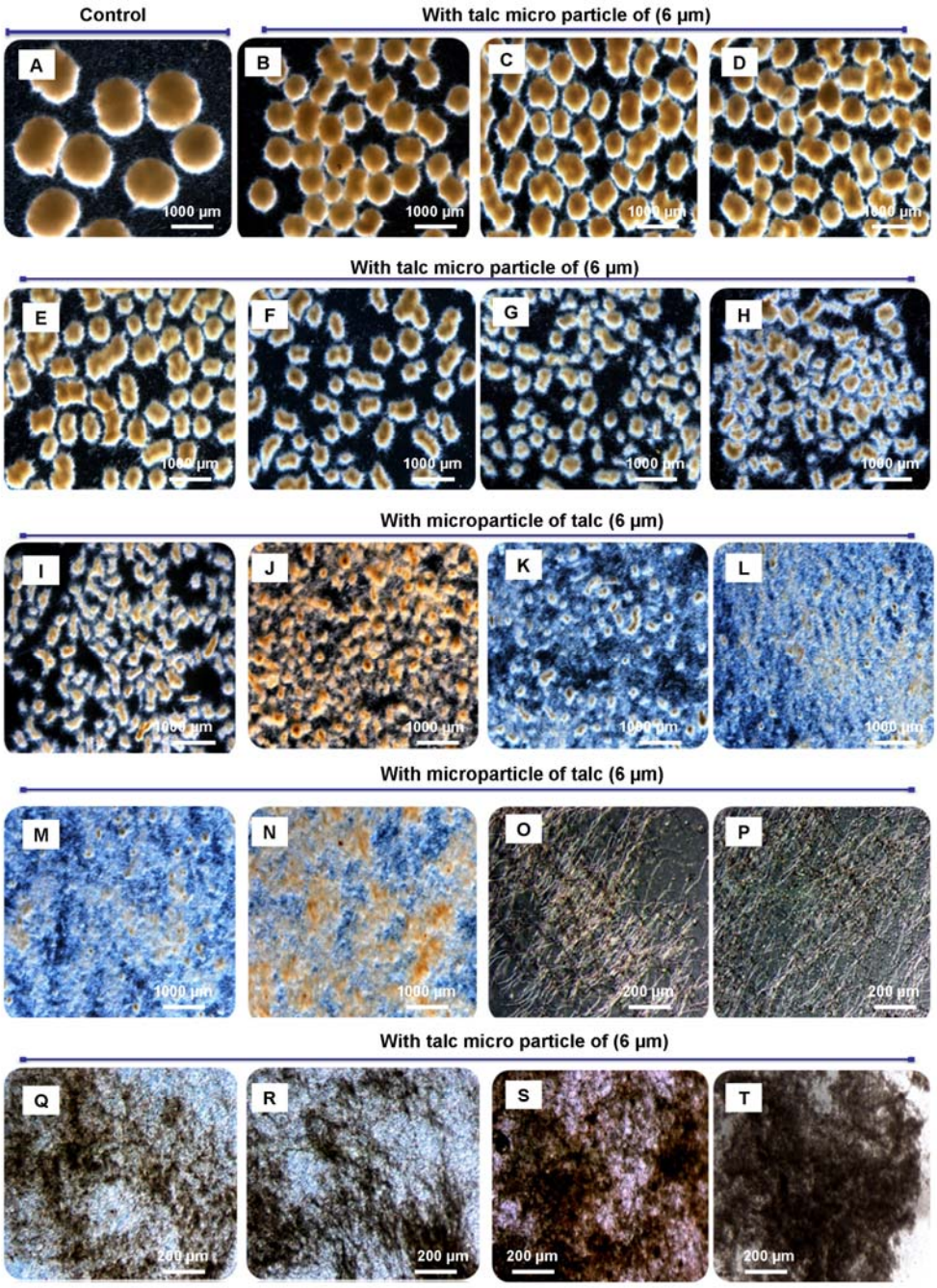

Figure 27: Morphology engineering of *Aspergillus niger* SKAn1015 by micro particle supplementation in submerged culture. Hydrous magnesium silicate (6 µm particle size) was added at varied concentration: control without talc (A), 10 mg/L (B), 0.1 g/L (C), 0.2 g/L (D), 0.3 g/L (E), 0.6 g/L (F), 1.0 g/L (G), 1.5 g/L (H), 2.0 g/L (I), 2.5 g/L (J), 3.0 g/L (K), 3.5 g/L (L), 4.0 g/L (M), 4.5 g/L (N), 5.0 g/L (O), 10 g/L (P), 15 g/L (Q), 20 g/L (R), 30 g/L (S) and 40-50 g/L (T). Image analysis was performed by light microscopy after 72 h of cultivation.

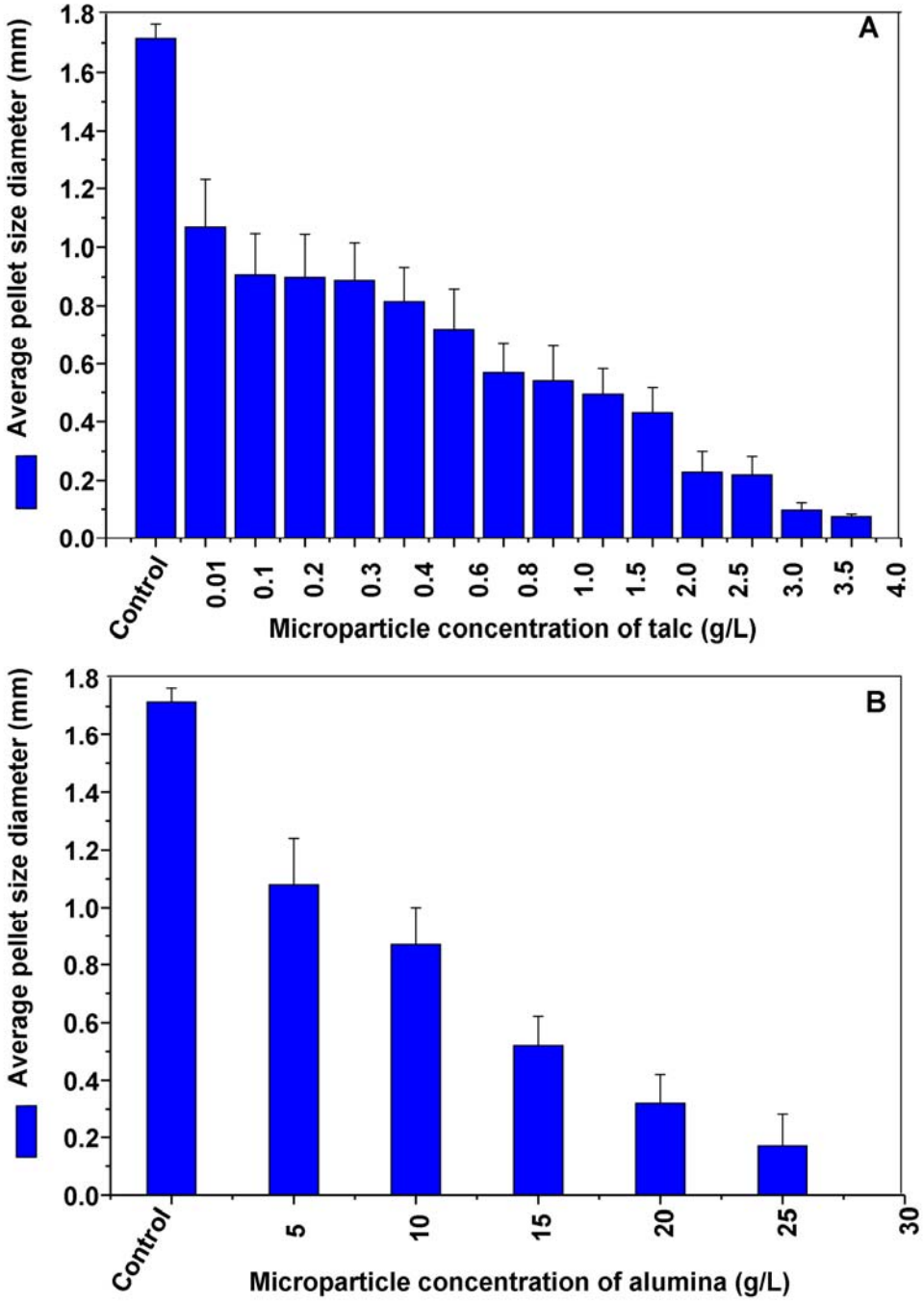

Figure 28: Design of a defined pellet size for *Aspergillus niger* SKAn1015 in submerged culture by addition of hydrous magnesium silicate micro particles (A) and aluminium oxide micro particles (B) at different concentrations. The pellet size was determined via image analysis of 100 pellets each by light microscopy after 72 h of cultivation.

In the presence of micro particles the morphology was strongly changed. Hereby, the properties of the added material obviously played an important role with respect to the resulting morphology. By variation of the size as well as the concentration of the

micro particles, a number of distinct morphological forms could be reproducibly created. With increasing particle concentration this ranged from the large pellets, formed in the control, via various smaller pellet forms with decreased size to freely dispersed mycelium (Figure 27B-T). Depending on the exact amount of the talc micro particles, a defined pellet size could be precisely adjusted, revealing the addition of micro particles as highly useful tool for defined morphology engineering of *A. niger* (Figure 28A). Moreover, also the particle size had an effect, whereby the most pronounced effects on morphology were attributed to the smallest particles. As an example, freely dispersed mycelium was formed for the 6 µm particles, whereas the only slightly larger material with 15 µm size resulted in small pellets (both at a concentration of 10 g/L). Particles based on aluminum oxide similarly affected also on morphology and allowed to precisely design the morphological shape of the cells. Increasing the concentration of aluminum oxide particles fungal pellets of decreasing size up to free mycelium were formed (Figure 29). Interestingly, more particles were required to achieve certain morphology as compared to the talc (6 µm) material (Figure 28B). This might be partly due to the larger particle size of alumina (14 µm).

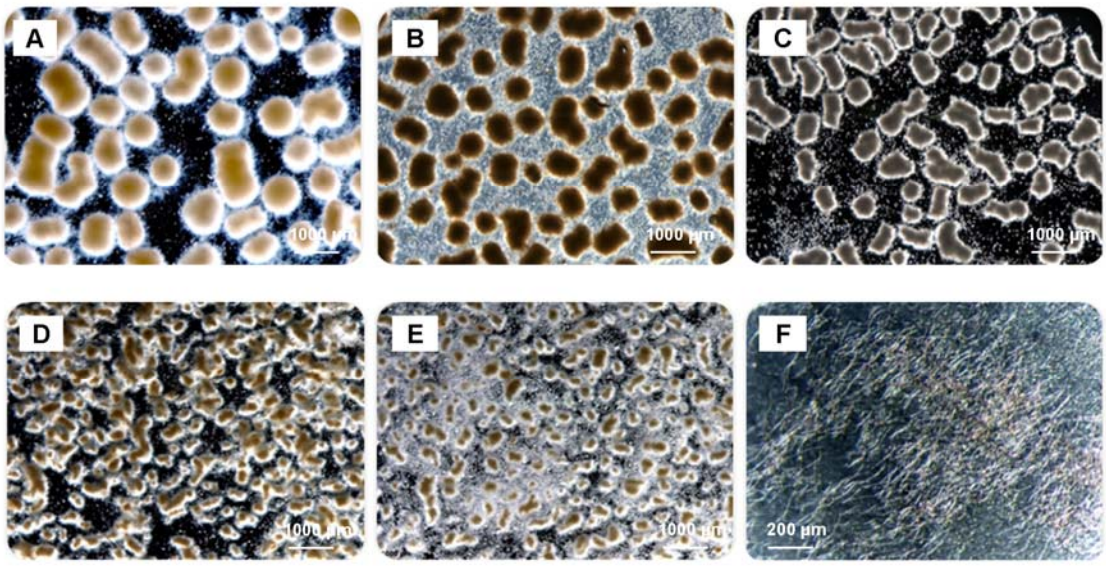

Figure 29: Morphology engineering of *Aspergillus niger* SKAn1015 by micro particle supplementation in submerged culture. Aluminum oxide (alumina, 14 µm particle size) was added at varied concentration: 5 g/L (A), 10 g/L (B), 15 g/L (C), 20 g/L (D), 25 g/L (E), and 30 g/L (F). Image analysis was performed by light microscopy after 72 h of cultivation.

6.1.3.2 Mechanism of interaction between micro particles and fungal cells

To get a further insight into the underlying mechanism of interaction between the micro particles and the cells, the morphological development of *A. niger* was monitored at different time points during the cultivation (Figure 30).

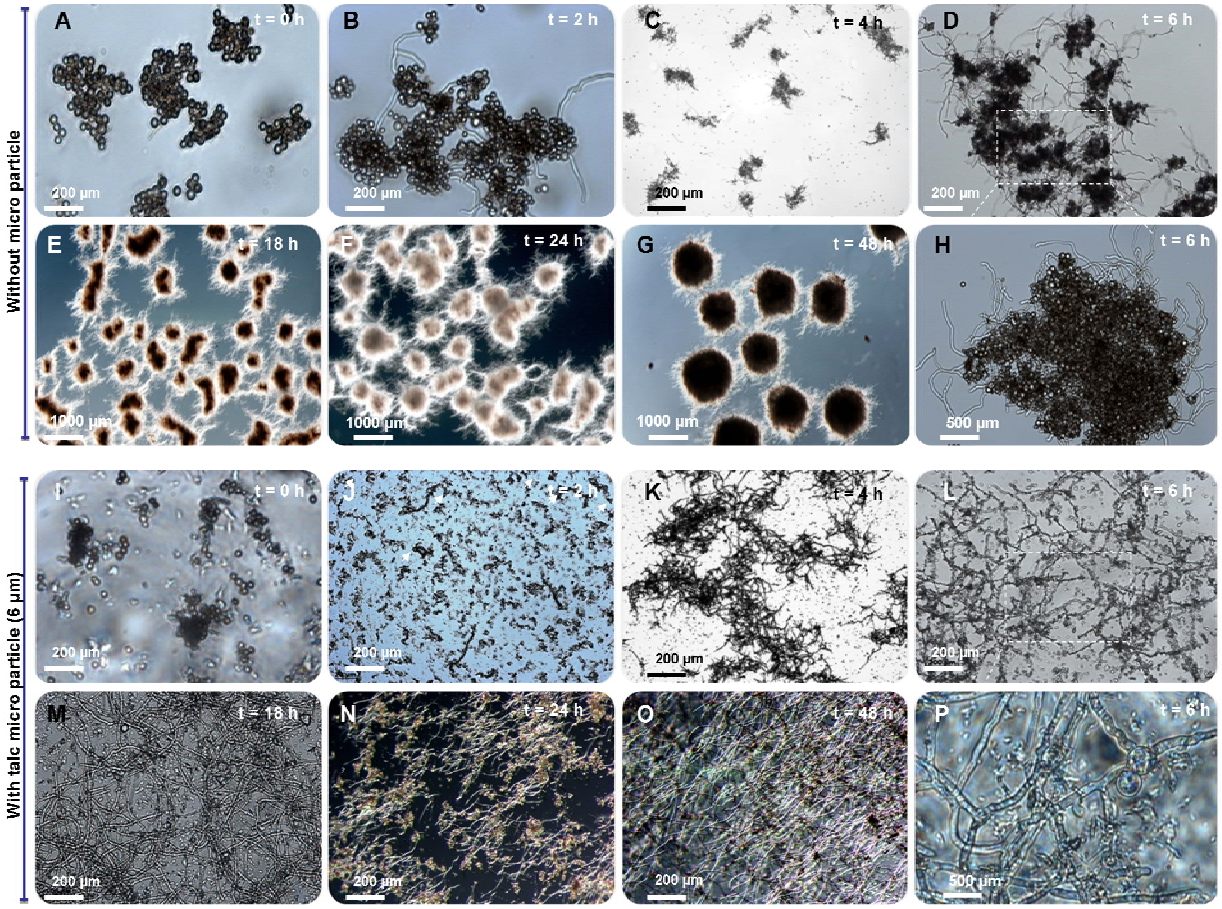

Figure 30: Influence of micro particle supplementation on morphological development of *Aspergillus niger* SKAn1015 in submerged culture after inoculation with spores. The pictures display the resulting morphology at different time points without particles (A-H) and with 10 g/L hydrous magnesium silicate micro particles (6 µm particle size) added to the culture prior to inoculation (I-P). Hereby, figures D and P display detailed views with higher magnification from the corresponding time of 6 h of cultivation. The arrows in subfigure J mark single spores which have partly germinated.

At the beginning, the spores were mainly present as large aggregates in both cultivations (Figure 30A-I). This conidia aggregation is typically observed in fungal submerged cultures. In the control culture these large agglomerates were then maintained during the following hours. Packed within these structures the

agglomerated conidia then germinated (Figure 30B), which further grew into large solid pellets of almost equal size obtained after 18 h (Figure 30C-H). This picture was completely changed when the talc material was present. Here, the initially present large spore agglomerates quickly disappeared. Already after 2 h mainly individual spores were present in the culture when the germination started (Figure 30J).

This resulted in a loosely mycelium later on (Figure 30K-P). Obviously, the micro particles disturbed the initial phase of spore aggregation which seems the major reason for the altered morphology. This was confirmed by the fact the morphology of *A. niger* was not changed as compared to the control when the micro particles were added at later stages of the cultivation (12 and 18 h). Possible interactions between spores and micro particles, causing the observed effects, could involve physical or chemical mechanisms. *A. niger* growing in medium that had been preincubated for 4 h with talc micro particles (5 g/L, 6 µm) followed by removal of the particles prior to inoculation formed pellets which had the same size than that in the control. Vice versa, the pre-incubated and potentially washed particles led to freely dispersed mycelium. From this, coating of the hydrophobic spores with talc chemicals potentially released from the particles does not appear as mainly responsible mechanism disallowing aggregation.

Microscopic studies further demonstrated that the main effect of micro particles lies in interference with the aggregation of conidia during the initial phase which determines the subsequent pellet size in fungal cultivations (Nielsen 1996). These obviously destroyed the initially present large aggregates and also reduced the formation of new aggregates. Thus mainly individual spores resulted in the presence of micro particles. Since this effect was also observed for aluminum-oxide-based micro particles, the chemical properties of the material seem not of major importance. We therefore conclude that a major role of micro particles in changing the morphology is based on a physical phenomenon and involves collision-induced aggregate disruption and probably also the hindrance of new spore–spore interactions as similarly suggested for hyphal inocula (Kaup et al. 2007). At this point, chemical interactions can, however, not be completely excluded as mechanism involved.

6.1.3.3 Production performance for different recombinant proteins

As shown above, the use of micro particles specifically allowed engineering of the morphology of *A. niger.* It was now interesting to see their impact on the production of industrially relevant enzymes by this filamentous fungus. For this purpose, three recombinant strains of *A. niger* which differed in the target enzyme as well as the genetic control of production were investigated. The strain SKAn1015 secretes fructofuranosidase as extracellular product into the broth under control of a constitutive promoter, whereby the strain AB1.13 accumulates glucoamylase as intracellular enzyme under control of an inducible promoter. *A. niger* ARAn701 co-expresses glucoamylase with a variant of GFP. All strains were cultured in shake flasks with and without particles. For *A. niger* SKAn1015, maximum fructofuranosidase activity in the supernatant, obtained after 72 h, was doubled by intentional addition of themicro particles (Figure 31A). This enhanced production was linked to a 50% decrease in pellet size as compared to the control. The formation of biomass, however, was only slightly affected holding both for the specific growth rate or the final biomass concentration. Interestingly, the presence of the micro particles strongly reduced the formation of oxalate as undesired by-product (Table 8).

Table 8: Influence of magnesium silicate micro particle supplementation (10 g/L) on enzyme production and by-product formation shake flask culture of *Aspergillus niger.*

	Specific activity (U/mgDW)		Oxalate (g/L)	
Morphology	**Pellet**	**Mycelium**	**Pellet**	**Mycelium**
Micro particles supplementation	**-**	**+**	**-**	**+**
***A. niger* AB1.13**	2.1±0.3	11.0±0.9	3.0	0.2
***A. niger* ARAn701**	1.9±0.2	9.3±0.3	3.4	0.9

The data given represent the final values for the three recombinant strains *Aspergillus niger* AB1.13 (glucoamylase), ARAn701 (glucoamylase), and SKAn1015 (fructofuranosidase) obtained after 72 h from three replicates for each strain. Data given represent the micro particle-enhanced cultures (+) and the control cultures without addition (-).

The stimulating effect by the talc particles was even more pronounced for glucoamylase production. *A. niger* AB1.13 was grown first on xylose. After 40 h of cultivation maltose was added to induce the glucoamylase production under control of the *gla*A promoter (Figure 31B). The final glucoamylase activity was increased

almost fourfold in the presence of the micro particles (61 U/mL) as compared to the control (17 U/mL).

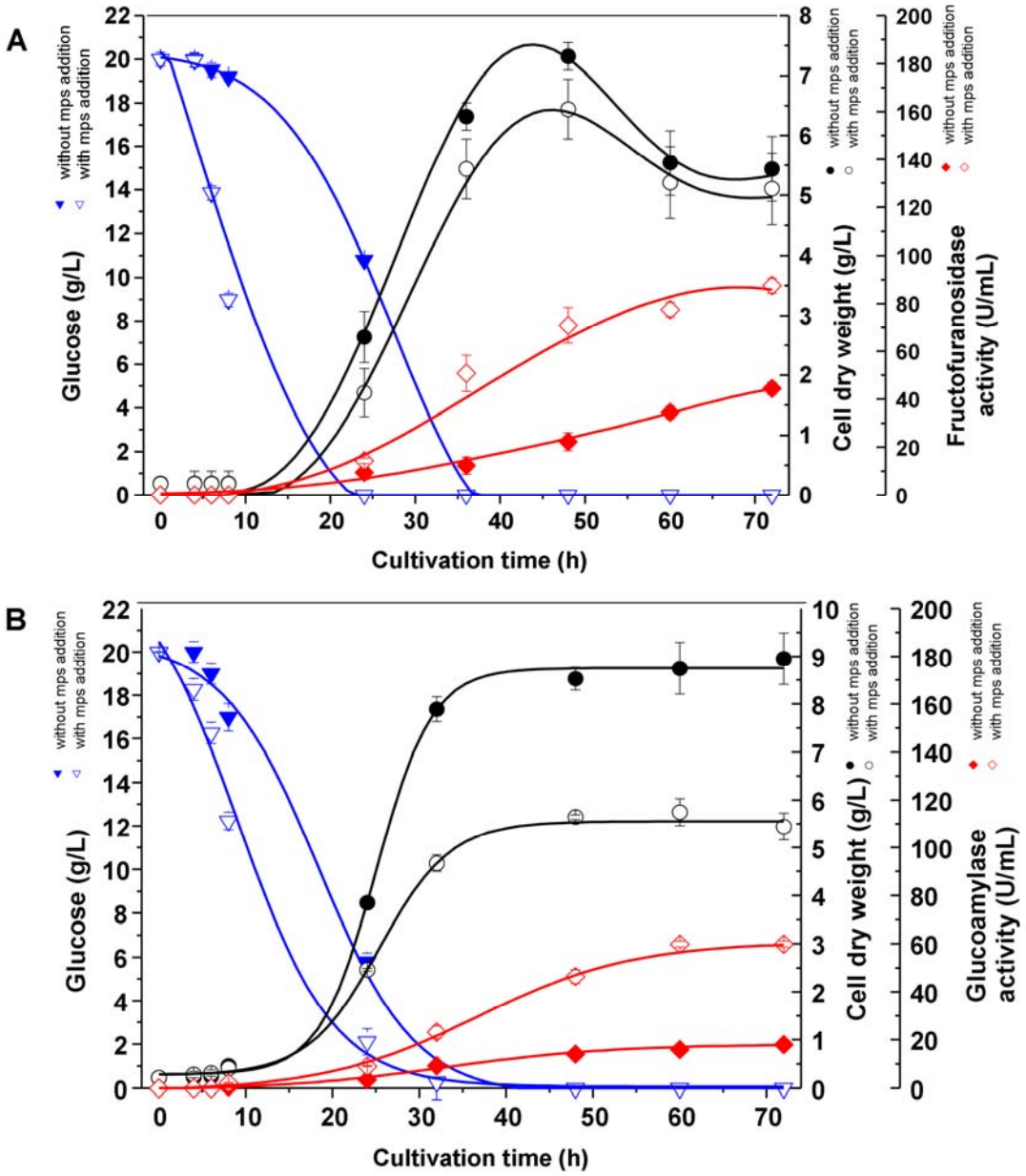

Figure 31: Influence of micro particle supplementation on growth and enzyme production characteristics in shake flask culture of *Aspergillus niger*. The data given are time profiles of fructofuranosidase activity and growth (A) of *A. niger* SKAn1015 as well as glucoamylase activity and growth of *A. niger* AB1.13 (B). Open symbols reflect cultures with supplemented talc micro particles (10 g/L, 15 mm). Solid symbols reflect control cultures without addition. Data given represent mean values and deviations from three replicates for each strain.

Interestingly, the opposite was observed for the formation of biomass, which was reduced by the added material from 9.0 g/L in the control culture to 5.5 g/L. Moreover, oxalate formation was significantly reduced (Table 8). Thus, the addition of

the micro particles specifically stimulated the formation of the desired product, which appears favorable for an industrial process. Accordingly, the specific glucoamylase activity obtained (11.0 U/mgDW vs. 2.1 U/mgDW) was substantially higher. Similar results were obtained for the related strain *A. niger* ARAn701 which also exhibited an increased production of glucoamylase and a reduced oxalate secretion in the presence of micro particles (Table 8). At this stage, one can conclude that the addition of micro particles to cultures of *A. niger* seems generally beneficial for the production of enzymes, whereby this holds for excreted as well as for intracellular products and also include constitutive as well as induced expression systems.

6.1.3.4 Spatial resolution of recombinant protein production in *A. niger*

Obviously, the micro particles specifically enhanced production of the target enzyme. Since this is a remarkable observation with respect to the biotechnological potential of *A. niger*, the origin of the enhanced production was investigated in more detail. The biomass of filamentous fungi is typically rather heterogeneous. Therefore, the extent of enzyme synthesis was spatially resolved across the different zones of the heterogeneous mycelial aggregates formed in the presence or absence of micro particles. This allowed identifying the biomass fractions actively involved in product formation. For this purpose, *A. niger* ARAn701 was applied. It co-expresses glucoamylase together with a variant of the GFP2 under control of the same promoter.

GFP expression via fluorescence intensity was localized in 70 µm thin cross-sections through the biomass aggregates obtained from cultures with and without micro particles. Figure 32A shows fluorescence intensity across a pellet of *A. niger* ARAn701 with about 1 mm diameter formed without addition of micro particles. Clearly, protein production was highest within a thin layer of about 75 µm thickness at the pellet surface. Inside the pellet, fluorescence was reduced but still visible with the exception of the inner core of about 500 µm which did not exhibit fluorescence (Figure 32).

This indicated that only a small fraction of the entire biomass is contributing significantly to product formation. The inner zones of the pellet were obviously reduced in production which is likely caused by diffusion limitation of oxygen or of

other nutrient typically associated with mycelial clumps. For loosely, dispersed mycelium formed upon addition of the micro particles, the picture looked completely different (Figure 32B). Intensive fluorescence was almost equally distributed across the entire biomass. This indicates that the interaction with micro particles created a highly active biocatalyst (Figure 33B-J). The enormously increased fraction of actively producing cells is a clear benefit as compared to normal pelleted culture

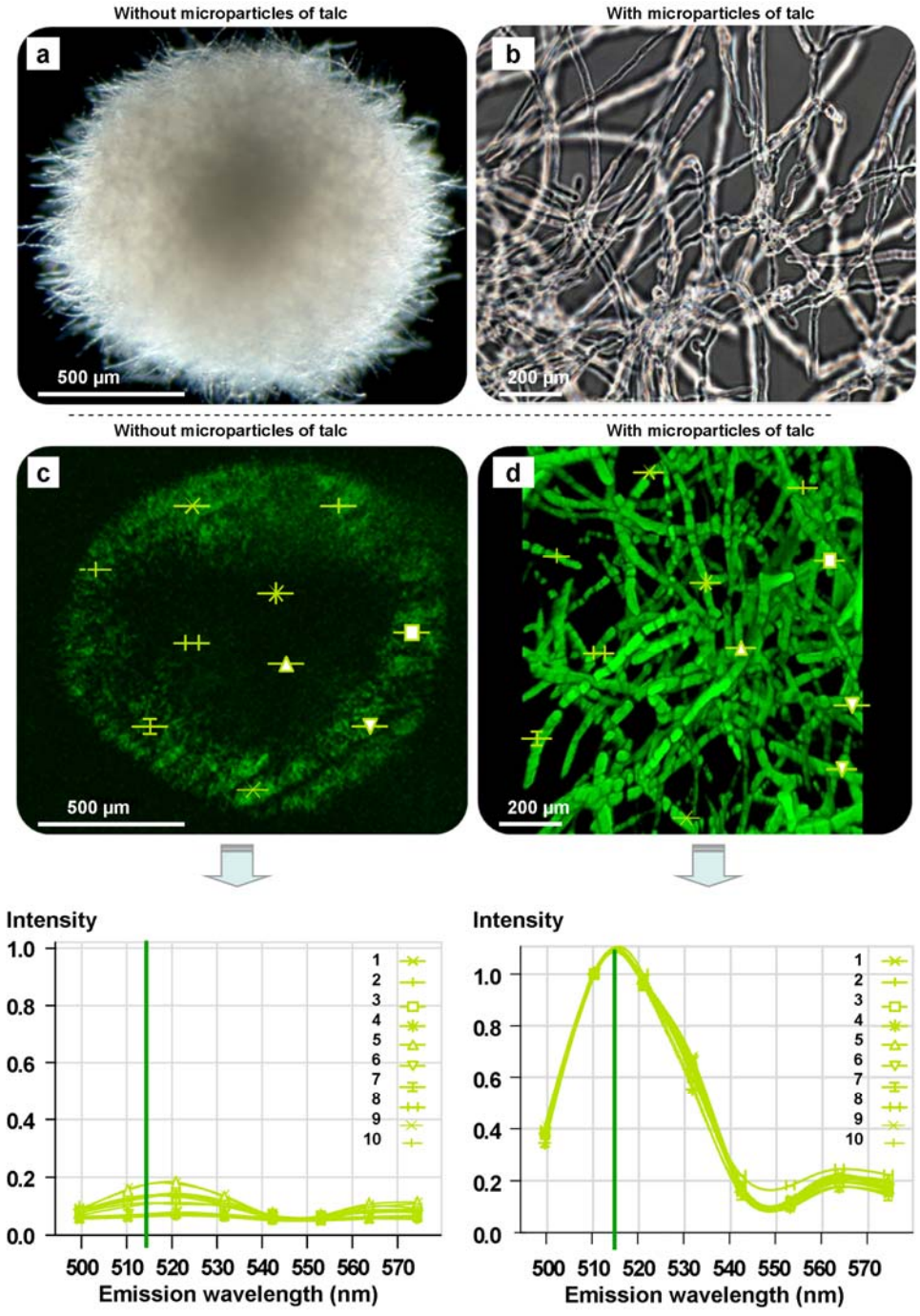

Figure 32: Spatial distribution of green fluorescent protein (GFP2) expression in *Aspergillus niger* ARAn701 pellets (A, control culture without micro particles) and

freely dispersed mycelium suspension (B, supplementation with talc micro particles, 10 g/L, 6 µm). The pictures were obtained by confocal laser scanning microscopy from 70 µm cross-sections through the corresponding cellular aggregates formed.

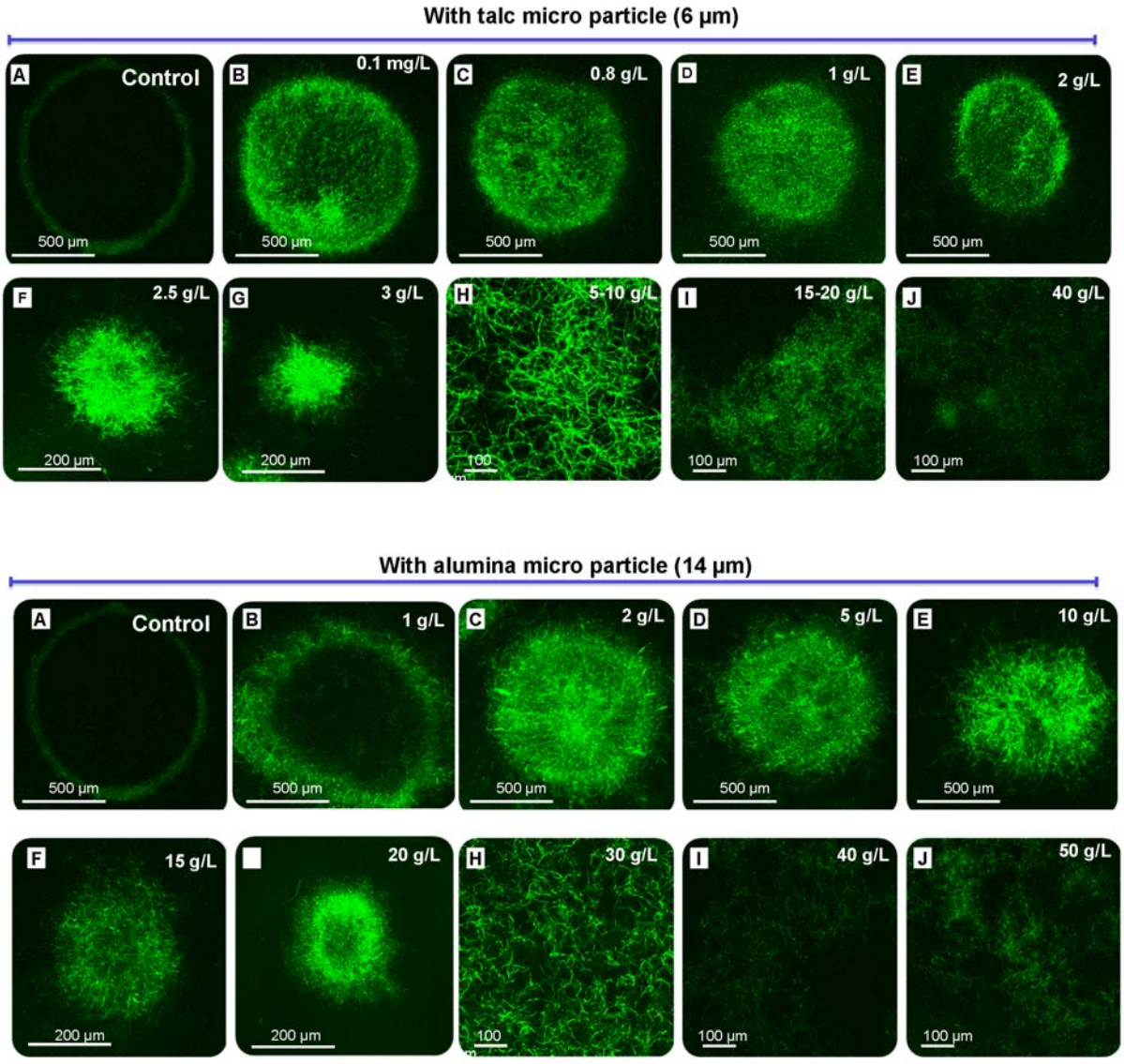

Figure 33: Spatial distribution of green fluorescent protein (GFP2) expression in *Aspergillus niger* ARAn701 pellets and freely dispersed mycelium by micro particle supplementation in submerged culture. Talc (Hydrous magnesium silicate, 6 µm particle size) was added at varied concentration: control without talc (A), 0.1 mg/L (B), 0.8 mg/L (C), 1 g/L (D), 2 g/L (E), 2.5 g/L (F), 3.0 g/L (G), 5-10 g/L (H), 15-20 g/L (I) and 40-50 g/L (I). Image analysis was performed by light microscopy after 72 h of cultivation. Aluminum oxide (14 µm particle size) was added at varied concentration: control culture without micro particles (A), 1 g/L (B), 2 g/L (C), 5 g/L (D), 10 g/L (E), 15 g/L (F), 20 g/L (G), 30 g/L (H), 40g/L (I) and 50 g/L (J). The pictures were obtained by confocal laser scanning microscopy from 70 µm cross-sections through the corresponding cellular aggregates formed.

6.1.3.5 Influence of particle concentration and size

Based on the above results the influence of size and concentration of the micro particles on production performance were investigated systematically. In comparative shake flask experiments with fructofuranosidase producing *A. niger* SKAn1015 the particle size was found to be an effective factor. An average diameter of 6 µm, reflecting the finest material tested, resulted in loosely mycelial growth and was found optimal for fructofuranosidase synthesis (Figure 34A). Already a slightly higher diameter of 15.2 µm resulted in a 35% reduced enzyme production, linked to a shift of morphology toward small size pellets. All cultures with micro particles, however, enabled significantly higher production than the control. For the optimum particle size of 6 µm, comparative experiments with varied concentration of the talc material in the range of 0–40 g/L were conducted. It turned out that also the particle concentration determines the production performance of *A. niger* to a large extent (Figure 34B).

Fructofuranosidase formation increased from 1 to 10 g/L particles. At 10 g/L, linked again to formation of freely dispersed mycelium, the highest fructofuranosidase activity of 135 U/mL was observed. At values exceeding 10 g/L, however, production collapsed to almost zero. This was linked to the formation of short mycelial fragments, indicating a negative effect of the particles in this high-concentration range. With increasing concentration of micro particles added the pellet size can be precisely decreased down to only small flocks and even freely dispersed mycelium. Hereby, the properties of the added material obviously play an important role.

For aluminium oxide (alumina), a higher concentration was required to achieve the same morphology as compared to talc. This might be attributed to the different particle size, expressed by the average diameter for talc (6 µm) and alumina (14 µm). Moreover, also the specific shape of the used particles is rather different, as illustrated by electron microscopy analysis (Figure 35A/B). At this point, it appears possible that the smooth, round-shaped alumina particles may have less impact to disrupt spore aggregates as compared to the sharp-edged silica particles. However, more detailed studies are necessary to really unravel the mechanisms of interaction between the fungus and the particles. For both materials, the production of fructofuranosidase exhibited an optimum (Figure 34), whereas the biomass formation was only slightly influenced (Figure 36).

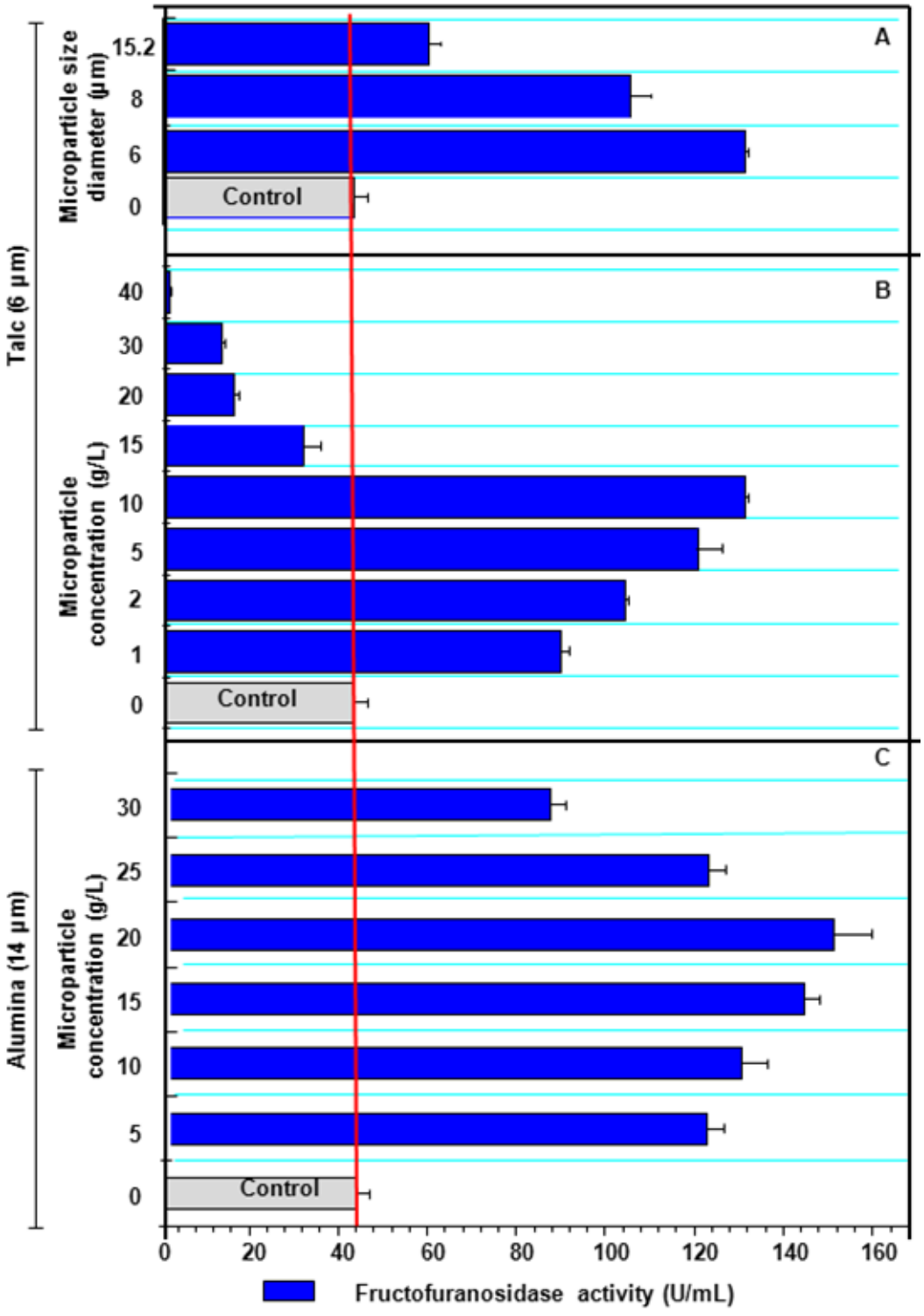

Figure 34: Fructofuranosidase activity in supernatant of *Aspergillus niger* SKAn1015 cultures at varied size of 10 g/L talc micro particles (A), varied concentration of 6 µm talc micro particles (B) and at varied concentration of 14 µm alumina micro particles (C).

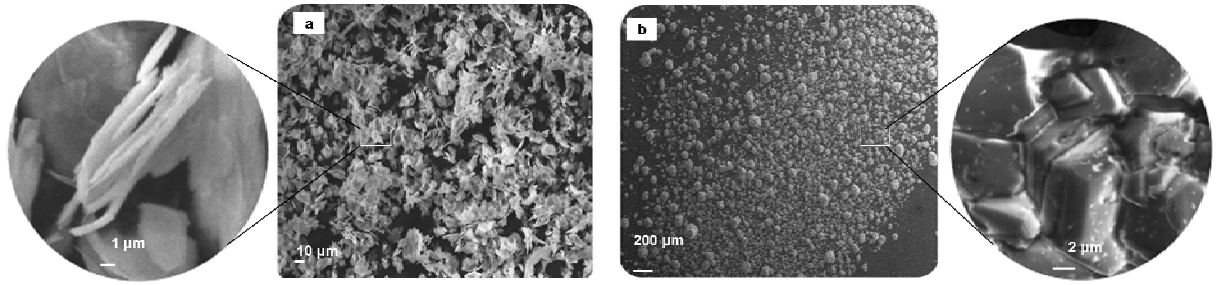

Figure 35: Structure of magnesium silicate (a: talc, 6 µm particle size) and aluminium oxide (b: alumina, 14 µm particle size) micro particles obtained by scanning electron microscopy.

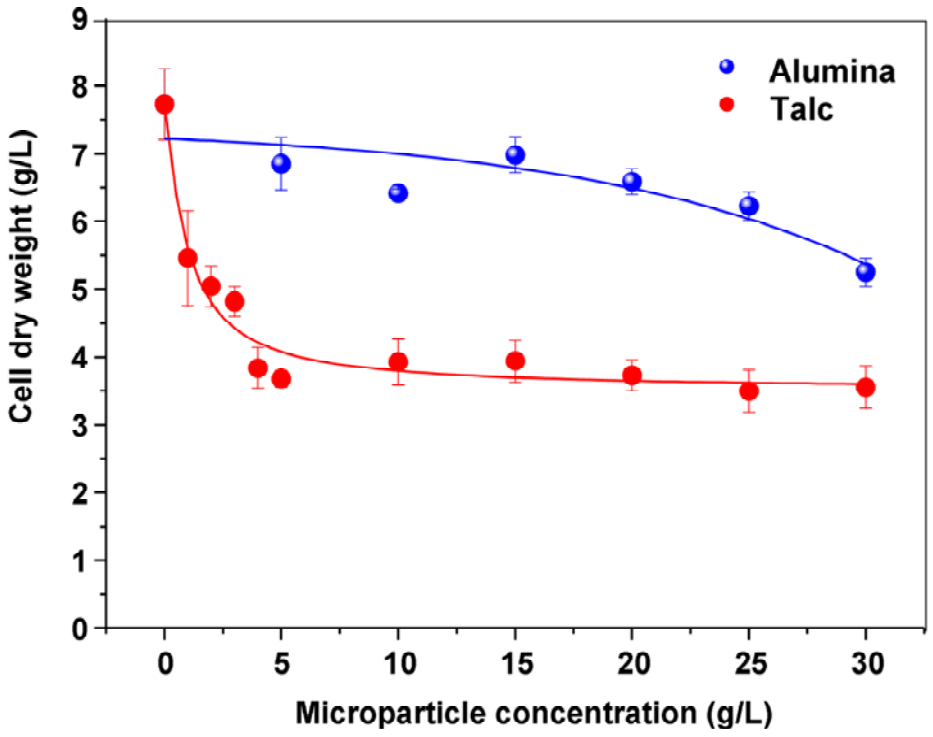

Figure 36: Influence of magnesium silicate (talc, 6 µm particle size) and aluminium oxide (alumina, 14 µm particle size) micro particles on the biomass by *Aspergillus niger* SKAn1015 in submerged culture.

6.1.3.6 Micro particle-enhanced batch-process

As shown above, volumetric activity of fructofuranosidase formed by *A. niger* SKAn1015 closely correlated with the morphology which could be adjusted appropriately through the addition of magnesium silicate micro particles. This was now utilized for production of fructofuranosidase in the bioreactor. Figure 37A-B display the time profile of the process run at pH 5.0 over 100 h in the presence of micro particles (6 µm, 10 g/L) or without addition (control).

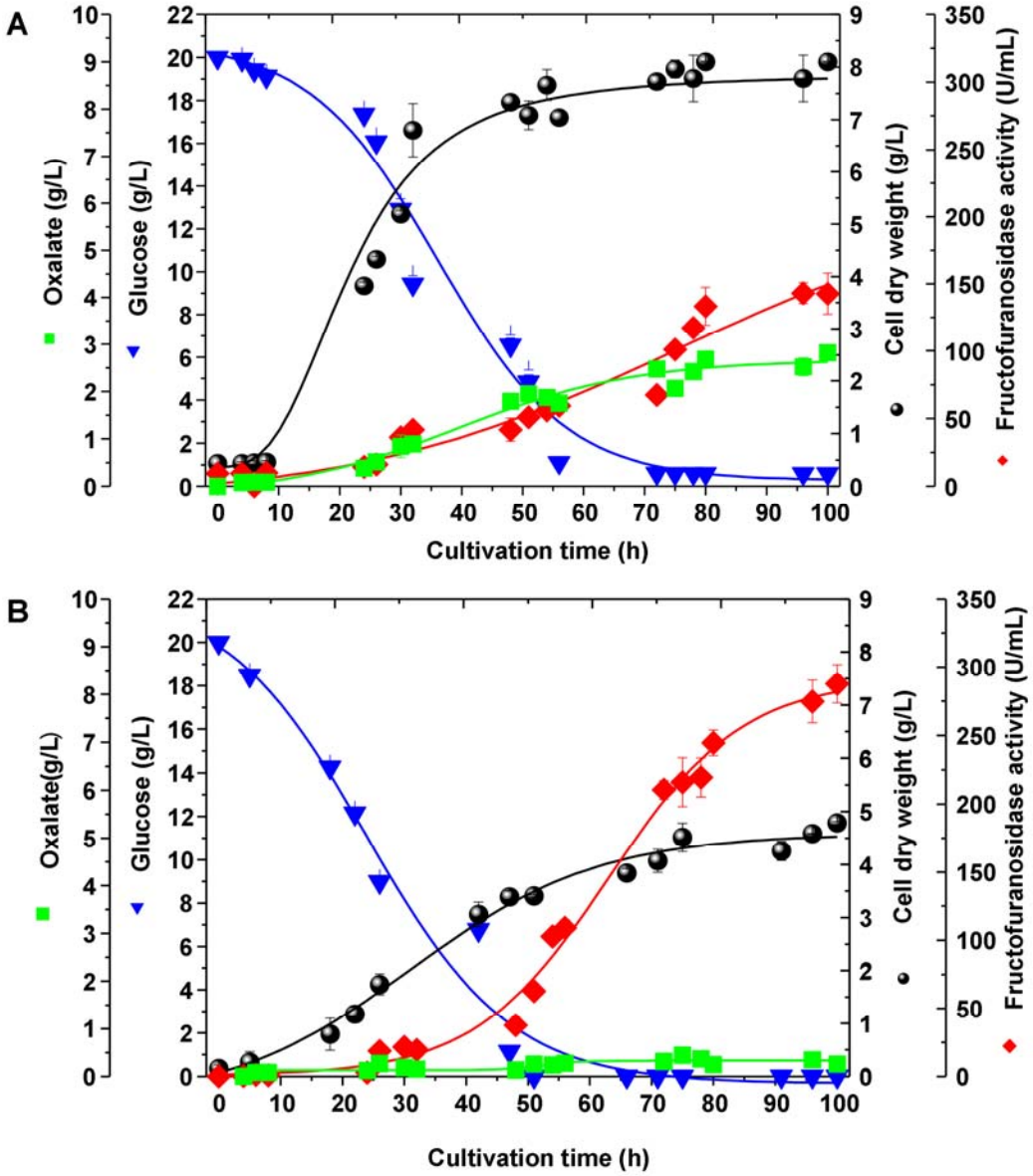

Figure 37: Time course of glucose, fructofuranosidase activity, and cell dry mass during submerged cultivation of *A. niger* SKAn1015 in a 3 L bioreactor in the absence (A) and presence of talc micro particles (10 g/L, 6 µm, B).

As described above, the micro particle-enhanced cultivation resulted in freely dispersed mycelium, whereas pelleted growth of *A. niger* was observed in the control. From early on, micro particles significantly stimulated the metabolic activity of *A. niger* as indicated by the faster uptake of glucose as sole source of carbon. With supplemented micro particles the fructofuranosidase activity in the broth reached a maximum value of more than 160 U/mL, which was about twice as high as compared to the control. Since the biomass formed was lower (4.6 g/L vs. 8.0 g/L) in the presence of the talc particles, the specific fructofuranosidase activity U/mg_{DW} was almost fourfold higher. Interestingly, the different morphology was further linked to a strong difference in by-product formation. Whereas in the control, *A. niger* secreted almost 3.2 g/L oxalate, formation of this compound was insignificant in the particle-enhanced cultivation process. Since pH was controlled at a value of 5.0 in both cultures, it can be excluded as parameter that could have driven differing acid formation. Overall, *A. niger* exhibited a significant improvement of its production performance in micro particle-enhanced cultivation. It is interesting to note that the talc material was rather inert under the conditions chosen. In a bioreactor control experiment without cells, the complete amount of 5.0 g/L of particles was recovered after 100 h.

Exemplified for glucoamylase and fructofuranosidase, particle supplementation strongly boosted production performance of *A. niger*. The titers were up to fivefold higher when the novel cultivation method was applied. Hereby, the investigated strains include a constitutive and an inducible expression system, as well as intracellular and extracellular enzymes. As shown, the strategy could be successfully transferred to a fructofuranosidase production process, where a final titer of 160 U/mL could be obtained. This value is about fourfold higher as compared to titers obtained until recently (Mussatto et al. 2009), underlining the enormous potential of the novel micro particle-based approach. Taking also the first successful example of chloroperoxidase production by the filamentous fungus *C. fumago* (Kaup et al. 2007) into account, the enhancing effects of micro particles seem of general nature and thus of high relevance for biotechnological processes with filamentous microorganisms.

The spatial resolution of enzyme production, visualized via co-expression of GFP with glucoamylase as the product of interest, clearly illustrated the origin of the enormous improvement. Obviously, the interaction of the cells with the

micro particles created a highly active biomass in which the dominating fraction of cells contributed to production. It was interesting to note, that protein production was obviously not restricted to hyphal tips as previously reported (Gordon et al. 2000; Vinck et al. 2005). This might display a further advantage of the novel cultivation approach. In contrast, production by pellets in the control culture was maximal only in a thin layer at the pellet surface, whereas most of the cells in the interior exhibited only weak or even no production. The superior morphology achieved thus was crucial to avoid limited availability of oxygen or other nutrients in the interior of pellets (De Nicolas-Santiago et al. 2006; Kelly et al. 2004; Zhang et al. 2007).

Here we demonstrate that, inoculated from spores, the morphology of *A. niger* can be precisely adjusted to a number of different distinct morphological forms by the addition of silicate micro particles. Through appropriate choice of size and concentration of the micro material different, distinct forms of pelleted growth with decreasing pellet size, freely dispersed mycelium, and even short hyphal fragments could be obtained. Beyond previous findings, our data show that the use of micro particles does not only enable free mycelium (Kaup et al. 2007), but even a rather precise engineering of morphology through fine tuned variation of particle size and concentration. This could open new possibilities to use micro particles for tailor-made morphology design in biotechnological production. The fact that other operational parameters can be left unchanged seems a positive side effect. As an alternative approach to adjust morphology to mycelium low pH could by far not yield the production performance of microparticle-enhanced cultivation. The use of micro particles could also be interesting as alternative to high stirring since increased energy costs can be avoided.

6.1.4 Targeted morphology design of hyper-productive bio-pellets

Pelleted growth (Figure 38A-B) displays an important industrial morphology. As example, it is beneficial for production of itaconic acid (Metz 1976) or citric acid (Gomez et al. 1988), glucoamylase (Xu et al. 2000) or penicillin (Nielsen et al. 1995b). Beyond direct production characteristics pellets provide a reduced viscosity of the culture fluid and thus improve mixing and oxygen transfer within the broth as well as a simplified separation of biomass.

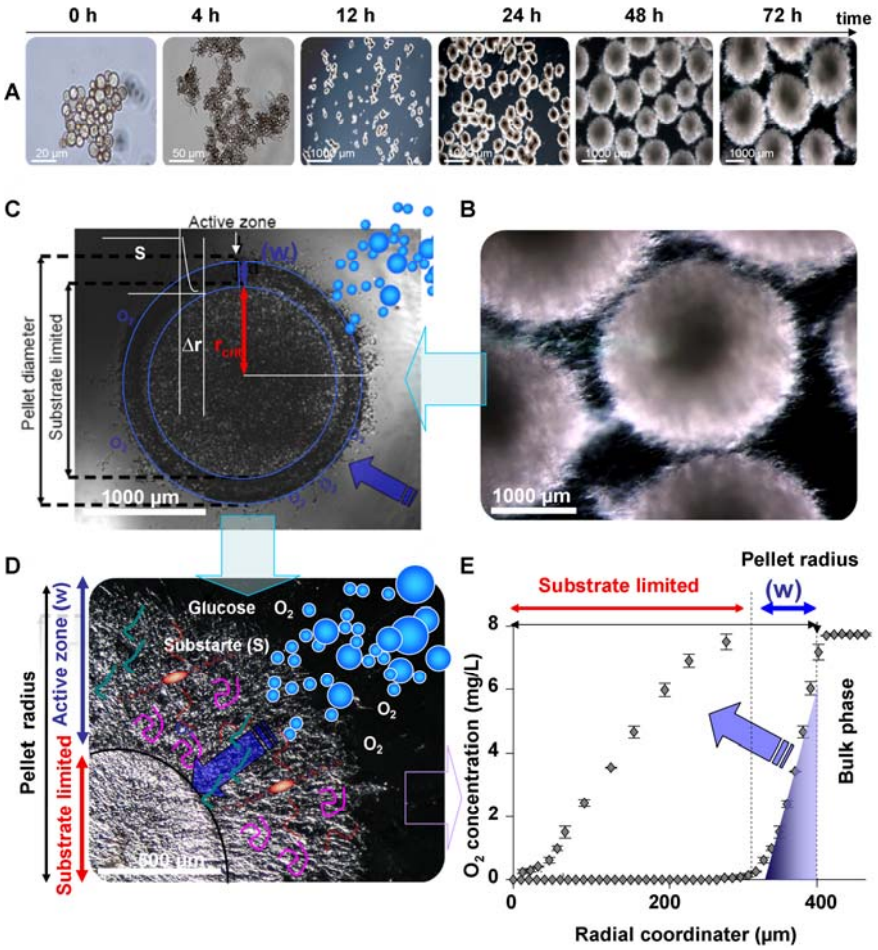

Figure 38: Photographs of macro-morphology (bio-pellet, A-B) of *A. niger* SKAn1015, principle sketch of radius and active layer within a pellet (C) and schematic representation of oxygen concentration profiles in pellet (D-E).

A severe disadvantage, however, is the low mass transfer within the pellet itself. Accordingly, the supply of oxygen and other nutrients to the cells especially in the pellet interior (Figure 38C-E) is typically limited (Hille et al. 2005; Nielsen 1996; Wittler et al. 1986).

Recent fluorescence analysis of GFP expressing reporter strains of *A. niger* visualized that only a thin layer at the pellet surface contributes to protein production, whereas the large inner part of the pellet was found inactive. In this regard, the present chapter demonstrates the design of superior bio-pellets of *A. niger* using a novel micro material added to the culture. Based on a broad screening among 15 different micro particle materials titanate (titanium silicate oxide, $TiSiO_4$, 8 µm) could be identified as most promising in providing bio-pellets. Exemplified for different recombinant *A. niger* strains, expressing the enzymes fructofuranosidase, glucoamylase and the model protein GFP the effect of this material on growth, production and morphology was studied in detail. The results could then be used to create high-producing bio-pellets of a distinct size with an inner core of titanate surrounded by active biomass.

6.1.4.1 Morphology of *A. niger* in the presence of titanate micro particles

Morphological analysis of *A. niger* now focussed on the cultivations with titanate particles (titanium silicate oxide, $TiSiO_4$, 8 µm) which had the most pronounced effect on recombinant protein production. Elevated levels of the micro material resulted in a remarkable change of the morphology. Surprisingly, *A. niger* maintained its pelleted growth in the presence of titanate over the whole tested concentration range. This differed strongly from the effects of other materials typically causing a shift from pelleted growth to free mycelia (Figure 39B). Most strikingly, the titanate particles were to a large extent associated with the biomass (Figure 39). Microscopic analysis revealed that depending on the amount of titanate present, different types of pellets were formed. The control pellet of about 2 mm size consisted of a rather dense outer layer of biomass and exhibited an unfilled centre, probably related to limited nutrient access in the inner part of the pellet (Figure 39A). With titanate levels below 5 g/L (Figures 38B, C) the overall pellet size was almost unaffected. The micro-material was found distributed within the pellet and obviously created a loose interior structure with a better biomass filling in the pellet core.

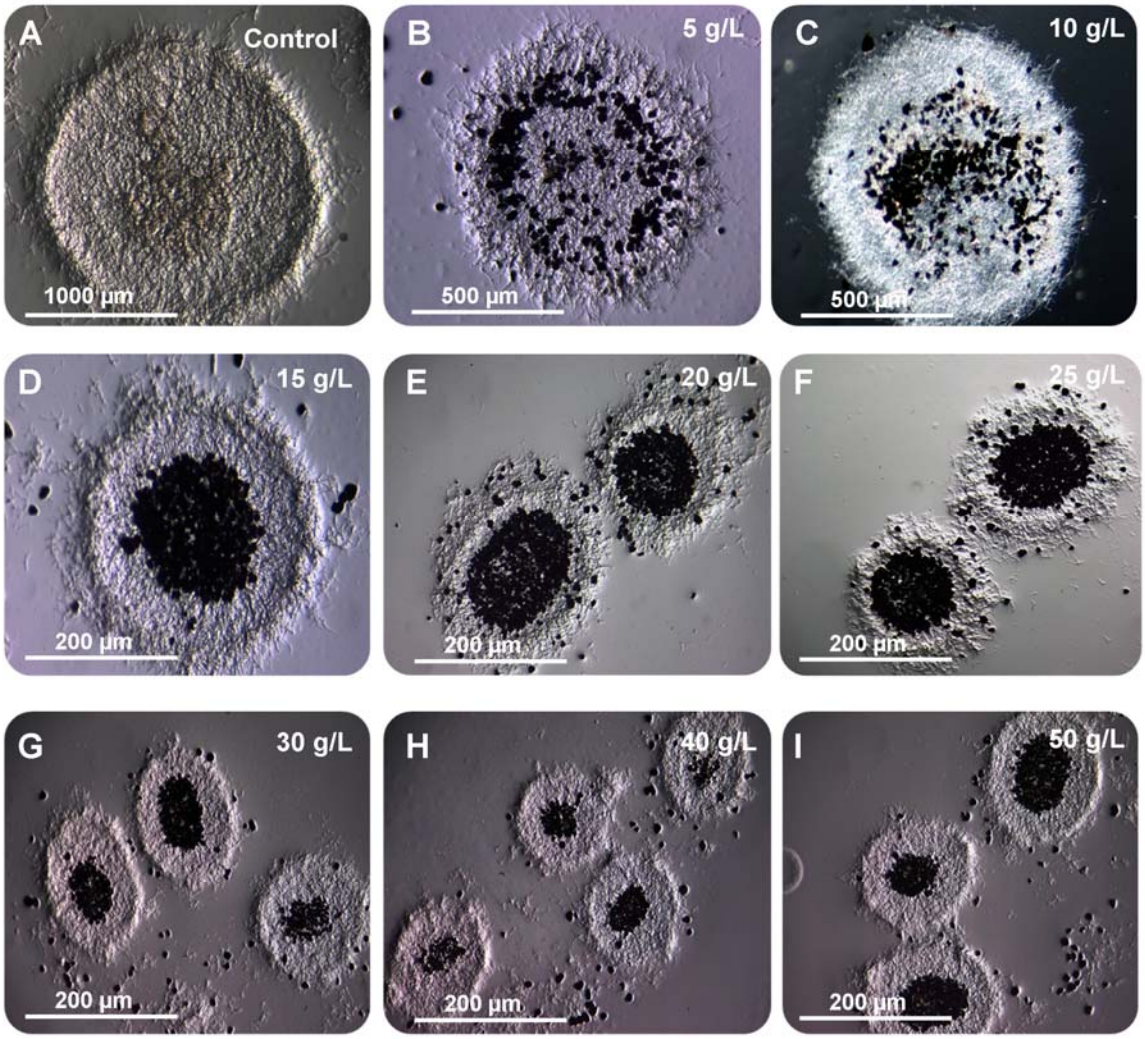

Figure 39: Bio-pellet design of *Aspergillus niger* SKAn1015 by titanate micro particle supplementation in submerged culture. Titanium silicate oxide (titanate, $TiSiO_4$, 8 µm particle size) was added at varied concentration: control without addition (A), 5 g/L (B), 10 g/L (C), 15 g/L (D), 20 g/L (E), 25 g/L (F), 30 g/L (G), 40 g/L (H), and 50 g/L (I). Image analysis was performed by light microscopy after 72 h of cultivation.

A completely different picture resulted for higher levels. Here, the titanate particles obviously aggregated in the initial phase of the cultivation and formed stable macro particles. They provided a solid support for growth of *A. niger* which subsequently covered the titanate cores with a 20 – 50 µm layer of mycelium during the culture. In addition, hyphae could be also observed in the inner zone between the titanate particles. Interestingly, the titanate aggregates varied in size between 20 and 150 µm in diameter depending on the amount of titanate initially added. Together with the outer cell layer this resulted in bio-pellets of differed sizes, amounts and composition. The small bio-pellet thus mainly consisted of cells, whereas the larger pellets were

mainly composed of titanate. Overall, a full range of macro-morphological pellet forms from dense pellets to specifically designed bio-pellets could be generated. The pellets were found stable during the whole culture.

6.1.4.2 Improvement of enzyme production by titanate micro particles

In addition to the initial screening that indicated the beneficial effect of titanate micro particles the impact on growth and enzyme formation was studied in more detail for the recombinant production of fructofuranosidase and glucoamylase in *A. niger* strain SKAn1015 and ARAn701, respectively (Figure 40).

Enzyme production was strongly boosted. The best results were obtained when a titanate concentration of 25 g/L was added. The resulting activities for fructofuranosidase (150 U/mL) and glucoamylase (185 U/mL) were 4 fold and 10 fold higher as compared to the control. Microscopic analysis further revealed that the pellet size could be designed rather precisely over almost one order of magnitude. Fungal pellets formed without addition reached an average pellet diameter of 1.72 mm. With the addition of titanate particles pellet diameters down to 0.30 mm could be achieved.

The bio-pellets remained stable throughout the whole cultivation and exhibited only a small variation in diameter. Growth seemed to be enhanced as well for both strains with increasing titanate levels, but care has to be taken since the gravimetric measurement probably overestimates the biomass formed due to the attached titanate, despite a correction for the micro particles present (Figure 40). The pH value of the cultures was unaffected by the addition of titanate.

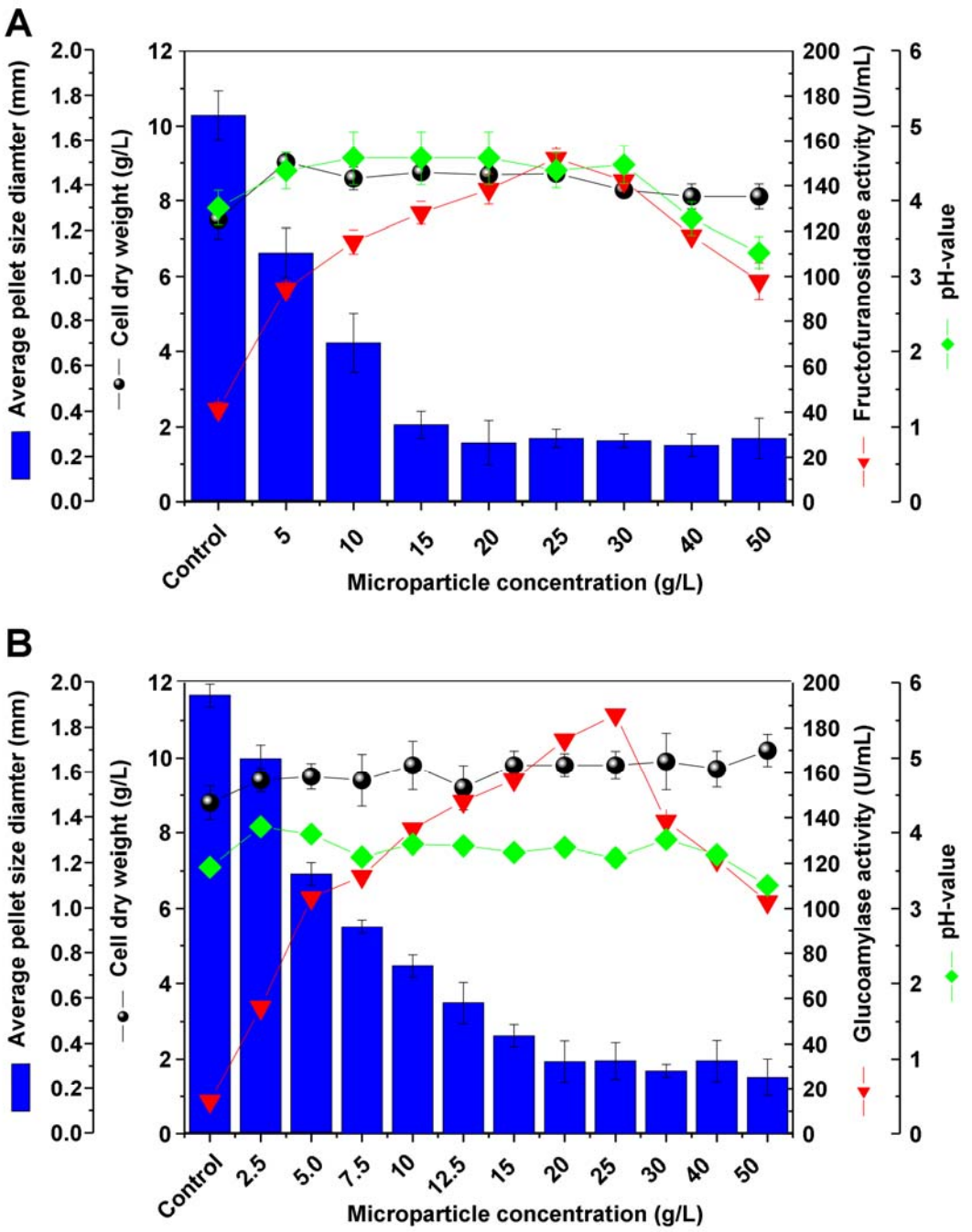

Figure 40: Fructofuranosidase and glucoamylase production by *A. niger* SKAn1015 (A) and *A. niger* ARAn701 (B) in batch culture without (control) and with addition titanate (8 µm) micro particles. The data comprise cell dry mass, average pellet size diameter, pH of the culture and enzyme activity after 72 h cultivation time as mean values from triplicate cultivations with corresponding deviation.

Influence of titanate on the specific surface of pellets and enzyme production

The volume-related specific surface of pellets (S_v) can be estimated by assuming all the pellets to have the same spherical shape. These geometric parameters S_v of pellets was estimated by following Eq. 8.

$$S_v = \frac{O_{pellet}}{V_{pellet}} = \frac{\pi * d^{2}_{pellet}}{\frac{\pi}{6} * d^{3}_{pellet}} = \frac{6}{d_{pellet}} \qquad (8)$$

Here, O_{pellet} is the surface of pellet, V_{pellet} is the volume of pellet and d_{pellet} is the average size diameter of pellet. The average size diameter (d_{pellet}) of pellet was determined via image analysis of 100 pellets each by light microscopy after 72 h of cultivation.

The results on the influence of titanate micro particle addition on S_v and enzyme production in both strain of *A. niger*, ARAn701 and SKAn1015, are presented in Figure 41.

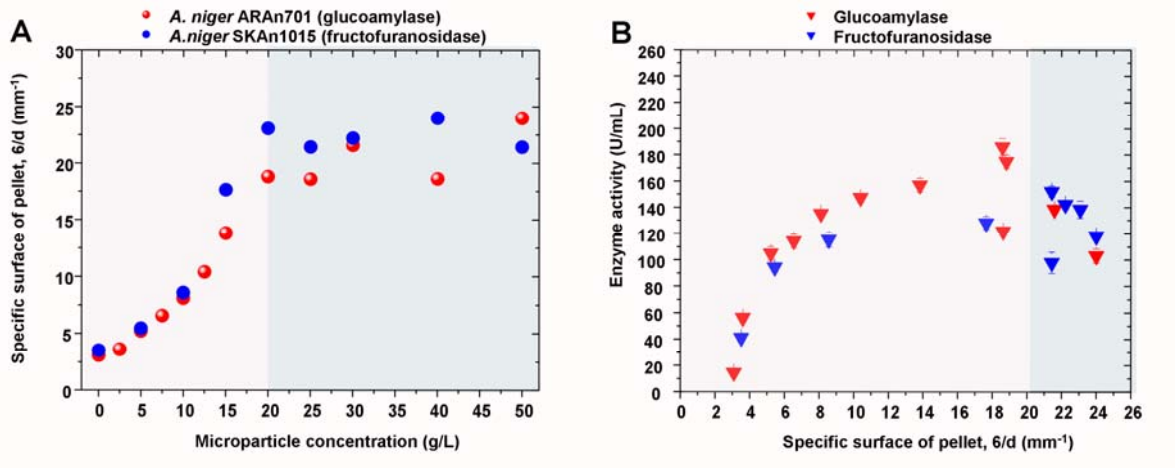

Figure 41: Influence of titanate (8 µm) micro particle addition on specific surface of pellets *Sv* (A) and enzyme production (B) of both strain of *A. niger* (ARAn701, SKAn1015).

Without titanate addition *A. niger* maintained its pelleted growth with an average pellet size diameter of 1.7 - 2.0 mm, corresponding to a small specific surface of pellets ($Sv = 6/d_{pellet}$) of 3.1 - 3.5 min^{-1} for ARAn701 and SKAn1015, respectively. By titanate micro particle addition the average pellet size diameters down to 0.2 - 0.3 mm could be achieved and the specific surface of pellets (24 min^{-1}) was 7 fold increased. The enzyme production in both strains, SKAn1015 and ARAn701, were strongly boosted. The larger specific surface of pellet created by titanate addition

caused an acceleration of enzyme production. The best results were obtained when a titanate concentration of 25 g/L was added. In both strains the results show that the enzyme production is dependent of specific surface of pellets created by addition of titanate micro particle, indicating that specific surface of pellet are involved in enhancement of oxygen supply, better mixing as well as mass and heat transfer,and thus, overall turnover rates in submerged cultivations. The nutrient/oxygen transfer seemed to be enhanced 7 fold with increasing of specific surface of pellets by addition of titanate microparticles. Specific surface of pellet have an important impact on penetration depths of substrates and, thus, the fraction of a pellet that is actually contributing to the pellet turnover. Mass transport in fungal bio-pellets is strongly coupled to pellet morphology (Hille et al. 2005, Hille et al. 2007). The specific rate of respiration of pellets was found to increase significantly with decrasing pellet size (Cronenberg et al. 1994). Pellets with a large specific surface of pellet of 20 mm^{-1} exhibited an enhanced enzyme activity. The resulting activities for fructofuranosidase and glucoamylase were 4 fold and 10 fold higher as compared to the control. The lower enzyme activity by control (large pellet, 2.0 mm, with a small specific surface of 3.5 min^{-1}) can be explained by the less nutrient/oxygen transfer, because at the central part of the pellet, the concentration of oxygen is always lower than that at the surface of pellet. Without raising the total energy input by aeration and agitation (volumetric power input) this results showed the potential utilization of the addition of titanate on the fungal bio-pellet morphology to improve the enzyme formation consequentially.

Spatial resolution of protein production in *A. niger* bio-pellets

It was now interesting to see, how the obviously increased production was distributed across the designed bio-pellets. The biomass of filamentous fungi is typically rather heterogeneous. Therefore, the extent of enzyme synthesis was spatially resolved across the different zones of the mycelial aggregates formed in the presence or absence of micro particles. For this purpose, *A. niger* ARAn701 was applied which co-expresses glucoamylase together with GFP2 under control of the same promoter. GFP expression via fluorescence intensity was localized in 70 µm thin cross sections through the biomass aggregates formed (Figure 42A-D). Figure 42 shows the microscopic picture and the corresponding fluorescence intensity across a pellet with about 1.5 mm diameter from a control experiment without addition of micro particles.

Clearly, protein production was highest within a thin layer of about 50 µm thickness at the pellet surface. Inside the pellet, fluorescence was strongly reduced.

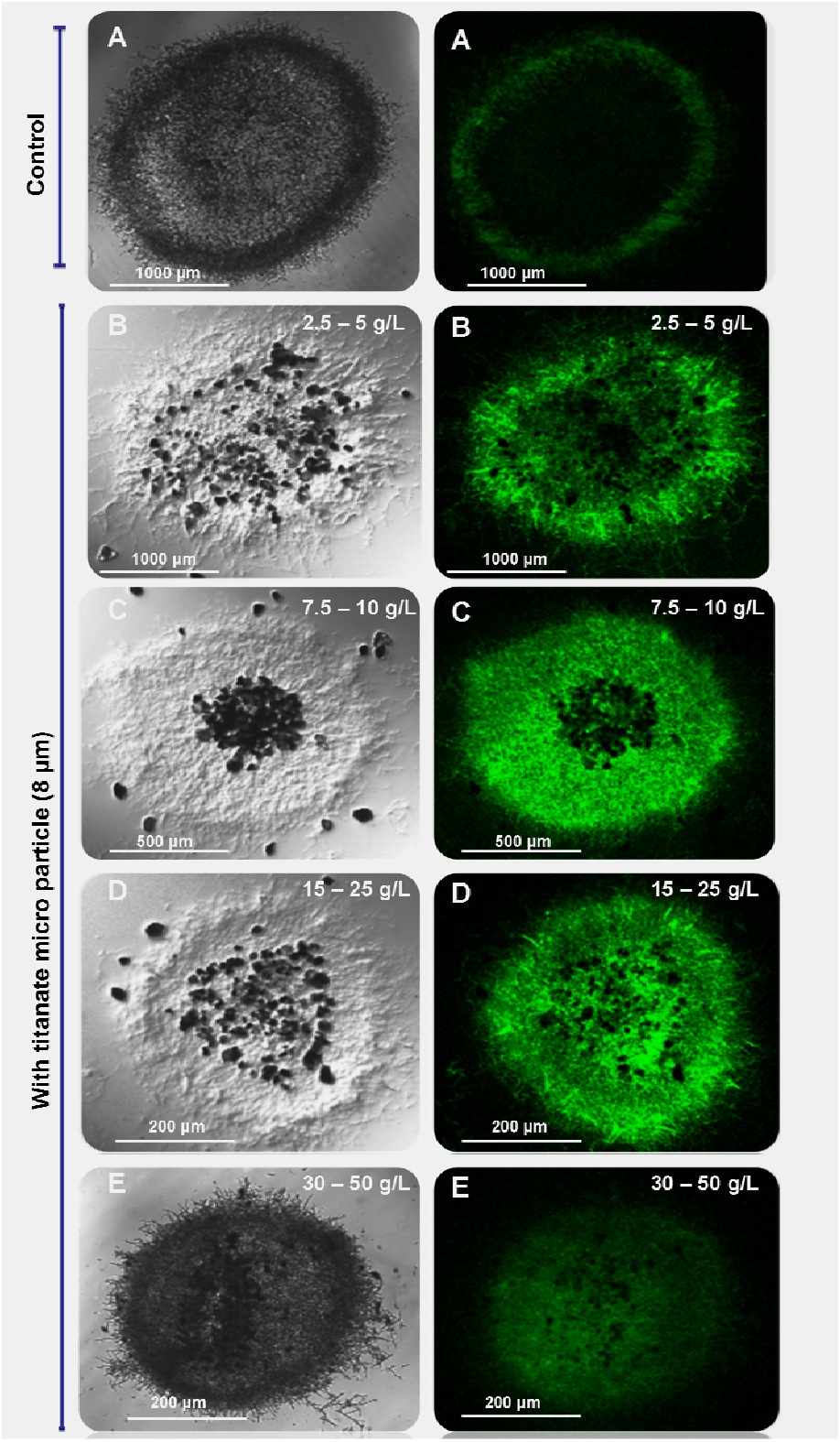

Figure 42: Spatial resolution of fluorescent protein production (GFP2) in recombinant *Aspergillus niger* ARAn701 pellets. The GFP2 expression was induced by start of the maltose feed after 40 h of cultivation. Samples were taken after induction 72 h of cultivation time. The pictures were obtained from 70 µm cross-sections through fungal aggregates by confocal laser scanning microscopy.

Obviously, only a small fraction of the entire biomass was contributing to product formation. In contrast, the interaction with the micro particles created smaller, but highly active bio-pellets of basically three different types. At low titanate concentration, a gradient of GFP expression within the pellet was still visible, although the thickness of the high-producing surface layer as well the contribution of the inner core were substantially higher, probably related to the looser inner pellet structure created (Figures 42B). In the medium concentration range, smaller pellets of about 1000 µm diameter exhibited a highly active biomass except for the small inner nucleus composed of the titanate aggregate (Figure 42C-E). With even higher concentration of titanate the 400 µm pellets exhibited maximum production performance. The GPF expression was rather high and equally distributed across the whole pellet. Above this optimum concentration, the overall production across the whole pellet was strongly reduced.

The present discovery seems especially useful for pellet based processes which have a long and strong industrial relevance for the production of itaconic acid (Metz 1976), citric acid (Gomez et al. 1988), glucoamylase (Xu et al. 2000) or penicillin (Nielsen et al. 1995b).

Beyond direct production characteristics pellets allow a reduced viscosity of the culture fluid and thus improve mixing and mass transfer as well as downstream processing by a simplified separation of biomass and culture fluid (Wucherpfennig et al. 2010). A severe disadvantage of pelleted growth, however, is the low mass transfer within the typically dense pellet. Accordingly, the supply of oxygen and other nutrients to the cells especially in the pellet interior is typically limited (Hille et al. 2005; Nielsen 1996; Wittler et al. 1986)The penetration depth of substrates and the fraction of pellet biomass which contributes to turnover and production, is directly linked to the mass transfer (Hille et al. 2009; Hille et al. 2005).

The addition of titanate micro particles of 8 µm size created superior pellet types. As compared to the control with only a thin surface layer involved in production, the use of titanate provided an increasing fraction of actively producing cells up to almost complete contribution of the entire pellet to protein production at 25 g/L titanate. The major reason is the surprising influence of the micro material. It was mainly found within the pellets. At low titanate concentration a statistical distribution of single particles inside the pellet could be observed, which changed into a rather dense titanate core in the pellet centre at higher levels. Overall, this caused a less dense

inner pellet structure beneficial for production. As positive side effect the biomass growing on this solid support exhibited a reduced depth as compared to normal pellet cultures so that problems with supply of oxygen and other nutrients can be minimized. Moreover, the size of the pellets could be strongly reduced by the micro particle addition from 1.7 to 0.3 mm. Overall this created a substantially larger surface for transport and nutrient uptake. In our opinion this might be a major driver to overcome limiting biomass growth, regarded as one of the main problems for achieving performance with filamentous fungi (Nielsen 1996). This becomes obvious from the fact that biomass growth was increased almost twofold by the use of titanate. It was interesting to note, that protein production was obviously not restricted to hyphal tips as previously reported (Gordon et al. 2000; Vinck et al. 2005). This might display a further advantage of the novel cultivation approach.

The overall response of cells to the titanate micro particles greatly differed from the effects to talc or alumina materials recently investigated mycelium (Kaup et al. 2007). Upon addition to cultures of *A. niger* and other filamentous fungi higher concentrations of talc and also alumina lead to free mycelium and even hyphal fragments. These materials are found typically outside the fungal aggregates and occur freely in the cultivation medium. Perhaps, this is one of the reasons for the different effect of titanate which aggregates itself from early on within the medium and is later trapped as solid support within the fungal aggregate. However, we are still far from understanding the complex process underlying the interaction between the micro particles and the cells.

Overall, the present chapter widens the goals for future work, especially towards understanding of the molecular mechanisms that link morphology with the underlying metabolic and regulatory networks. The use of different micro particle materials allow a targeted and rather precise engineering of cellular morphology into free mycelium (Kaup et al. 2007) and now also into superior bio-pellets (this work) which creates novel possibilities for future design and optimization of bioprocesses with *A. niger* and also other fungi. Based on this result, it was shown that the addition of selected titanate micro particles (8 µm) manipulate fungal bio-pellet morphology and enhance enzyme production, supplementary experiments and new insights into the potential mechanisms of the effects of the titanate micro particles were needed.

Due to the fast development in image analysis techniques it is possible to study the growth kinetics of filamentous microorganisms in more detail than previously.

However, it is important to apply mathematical models of mass transport and turnover in fungal biopellets that describe morphology and growth of filamentous fungi, such as characterization of biopellet morphology, measurement and simulation of morphological development, and a mathematical model of apical growth, septation, and branching to extract information about the underlying mechanisms from experimental data such as effective diffusion coefficient (D_{eff}). This can be used as a parameter in equations for the description and calculation of mass transport and turnover (Hille et al. 2009; Hille et al. 2005; Nielsen 1996; Znidarsic and Pavko 2001). There are many useful published models regarding nutrient diffusion which could have been used to further illuminate the effects of morphology changes and to predict productivity changes, and so to compare with the findings here.

Furthermore, utilizing the selected micro material of titanate and the optimal concentration of 25 g/L the process could be transferred from shake flask into batch or fed-batch process operated in the industrially relevant stirred tank (STR) type bioreactor. Thus the direct relevance could be shown towards manipulation of enzyme productivity in a highly productive system.

6.2 Optimized Bioprocess for Production of Fructofuranosidase as Biocatalyst for High-Value Neo-Sugars

6.2.1 Medium design

When developing biotechnological processes for batch or fed-batch cultivation, designing a defined cultivation medium is of critical importance because medium composition can significantly affect product yield and titer. It would be advantageous to designed culture media that contain all the nutrients in exactly the amount with only a carbon, energy source and a nitrogen source required, so that all nutrients would be consumed to completion at the end of the ptocess. Additionally, medium cost can substantially affect overall process economics. On the other hand, medium composition can also affect the ease and cost of downstream product separation, for example in the separation of protein products from a medium containing protein and are desired mainly in research laboratories due to the modelling of process.

Fructofuranosidases receive increasing interest as industrial biocatalysts for the synthesis of prebiotic neo-sugars. This high potential demands for efficient strains and bioprocesses enabling industrially feasible fructofuranosidase production. In this regard, a number of studies have previously aimed at the isolation of fructofuranosidaseproducing strains from nature (Cuervo et al. 2007) or the screening for suitable production media (Balasubramaniem et al. 2001). Most of these studies, however, resulted in relatively low production efficiency, which might be attributed to the fact that wild-type strains were employed and processes were performed in shake flask cultures. Towards an efficient production of fructofuranosidase, it appears important to develop efficient bioprocesses based on efficient media formulations and process conditions for tailor-made production strains. In a first step towards an optimized medium, the influence of carbon source, nitrogen source, and trace elements on production was studied. For this purpose, screening experiments in shake flasks were set up in triplicate each (Figure 43).

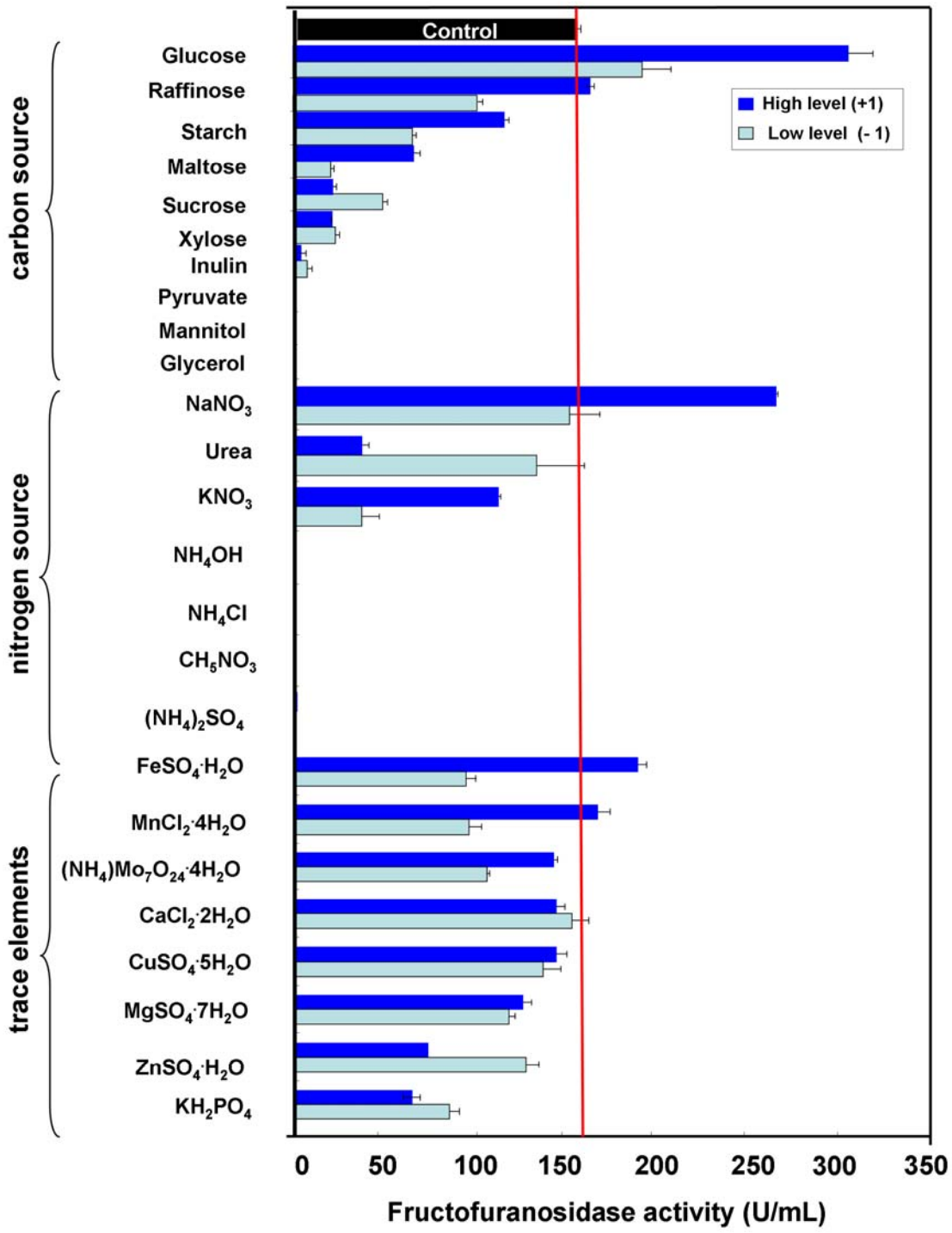

Figure 43: Identification of key nutrients for fructofuranosidase production by *Aspergillus niger* SKAn1015 using one-factor-at-a-time (OFAT) experiments in shake flasks. The fructofuranosidase activity, given as average with corresponding deviation from three replicate incubations, was determined after 100 h of cultivation. The control experiment was carried out with the basic medium containing 20 g/L glucose and 6 g/L sodium nitrate and corresponding trace elements. For the carbon sources tested, the low- and highlevel conditions refer to 10 and 30 g/L. The low- and high-level concentrations for the nitrogen source were 3 and 12 g/L. Similarly, the low and high level for the trace elements corresponded to 50% and 200% of the concentration in the basic medium.

Table 9: Levels of factors used in the CCD for optimizing media for growth and the fructofuranosidase production by *Aspergillus niger* SKAn1015

Symbol	Independent factors	Units	Coded levels				
			-2	-1	0	+1	+ 2
			Uncoded levels				
x_1	Glucose	(g/L)	10	20	30	40	50
x_2	$NaNO_3$	(g/L)	03	06	09	12	15
x_3	$FeSO_4 \cdot 7H_2O$	(mg/L)	1.5	3.0	4.5	6.0	7.5
x_4	$MnCl_2 \cdot 4H_2O$	(mg/L)	0.5	1.0	1.5	2.0	2.5

Table 10: Experimental design matrix and results of medium optimization for growth and fructouranosidase production by *Aspergillus niger* SKAn1015. The coded variables are glucose (x_1), sodium nitrate (x_2), $FeSO_4 \cdot 7H_2O$ (x_3), and $MnCl_2 \cdot 4H_2O$ (x_4). The concentrations corresponding to the coded factors (-2, -1, 0, +1, +2) are 10, 20, 30, 40, and 50 g/L for glucose, 3, 6, 9, 12, and 15 g/L for sodium nitrate, 1.5, 3.0, 4.5, 6.0, and 7.5 mg/L $FeSO_4 \cdot 7H_2O$, and 0.5, 1.0, 1.5, 2.0, and 2.5 mg/L for $MnCl_2 \cdot 4H_2O$

Coded factor						$Y_{biomass}$ (g/L)		Y_{FFase} (U/mL)	
Run	x_1	x_2	x_3	x_4	Design	Experimental	Predicted	Experimental	Predicted
1	-1	-1	-1	-1	**Full**	04.88	05.01	031	034
2	+1	-1	-1	-1	**factorial**	08.91	08.52	173	164
3	-1	+1	-1	-1	**design**	08.13	07.79	153	132
4	+1	+1	-1	-1	**2^4=16**	11.52	10.95	205	193
5	-1	-1	+1	-1		06.70	07.26	050	058
6	+1	-1	+1	-1		10.69	10.59	164	171
7	-1	+1	+1	-1		09.53	09.04	227	218
8	+1	+1	+1	-1		11.54	12.02	245	268
9	-1	-1	-1	+1		06.53	06.58	094	089
10	+1	-1	-1	+1		09.45	09.63	167	174
11	-1	+1	-1	+1		09.35	09.13	151	140
12	+1	+1	-1	+1		11.87	11.83	167	171
13	-1	-1	+1	+1		08.24	08.49	128	135
14	+1	-1	+1	+1		10.50	11.36	164	187
15	-1	+1	+1	+1		09.14	10.05	233	258
16	+1	+1	+1	+1		13.00	12.56	101	272
17	-2	0	0	0	**8 Star**	04.86	04.54	015	024
18	+2	0	0	0	**points**	10.45	10.56	182	164
19	0	-2	0	0		07.30	06.63	060	050
20	0	+2	0	0		10.16	10.61	168	184
21	0	0	-2	0		09.49	10.19	185	216
22	**0**	**0**	**+2**	**0**		**14.09**	**13.18**	**397**	**387**
23	0	0	0	-2		08.33	08.79	171	165
24	0	0	0	+2		11.58	10.91	238	217
25	0	0	0	0	**6 Center**	11.69	10.93	205	190
26	0	0	0	0	**points**	00.47	10.93	178	190
27	0	0	0	0		10.22	10.93	184	190
28	0	0	0	0		10.98	10.93	160	190
29	0	0	0	0		11.49	10.93	189	190
30	0	0	0	0		10.71	10.93	206	190

Table 11: Statistical analysis of central composite medium design for cell dry weight $Y_{biomass}$ (gramm per liter) and fructofuranosidase Y_{FFase} (units per milliliter) production by *Aspergillus niger* SKAn1015.

Source	Sum of squares	*df*	Mean square	*F* value	*p* value
Fructofuranosidase activity Y_{FFase} (U/mL)					
Model	268.16	14	19.15	10.73	<0.0001*
A: Glucose (x_1)	051.72	1	51.72	28.98	<0.0001*
B: $NaNO_3$ (x_2)	045.45	1	45.45	25.46	<0.0001*
C: $FeSO_4 \cdot 7H_2O$ (x_3)	015.75	1	15.75	08.82	0.0095
D: $MnCl_2 \cdot 4H_2O$ (x_4)	001.48	1	01.48	00.83	0.3769
AB	025.20	1	25.21	14.13	0.0019
AC	007.29	1	07.29	04.08	0.0616
AD	015.43	1	15.43	08.65	0.0101
BC	000.14	1	00.14	00.01	0.7861
BD	014.10	1	14.10	07.90	0.0132
CD	0.8000	1	00.80	00.45	0.5127
A^2	047.60	1	47.60	26.67	0.0001
B^2	022.19	1	22.19	12.40	0.0031
C^2	013.55	1	13.55	07.59	0.0147
D^2	0.1600	1	00.16	0.087	0.7722
Residual	026.77	15	01.78		
Lack of Fit:	024.72	10	02.47	06.02	0.0305
Pure Error	002.05	5	00.41		
Cor Total	294.93	29			
Cell dry weight $Y_{biomass}$ (g/L)					
Mosel	129.57	14	09.26	017.9	<0.0001*
A: Glucose (x_1)	054.50	1	54.50	105.6	<0.0001*
B: $NaNO_3$ (x_2)	023.79	1	23.79	046.1	<0.0001*
C: $FeSO_4 \cdot 7H_2O$ (x_3)	013.37	1	13.37	025.9	<0.0001*
D: $MnCl_2 \cdot 4H_2O$ (x_4)	006.70	1	06.70	012.9	0.0026
AB	0.1300	1	00.13	00.24	0.6288
AC	0.0330	1	00.03	00.06	0.8036
AD	0.2100	1	00.21	00.41	0.5320
BC	1.0100	1	01.01	01.96	0.1820
BD	0.0520	1	00.05	00.10	0.7555
CD	0.1100	1	00.11	00.22	0.6442
A^2	019.53	1	19.53	37.84	0.0001
B^2	09.090	1	09.09	17.61	0.0008
C^2	00.990	1	00.99	01.91	0.1867
D^2	1.9800	1	01.98	03.84	0.0687
Residual	007.74	15	00.52		
Lack of Fit:	006.08	10	00.61	01.83	0.2615
Pure Error	001.66	5	00.33		
Cor Total	137.30	29			

df degree of freedom, *Variable terms have significant effect on fructofuranosidase production and biomass.

This included the test of alternative carbon and nitrogen sources as well as the variation of the level of the investigated nutrients. On the basic medium (control), *A. niger* secreted 160 U/mL fructofuranosidase. Among all studies, four conditions allowed a production of fructofuranosidase, which was higher than in the control. From a variety of carbon sources tested, the medium with 30 g/L glucose resulted in the highest enzyme activity. $NaNO_3$ at a level of 12 g/L was found to be the most suited nitrogen source for production. The screening experiments further revealed a beneficial effect of elevated levels of the trace elements Mn^{2+} and Fe^{2+} on enzyme production. The four nutrients glucose, $NaNO_3$, $MnCl_2 \cdot 4H_2O$, and $FeSO_4 \cdot 7H_2O$, were considered for further medium optimization (Table 9). The strategy based on central composite design experiments with estimation of optimal nutrient levels using a quadratic model. In total, 30 different nutrient combinations were designed for this purpose and then tested in shake flask studies with three replicates each.

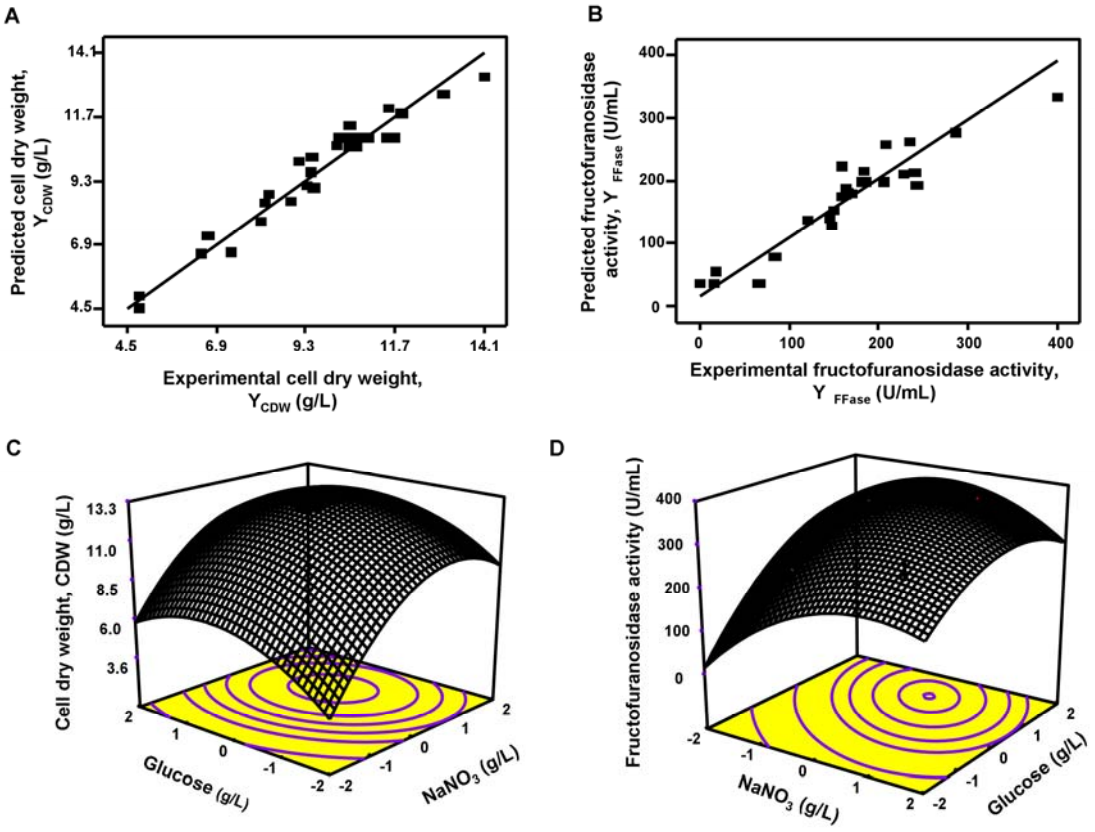

Figure 44: Medium design for cell dry weight (A) and fructofuranosidase production (B) by *Aspergillus niger* SKAn1015. The data shown comprise the measured enzyme activity on 30 different nutrient combinations as well as theoretical values predicted by the quadratic model used to identify the optimum medium composition. Influence of glucose and $NaNO_3$ on cell dry weight (C) and fructofuranosidase production (D) as predicted by the model. The interaction is visualized by a response surface plot.

The results from all experiments with the information on the corresponding medium composition are summarized in Table 10 and Table 11. Depending on the medium, the observed enzyme activity ranged from about 40 to almost 400 U/mL, underlining that the investigated nutrients obviously strongly influenced production. The experimental data were then fitted with a second-order polynomial expression.

The cell dry weight ($Y_{biomass}$) and fructofuranosidase activity (Y_{FFase}) could be expressed as function of the concentration of glucose (x_1), $NaNO_3$ (x_2), $MnCl_2 \cdot 4H_2O$ (x_3), and $FeSO_4 \cdot 7H_2O$ (x_4) by the following equation 8 and equation 9:

$$\begin{aligned} Y_{biomass} &= 10.93 + 1.51x_1 + 1x_2 + 0.75x_3 + 0.53x_4 - 0.089x_1x_2 \\ &- 0.045x_1x_3 - 0.11x_1x_4 - 0.25x_2x_3 - 0.057x_2x_4 - 0.085x_3x_4 \\ &- 0.84{x_1}^2 - 0.58{x_2}^2 + 0.19{x_3}^3 - 0.27{x_4}^2 \end{aligned} \quad (8)$$

$$\begin{aligned} Y_{FFase} &= 105 + 19x_1 + 21x_2 + 17x_3 + 7x_4 - 8x_1x_2 \\ &- 0.5x_1x_3 + 5x_1x_4 + 9x_2x_3 - 5x_2x_4 + 4x_3x_4 \\ &- 13{x_1}^2 - 11{x_2}^2 + 13{x_3}^3 + 0.05{x_4}^2 \end{aligned} \quad (9)$$

The comparison of the experimental biomass and enzyme activity with the corresponding values predicted by the model revealed a good correlation (Figure 44A). The high coefficient of regression (R = 0.94 and R = 0.90) indicated a high goodness of fit. Statistical treatment of the data further underlined a highly consistent data set and high confidence for the obtained parameters (Figure 44A-B). Exemplified for glucose and sodium nitrate, the 3-D response surface plot, determined from the obtained regression model, illustrates the strong effect of the key nutrients on production as well as the prediction of an optimal combination (Figure 44C-D). The optimal medium identified by the model contained 30 g/L glucose, 9 g/L $NaNO_3$, 1.5 mg/L $MnCl_2 \cdot 4H_2O$, and 7.5 mg/L $FeSO_4 \cdot 7H_2O$, respectively. For these conditions, a maximum enzyme activity of 400 U/mL in shake flask culture was predicted, almost threefold more than in the original medium.

6.2.2 Batch Bioprocess

The optimal medium was first compared in shake flasks to the original basic medium. On the original medium, *A. niger* SKAn1015 grew only to a maximum dry weight of 8.2 g/L. The enzyme activity reached 160 U/mL after 100 h of cultivation. Cultured on the new medium formulation, the strain revealed significantly improved performance. It reached a maximum dry weight of 12.8 g/L. The achieved enzyme activity of 400 U/mL corresponded nicely to the predicted value. The production performance of *A. niger* SKAn1015 on both media was then evaluated in bioreactor (Figure 45A-B).

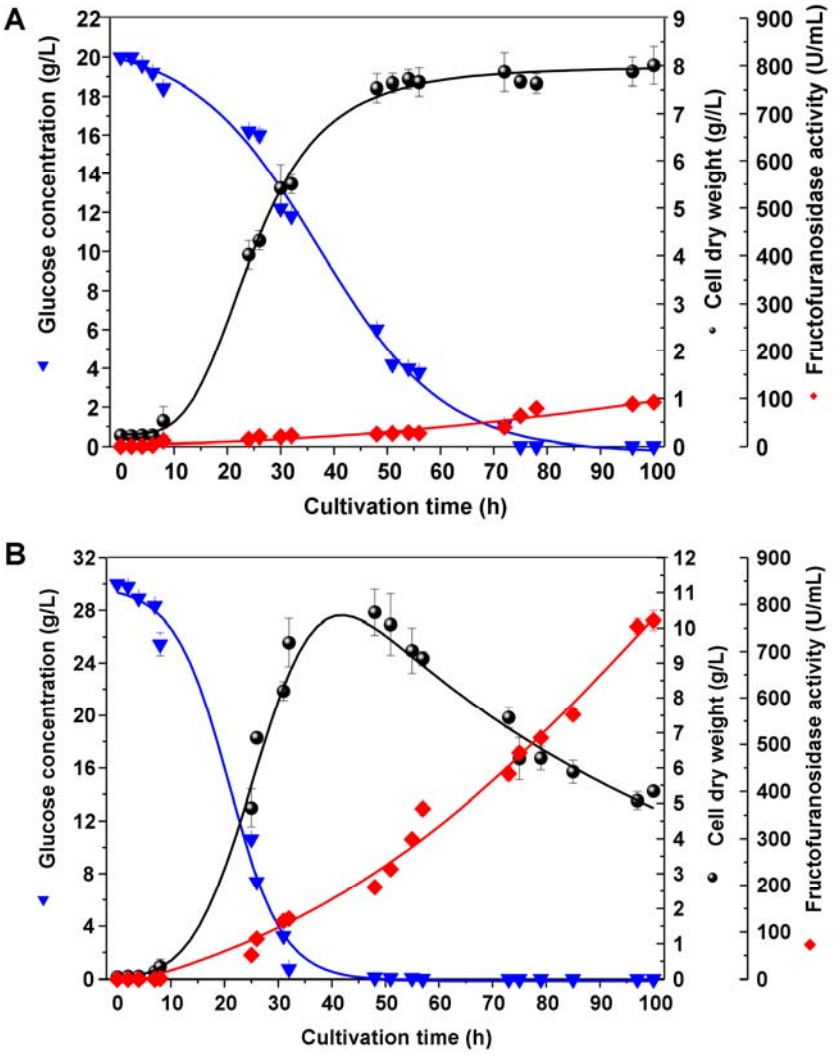

Figure 45: Fructofuranosidase production by *Aspergillus niger* SKAn1015 in batch culture using 3 L stirred tank bioreactors on the original basic medium (A) and the optimized medium (B). The data comprise the time profile for glucose, cell dry weight, and enzyme activity over the cultivation time of 100 h as mean values from two replicate cultivations with corresponding deviations.

On the newly designed medium, the strain grew much faster and reached a higher biomass concentration. Most impressively, the fructofuranosidase activity was more than sevenfold higher (750 U/mL) as compared to the control (100 U/mL).

6.2.3 Fed-batch bioprocess

Compared with traditional batch operation, fed-batch operation mode often offers an improved efficiency. This was now exploited by transferring the production into a fed-batch process (Figure 46A). After an initial batch phase of 30 h, the feed, which contained a concentrated form of the optimal nutrient mixture, was started. The intermittent feed with a total volume of 1 L was adjusted such that the glucose level in the culture was maintained above 1 g/L ensuring sufficient supply of the culture with the carbon source. The process was characterized by efficient growth of *A. niger* SKAn1015, meaning that 14 g/L of dry biomass were observed after about 80 h of cultivation time. The cells formed the characteristic pellet structure of filamentous fungi in submerged culture (Figure 47A). During the first 50 h, the consumed glucose was partly oxidized into gluconate. Both substrates were then concurrently metabolized for the remaining process. The maximum fructofuranosidase activity (600 U/mL) was observed after about 100 h. The product level then dropped to a final value of 350 U/mL corresponding to a specific activity of 200 $U/mg_{protein}$. Overall, the performance of the fed-batch process, at least at this stage, was not better than that of the batch operation.

6.2.4 Micro particle-enhanced fed-batch-process

For a further optimization of enzyme production in fed-batch mode, the batch medium was now additionally supplemented with inorganic talc microparticles (6 µm, 5 g/L), previously proven in shake flasks studies to stimulate production. All other process parameters remained unchanged. The cultivation profile of this microparticle-enhanced process is shown in Figure 46B.

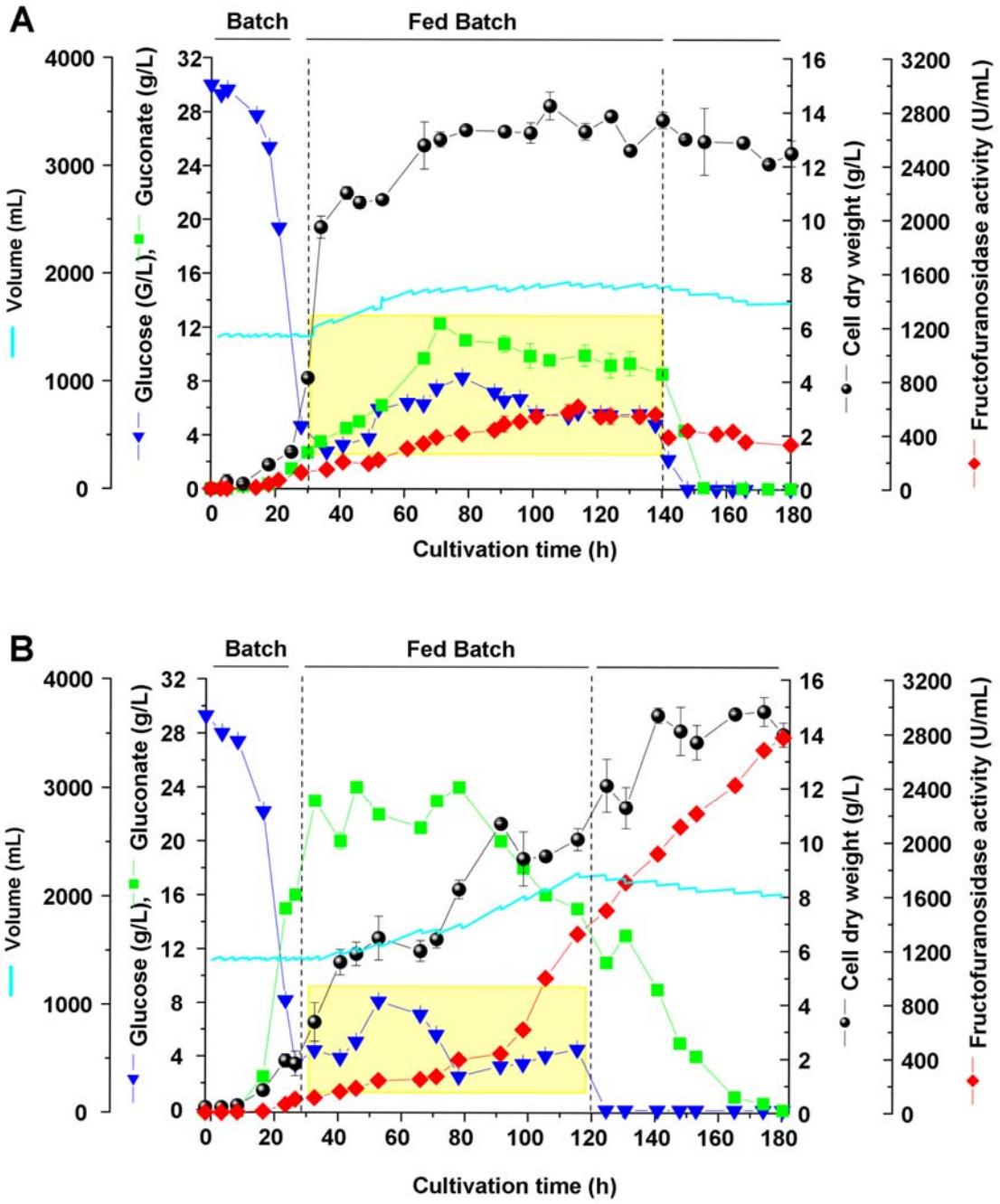

Figure 46: Fructofuranosidaseproduction by *Aspergillus niger* SKAn1015 in fed-batch culture on the optimized medium without (A) and with addition of talc micro particles (6 µm, 5 g/L; B) using 3 L stirred tank bioreactors. The data comprise the time profile for glucose, gluconate, cell dry weight, and enzyme activity over 180 h cultivation time as mean values from two replicate cultivations with corresponding deviations.

It differed dramatically from the normal fed-batch process. Most strikingly, the fructofuranosidase activity reached a final value of 2,800 U/mL, meaning that the addition of the microparticles increased production dramatically. This was also observed for the specific enzyme activity (820 U/$mg_{protein}$).Cells grew as freely

dispersed mycelium for the whole cultivation process (Figure 47B). In addition to the morphology, the talc material obviously influenced the metabolic properties of *A. niger* SKAn1015. Compared to the normal fed-batch, the formation of gluconate was clearly stimulated at the expense of growth. This was especially pronounced in the first 80 h.

Here, gluconate reached a maximum level of 24 g/L. Together with the added glucose, gluconate was completely re-used towards the end of the process. Interestingly, growth and enzyme production were maintained until the end of the process, which seems one of the major benefits as compared to the control fed-batch. SDS-PAGE analysis of the supernatant at the end of the micro particle enhanced fed-batch confirmed strong of fructofuranosidase, represented by the protein band at 110-120 kDa, by the recombinant strain (Figure 48).

The target enzyme was secreted almost exclusively, underlining the high specificity of production. In addition, only one band was visible at about 80 kDa. This coincided with low but significant activity of glucoamylase (90 U/mL) observed in the supernatant at the end of the process. A rough estimation via the volume of the observed bands revealed that fructofuranosidase accounted for about 85% of the totally excreted protein in the culture supernatant.

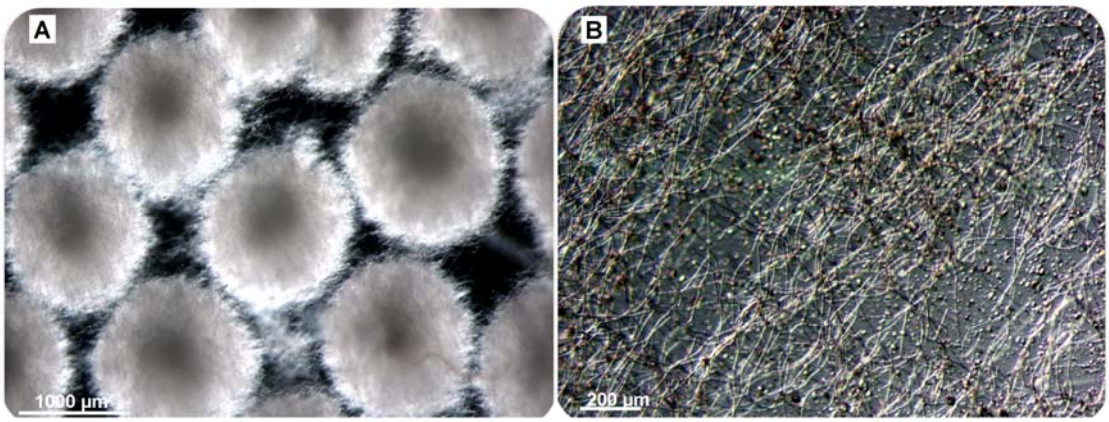

Figure 47: Morphology of *Aspergillus niger* SKAn1015 after 72 h of a normal fed-batch-cultivation (A) and a micro particle-enhanced fed-batch cultivation (B) with addition of talc micro particles (6 µm, 5 g/L).

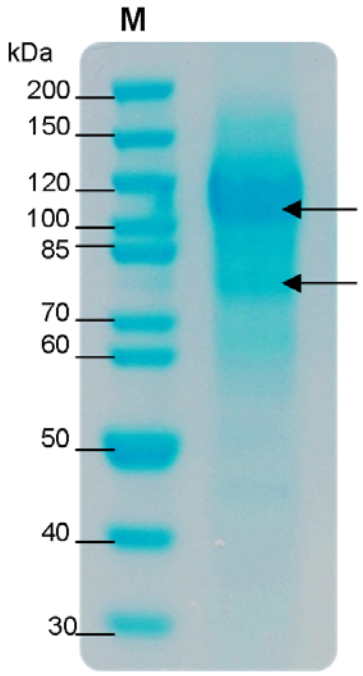

Figure 48: Sodium dodecyl sulfate-polyacrylamide gel electrophoresis analysis of culture supernatant (180 h) from *Aspergillus niger* SKAn1015 in fed-batch production with optimized medium and addition of talc micro particles. The left lane 1 (M) shows a molecular weight marker (Fermentas SM0661). The strong band at about 110-120 kDa corresponds to fructofuranosidase (Zuccaro et al. 2008). The total protein secreted was attributed to fructofuranosidase and to the other visible protein band at 80 kDa. The relative amount of fructofuranosidase was estimated as volume of the corresponding band related to that of all protein bands.

6.2.5 Impact of morphology on enzyme production

Obviously, the micro particles specifically enhanced production of the target enzyme by *A. niger* in the fed-batch culture. *A. niger*, grown in the presence of the micro particles, exhibited a specifically higher production level, especially during the second half of the fermentation. To unravel the link between the production behavior and the obviously affected morphology, enzyme production was spatially resolved during the fed-batch process within the different fungal aggregates, mycelium, and pellet, employing a GFP-expressing variant of *A. niger*. Production was hereby localized in 70 µm thin cross-sections through biomass aggregates obtained from cultures with and without micro particles (Figuer 49). In both cases, GFP expression was immediately initiated after the induction by maltose after 40 h. Protein production in the pellet-based process, however, occurred only within a thin layer at the pellet surface (Figuer 49A–D).

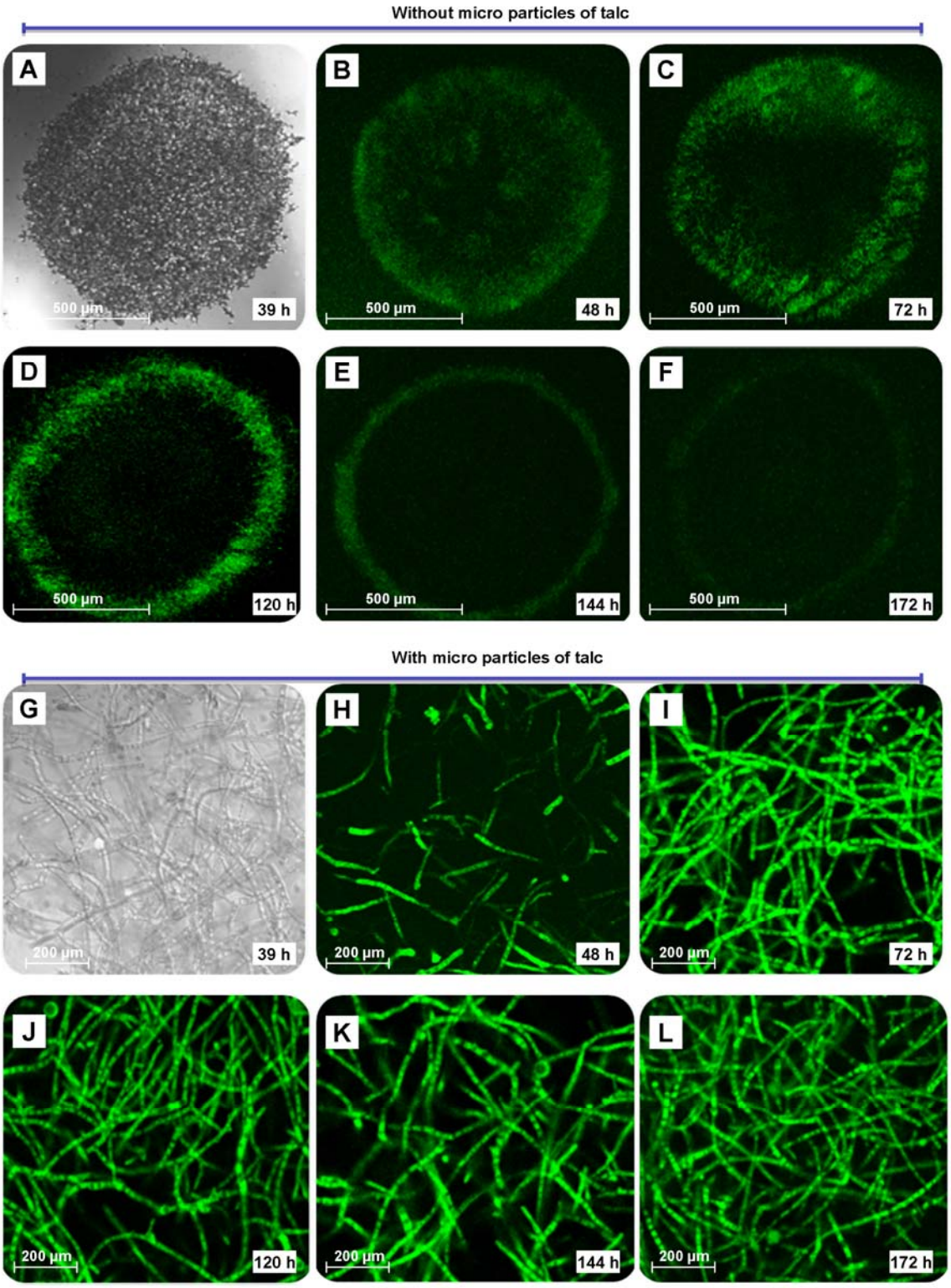

Figure 49: Spatial resolution of fluorescent protein production (GFP2) in recombinant *Aspergillus niger* ARAn701 pellets (A–F, normal fedbatch cultivation) and freely dispersed mycelium (G–l, fed-batch cultivation with addition of 5 g/L talc micro particles of 6 µm diameter). GFP2 expression was induced by start of the maltose feed after 40 h of cultivation. Samples were taken before induction (39 h) and after 48, 72, 120, 144, and 172 h of cultivation time. The pictures were obtained from 70 µm cross-sections through fungal aggregates by confocal laser scanning microscopy

For the micro particle-enhanced process, intensive fluorescence was present across the entire mycelium (Figure 49E-F). Protein production remained high until 180 h. This indicates that the interaction with micro particles created a productive biocatalyst remaining highly active during the entire process. The inner pellet did not contribute to production, probably due to diffusion limitation of oxygen or of other nutrients. Despite glucose was still present, production in the surface layer markedly decreased after about 120 h, so that almost completely inactive pellets remained for a large time period of the process.

Table 12: Production of extracellular fructofuranosidase by *Aspergillus niger* SKAn1015 using different processes in flasks and in bioreactor with original and optimized medium combined without and with microparticle addition.

Process (cultivation time)	**Batch (100h)**					**Fed-batch (180h)**	
	Shake flasks		**Bioreactor**			**Bioreactor**	
Medium	**Basic**	**Opt.**	**Basic**	**Opt.**	**Opt.**	**Opt.**	**Opt.**
Morphology	Pellet	Pellet	Pellet	Pellet	Mycelium	Pellet	Mycelium
Microparticle addition*	−	−	−	−	+	−	+
Cell dry weight, CDW (g/L)	5.6±1	8.5±0	8.2±0	5.3±1	3.6±0	12.5±1	13.5±0.4
Protein (mg/mL)	0.8±0	1.3±0	0.9±0	2.0±0	2.1±0	1.7±0	03.4±0.2
Volumetric activity (U/mL)	92±6	400±20	160±10	750±20	860±30	350±20	2,800±40
Productivity (U/L*h)	920	4,000	1,600	7,500	8,600	1,940	15,600
Specific activity (U/mg$_{protein}$)	115	310	180	380	410	206	820

* −/+ without/with microparticles of hydrous magnesium silicate (6 µm, 5 g/L)

In summary an optimized bioprocess for production of fructofuranosidase by the recombinant strain *A. niger* SKAn1015 was developed (Table 12). As first step, the production medium was systematically optimized using a modelling-based statistical approach. Among various carbon sources tested, glucose allowed fastest growth and also resulted in the highest enzyme activity. Previous fructofuranosidase production processes are almost exclusively based on sucrose and require high substrate concentration of typically more than 200 g/L. This is obviously due to the fact that these high sucrose levels are needed to induce fructofuranosidase expression in wildtype strains (Chen and and Liu 1996). Accordingly, other sugars including glucose typically enable fast growth, but only low enzyme production (Zuccaro et al.

2008). This was not observed for the recombinant strain *A. niger* SKAn1015, which expresses the fructofuranosidase encoding gene under control of the strong constitutive promoter *pki*A and is thus released from undesired endogenous control mechanisms. Due to this, the superior efficiency of glucose regarding growth as compared to sucrose (Figure 43) could now be fully exploited for fructofuranosidase production which seems a major advantage. As further benefit, efficient enzyme production was possible even at a low glucose level below 5 g/L (Figure 46B). This facilitates the setup of efficient fed-batch processes with limited feeding and complete consumption of the carbon source (Table 13).

Table 13: Efficiency of biotechnological fructofuranosidase production by different organisms

Organism and process parameters	**Extracellulare fructofuranosidase activity (U/mL)***	**References**
Aspergillus niger SKAn1015		
Batch, glucose	780	In this work
Fed batch, glucose	2,800	In this work
Aspergillus niger SKAn1015	280	(Driouch et al 2010)
Aspergillus niger ATCC20611	41	(Hidaka et al.1988)
Aspergillus niger NRRL4337	9	(Hidaka et al.1988)
Aspergillus japonicus IFO 4060	25	(Hayashi et al. 1992)
Batch: flasks, Sucrose		
Aspergillus japonicus TIT-KJ1 (immobilized)	1	(Cruz et al. 1998)
Batch: flasks, glucose		
*Aureobasidium pullulan*s	54	(Shin et al. 2004)
Batch: flasks, sucrose		
*Aureobasidium pullulan*s KCTC 6353	55	(Shin et al. 2004)
Batch: flasks, sucrose		
*Aureobasidium pullulan*s KCTC 6789	10	(Shin et al. 2004)
Batch: flasks, sucrose		
Aspergillus japonicus JN19	55	(Wang and Zhou 2006)
Batch: flasks, sucrose		
Aspergillus oryzae IAM-2609pp13	4	(Yoshikawa et al. 2006)
Penicillium purpurogenum	61	(Dhake and Patil 2007)
Batch: flasks, sucrose		
Aureobasidium pullulans DSM 2404	12	(Yoshikawa et al. 2007)
Aspergillus japonicus ATCC 20236 (immobilized)	43	(Mussatto et al. 2008)
Batch: flasks, sucrose		
Aspergillus japonicus ATCC 20236 (immobilized)	41	(Mussatto et al. 2009)
Repeated batch: flasks, sucrose		
Aspergillus niveus	5	(Guimaraes et al. 2009)
Batch: flasks		

* The extracellular enzyme activity given refers to a measurement temperature of 55 °C

Concerning the nitrogen source, recent studies revealed interesting effects of the chosen ingredient on production properties and the morphology of the cells (Balasubramaniem et al. 2001). It appeared that the higher enzyme activity on corn steep liquor, as compared to inorganic salts containing nitrate or ammonium, was indirectly related to the fact that the complex nitrogen source resulted in loose pellets or hyphae, whereas the salts led to pelleted growth. These medium-dependent morphology effects were no more required in the present work, since the intentional addition of micro particles allowed a direct and precise engineering of the morphology into the desired hyphal form. Accordingly, sodium nitrate could be efficiently used. It should be noticed that also complex nitrogen sources, such as peptone or yeast extract, enabled efficient production, but were not considered since we aimed at a fully defined medium towards a robust, reproducible production process avoiding batch-to-batch variation, typically faced on complex nutrients. Among the microelements, Fe^{2+} and Mn^{2+} were identified as key nutrients. Their importance for fructofuranosidase production has not been observed before (Maiorano et al. 2008), which might be explained by the altered control of enzyme expression in *A. niger* SKAn1015 as compared to wild-type strains. It is interesting to note that in contrast to the present work, both trace elements have tobe limiting for efficient production of citric acid (Papagianni 2007). The production of this organic acid demands for a downregulation of the tricarboxylic acid (TCA) cycle at the level of citric acid. This can be achieved by the lack of Fe^{2+} and Mn^{2+} required as cofactors of downstream TCA cycle enzymes. The stimulating role of the two metals here might indicate that an actively operating TCA cycle, supplying energy and building blocks, is needed to achieve high enzyme titers in *A. niger* SKAn1015. The subsequent optimization of the level of glucose, nitrate, Fe^{2+}, and Mn^{2+} using central composite design allowed a threefold increase of fructofuranosidase in shake flask. This underlines the high value of a systematic, modelling-based medium design (Babu et al. 2008). Subsequently, the process was transferred from shake flask into bioreactor for further optimization. This step appears especially important, since for the production of fructofuranosidase, such investigations are quite rare (Maiorano et al. 2008). Already in batch operation, this allowed a higher enzyme production (Table 12). The increased enzyme level might be due to better aeration or mixing patterns provided in the bioreactor. When transferred into a fed-batch environment with intermittent feeding of glucose and the addition of microparticles, a

fructofuranosidase activity of 2,800 U/mL could be finally achieved. Starting from the original medium in batchoperated shake flasks (140 U/mL), the product level could thus be optimized by a factor of 20. Among all fructofuranosidase-producing studies, providing data on the extracellular enzyme activity, values up to about 280 U/mL could be achieved so far (Table 13). The enzyme activity by the microparticle-enhanced fed-batch process on minimal medium is more than tenfold higher.

Moreover, the process was characterized by a high specificity of production. Fructofuranosidase accounted to about 85% of the totally secretion protein as verified by SDS-PAGE gel analysis. Taking the measured protein concentration in the culture supernatant into account (Table 12), this roughly corresponds to about 3 g/L of fructofuranosidase. It seems likely that glucoamylase formed as endogenous enzyme of the applied strain on glucose represents the weak protein band at around 80 kDa (Venkataraman et al. 1975). The presence of glucoamylase was, however, rather low. Its enzymatic activity (90 U/mL) was only 3% as compared to that of fructofuranosidase (2,800 U/mL). Future metabolic engineering of *A. niger* SKAn1015 could aim at disruption of the encoding gene to completely prevent formation of glucoamylase and achieve an even more pure culture supernatant.

Summarizing, the presented bioprocess strategy appears as a milestone towards future industrial fructofuranosidase production. A key to success seems the highly active mycelial biocatalyst present during the whole fed-batch process, exhibiting superior production properties as compared to the pelleted form, which only provided a small fraction of actively producing cells.

A key criterion for the developed process is the selectivity at which the target enzyme fructofuranosidase is produced. Previous separation of the supernatant at the end of the micro particle enhanced cultivation process by 1-D SDS-PAGE revealed the presence of only a few proteins. From enzyme activity measurements and the estimated molecular weights, it was concluded that the culture supernatant mainly contains fructofuranosidase as a dominant product and small amounts of glucoamylase. The estimation via the volume of the observed bands in 1-D gels revealed that fructofuranosidase accounted for about 85% of the totally excreted protein in the culture supernatant, indicating a highly specific production process. These findings were confirmed by MALDI-TOF MS analysis of the two proteins excised from the gel which allowed clear identification of the two proteins as

fructofuranosidase as dominating product (120 kDa) and glucoamylase (80 kDa), respectively (Table 14). Future rational based approaches such as metabolic engineering of *A. niger* SKAn1015 could aim at disruption of the encoding glucoamylase gene to completely prevent its formation, if needed.

Table 14: Expressed extracellular enzymes of *Aspergillus niger* SKAn1015 identified by MALDI-TOF-MS analysis. The two bands represent the two major proteins produced and previously attributed to fructofuranosidase (band 1) and glucoamylase (band 2) by enzyme activity measurement and molecular weight. For identification, bands were manually excised from the gel, cut into small pieces and prepared for peptide digestion by trypsin addition. Peptide mass fingerprints and peptide fragmentation data were analysed using an UltrafleXterme™ TOF/TOF mass spectrometer (Bruker Daltonic GmbH, Bremen, Germany) and subsequently processed using FlexAnalysis™ 3.0 and the BiotoolsTM 3.2 program of the software-package Masslynx™. The Mascot 2.2 search program was used for protein identification with the annotated *Aspergillus niger* genome (EMBL: http://www.ebi.ac.uk/genomes/eukaryota.html).

Band	Accession	NCBI protein	Searched/ matched peptides	Score*	Sequence coverage (%)
1	gi | 485547	beta-Fructofuranosidase	32/8	67	18
2	gi | 224027	Glucoamylase G1	37/9	103	26

* Proteins with a score of more than 52 were regarded as significant

6.2.2 Application of recombinanat fructofuranosidase for biosynthesis of neo-sugars

It was now relevant to evaluate the full value of the developed process by application of the produced enzyme to a biotransformation of substantial commercial interest. For this purpose additional experiments coupling the steps of production of fructofuranosidase by *A. niger* using the described micro particle based process, enzyme preparation from the culture broth and its application to the biosynthesis of high-value neo-sugars of the inulin type (Figure 50A) was now carried out.

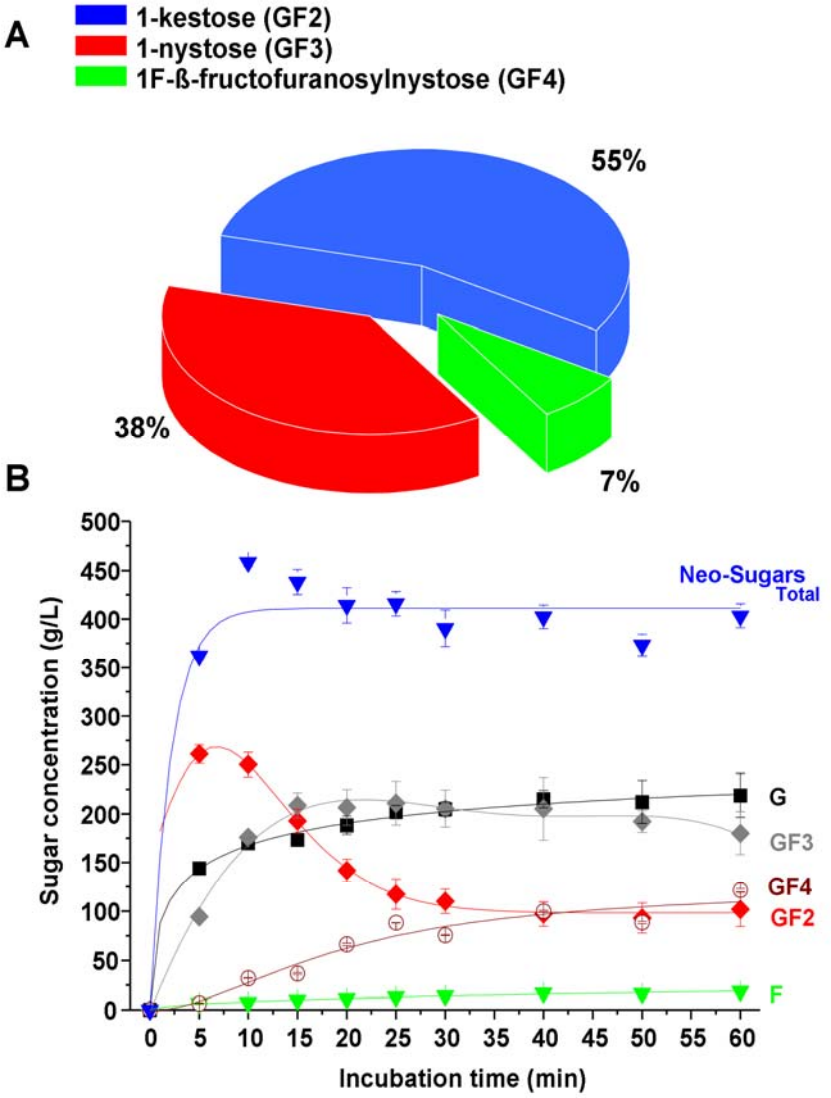

Figure 50: Enzymatic reaction including transfructorylation towards GF1, Sucrose; GF2, 1-kestose, GF3, 1-nystose and GF4, 1F-fructofuranosylnystose (A). Biosynthesis of neo-sugars of the inulin type by recombinant fructofuranosidase (B). Batch production of neo-sugars by fructofuranosidase produced by recombinant *A. niger* SKAn1015 in a micro particle enhanced batch process. The reaction conditions in the enzymatic conversion were: fructofuranosidase activity 860 U/mL; 500 g/L sucrose; 50°C; pH 5.4. Sugars and neo-sugars were quantified by HPLC using external calibration with pure standards.

Fructofuranosidase was produced in submerged culture by a micro particles enhanced batch-process using the recombinant strain *A. niger* SKAn1015 as described previously. Operated in normal batch mode, an enzyme level of 900 U/mL was obtained after 100 h.

The culture supernatant (20 mL), clarified from cells and micro particles by filtration through a cellulose acetate filter (pore size 20 µm, Sartorius, Göttingen, Germany), was mixed with 90 mL sucrose solution (pH 5.4, 50 mM phosphate buffer) to an initial concentration of 500 g/L sucrose and subsequently incubated under slight rotation (120 rpm) at 50°C. Within only 10 minutes, sucrose was almost completely converted into the desired products, indicated by the high level of about 450 g/L neo-sugars (Figure 50B). The formed products comprised the high value compounds 1-kestose (55%), 1-nystose (38%) and 1F-β-fructofuranosylnystose (7%), respectively (Figure 49A). By extension of the incubation time, the product spectrum could be successfully shifted towards the higher weight neo-sugars, i.e., 1F-β-fructofuranosylnystose. During this time a slight decrease of the total amount of neo-sugars was observed which might be due to hydrolysis. The transfructosylating and hydrolytic activity ratio was 25, matching nicely with previous observations for this recombinant fungal fructofuranosidase (Zuccaro et al. 2008). Variation of the substrate of sucrose analogues i.e. galactose-fructose, mannose-fructose, fructose-fructose and xylose-fructose (R-fructose) might be an interesting option to extend the product range of the produced recombinant fructofuranosidase from *A. niger* SKAn1015 (Baciu et al. 2005; Seibel et al. 2006; Zuccaro et al. 2008). This has exciting potential for the development of novel sugars derivatives (Kralj et al. 2008). Overall, the results demonstrate that the novel approach of targeted morphology engineering is an effective strategy for biotechnological enzyme production by filamentous fungi. Any negative interference with subsequent application of the enzyme produced for biocatalysis was did not observe. In fact, with minimal pre-treatment the enzyme obtained allowed highly efficient bioconversion towards prebiotics of commercial interest. Due to the wide use of filamentous fungi the application potential of micro particles in fungal fermentations appears large.

6.3 Metabolic Flux Analysis and Design

As shown the creation of an *A. niger* strain with high expression of the recombinant product encoding gene (Fleissner and Dersch 2010), medium design and bioprocess optimization was enabled an efficient production process for fructofuranosidase. Neo-sugars of the inulin type, prebiotics with substantial commercial interest. This promising situation now drives increasing interest on the underlying metabolism of *A. niger* towards further optimization. Hereby, metabolic flux analysis has proven as powerful method to unravel key production characteristics and metabolic engineering targets due to the close correlation of the metabolic fluxes to the cellular phenotype. Concerning *A. niger,* metabolic flux analysis which evolved from pioneering studies on small stoichiometric models (Pedersen et al. 2000b; Schmidt et al. 1999) has revealed that fluxes in *A. niger* are flexible depending on the nutrient status, genetic background or the type of product formed (Andersen et al. 2008; Meijer et al. 2009). Obviously, the filamentous fungus re-distributes the flux of carbon to adjust its metabolism to the environmental conditions or the actual requirement for product biosynthesis. This appears most relevant to the production of fructofuranosidase.

In this chapter the elucidation of intracellular fluxes in two strains of *A. niger,* the fructofuranosidase producing recombinant strain SKAn1015 and the parent wild type strain SKANip8 was reported. On the basis of ^{13}C-labelling experiments during batch cultivation the study focussed on the major pathways of the carbon core metabolism under conditions of optimal production, recently identified (Driouch et al. 2010a, Driouch et al. 2010b). A compartmented large-scale metabolic model of the central metabolism of *A. niger* (Figure 19) was used in combination with metabolic flux ratio analysis (Zamboni et al. 2005) to estimate the in vivo metabolic fluxes from ^{13}C labelling data of proteinogenic amino acids measured by GC-MS, measured extracellular rates, and anabolic fluxes.

Beyond a detailed investigation of the underlying metabolic physiology on the flux level, the integration of in vivo flux data with in silico flux data, obtained from elementary flux mode analysis for the same metabolic network was applied for model based strain design. This appears particularly important in recombinant protein production requesting for additional targets in central metabolism complementing the overexpression of the recombinant gene itself.

6.3.1 Growth and production performance

The effect of recombinant fructofuranosidase expression on the physiology of *A. niger* was first assessed in comparative batch cultures of the wild type SKANip8 and the recombinant strain SKAn1015 (Figures 51A-C), which expresses the target enzyme under control of the constitutive *pki*A promoter.

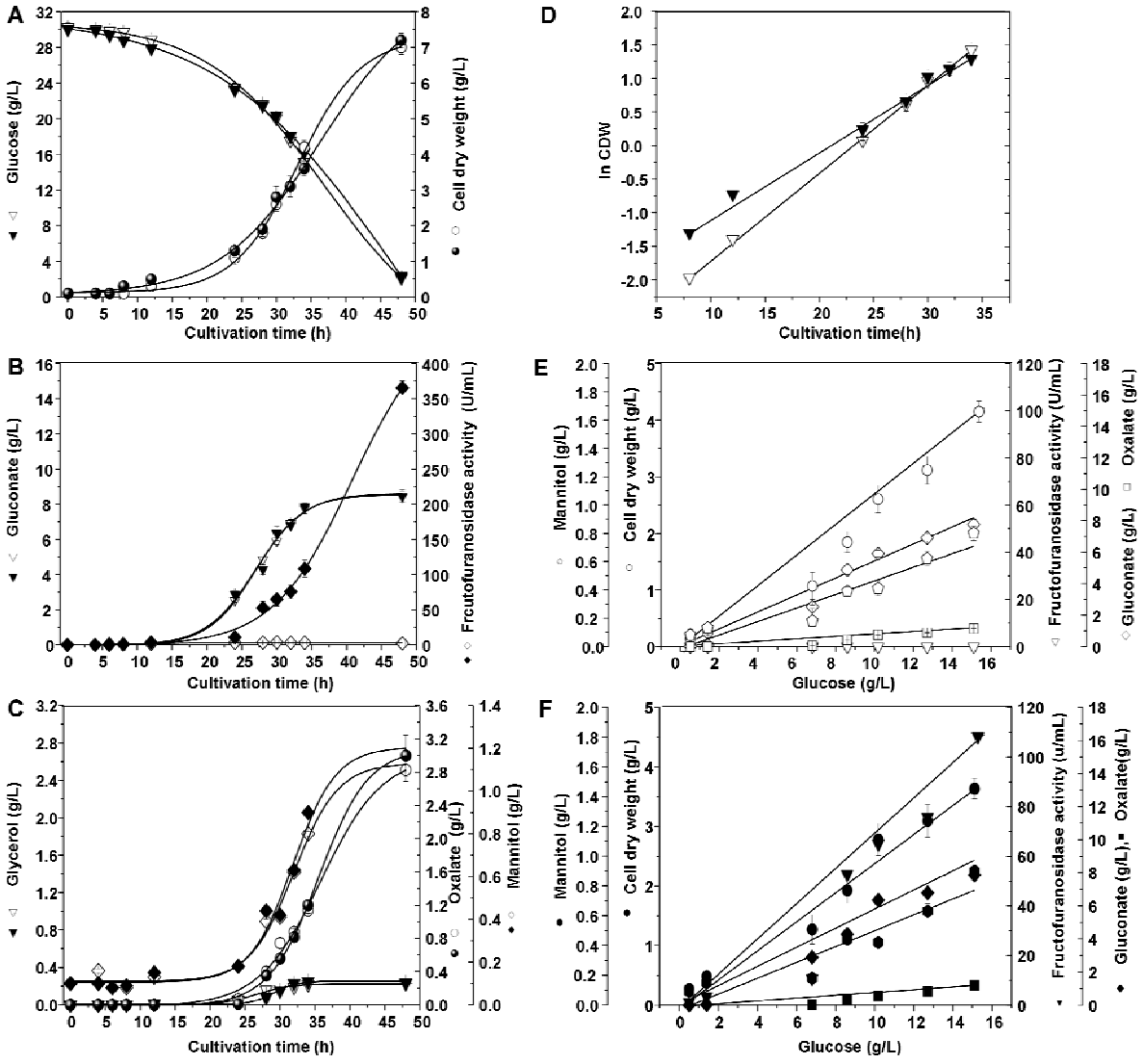

Figure 51: Cultivation profile of *Aspergillus niger* SKANip8 (wild type) and SKAn1015 (recombinant fructofuranosidase producer) during batch growth on defined medium with glucose and nitrate. Open symbols reflect the wild type, solid symbols the recombinant strain. Data given represent mean values and deviations from three replicate cultures for each strain.

The recombinant strain accumulated about 370 U/mL of fructofuranosidase after 48 h, whereas production in the wild type strain was negligible. The electrophoretic analysis of the culture supernatant of the recombinant strain reflected fructofuranosidase (120 kDa) as dominating protein (Figure 52).

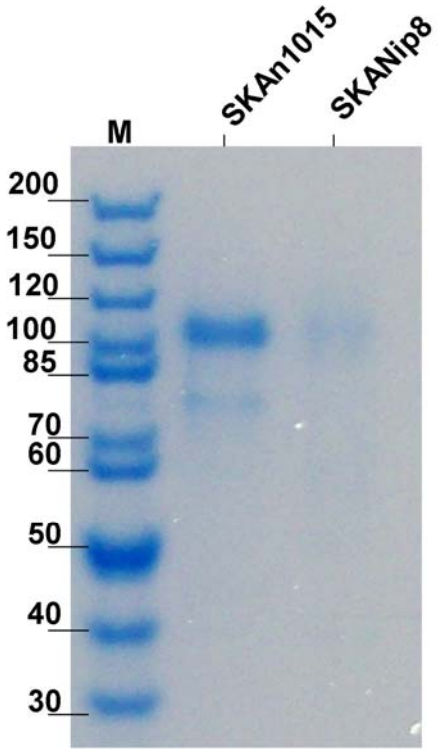

Figure 52: Sodium dodecyl sulphate-polyacrylamide gel electrophoresis analysis of culture supernatant from *Aspergillus niger* SKANip8 and SKAn1015. The left lane (M) shows the molecular weight marker. The strong band at about 110-120 kDa corresponds to fructofuranosidase (Zuccaro et al. 2008).

The relative quantification of the enzyme level via the volume of all observed bands in the 1-D gel revealed that fructofuranosidase accounted for 95 % of the totally excreted protein. Taking the total protein concentration in the culture supernatant into account (Table 15), this corresponds to an enzyme titre of 0.4 g/L of fructofuranosidase formed after 48 h. In contrast, the reference strain did not exhibit production (Figure 51). After an initial phase of spore swelling and germination, both strains grew exponentially until about 48 h of cultivation. During this period glucose as sole carbon source was completely consumed. Hereby the specific growth rate of 0.10 h^{-1} (producer) and 0.11 h^{-1} (wild type) did not differ significantly.

Table 15: Physiology of *Aspergillus niger* SKANip8 (wild type) and SKAn1015 (recombinant fructofuranosidase producer) during batch cultivation on glucose and nitrate. The data represent the exponential phase obtained from three replicates for each strain.

	SKANip8 Wild type	**SKAn1015 Producer**
Cell dry weight (g/L)	7.0±0.2	7.2± 0.2
Specific growth rate (h^{-1})	0.11±0.01	0.10±0.01
Biomass yield on glucose (g/g)	0.37±0.02	0.36±0.02
Spec. glucose uptake rate (mmol/g*h)	1.59±0.01	1.51±0.01
Fructofuranosidase activity (U/mL)	0±0	370±6
Spec. fructofuranosidase activity (U/mg)	0±0	51±2
Protein concentration (g/L)	0±0	0.4 ±0.1

The wild type strain reached a slightly higher biomass concentration. It was interesting to note that, under producing and under non-producing conditions, only 70 % of the glucose was channelled into the central metabolism, but 30 % was directly converted into gluconate accumulating up to 8 g/L in the medium. This organic acid displayed the major by-product. In addition, minor amounts of oxalate, mannitol and glycerol were detected. The levels of the by-products did not differ significantly between both strains. Beyond the phase of 48 h growth ceased and the biomass concentration remained constant (data not shown). However, cells maintained metabolic activity, which was linked to re-utilization of gluconate as carbon source and continuing enzyme secretion. Overall, the three biological replicates for each strain exhibited high agreement which underlines the consistency of the data.

A crucial pre-requisite for valid flux data in batch culture was balanced growth linked to pseudo-steady state. From batch cultures, this can be deduced from constant kinetic and stoichiometric characteristics of the cells, as well as from isotopic steady-state (Becker et al. 2008). Careful revision of the investigated process confirmed metabolic steady-state up to 35 h for both strains. During this period, cells grew exponentially with a constant specific growth rate (Figure 51D). Moreover, the yield coefficients for growth and by-products remained constant over time (Figures 51E-F). Isotopic steady-state was proven by verifying constant labelling patterns of the proteinogenic amino acids during the cultivation (see Appendix B-C). This enabled

valid ^{13}C metabolic flux analysis on the growth related production of fructofuranosidase. For the calculation, the corresponding time averaged yield coefficients and rates during this initial phase (Table 15) as well as the GC-MS labelling data (see Appendix B-C) of the cultivation were considered for the flux calculation.

6.3.2 Metabolic pathway fluxes in the wild type

Central carbon metabolism of *A. niger* was studied by adapting the metabolic flux ratio analysis (METAFoR) previously used for other eukaryotic microorganisms (Blank et al. 2005; Blank and Sauer 2004) on the basis of a thorough evaluation of the compartmented network structure. A qualitative inspection of the metabolic flux ratios estimated from the labelling data reveals that glucose-grown *A. niger* exhibits simultaneous contribution of glycolysis and pentose phosphate pathway (PPP) to the break-down of glucose (Table 15). The flux through malic enzyme as an additional alternative for NADPH production was found to be zero, indicating the PPP as major source for NADPH. Also, cytosolic phosphoenolpyruvate carboxykinase was found inactive.

The overall flux distribution in the central metabolism was estimated on basis of the compartmented stoichiometric model of the *A. niger* metabolism (Figure 53), the measured extracellular rates (Table 15), the metabolic flux ratios as ^{13}C-constraints (Table 16) and known precursor requirements for anabolism and fructofuranosidase biosynthesis (see Appendix D). As major physiological characteristics, *A. niger* revealed an oxidative metabolism with cyclic operation of the TCA cycle (Figure 53). Pyruvate and to a lower extent oxaloacetate were the major precursors transported into the mitochondrion. About 30% of the up-taken glucose was directed through the PPP. The flux was obviously higher than required for anabolic demands by this pathway so that a substantial amount of carbon was redirected back into the glycolytic chain at the level of fructose 6-phosphate and glyceraldehyde 3-phosphate. This confirmed the important role of the PPP to the NADPH supply. It was now interesting to see how *A. niger* corresponded to the metabolic burden imposed by expression of fructofuranosidase.

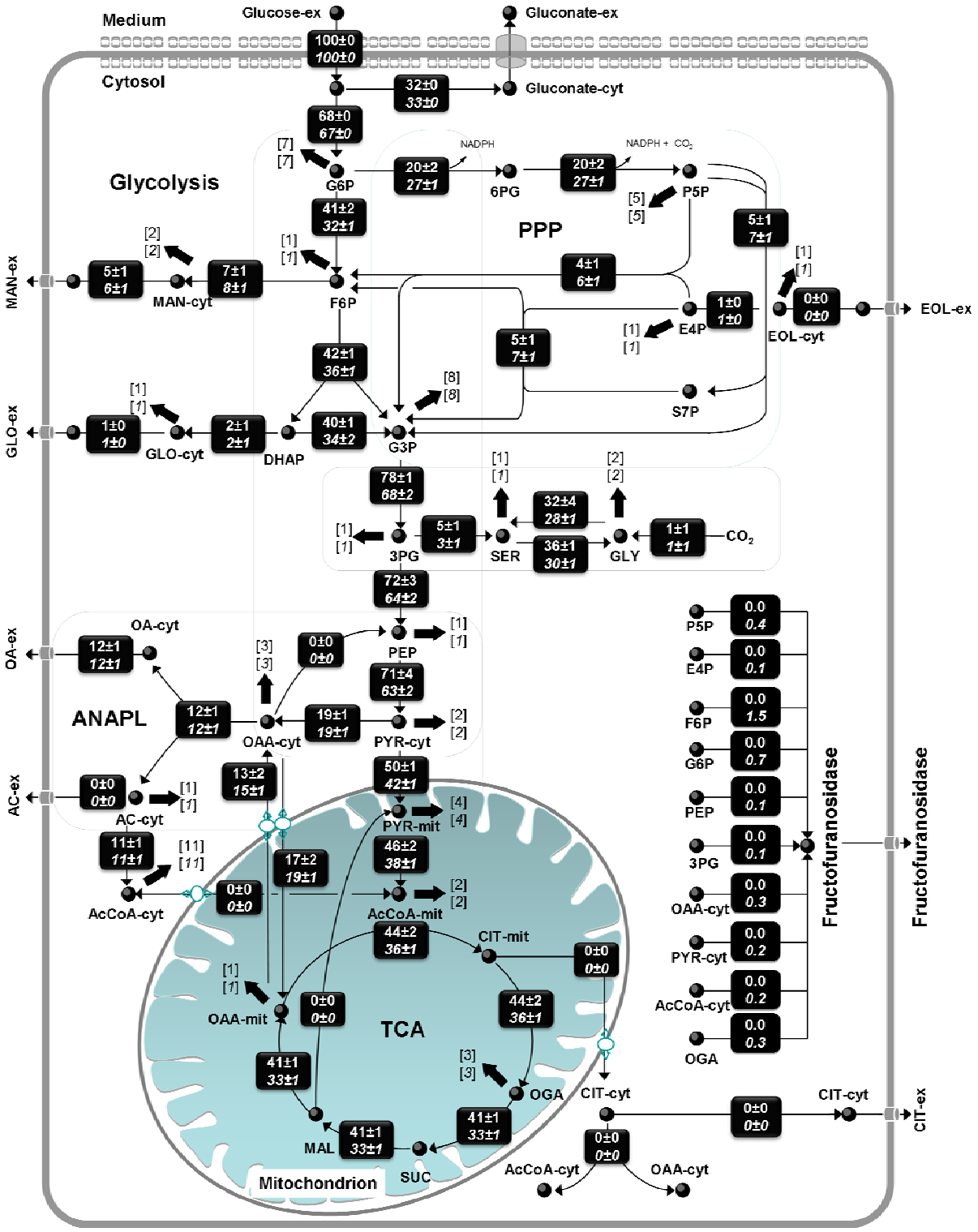

Figure 53: Metabolic flux distribution of *Aspergillus niger* SKANip8 (wild type, top) and SKAn1015 (recombinant fructofuranosidase producer, bottom) during batch growth on defined medium with glucose and nitrate. All fluxes are normalized to the specific glucose uptake rate which was 1.59 ± 0.01 mMol/g/h for the wild type and 1.51 ± 0.01 mMol/g/h for the producer. The complete set of reactions and abbreviations of the underlying stoichiometric model is listed in Appendix A.

Table 16. Metabolic flux ratios of the wild type *Aspergillus niger* SKANip8 and the fructofuranosidase producing strain *Aspergillus niger* SKAn1015 obtained from [1-^{13}C] and [U-^{13}C] glucose experiments.

Strains	Fraction of total pool (%) (Mean ± SD)	
	SKANip8 Wild type	**SKAn1015 Producer**
Glycolysis and PP pathway		
SER through Glycolysis	27±1	33±1
R5P from G6P (ld)	24±2	11±1
R5P from T3P and S7P (*tkl* reaction)	30±3	36±1
R5P from E4P (*tkl/tal* reaction)	47±1	55±2
E4P from TK	67±3	67±1
C1-Metabolism		
SER from GLY	39±1	41±1
GLY from SER	66±1	67±1
Labeled CO_2	51±3	53±1
Glycolysis, ANAPL and TCA cycle		
PEP-cyt from OAA-cyt (*pepck*)	00±0	00±0
OAA-cyt from PYR-cyt	60±1	80±1
AcCoA-mit from PYR-mit	n.d	104±1
OAA-mit from ANAPL	50±1	74±1
OAA-mit from ANAPL (old)	41±1	48±1
PYR-mit from MAL (*me*, ud)	0±0	0±0
PYR-mit from MAL (*me,* ld)	0±0	0±0

lb: lower bound, up: upper bound, *tkl*: transketolase, *tal*: transaldolase, *pepck:* PEP caboxykinase, *me*: malic enzyme, n.d.: not detectable because the fragment needed for tracing this activity was absent, SD: standard deviation.

6.3.3 Response of metabolic pathway fluxes to recombinant fructofuranosidase production

The recombinant strain exhibited a strong up-regulation of the carbon flux into the PP pathway, whereas the flux through the glycolysis was reduced (Figure 54). Directly linked to the elevated demand for glucose 6-phosphate and fructose 6-phosphate as sugar precursors of the highly glycosylated fructofuranosidase in the recombinant strain, the flux towards the lower glycolytic chain was lower. As a result, the overall carbon flux entering the cytosolic pyruvate pool was reduced by more than 10 %. This caused a significantly decreased TCA cycle flux in the recombinant strain. In addition to these obvious flux differences, other reactions were found rather similar

between the two strains. Cytosolic phosphoenolpyruvate carboxykinase *(pepck)* and mitochondrial malic enzyme (*me)* were found inactive. Moreover, both strains revealed a high anaplerotic flux towards cytosolic oxaloacetate, which was to a large extent channelled into the by-product oxalate and only partly served for anabolic purposes.

6.3.4 In silico pathway analysis of recombinant fructofuranosidase production

Structural properties of the metabolic network of *A. niger* for recombinant production of fructofuranosidase were studied using elementary flux mode analysis. Assuming glucose as carbon source and nitrate as nitrogen source, 109,661 different elementary modes resulted. The modes differed substantially in the corresponding yield for the enzyme or the biomass (Figure 54).

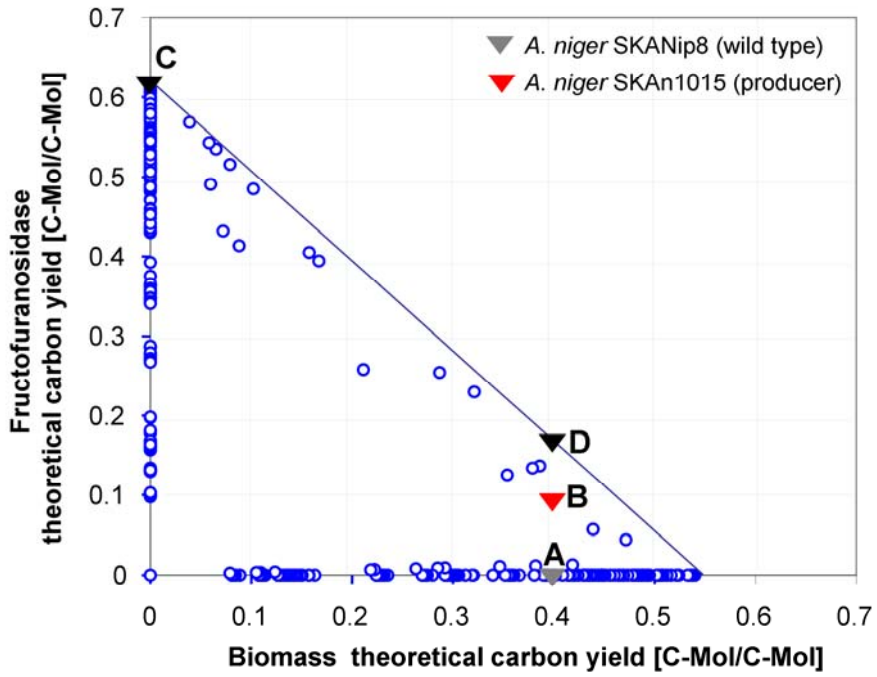

Figure 54: Metabolic states of *Aspergillus niger* assessed from in vivo and in silico flux analysis (Melzer et al. 2009). The data comprise the set of elementary modes for fructofuranosidase and biomass production on glucose and nitrate and were taken from (Melzer et al. 2009). The solution space of the elementary modes, represented by the open circles dots, is marked through the interior as well as the sides of the rectangular triangle. The modes on the axes represent extreme modes exclusively linked to production of fructofuranosidase or biomass. Additionally the experimentally observed metabolic states of the wild type *A. niger* SKANip8 (A) and the recombinant strain *A. niger* SKAn1015 (B) are shown. The other states reflect the theoretical optimum for fructofuranosidase production at zero growth (C) and for the biomass yield resulting for the producing strain (D).

The dominating fraction of modes was linked to exclusive production of either fructofuranosidase or biomass, respectively. Overall, 43% of the modes (47,508) were linked to fructofuranosidase production. Simultaneous biomass and fructofuranosidase production was observed for 2.7% of the modes (2,950). The maximum theoretical carbon yield for fructofuranosidase was 0.61 C-Mol/C-Mol, i.e. the upper left corner of the triangle (Figure 54).

6.3.5 Integration of in silico and in vivo pathway fluxes for strain design

In addition to the evaluation of the overall performance of *A. niger*, the large set of elementary modes contained unique in silico flux distributions for various metabolic states. These were now analysed further considering elementary modes that displayed simultaneous production of the enzyme and biomass and matched the observed phenotype of the studied strains. It was particularly interesting to see, how the different reactions correlated with the production of the recombinant enzyme. For this purpose, flux correlation coefficients (α_{silico}), quantifying the correlation of each flux (v_i) with the target flux (v_j) were extracted via correlation analysis of the corresponding elementary modes (Eq. 10).

$$\alpha_{silico} = \frac{\mathrm{cov}(v_j, v_i)}{\delta_j^2} \qquad (10)$$

Overall, a quite diverse picture resulted for the different reactions of the *A. niger* network with glucose and nitrate as substrates. Positive values resulted e. g. for the PPP reactions, illustrating that the underlying fluxes increase with higher fructofuranosidase production, whereas the opposite was found for the TCA cycle or the formation of by-products (Table 15). Complementary, flux correlation coefficients were also extracted from the in vivo flux data sets of the two compared *Aspergillus* strains (Figure 54). Again, this was carried out for each flux (v_i) related to the flux towards fructofuranosidase production (v_j), Eq. 11.

$$\alpha_{vivo} = \frac{\mathrm{cov}(v_j, v_i)}{\delta_j^2} \qquad (11)$$

The result directly visualizes the flux response to the metabolic burden of product formation and allows to differentiate between increased (positive value), decreased (negative value) and unaffected (zero value) reactions (Table 17).

Notably, the integration of the computational and the experimental flux data revealed that – upon expression of the recombinant enzyme, fluxes in *A. niger* were influenced quite differently with regard to the predicted optimum (Figure 55).

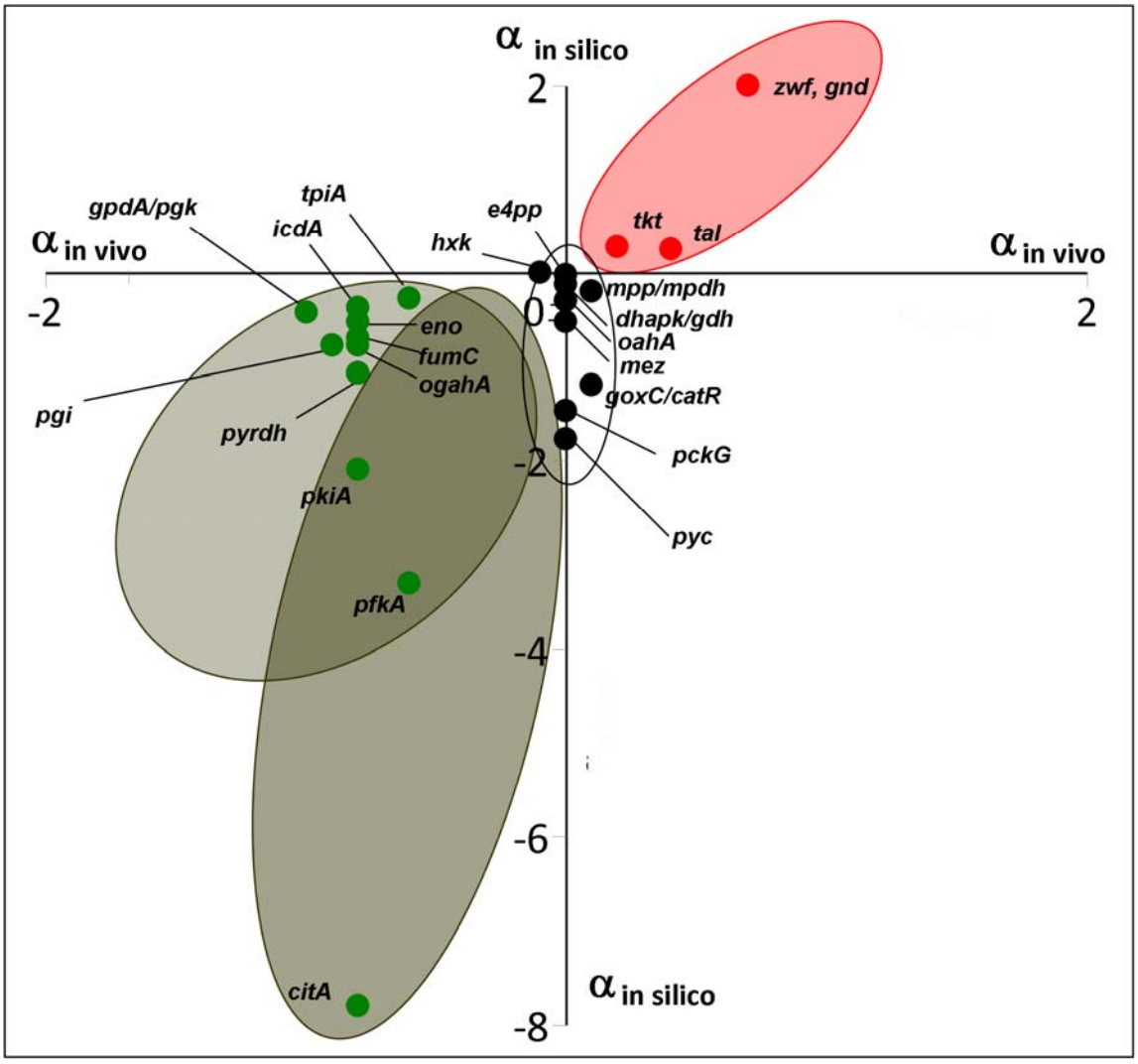

Figure 55: Integration of in silico and in vivo pathway fluxes for strain design.

Table 17. Integration of in silico and in vivo pathway fluxes of *Aspergillus niger* for strain design towards improved fructofuranosidase production.

Gene	ANgxx number	$\alpha_{in\text{-}vivo}$	$\alpha_{in\text{-}sil}$
goxC/catR	**An01g14740/An01g01550**	0.1	-1.2
hxk	**An02g14380**	-0.1	0
pgi	**An16g05420**	-0.9	-0.8
pfkA/fda	**An18g01670/An02g07470**	-0.6	-3.3
tpiA	**An02g04920**	-0.6	-0.3
gpd/pgk	***An16g01830*/An08g02260**	-1.0	-0.4
enol	**An18g06250**	-0.8	-0.5
pkiA	**An07g08990**	-0.8	-2.1
zwf/gnd	**An02g12140/An11g06120**	0.7	2.0
rpe/rpi/tkt1	**An11g02040/An02g02930/An02930**	0.2	0.3
tkt2/tal	**An07g03850/An08g06430**	0.4	0.2
pyc	**An04g02090**	0	-1.7
acsmpp/mpdh	**An02g14380/An06g00750**	0.1	-0.2
dhapk/gdh	**An15g02200/An18g05480**	0	-0.1
pckG	**An05g02550**	0	-1.5
oahA	**An10g00820**	0	-0.3
pyrdh	**An07g09530**	-0.8	-1.1
citA	**An09g06680**	-0.8	-7.8
icdA	**An08g05580**	-0.8	-0.4
ogahA	**An08g02970**	-0.8	-0.8
sucD	**An14g04395**	-0.8	-1.1
fumC	**An12g07850**	-0.8	-0.7
mdh	**An07g03850**	-0.8	-1.1
mez	**An12g00160**	0	-0.5
e4pp, er	**An01g06970**	0	-0.02

6.3.6 Flux response to cellular burden imposed by production

The recombinant *A. niger* SKAn1015, expressing recombinant fructofuranosidase under control of a constitutive promoter, revealed efficient secretion of the target product as compared to its parent strain. As shown the organism was capable to maintain its overall growth behaviour despite the significant cellular demand for biosynthesis of the large, highly glycosylated protein. Production was accompanied by a change in the fluxes through the PPP and the TCA cycle. All of the observed changes were mediated through flux redistribution, as the expression of the recombinant gene itself was the only genetic perturbation performed. The PPP is the major pathway for production of NADPH, especially in *A. niger* obviously lacking contribution of malic enzyme to supply of this cofactor. The relative flux through the oxidative PP pathway normalized to the glucose uptake rate was 27% in the fructofuranosidase-producing strain SKAn1015 and thus higher as compared to the

wild type SKANip8 (20%). NADPH is particularly required for biosynthesis of fructofuranosidase, so that the flux increase probably reflects the increased demand for this cofactor in the recombinant strain.

Similar findings result from comparative flux analysis of wild type and amylase-producing strains of *A. oryzae* (Pedersen et al. 1999). In this light the use of nitrate as nitrogen source, requiring NADPH for reduction to ammonia (Diano et al. 2006) might compete with production. Both strains revealed flux differences in anabolic reactions and the steps of the TCA cycle. The central metabolites, pyruvate and oxaloacetate, display important branch points of central carbon metabolism and organic acid production (Meijer et al. 2007). Pyruvate can enter the TCA cycle localized in the mitochondria in two ways: either involving oxidative decarboxylation into acetyl-CoA via pyruvate dehydrogenase or carboxylation into oxaloacetate by pyruvate carboxylase in the cytosol. The two strains recruit both pathways for this purpose. The comparison with ^{13}C-data sets from other *Aspergilli* illustrates that the observed flux pattern, i.e. the changing contribution of the PPP and the TCA cycle displays a general feature of the underlying carbon core metabolism in filamentous fungi (Figure 56).

Among various reactions of the central metabolism, these two pathways reveal the highest flexibility and obviously play a central role for the cells to cope with different environments or cellular burdens. As example, the relative PPP flux can increase to almost 60%, as observed for glucoamylase producing *A. niger* during batch cultivation (Pedersen et al. 2000b), but can also exhibit low values of 20%, as reported here or from previous chemostat culture of *A. nidulans* (David et al. 2003). Notably, metabolic flexibility in yeasts is also mediated via flux adaptation through the PPP and the TCA cycle (Blank et al. 2005; Blank and Sauer 2004).

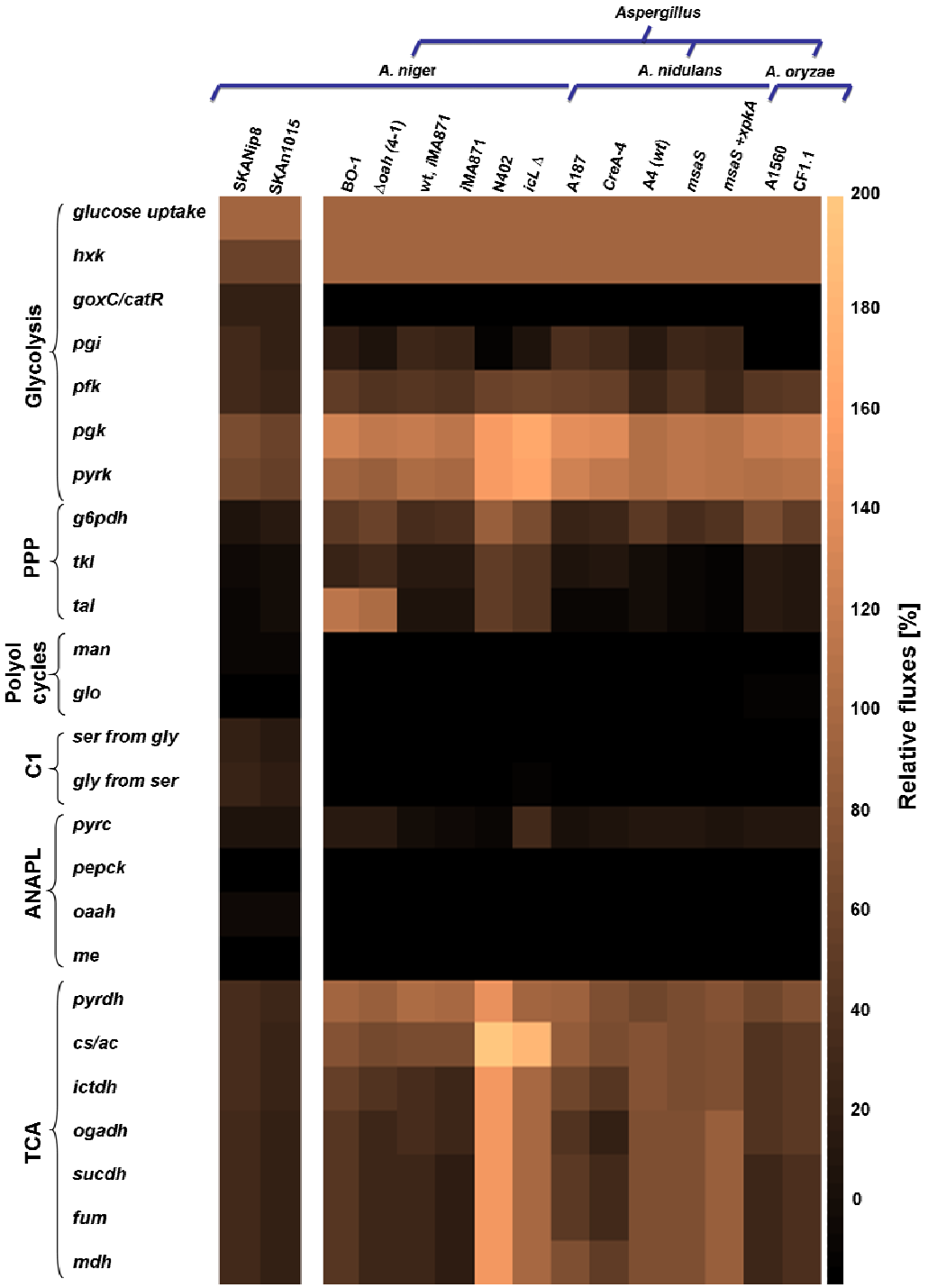

Figure 56: Metabolic flux fingerprints of *A. niger* SKANip8 and SKAn1015 (this work) and of previously reported *Aspergillus* species from ^{13}C-experiments involving, a wild-type strain (A150) and a recombinant strain (CF1.1) of *A. oryzae* producing α-amylase studied in chemostat culture (Pedersen et al. 1999), two glucoamylase producing strains of *A. niger* (BO-1 and a oxalic acid negative mutant from batch cultivation (Pedersen et al. 2000b), a reference strain (A187) and a Δ*cre*A mutant and *A. nidulans* from batch cultivation and polyketides production by three strain of A. nidulans including wt, *msa*S, *msas+xpk*A (David et al. 2005; Panagiotou et al. 2009) and different strains of *A. niger* including a Δ*oah* mutant (Andersen et al. 2008) and an isocitrate lyase overexpressing strain AB4.1 (Meijer et al. 2009).

6.3.7 Integration of in silico and in vivo metabolic states for strain evaluation and design.

The integrated analysis of in vivo and in silico flux data now provides a design space for strain engineering that can make use of the underlying physiology observed in the production process. Corresponding to their production behaviour the two strains can be placed within the resulting triangle space spanned by elementary flux mode analysis. This results in the two metabolic states A (wild type) and B (producer). Clearly, the recombinant strain exhibits an improved yield as compared to its parent strain, but production is still far from the theoretical optimum. Moreover, it becomes clear that the achieved increase in production is not linked to negative effects on growth, as the biomass yield is maintained. The distance between the actual flux state of the producer (B) and the theoretical optimum (C) suggests an enormous remaining potential for future optimization (Figure 54). Obviously, the observed yield in the recombinant producer displays only 17% of the maximum potential, suggesting that further strain engineering appears generally promising. Furthermore it can be predicted that the optimization of fructofuranosidase-producing *A. niger* SKAn1015 towards higher protein yields, beyond a certain limit, would be inherently linked to reduced growth performance. The maximum production possible for the observed biomass yield of the recombinant strain (Table 15) is given by the metabolic state D, located on the boundary of the solution space. The predicted fructofuranosidase yield of 0.18 C-Mol/C-Mol is thus only slightly higher. Beyond this remaining limit, increased protein production directly goes at the expense of growth. From the metabolic viewpoint, fructofuranosidase and biomass production compete for common amino acid and sugar building blocks, cofactors and energy. This has direct consequences for the evaluation of strain and process engineering. At a certain point of development, negative growth effects are inherently caused by the imposed metabolic state, but do not necessarily indicate a wrong strain engineering strategy. Alternatively, a two-step cultivation process decoupling growth and enzyme production in different phases might be attractive to overcome the predicted limitations.

To fully account for the high complexity of the underlying networks and select valid targets out of many possible candidates, systems-wide modelling approaches including OptKnock (Suthers et al. 2007) OptGene (Patil et al. 2005), minimization of

metabolic adjustment (Segre et al. 2002) or flux design (Trinh et al. 2008) have emerged from the rapidly increasing amount of genome-scale models. These are attractive from their straightforward strategy to directly exploit stoichiometric network information and allow broad simulation studies on various aspects (Kim et al. 2008). They, however, do not consider physiological information on the system to be optimized, e.g. on the level of regulation. To integrate physiology into strain design, the present work combines the power of computational network simulation with the resolution of experimental network analysis on the flux level (Figure 54). This appears particularly important in recombinant protein production requesting for additional targets in central metabolism complementing the overexpression of the recombinant gene itself.

In this regard, the integration of in silico and in vivo analysis allowed evaluating the relevance of each reaction from its position in the flux correlation plot. Shortly, the origin of the figure displays the starting point of development. The distance of a reaction from the origin in y-direction indicates the predicted potential of changing the corresponding flux for optimization in silico, whereas the distance in x-direction showed the realized flux alteration in vivo. Notably, specific reactions were highlighted as most relevant within a pathway. This resulted for *zwf/gnd* within the PPP, *citA* (TCA cycle) or *pfkA* (glycolysis) which all display interesting candidates for further optimization. Other enzymes from the same pathways seem of lower relevance. Some reactions, including *pyc* or *pckG* or by-product forming pathways showed no or only a slight change in vivo, despite they obviously exhibit a potential for improved production. This could indicate inherent regulation mechanisms which prevent flux changes and therefore might be investigated further. A number or reactions close to the origin are identified as only slightly important.

This might narrow down the number of mutants to be potentially constructed in future strain engineering work. With regard to fructofuranosidase production, attenuation of phosphofructokinase (*pfkA*) or of citrate synthase (*citA*), deletion of by-product formation and amplification of glucose 6-phosphate dehydrogenase (*zwf*) emerge as important targets to be tested. Their relevance is partly confirmed from other filamentous fungi (Figure 55). Overall, the integration of in silico and in vivo fluxes might be a useful extension and complementation of recent concepts such as a

bi-level optimization (OptReg) on the basis of experimental flux data and regulation strength parameters (Pharkya and Maranas 2006), flux converging pattern analysis using real fluxes as constraints for predictions (Park et al. 2010) or design-based systems metabolic engineering strategies (Becker et al. 2011).

7 CONCLUSIONS AND FUTURE PERSPECTIVES

The present work describes comprehensive systems biotechnology studies of *Aspergillus niger* towards optimized production of recombinant proteins. This combined systems-wide analysis, fluxome analyses by ^{13}C-isotope studies, in silico design and process-driven engineering of the bioreactor environment.

Micro particles for tailor-made fungal morphology and enhanced enzyme production.

The close link between fungal morphology and productivity could be exploited to create superior morphoggy of *A. niger*, i.e. free dispersed mycelium or high-actively bio-pellets for enhanced enzyme production. With increasing concentration of micro particles added the pellet size could be precisely adjusted down to even freely dispersed mycelium. The properties of the added material obviously played an important role. For alumina, a higher concentration was required to achieve the same morphology as compared to talc. This might be attributed to the different particle size, expressed by the average diameter for talc (6 µm) and alumina (14 µm). Moreover, also the specific shape of the used particles is rather different, as illustrated by electron microscopy analysis. At this point, it appears possible that the smooth, round-shaped alumina particles may have less impact to disrupt spore aggregates as compared to the sharp-edged silica particles. However, detailed studies are necessary to really unravel the mechanisms of interaction between the fungus and the particles. For both materials, the production of fructofuranosidase exhibited an optimum. The biomass formation was strongly influenced, additionally; the accumulation of the undesired by-product oxalate was suppressed by up to 90%. The overall response of the cells to the micro particles was not a general stimulation of metabolism but a rather complex change of physiology. This opens new avenues for future work, especially toward understanding of the molecular mechanisms that link morphology with the underlying metabolic and regulatory networks. Moreover, others material to the tested organic particles could be used with non-genetically modified organism biomass and functionalized particles e.g. in situ product removal as a tool for bioprocessing (ISPR) to improve yield or productivity.

Micro particle-enhanced bioprocess for production of fructofuranosidase.

The beneficial influence of the micro material on important metabolic characteristics of *A. niger* opens a new strategy for superior enzyme production. This was demonstrated for fructofuranosidase production by recombinant *A. niger* SKAn1015. Fructofuranosidase is an important industrial biocatalyst for the synthesis of neo-sugars as functional food ingredients. Combined with model based medium design, identifying elevated levels of glucose, $NaNO_3$, $MnCl_2 \cdot 4H_2O$ and $FeSO_4 \cdot 7H_2O$ as beneficial, and the development of a suitable bioprocess strategy the application of talc micro particles allowed highly efficient enzyme production. When transferred into a fed-batch environment with intermittent feeding of glucose, a high fructofuranosidase activity of 2,800 U/mL, corresponding to an enzyme titre of about 3 g/L could be achieved. Starting from the original medium in batch operated shake flasks (140 U/mL) the enzyme level could thus be optimized by a factor of twenty. Compared to all fructofuranosidase-producing processes reported so far, the achieved enzyme titre by the micro particle-enhanced fed-batch process on minimal medium is more than tenfold higher, underlining the enormous potential of the use of micro particles. Future rational based approaches such as metabolic engineering of *A. niger* SKAn1015 could aim at disruption of the encoding glucoamylase gene to completely prevent its formation, if needed.

Application of neo-sugars from *Aspergillus niger* fructofuranosidase.

To fuller assess the potential of the process, additional experiments coupled the steps of production of fructofuranosidase by *A. niger* SKAn1015 using the described micro particle based process, enzyme preparation (900 U/mL) from the culture broth of a micro particles enhanced batch-process using the recombinant strain SKAn1015 after 100 h cultivation time and its application to the biosynthesis of high-value neo-sugars was carried out. The produced culture supernatant (20 mL) with the secreted enzyme, clarified from cells and micro particles by filtration, was indubed of 500 g/L sucrose. Within only 10 minutes, sucrose was almost completely converted into the desired products, indicated by the high level of about 450 g/L neo-sugars. The formed products comprised the high value compounds 1-kestose (55%),

1-nystose (38%) and 1F-β-fructofuranosylnystose (7%), respectively. Variation of the substrate to sucrose analogues such as galactose-fructose, mannose-fructose, fructose-fructose and xylose-fructose could be an interesting option to extend the product range of the produced recombinant fructofuranosidase.

Metabolic flux analysis and design - Impact of recombinant protein production on in vivo and in silico fluxes.

Using ^{13}C-based metabolic flux ratio analysis, which provides a bird's-eye view of flux distribution, the complex, compartmented metabolism of both strains (producer SKAn1015 and wild type SKNip8) was compared on the flux level. The production of fructofuranosidase was linked to significant flux changes, most notably including an elevated flux through the PPP as major source of NADPH and an attenuated flux through the TCA cycle. Anaplerotic enzymes such as phosphoenolpyruvate carboxykinase, malic enzyme or the glyoxylate shunt were found inactive in both strains. In addition, characteristics of the metabolic network of *A. niger* were studied in silico using elementary flux mode analysis. The integration of measured and predicted flux changes for optimum performance allowed a quantitative evaluation of the achieved strain optimization. Beyond the expression of the recombinant protein itself, which is typically realized in protein production, this visualized targets in central metabolism, e.g. *zwf*, *citA* or *pfkA* supporting production as useful next steps in strain engineering.

Overall, the result reveals new detailed insights into glucose metabolism and its relation to fructofuranosidase production by *A. niger*, which can be used to design strategies for further improvements in the rate of fructofuranosidase production using design-based systems metabolic engineering which enables blocking the by-product pathway such as oxalate by deletion of *oahA* gene or amplification of the some enzyme leading to NADPH regeneration for the overproduction of the target product. The traditional oxidative and non-oxidative PPP could be enhanced with addition of *zwf/gnd* and/or *tkt* and *tal* genes, respectively. Glycolysis and TCA cycle could be enhanced by attenuation of *pkiA* and *pfkA* genes or *cit*A gene, respectively. Future metabolic engineering of *A. niger* SKAn1015 could aim at disruption of gene encoding glucoamylase and increase product purity. Along with in silico design using

elementary flux modes, the in vivo information gained from process optimization and ^{13}C-based metabolic flux ratio analysis, port in the present work can aid improvements of bioprocesses using these interesting filamentous fungi. In vivo and in silico flux analysis, suggests the identifiied enzyme as promising targets for metabolic engineering of the recombinant strain SKAn105. This strategy could be generally used to identify priority sorted amplification and attenuation targets for metabolic engineering purposes under various conditions and thus displays a useful strategy to be incorporated into efficient strain and bioprocess optimization, however, recombinant strains do not necessarily grow optimally.

Overall, the results of this thesis provide important a connection between morphology and productivity and give insights into metabolic of *A. niger* and thus key data towards a better biotechnological process for recombinant proteins production in the cell factory *A. niger*. Other fascinating metabolic effects of micro particles on the metabolic flux distribution of *A. niger* under different forms as previously demonstrated towards the recombinant fructofuranosidase production can be investigated using this systems biotechnology approach in the future.

8 LIST OF SYMBOLS

8.1 Abbreviations

Precursor

3PG	3-phosphoglycerate
AC	acetate
AcCoA	acetyl CoA
CIT	citrate
CO_2	carbon dioxide
DHAP	dihydroxyacetone-phosphate
E4P	erythrose 4-phosphate
EOL	erytrithol
F6P	fructose 6-phosphate
FUM	fumarate
G3P	glyceraldehyde 3-phosphate
G6P	glucose 6-phosphate
GLO	glycerol
ICT	isocitrate
MAL	malate
MAN	mannitol
OA	oxalate
OAA	cytosolic oxaloacetate
OGA	α-ketoglutarate
P5P	pentose 5-phosphate
PEP	phosphoenolpyruvate
S7P	sedoheptulose 7-phosphate
SUC	succinate
cyt	cytosolic
mit	mitochondrial
ex	extracellular

Enzyme

6pgdh	6-phosphogluconate dehydrogenase
acs	acetyl-CoA synthase (acetate-CoA ligase)
ct/ac	citrate synthase/ aconitase
ctl/acs	citrate lyase/acetate-CoA ligase
dhapk	DHAP kinase
dhapp	DHAP phosphatase
e4pp/er	erythrose 4-phosphate phosphatise/erythrose reductase
eno	enolase
Fpp	fructose 6-phosphate phosphatase
Fum	fumarase
g3pdh	NAD-dependent glycerol 3-phosphate dehydrogenase
g3pp	glycerol 3-phosphate phosphatise
g*6pdh*	gucose 6-Phosphate dehydrogenase
gdh	NAD/NADP-dependent glycerol dehydrogenase
gk	glycerol kinase
hxk	hexokinase
Icdh	isocitrate dehydrogenase
Icl	isocitrate lyase
Mdh	malate dehydrogenase
Mpdh	mannitol-phosphate dehydrogenase
me	malic enzyme
mpdh	mannitol 1-phosphate dehydrogenase
mpp	mannitol 1-phosphate phosphatase
ms	malate synthse
oaah	oxaloacetate hydrolase
ogdh	α-ketoglutarate dehadrogenase
pepck	phosphoenolpyruvate carboxykinase
pfk	6-phosphofructokinase
pgi	glucose 6-phosphate isomerise
pgk	phosphoglycerate kinase
pyrc	pyruvate carboxylase
pyrdh	pyruvate dehydrogenase
pyrk	pyruvate kinase

r5pe	ribulose 5-phosphate -epimerase
r5pi	ribulose 5-phosphate -isomerase
sucdh	succinate dehydrogenase
tal	transaldolase
tkl	transketolase

Amino acids

ALA	alanine
ASP	aspartate
GLU	glutamate
GLY	glycine
HIS	histidine
ILE	isoleucine
LEU	leucine
LYS	lysine
PHE	phenylalanine
PRO	proline
SER	serine
THR	threonine
TYR	tyrosine
VAL	valine

8.2 Latin Symbols

Symbol	Unit	Description
C	[g/L]	concentration
C_p	[mg/mL]	protein concentration
C_s	[Mol/m^3]	substrate concentration
D_{eff}	[m^2/s]	effective diffusion coefficient
M	[g/Mol]	molar mass
N		number of experiments
Q		total distribution
Qs	[Mol/g_{CDw}*h]	specific substrate uptake rate
R		correlation coefficient
R^2		coefficient of determination
T		target metabolite
U		mixture of [U-^{13}C] and natural glucose
V	[mL]	volume
X	[g/L]	biomass concentration
X_{50}		average particle size diameter
Y	[C-Mol/C-Mol]	yield coefficient

8.3 Greek Symbols

Symbol	Unit	Description
±α		axial points
f		fractional contribution in the response
i		number of metabolites
j		number of reactions
r_{crit}		critical radius
r_s	[mMol/gCDW*h]	glucose uptake rate
v	[mMol/gCDW*h]	metabolic flux
Y		response of a process
β		squared coefficient
Δr		thickness in pellets
ε		represents the noise or error observed
η		response surface
ρ	[g/cm^3]	density at 20-25 °C
ρ_{Pellet}	[kg/m^3]	pellet density
μ	[1/h]	specific growth rate
ν	[C-Mol/C-Mol]	flux yield
ξ	[C-Mol/Mol]	molar carbon content
t	[h]	time

8.4 List of Indices

Indices	Description
+/-1	high level / low level
1	100% of [1-^{13}C]glucose
aa	amino acids
Alumina	aluminium oxide
ANAPL	anaplerotic
ANOVA	analysis of variance
CCD	central composite design
cDNA	complementary DNA
CDW	cell dry weight
CLSM	confocal laser scanning microscopy
CO_2	carbon dioxide
CP	centre point
DoE	design of experiments
EMFA	elementary flux mode analysis
FD	factorial design
FFase	beta-fructofuranosidase
GA	glucoamylase
GC-TOF-MS	gas chromatography–time-of-flight mass spectrometry
GFP	green fluorescent protein
GLP	glyoxylate pathway
GRAS	generally recognised as safe
HPLC	high performance liquid chromatography
LC-MS	liquid chromatography mass spectrometry
M	precursor
M_0	fractional abundance of fragments withmonoisotopic mass
MALDI-TOF-MS	matrix assisted laser desorption ionization - time of flight mass spectrometry
max	maximal
MDV	mass isotopomer distribution vector
METAFoR	metabolic flux ratio analysis
M_i	abundances of molecules with higher masses
MS	mass spectrometry techniques
NMR	nuclear magnetic resonance
O_2	oxygen
OFAT	one-factor-at-a-time
P	product
P/V	volumetric power input
RSM	response surface methodology
S	substrate
sc-FOS	short chain fructooligosaccharides (neo-sugars)
SDS-PAGE	sodium dodecyl sulfate polyacrylamide gel electrophoresis
SEM	scanning electron microscope
Talc	magnesium silicate
TCA	tricarboxilic acid cycle
up	upper bound

9 LIST OF REFERENCES

Alvarez-Vasquez F, González-Alcon C, Torres NV. 2000. Metabolism of citric acid production by *Aspergillus niger*: model definition, steady-state analysis and constrained optimization of citric acid production rate. Biotechnol. Bioeng. 70:82-108.

Amanullah A, Christensen LH, Hansen K, Nienow AW, Thomas CR. 2002. Dependence of morphology on agitation intensity in fed-batch cultures of *Aspergillus oryzae* and its Implications for recombinant protein production. Biotechnol. Bioeng. 77:815-826.

Andersen MR, Lehmann L, Nielsen J. 2009. Systemic analysis of the response of *Aspergillus niger* to ambient pH. Gen. Biol. 10:R47.1-R47.14.

Andersen MR, Nielsen ML, Nielsen J. 2008. Metabolic model integration of the bibliome, genome, metabolome and reactome of *Aspergillus niger*. Mol. Syst. Biol. 4:178.

Andersen MR, Nielsen N. 2009. Current status of systems biology in *Aspergilli*. Funga.l Genand. Biol. 46:180-190.

Askenazi M, Driggers EM, Holtzman DA, Norman TC, Iverson S, Zimmer DP, Boers M-E, Blomquist PR, Martinez EJ, Monreal AW and others. 2003. Integrating transcriptional and metabolite profiles to direct the engineering of lovastatin-producing fungal strains. Nat. Biotechnol. 21:150-156.

Babu SI, Ramappa S, Guru MD, Sunanda KK, Sita KK, Subba RG. 2008. Optimization of medium constituents for the production of fructosyltransferase (FTase) by *Bacillus subtilis* using response. Res. Microbiol. 3:114-121.

Baciu IE, Jördening HJ, Seibel J, Buchholz K. 2005. Investiga- tions of the transfructosylation reaction by fructosyltransferase from *B. subtilis* NCIMB 11871 for the synthesis of the sucrose analogue galactosyl-fructoside. J. Biotechnol. 116:347-357.

Baker S. 2006. *Aspergillus niger* genomics: past, present and into the future. Med. Mycol. 44:17-21.

Balasubramaniem A, Nagarajan K, Paramasamy G. 2001. Optimization of media for fructofuranosidase production by *Aspergillus niger* in submerged and solid state fermentation. Process. Biochem. 37:331-338.

Becker J, Klopprogge C, Wittmann C. 2008. Metabolic responses to pyruvate kinase deletion in lysine producing *Corynebacterium glutamicum*. Microb. Cell. Fact. 7:8.

Becker J, Zelder O, Häfner S, Schröder H, Wittmann C. 2011. From zero to hero-Design-based systems metabolic engineering of *Corynebacterium glutamicum* for l-lysine production. Metab. Eng. 13:159-168.

Beine R, Valente AR, Biedendieck R, Jahn D, Seibel J. 2009. Directed optimization of biocatalytic transglycosylation processes by the integration of genetic algorithms and fermentative approaches into a kinetic model. Pro. Biochem. 44:1103-1114.

Bizukojc M, Ledakowicz S. 2010. The morphological and physiological evolution of *Aspergillus terreus* mycelium in the submerged culture and its relation to the formation of secondary metabolites. W. J. Microbiol. Biotechnol. 26: 41-54.

Blank LM, Lehmbeck F, Sauer U. 2005. Metabolic-flux and network analysis in fourteen hemiascomycetous yeasts. FEMS. Yeast. Research. 5:545-558.

Blank LM, Sauer U. 2004. TCA cycle activity in *Saccharomyces cerevisiae* is a function of the environmentally determined specific growth and glucose uptake rates. Microbiol. 150:1085-1093.

Blom RH, Pfeifer VF, Moyer AJ, Traufrer DH, Conway HF, Crocker CK, Farison RE, Hannibal DV. 1952. Sodium gluconate production. Fermentation with *Aspergillus niger*. Ind. Eng. Chem. 44:435-440.

Boddy LM, Berges T, Barreau C, Vainstein MH, Dobson MJ, Ballance DJ, Peberdy JF. 1993. Purification and characterisation of an *Aspergillus niger* invertase and its DNA sequence. Curr. Genet. 24:60-66.

Boel E, Hjort I, Svensson B, Norris F, Norris KE, Fiil NP, Norris KE, Fiil NP. 1984. Glucoamylases G1 and G2 from *Aspergillus niger* are synthesized from two different but closely related mRNAs. EMBO. J. 3:1097-1102

Bok J, Hoffmeister D, Maggio-Hall L, Murillo R, Glasner JD, Keller NP. 2006. Genomic mining for *Aspergillus* natural products. Chem. Biol. 13 31–37.

Bolten CJ, Kiefer P, Letisse F, Portais JC, Wittmann C. 2007. Sampling for metabolome analysis of microorganisms. Anal. Chem. 79:3843-3849.

Box GEF, Wilson KB. 1951. On the experimental attainment of optimum condition. J. Stat. Soc. 13:1-45.

Brock TD, Madigan MT. 1994. Biology of microorganism. Prantic Hall. Englewood Cliffs. New Jersey, USA.

Carberry S, Doyle S. 2007. Proteomic studies in biomedically and industrially relevant fungi. Cytotechnol. 53:95-100.

Carlsen M, Spohr AB, Nielsen J, Villadsen J. 1996. Morphology and Physiology of an alpha Amylase Producing Strain of *Aspergillus oryzae* during Batch Cultivations. Biotechnol. Bioeng. 49:266-276.

Carmichael RD, Pickard MA. 1989. Continuous and batch production of chloroperoxidase by mycelial pellets of *Caldariomyces fumago* in an airlift fermenter. Appl. environ. Microbiol. 44:17-20.

Casas López JL, Sánchez Pérez JA, Fernández Sevilla JM, Rodríguez Porcel EM, Chist iY. 2005. Pellet morphology, culture rheology and lovastatin production in cultures of *Aspergillus terreus*. J. Biotechnol. 116:61-77.

Chen WC, and Liu CH. 1996. Production of fructofuranosidase by *Aspergillus japonicus*. Enzy. Microbial. Technol. 18:153-160.

Coutinho PM, Andersen MR, Kolenova K, vanKuyk PA, Benoit I, Gruben BS, Trejo-Aguilar B, Visser H, van Solingen P, Pakula T and others. 2009. Post-genomic insights into the plant polysaccharide degradation potential of *Aspergillus nidulans* and comparison to *Aspergillus niger* and *Aspergillus oryzae*. Fungal. Genet. Biol. 1:161-169.

Cox PW, Paul GC, Thomas CR. 1998. Image analysis of the morphology of filamentous micro-organisms. Microbiol. 144:817-827.

Cronenberg CCH, Ottengraf SPP, van den Heuvel JC, Pottel F, Sziele D, Schiigerl K, Bellgardt KH. 1994. Influence of age and structure of *Pencillium* on the internal concentration profiles chrysogenum pellets. Biopro. Eng. 10:209-216.

Cruz R, Cruz VD, Belini MZ, Belote JG, Vieira CR. 1998. Production of fructooligosaccharides by mycelia of *Aspergillus japonicus* immobilized in calcium alginate. Biores. Technol. 65:139-143.

Cubitt AB, Heim R, Adams SR, Boyd AE, Gross LA, Tsien RY. 1995. Understanding, improving and using green fluorescent proteins. Trends. Biochem. 20:448-455.

Cuervo RF, Ottoni CA, Silva ES, Matsubara RS, Carter JM, Magossi LR, Wada MAA, Rodrigues MFA, Guilarte BM, Maiorano AE. 2007. Screening of b-fructofuranosidaseproducing microorganisms and effect of pH and temperature on enzymatic rate. Appl. Microbiol. Biotechnol. 75:87-93.

Cui YQ, Lans RGJMvd, Luyben KCAM.1998. Effects of dissolved oxygen tension and mechanical forces on fungal morphology in submerged fermentation. *Biotechnol. Bioeng.* 57(4):409-419.

Daly DS, Anderson KK, Panisko EA, Purvine SO, Fang R, Monroe ME, Baker SE. 2008. Mixed-effects statistical model for comparative LC-MS proteomics studies. J. Prote. Res. 7 1209-1217.

David H, Akesson M, Nielsen J. 2003. Reconstruction of the central carbon metabolism of *Aspergillus niger*. Eur. J. Biochem. 270:4243-4253.

David H, Hofmann G, Oliveira A, Jarmer H, Nielsen J. 2006. Metabolic network driven analysis of genome-wide transcription data from *Aspergillus nidulans*. Genome. Biol. :doi:10.1186/gb-2006-7-11-r108.

David H, Krogh AM, Roca C, Akesson M, Nielsen J. 2005. CreA influences the metabolic fluxes of *Aspergillus nidulans* during growth on glucose and xylose. Microbiol. 151:2209-2221.

David H, Ozcelik I, Hofmann G, Nielsen J. 2008. Analysis of *Aspergillus nidulans* metabolism at the genome-scale. BMC. Genomics. :doi:10.1186/1471-2164-9-163.

De Nicolas-Santiago S, Regalado-Gonzalez C, Garcia-Almendárez B, Fernández FJ, Tellez-Jurado A, Huerta-Ochoa S. 2006. Physiological, morphological, and mannanase production studies on *Aspergillus niger* uam-gs1 mutants. Electron. J. Biotechnol. ISSN:0717-3458.

Debets F, Swart K, Hoekstra R, Bos CJ. 1956. Genetic maps of eight linkage groups of *Aspergillus niger* based on mitotic mapping. Curr. Genet. 23:47-53.

Deckwer WD, D. J, Hempel D, Zeng AP. 2006. Systems biology approaches to bioprocess. Eng. Life. Sci. N:455-469.

Denison SH. 2000. pH regulation of gene expression in fungi. Fungal. Genet. Biol. 29:61-71.

Dhake AB, Patil MB. 2007. Effect of substrate feeding on production of fructosyltransferase by *Penicillium purpurogenum*. Braz. J. Microbiol. 38:194–199.

Diano A, Bekker-Jensen S, Dynesen J, Nielsen J. 2006. Polyol synthesis in *Aspergillus niger*: Influence of oxygen availability, carbon and nitrogen sources on the metabolism. Biotechnol. Bioeng. 94:899-908.

Domingues FC, Queiroz JA, Cabral JMS, Fonseca LP. 2000. The influence of culture conditions on mycelium structure and cellulose production by *Trichoderma reesei* Rut C-30. Enzyme. Microb. Technol. 26:394-401.

Driouch H, Roth A, Dersch P. 2011. Filamentous fungi in good shape: Microparticles for tailor-made fungal morphology and enhanced enzyme production. Bioeng. Bugs 2:1-5.

Driouch H, Roth A, Dersch P, Wittmann C. 2010a. Optimized bioprocess for production of fructofuranosidase by recombinant *Aspergillus niger*. Appl. Microbiol. Biotechnol. 87:2011-2024.

Driouch H, Sommer B, Wittmann C. 2010b. Morphology engineering of *Aspergillus niger* for improved enzyme production. Biotechnol. Bioeng. 105:1058-1068.

El-Enshasy H, Hellmuth K, Rinas U.1999. Fungal morphology in submerged cultures and its relation to glucose oxidase excretion by recombinant *Aspergillus niger*. *Appl. Biochem. Biotechnol.* 81(1):1-11.

El-Enshasy HA, Kleinea J, Rinas U. 2006. Agitation effects on morphology and protein productive fractions of filamentous and pelleted growth forms of recombinant *Aspergillus niger*. Process. Biochem. 41:2103-2112.

Fedorova N, Khaldi N, Joardar V, Maiti R, Amedeo P, Anderson M, Crabtree J, Silva J, Badger J, Albarraq A and others. 2008. Genomic islands in the pathogenic filamentous fungus *Aspergillus fumigatus*. PLoS. Genet. 4:4-e1000046.

Fernandez RC, Maresma BG, Juarez A, Martinez J. 2004. Production of fructooligosaccharides by β-fructofuranosidase from *Aspergillus sp.* 27H. J. Chem. Techol. Biotechnol. 79:268-272.

Fernie A, Trethewey R, Krotzky A, Willmitzer L. 2004. Metabolite profiling: from diagnostics to systems biology. Nat. Rev. Mol. Cell. Biol. 5:763-769.

Fiaux J, Cakar PZ, Sonderegger M, Wüthrich K, Szyperski T, Sauer U. 2003. Metabolic-Flux Profiling of the Yeasts *Saccharomyces cerevisiae* and *Pichia stipitis*. Eukaryotic. Cell. 2:170-180.

Finkelstein DB. 1987. Improvement of enzyme production in *Aspergillus*. Ant. Van. Leeuw. 53:349-352.

Fischer E, Sauer U. 2003. A novel metabolic cycle catalyzes glucose oxidation and anaplerosis in hungry *Escherichia coli*. J. Biological. chem. 47:46446-46451.

Fleissner A, Dersch P. 2010. Expression and export: recombinant protein production systems for *Aspergillus*. Appl. Microbiol. Biotechnol. 87:1255–1270.

Fowler T, Berka RM, Ward M. 1990. Regulation of the glaA gene of *Aspergillus niger*. Curr. Genet. 18:537-545.

Fredlund E, Blank LM, Schnürer J, Sauer U, Passoth V. 2004. Oxygen- and glucose-dependent regulation of central carbon metabolism in *Pichia anomala*. Appl. Env. Microbiol. 70:5905-5911.

Friedrich J, Cimerman A, Steiner W. 1989. Submerged production of pectolytic enzymes by *Aspergillus niger* effect of different aeration/agitation regimes. Appl. Microbiol. Biotechnol. 31:490-494.

Frisvad JC, Rank C, Nielsen KF, Larsen TO. 2009. Metabolomics of *Aspergillus fumigatus*. Med. Mycol. 1:53-71.

Fürch T, Hollmann R, Wittmann C, Wang W, Deckwer WD. 2007. Comparative study on central metabolic fluxes of *Bacillus megaterium* strains in continuous culture using ^{13}C-labelled substrates. Bioprocess. Biosyst. Eng. 30:47-59.

Galagan JE, Calvo SE, Borkovich KA. 2003. The genome sequence of the filamentous fungus *Neurospora crassa*. Nature 422:859-868.

Galbraith JC, Smith JE. 1969. Filamentous growth of *Aspergillus niger* in submerged shake culture. Trans. Bri. Mycological. Soci. 52:237-246.

Gheshlaghi R, Scharer JM, Moo-Young M, Douglas PL. 2007. Metabolic flux analysis for optimizing the specific growth rate of recombinant *Aspergillus niger*. Bioprocess. Biosyst. Eng.:doi: 10.1007/s00449-007-0136-x.

Gibbs PA, Seviour RJ, Schmid F. 2000. Growth of filamentous fungi in submerged culture: Problems and possible solutions. Crit. Rev. Biotechnol. 20:17-45.

Goffeau A. 1998. The yeast genome. Pathol. Biol. 46:96-97.

Gomez R, Schnabel I, Garrido J. 1988. Pellet growth and citric acid yield of *Aspergillus niger* 110. Enzy. Microb. Technol. 10:188-191.

Gordon CL, Archer DB, Jeenes DJ, Doonan JH, Wells B, Trinci AP, Robson GD. 2000. A glucoamylase::GFP gene fusion to study protein secretion by individual hyphae of *Aspergillus niger*. J. Microbiol. Meth. 42:39-48.

Grimm LH, Kelly S, Krull R, Hempel DC. 2005. Morphology and productivity of filamentous fungi. Appl. Microbiol. Biotechnol. 69:375-384.

Guimaraes LHS, Somera AF, Terenzi HF, Polizeli MLTM, Jorge JA. 2009. Production of fructofuranosidases by *Aspergillus niveus* using agroindustrial residues as carbon sources: Characterization of an intracellular enzyme accumulated in the presence of glucose. Process. Biochem. 44:237-241.

Gutierrez-Alonsto P, Fernandez-Arrojo L, Plou FJ, Fernandez-Lobato M. 2009. Biochemical characterization ofa fructofuranosidase from *Rhodotorula dairenensiswith* transfructosylating activity. Fed. Europ. Microbiol. Soc. 9 768-773.

Haack MB, Olsson L, Hansen K, Eliasson LA. 2006. Change in hyphal morphology of *Aspergillus oryzae* during fed-batch cultivation. Appl. Microbiol. Biotechnol. 70:482-487.

Hamer L. 1997. Sequencing of filamentous fungal genomes. Fungal. Genet. Biol. 21:8-10.

Haverkorn van Rijsewijk BR, Nanchen A, Nallet S, Kleijn RJ, Sauer U. 2011. Large-scale (13)C-flux analysis reveals distinct transcriptional control of respiratory and fermentative metabolism in *Escherichia coli*. Mol. Syst. Biol 7:477.

Hayashi S, Matsuzaki K, Takasaki Y, Ueno H, Imada K. 1992. Production of fructofuranosidase by *Aspergillus japonicus*. W. J. Microbiol. Biotechnol. 8:155-159.

Hemmersdorfer H, Leuchtenberger A, Wardsack C, Ruttloff H. 1987. Influence of culture conditions on mycelial structure and polygalactorunidase synthesis of *Aspergillus niger*. J. Basic. Microbiol. 27:309-315.

Hidaka H, Hirayama M, Sumi N. 1988. A fructooligosaccharide-producing enzyme from *Aspergillus niger* ATCC20611. Agric. Biol. Chem . 52:1181–1187.

Hille A, Neu R, Hempe DC, Horn H. 2009. Effective diffusivities and mass fluxes in fungal biopellets. Biotechnol. Bioeng. 103:1202–1213.

Hille A, Neu TR, Hempel DC, Horn H. 2005. Oxygen profiles and biomass distribution in biopellets of *Aspergillus niger*. Biotechnol. Bioeng. 92:614-623.

Jimenez-Tobon G, Penninck MJ, Lejeune R. 1997 The relationship between pellet size and production of Mm(II) peroxidise by *Phanerochaete chrysosporium* in submerged culture. Enzy. Microb. Technol. 21: 537-542.

Jones M. 2007. The first filamentous fungal genome sequences: *Aspergillus* leads the way for essential everyday resources or dusty museum specimens? Microbiol. 153 1-6.

Jouhten P, Pitkänen E, Pakula T, Saloheimo M, Penttilä M, Maaheimo H. 2009. 13C-metabolic flux ratio and novel carbon path analyses confirmed that *Trichoderma reesei* uses primarily the respirative pathway also on the preferred carbon source glucose. BMC. Syst. Biol. 3:104.

Jung KH, Yun JW, R KK, Y. LJ, Lee JH. 1989. Mathematical model for enzymatic production of fructooligosaccharides from sucrose. Enzy. Microb.Technol. 11:491-494.

Kaup BA, Ehrich K, Pescheck M, Schrader J. 2007. Microparticle-enhanced cultivation of filamentous microorganisms: increased chloroperoxidase formation by *Caldariomyces fumago* as an example. Biotechnol. Bioeng. 99:491-198.

Kelly S, Grimm LH, Brendind C, Hempel DC, Krull R. 2006a. Effects of fluid dynamic induced shear stress on fungal growth and morphology. Process. Biochem. 41:2113-2117.

Kelly S, Grimm LH, Hengstler J, Schultheis E, Krull R, Hempel DC. 2004. Agitation effects on submerged growth and product formation of *Aspergillus niger*. Bioproc. Biosyst. Eng. 26:315-323.

Kelly S, Grimm LH, Jonas R, Hempel DC, Krull R.2006b. Investigations of the Morphogenesis of Filamentous Microorganisms. *Engineering Life Science* 6(5):475-480.

Kiefer P, Heinzle E, Zelder O, Wittmann C. 2004. Comparative metabolic flux analysis of lysine-producing *Corynebacterium glutamicum* cultured on glucose or fructose. Appl. Environ. Microbiol. 70:229-239.

Kim HU, Kim TY, Lee SY. 2008. Metabolic flux analysis and metabolic engineering of microorganisms. Mol. Biosyst. 2:113-120.

Kim JS, Homgseok Y, Hyun UK, Hyung SC, Tae YK, Han MW, L. SY. 2006. Resources for Systems Biology Research. J. Microbiol. Biotechnol.:832-848.

Kim Y, Nandakumar M, Marten M. 2007. Proteome map of *Aspergillus nidulans* during osmoadaptation. Fungal. Genet. Biol. 44:886-895.

Kohlstedt M, Becker J, Wittmann C. 2010. Metabolic fluxes and beyond - systems biology understanding and engineering of microbial metabolism. Appl. Microbiol. Biotechnol. 88:1065-1075.

Kouskoumvekaki I, Yang Z, Jónsdóttir S, Olsson L, Panagiotou G. 2008. Identification of biomarkers for genotyping *Aspergilli* using nonlinear methods for clustering and classification. . BMC. Bioinform. 9:59.

Kralj S, Buchholz K, Dijkhuizen L, Seibel J. 2008. Fructansucrase enzymes and sucrose analogues: A new approach for the synthesis of unique fructo-oligosaccharides Biocat. Biotransform. 26:32-41.

Krull R, Cordes C, Horn H, Kampen I, Kwade A, Neu TR, Nörtemann B. 2010. Morphology of filamentous fungi: linking cellular biology to process engineering using *Aspergillusniger*. Biosyst. Eng. II. Adv. Bioch. Eng. Biotechnol. 121:doi 10.1007/10-2009-60.

L'Hocine L, Wang Z, Jiang B, Xu S. 2000. Purification and partial characterization of fructosyltransferase and invertase from *Aspergillus niger* AS0023 J. Biotechnol. 81:73-84.

Lee BH. 1991. Bioconversion of Starch Wastes. In: Bioconversion of Waste Materials to Industrial Products. Edited by M.AM. N Y. Els.Appl. Sci.:265 - 291.

Lee SY, Lee DY, Kim TY. 2005. Systems biotechnology for strain improvement. Tre. Biotechnol. 23:doi:10.1016/j.tibtech.2005.05.003.

Li Q, Harvey LM, McNeil B.2008. Oxygen enrichment effects on protein oxidation, proteolytic activity and the energy status of submerged batch cultures of *Aspergillus niger* B1-D. *Process. Biochem.* 43(3):238-243.

Lin PJ, Scholz A, Krull R. 2010. Effect of volumetric power input by aeration and agitation on pellet morphology and product formation of *Aspergillus niger*. Biochem. Eng. J. 49:213-220.

Liu Y, Liao W, Chen S. 2008. Study of pellet formation of filamentous fungi *Rhizopus oryzae* using a multiple logistic regression model. Biotechnol. Bioeng. 99 117-128

Lu X, Sun J, Nimtz M, Wissing J, Zeng AP, Rinas U. 2010. The intra- and extracellular proteome of *Aspergillus niger* growing on defined medium with xylose or maltose as carbon substrate. Microbial. Cell. Fact. 9:23.

Lubertozzi D, Keasling JD. 2009. Developing *Aspergillus* as a host for heterologous expression. Biotechnol. Adv. 27:53–75.

Maaheimo H, Fiaux J, Cakar ZP, Bailey JE, Sauer U, Szyperski T. 2001. Central carbon metabolism of *Saccharomyces cerevisiae* explored by biosynthetic fractional ^{13}C-labelling of common amino acids. Eur. J. Biochem. 268:2464-2479.

Machida M, Asai K, Sano M, Tanaka T, Kumagai T, Terai G, Kusumoto KI, Arima T, Akita O, Kashiwagi Y and others. 2005. Genome sequencing and analysis of *Aspergillus oryzae*. Nature. 438: 1157-1161.

Maeda H, Sano M, Maruyama Y, Tanno T, Akao T, Totsuka Y, Endo M, Sakurada R, Yamagata Y, Machida M and others. 2004. Transcriptional analysis of genes for energy catabolism and hydrolytic enzymes in the filamentous fungus *Aspergillus oryzae* using cDNA microarrays and expressed sequence tags. Appl. Microbiol. Biotechnol. 65:74-83.

Magnuson JK, Lasure LL. 2004. Organic acid production by filamentous fungi. Edited Jan Lene Lange. Agri. Medi.:307-340.

Mainwaring DO, Wiebe MG, Robson GD, Goldrick M, Jeenes DJ, Archer DB, Trinci APJ. 1999. Effect of ph on henn egg white lysozyme production and evolution of a recombinant strain of *Aspergillus niger*. J. Biotechnol. 75 1-10.

Maiorano EA, Piccoli RM, da Silva ES, Rodrigues DAMF. 2008. Microbial production of fructosyltransferases for synthesis of pre-biotics. Biotech. Lett. 30:1867-1877.

Malavazi I, Savoldi M, da Silva Ferreira M, Soriani F, Bonato P, de Souza Goldman M, Goldman G. 2007. Transcriptome analysis of the *Aspergillus nidulans* AtmA (ATM, Ataxia-Telangiectasia mutated) null mutant. Mol. Microbiol. 66:74–99.

Malavazi I, Savoldi M, Di Mauro S, Menck C, Harris S, Goldman M, Goldman G. 2006. Transcriptome analysis of *Aspergillus nidulans* exposed to camptothecin-induced DNA damage. Eukaryot. Cell. 10:1688-1704.

Mandenius CF, Brundin A. 2008. Bioprocess optimization using design-of-experiments methodology. Biotechnol. Prog. 24:1191-1203.

Mattern IE, van Noort JM, van den Berg P, Archer DB, Roberts IN, van den Hondel CAMJJ. 1992. Isolation and characterization of mutants of *Aspergillus niger* deficient in extracellular proteases. Mol. Gen. Genet . 234:332-336.

McIntyre M, Dynesen J, Nielsen J. 2001a. Morphological characterization of *Aspergillus nidulans*: growth, septation and fragmentation. Microbiol. 147:239-246.

McIntyre M, Müller C, Dynesen J, Nielsen J. 2001b. Metabolic engineering of the morphology of *Aspergillus*. Adv. Biochem. Eng. Biotechnol. 73:103-128.

Meijer S, Otero J, Olivares R, Andersen MR, Olsson L, Nielsen J. 2009. Overexpression of isocitrate lyase-glyoxylate bypass influence on metabolism in *Aspergillus niger*. Metab. Eng. 11:107-116.

Meijer S, Panagiotou G, Olsson L, Nielsen J. 2007. Physiological characterization of xylose metabolism in *Aspergillus niger* under oxygen-limited conditions. Biotechnol. Bioeng. 98:462-475.

Melzer G. 2010. Metabolic network analysis of the cell factory *Aspergillus niger*. Cuvillier-Verlage Göttingen 1-Band 47:ISBN: 978-3-86955-456-3, ISSN: 1431-7230.

Melzer G, Dalpiaz A, Grote A, Kucklick M, Göcke Y, Jonas R, Dersch P, Franco-Lara E, Nörtemann B, Hempel D. 2007. Metabolic flux analysis using stoichiometric models for *Aspergillus niger*: comparison under glucoamylaseproducing and non-producing conditions. J. Biotechnol.:405-417.

Melzer G, Esfandabadi ME, Franco-Lara E, Wittmann C. 2009. Flux design: In silico design of cell factories based on correlation of pathway fluxes to desired properties. BMC. Syst. Biol. 3:120.

Metz B. 1976. From pulp to pellet. PhD thesis. Delft Technical University of The Netherlands.

Michal G. 1999. Biochemical pathways. Heidelberg / Berlin: Spektrum Akademischer Verlag.

Mitard A, Riba JP. 1988. Morphology and growth of *Aspergillus niger* ATCC 26036 cultivated at several shear rates. Biotechnol. Bioeng. 32:835-840.

Mogensen J, Nielsen H, Hofmann G, Nielsen J. 2006. Transcription analysis using high-density microarrays of *Aspergillus nidulans* wild type and creA mutant during growth on glucose or ethanol. Fungal. Gen. Biol. 43:593-603.

Montgomery DC. 2001. Design and analysis of experiments. John. Wiley & sons, Inc. USA.

Mussatto S, Rodrigues L, Teixeira J.2009. β-Fructofuranosidase production by repeated batch fermentation with immobilized *Aspergillus japonicus*. J. Ind. Microbiol. Biotechnol. 36(7):923-928.

Nakakuki T. 2002. Present status and future of functional oligosaccharide development in Japan. Pure. Appl. Chem. 74:1245–1251.

Nanchen A, Fuhrer T, U. Saue U. 2006. Determination of metabolic flux ratios from ^{13}C-experiments and gas chromatography-mass spectrometry data: protocol and principles. Meth. Molec. Biol. 358:doi: 10.1007/978-1-59745-244-1-11.

Nevalainen H, Te'o V, Penttilä MJ, Pakula T. 2005. Heterologous gene expression in filamentous fungi: A holistic view Alert. Appl. Mycol. Biotechnol. 5:211-237.

Nielsen J. 1996. Modelling the morphology of filamentous microorganisms. Tibetch. 14:438-443.

Nielsen J. 1997. Physiological engineering aspects of *Penicillium chrysogenum*. W. Sci. Pub.Co. Pte. Ltd. 61:138.

Nielsen J, Johansen CL, Jacobsen M, Krabben P, Villadsen J.1995a. Pellet formation and fragmentation in submerged cultures of *Penicillium chrysogenum* and its relation to penicillin production. Biotechnol. Bioeng. 11(1):93-8.

Nielsen J, Johansen CL, Jacobsen M, Krabben P, Villadsen J. 1995b. Pellet formation and fragmentation in submerged cultures of *Penicillium chryrsogenum* and its relation to penicillin production. Biotech. Prog. 11 93-98.

Nielsen J, Krabben P.1995. Hyphal growth and fragmentation of *Penicillium chrysogenum* in submerged cultures. *Biotechnol. Bioeng.* 46(6):588-98.

Nierman W, Pain A, Anderson M, Wortman J, Kim H, Arroyo J, Berriman M, Abe K, Archer D, Bermejo C and others. 2005. Genomic sequence of the pathogenic and allergenic filamentous fungus *Aspergillus fumigatus*. Nature. 438:1151-1156.

O'Donnell D, Wang L, Xu J, Ridgway D, Gu T, Moo-Young M. 2001. Enhanced heterologous protein production in *Aspergillus niger* through pH control of extracellular protease activity. Biochem. Eng. J. 8:187-93.

Panagiotou G, Andersen MR, Grotkjaer T, Regueira TR, Nielsen J, Olsson L. 2009. Studies of the production of fungal polyketides in *Aspergillus nidulans* by using systems biology tools. Appl. Env. Microbiol. 75:2212–2220.

Papagianni M. 2004. Fungal morphology and metabolite production in submerged mycelial processes. Biotechnol. Adv. 22:189-259.

Papagianni M. 2007. Advances in citric acid fermentation by *Aspergillus niger*: Biochemical aspects, membrane transport and modelling. Biotechnol. Adv. 5:244-263.

Papagianni M, Joshi N, Moo-Young M. 2002 Comparative studies on extracellular protease secretion and glucoamylase production by free and immobilized *Aspergillus niger* cultures. J. I. Microbiol. Biotechnol. 5:259-263.

Papagianni M, Mattey M. 2006. Morphological development of *Aspergillus niger* in submerged citric acid fermentation as a function of the spore inoculum level. Application of neural network and cluster analysis for characterization of mycelial morphology. Microbial. Cell. 5:3-12.

Papagianni M, Mattey M, Kristiansen B. 1998. Citric acid production and morphology of *Aspergillus niger* as function of the mixing intensity in a stirred tank and tubular loop bioreactor. Biochem. Eng. J. 2 197-205.

Park JM, Kim TY, Lee SY. 2010. Prediction of metabolic fluxes by incorporating genomic context and flux-converging pattern analyses. PNAS 107:14931–14936.

Patil KR, Rocha I, Forster J, Nielsen J. 2005. Evolutionary programming as a platform for in silico metabolic engineering. BMC Bioinform. 6:308.

Pedersen H, Beyer M, Nielsen J. 2000a. Glucoamylase production in batch, chemostat and fed-batch cultivations by an industrial strain of *Aspergillus niger*. Appl. Microbiol. Biotechnol. 53:272-277.

Pedersen H, Carlsen M, Nielsen J. 1999. Identification of enzymes and quantification of metabolic fluxes in the wild type and in a recombinant *Aspergillus oryzae* strain. Appl. Env. Microbiol. 65:11-19

Pedersen H, Christensen B, Hjort C, Nielsen J. 2000b. Construction and characterization of an oxalic acid nonproducing strain of *Aspergillus niger*. Metab. Eng. 41:34-41.

Pel HJ, de Winde JH, Archer DB, Dyer PS, Hofmann G, Schaap PJ, Turner G, de Vries RP, Albang R, Albermann K. 2007. Genome sequencing and analysis of the versatile cell factory *Aspergillus niger* CBS 513.88. Nat. Biotechnol. 25:221-231.

Petzoldt K. 1971. Mischfermentation von zwei steroid-umwandelnden Mikroorganismen. Chem. Ing. Techn. 43:1-2.

Pharkya P, Maranas CD. 2006. An optimization framework for identifying reaction activation/inhibition or elimination candidates for overproduction in microbial systems. Metab. Eng. 8:1-13.

Pocsi I, Miskei M, Karanyi Z, Emri T, Ayoubi P, Pusztahelyi T, Balla G, Prade R. 2005. Comparison of gene expression signatures of diamide, H_2O_2 and menadione exposed *Aspergillus nidulans* cultures-linking genome-wide transcriptional changes to cellular physiology. BMC. Genom. 6:182.

Prathumpai W, Gabelgaard JB, Wanchanthuek P, van de Vondervoort PJ, de Groot MJ, McIntyre M, Nielsen J. 2003. Metabolic control analysis of xylose catabolism in *Aspergillus*. Biotechnol. Prog. 19:1136-1141.

Punt PJ, van Biezen N, Conesa A, Albers A, Mangnus J, van den Hondel C. 2002. Filamentous fungi as cell factories for heterologous protein production. Trends. Biotechnol. 20:200-206.

Roth AHFJ, Dersch P. 2010. A novel expression system for intracellular production and purification of recombinant affinity-tagged proteins in *Aspergillus niger*. Appl. Microbiol. Biotechnol. 86:659-670.

Rowley BI, Pirt SJ. 1972. Melanin production by *Aspergillus nidulans* in batch and chemostat cultures. J. Gen. Microbiol. 72 553-563.

Rubio MC, Maldonado MC. 1995. Purification and Characterization of Invertase from *Aspergillus niger*. Curr. Microbiol. 31:80-83.

Ruijter GJ, van de Vondervoort PJI, Visser J. 1999. Oxalic acid production by *Aspergillus niger*: An oxalate-non-producing mutant produces citric acid at pH 5 and in the presence of manganese. Microbiol. 145:2569-2576.

Sanchez OF, Rodriguez AM, Silva E, Caicedo LA. 2008. Sucrose biotransformation to fructooligosaccharides by *Aspergillus sp*. N74 Free Cells. Food. Biopro. Technol.: doi:10.1007/s11947-008-0121-7.

Sangeetha PT, Ramesh MN, Prapulla SG. 2005a. Fructooligosaccharide production using fructosyl transferase obtained from recycling culture of *Aspergillus oryzae* CFR 202. Process. Biochem. 40:1085-1088.

Sangeetha PT, Ramesh MN, Prapulla SG. 2005b. Recent trends in the microbial production, analysis and application of Fructooligosaccharides. T. F. Sci. Techn. 16 442-457.

Sauer U. 2004. High-throughput phenomics: experimental methods for mapping fluxomes. Curr. Opin. Biotechnol. 15:58-63.

Schmidt K, Norregaard LC, Pedersen B, Meissner A, Duus J, Nielsen J, Villadsen J. 1999. Quantification of intracellular metabolic fluxes from fractional enrichment and 13C-13C coupling constraints on the isotopomer distribution in labeled biomass components Metab. Eng. 1:166-179.

Schrickx JM, Krave AS, Verdoes JC, van den Hondel CA, Stouthamer AH, van Verseveld HW. 1993. Growth and product formation in chemostat and recycling cultures by *Aspergillus niger* N402 and a glucoamylase overproducing transformant,provided with multiple copies of the glaA gene. J. Gen. Microbiol. 139:2801-2810.

Segre D, Vitkup D, Church GM. 2002. Analysis of optimality in natural and perturbed metabolic networks. PNAS 99:15112-15117.

Seibel J, Moraru R, Götze S, Buchholz K, Na'amnieh S, Pawlowski A, Hecht HJ. 2006. Synthesis of sucrose analogues and the mechanism of action of Bacillus subtilis *fructosyltransferase* (levansucrase). Carbohydr. Res. 341:2335-2349.

Sheu DC, Duan KJ, Cheng CY, Bi JL, Chen JL. 2002. Continuous production of high-content fructooligosaccharides bya complex cell system. Biotechnol. Prog. 18:1282-1286.

Shin HT, Baig SY, Lee SW, Suh DS, Kwon ST, Lim YB, Lee JH. 2004. Production of fructo-oligosaccharides from molasses by *Aureobasidium pullulans* cells. Bioresource. Technol. 93:59-62.

Sims AH, Gent ME, Lanthaler K, Dunn-Coleman NS, Oliver SG, Robson GD. 2005. Transcriptome analysis of recombinant protein secretion by *Aspergillus nidulans* and the unfolded-protein response in vivo. Appl. Environ. Microbiol. 71:2737-2747.

Smith JJ, Lilly MD, Fox RI. 1990. The effect of agitation on the morphology and penicillin production of *Penicillium chrysogenum*. Biotechnol. Bioeng. 35:1011-1023.

Sola A, Maaheimo H, Ylönen K, P F, T S. 2004. Amino acid biosynthesis and metabolic flux profiling of *Pichia pastoris*. Eur. J. Biochem. 271:2462-2470.

Stephanopoulos G. 2007. Challenges in engineering microbes for biofuels production. Sci. 315:801-804.

Suthers PF, Burgard AP, Dasika MS, Nowroozi F, Van Dien S, Keasling JD, Maranas CD. 2007. Metabolic flux elucidation for large-scale models using 13C labeled isotopes. Metab. Eng. 9:387-405.

Szyperski T. 1995. Biosynthetically directed fractional ^{13}C-labelling of proteinogenic amino acids. An efficient tool to investigate intermediary metabolism. Eur. J. Biochem. 232:433-448.

Szyperski T, Glaser RW, Hochuli M, Fiaux J, Sauer U, Bailey J, Wüthrich K. 1999. Bioreaction network topology and metabolic flux ratio analysis by biosynthetic fractional ^{13}C labelling and two-dimensional NMR spectroscopy. Metab. Eng. 1(189-197).

Tamano K, Sano M, Yamane N, Terabayashi Y, Toda T, Sunagawa M, Koike H, Hatamoto O, Umitsuki G, Takahashi T and others. 2008. Transcriptional regulation of genes on the non-syntenic blocks of *Aspergillus oryzae* and its functional relationship to solid-state cultivation. Fungal. Genet. Biol. 45 139-151.

Teng Y, Xu Y, Wang D. 2009. Changes in morphology of *Rhizopus chinensis* in submerged fermentation and their effect on production of mycelium-bound lipase. Bioproc. Biosyst. Eng. 32:397-405.

Torres N, Regalado C, Sorribas A, Cascante M. 1993 Modeling of cell processes with applications to biotechnology and medicine: Quality assessment of a metabolic model and system analysis of citric acid production by *Aspergillus niger*. Modern. Tre. in Biotherm. Plenum. Press.:115–124.

Torres N, Voit E, Glez-Alcón C, Rodríguez F. 1998. A novel approach to design of overexpression strategy for metabolic engineering. Application to the carbohydrate metabolism in the citric acid producing mould *Aspergillus niger*. Biotechnol. Adv. 36:177-184.

Torres NV. 1994. Modeling approach to control of carbohydrate metabolism during citric acid accumulation by *Aspergillus niger*: II. Sensitivity analysis. Biotechnol. Bioeng. 44:112-118.

Trinh CT, Unrean P, Srienc F. 2008. Minimal *Escherichia coli* cell for the most efficient production of ethanol from hexoses and pentoses. App.l Environ. Microbiol. 74:3634-3643.

Tucker KG, Thomas CR. 1992. Mycelial morphology, the effect of spore inoculum level. Biotechnol. Lett. 14:1071-1074.

van Brunt J. 1986. Fungi: The perfect hosts? Biotechnol. Adv. 4:1057-1062.

Van Hartingsveldt W, Mattern IE, Van Zeijl CM, Pouwels PH, Van den Hondel CA. 1987. Development of a homologous transformation system for *Aspergillus niger* based on the pyrG gene. Mol. Gen. Genet. 206:71-5.

Vats P, Sahoo DK, Banerjee UC. 2004. Production of phytase (myo-inositolhexakisphosphate phosphohydrolase) by *Aspergillus niger* van teighem in laboratory-scale fermenter. Biotechnol. Prog. 20:737-743.

Vecht-Lifshitz SE, Magdassi S, S. B. 1990. Pellet formation and cellular aggregation in *Streptomyces tendae*. Biotechnol. Bioeng. 35:890-896.

Venkataraman K, Manjunath P, Raghavandra MRR. 1975. Glucoamylases of *Aspergillus niger* NRRL 330. Ind. J. Biochem. Biophys. 12:107–114.

Vinck A, Terlou M, Pestman wR, Martens EP, Ram AF, van den Hondel CAMJJ, Wösten HAB. 2005. Hyphal differentiation in the exploring mycelium of *Aspergillus niger*. Molecular. Microbiol. 58:693-699.

Wang L, Ridgway D, Gu T, Moo-Young M. 2003. Effects of process parameters on heterologous protein production in *Aspergillus niger* fermentation. J. Chem. Technol. Biotechnol. 78:1259-1266.

Wang L, Ridgway D, Gu T, Moo-Young M. 2005. Bioprocessing strategies to improve heterologous protein production in filamentous fungal fermentations. Biotechnol. Adv. 23:115-129.

Wang LM, Zhou HM. 2006. Isolation and identification of a novel *Aspergillus japonicus* JN19 producing fructofuranosidase and characterization of the enzyme. J. Food. Biochem. 30:641-658.

Wiechert W. 2002. An introduction to 13C-metabolic flux analysis. Gen. Eng. 24:215-238.

Wiechert W, Möllney M, Petersen S, de Graaf AA. 2001. A universal framework for ^{13}C-metabolic flux analysis. Metab. Eng. 3:265-283.

Wittler R, BaumgartI H, Lübbers DW, Schügerl K. 1986. Investigations of oxygen transfer into *Penicillium chrysogenum* pellets by microprobe measurements. Biotechnol. Bioeng. 28:1024–1036.

Wittmann C. 2007. Fluxome analysis using GC-MS. Microb. Cell. Fact. 6:6.

Wittmann C, Hans M, Heinzle E. 2002. In vivo analysis of intracellular amino acid labelings by GC-MS. Analytical. Biochem. 307:379-382.

Wittmann C, Heinzle E. 2002. Genealogy profiling through strain improvement by using metabolic network analysis: metabolic flux genealogy of several generations of lysine-producing corynebacteria. Appl. Environ. Microbiol. 68:5843-5859.

Wongwicharn A, McNeil B, Harvey LM. 1999. Effect of oxygen enrichment on morphology, growth, and heterologous protein production in chemostat cultures of *Aspergillus niger* B1-D. Biotechnol. Bioeng. 65:416-424.

Wucherpfennig T, Kiep KA, Driouch H, Wittmann C, Krull R. 2010. Morphology and rheology in filamentous cultivations. Adv. Appl. Mircobio. 72:89 136, Academic Press, ISBN: 978-0-12-380989-6.

Xu J, Wang L, Ridgway D, Gu T, Moo-Young M. 2000. Increased heterologous protein production in *Aspergillus niger* fermentation through extracellular proteases inhibition by pelleted growth. Biotechnol. Bioeng. 16:222-227.

Yanai K, Nakane A, Kawate A, Hirayama M. 2001. Molecular cloning and characterization of the fructooligosaccharide-producing beta-fructofuranosidase gene from *Aspergillus niger* ATCC 20611. Biosci. Biotechnol. Biochem. 65:766-773.

Yang F, Larry G, Moss GN, Phillips J. 1996. The molecular structure of green fluorescent protein. Nat. Biotechnology. 14:1246 - 1251.

Yoshikawa J, Amachi S, Shinoyama H, Fujii T. 2006. Multiple fructofuranosidases by *Aureobasidium pullulans* DSM2404 and their roles in fructooligosaccharide production. FEMS. Microbiol. Lett. 265:159–163.

Yoshikawa J, Amachi S, Shinoyama H, Fujii T. 2007. Purifuction and some properties of beta-fructofuranosudase I formed by *Aureobasidium pullulans* DSM 2404. J. Biosci. Bioeng. 103:491-493.

Yu J, Cleveland T, Nierman W, Bennett J. 2005. *Aspergillus flavus* genomics: gateway to human and animal health, food safety, and crop resistance to diseases. Rev. Iberoam. Micol. 22:192-202.

Yuan XL, Goosen C, Kools H, van der Maarel MJ, van den Hondel CA, Dijkhuizen L, Ram AF. 2006. Database mining and transcriptional analysis of genes encoding inulin-modifying enzymes of *Aspergillus niger*. Microbiol. 152:3061-3073.

Yun JW. 1996. Fructooligosaccharides-Occurrence, preparation, and application. Enzy. Microbiol. Techn. 19:Doi:10.1016/0141-0229(95)00188-3.

Zamboni N, Fendt SM, Rühl M, Sauer U. 2009. ^{13}C-based metabolic flux analysis. Nat. Proto. 4:878-892.

Zamboni N, Fischer E, Sauer E. 2005. FiatFlux - a software for metabolic flux analysis from 13C-glucose experiments. BMC. Bioinform. 6:209.

Zamboni N, Sauer U. 2009. Novel biological insights through metabolomics and 13C-flux analysis. Curr. Opin. Microbiol. 5:553-558.

Zhang ZY, Jin B, Kelly JM. 2007. Effects of cultivation parameters on the morphology of *Rhizopus arrhizus* and the lactic acid production in a bubble column reactor. Eng. Life. Sci. 7:490-496.

Znidarsic P, Pavko A. 2001. The morphology of filamentous fungi in submerged cultivations as a bioprocess parameter. morphology of filamentous fungi. Food. Technol. Biotechnol. 39:237–252.

Zuccaro A, Götze S, Kneip S, Dersch P, Seibel J. 2008. Tailor-made fructooligosaccharides by a combination of substrate and genetic engineering. Chem. Bio. Chem. 9:143-149.

10 APPENDIX

A. Stoichiometric Metabolic Model of *Aspergillus niger*.

In the following, the metabolic reactions of the metabolism of *Aspergillus niger* were derived from the recently published genome scale metabolic model (Andersen et al. 2008) and from literature (David et al. 2005; Diano et al. 2006; Melzer et al. 2009).

v_i	**Reactions**
Glucose uptake	
v_1:	Glucose + ATP > G6P
Glycolysis and PP Pathway	
v_2:	Glucose + 0.5 O_2 > Gluconate-cyt
v_3:	G6P = F6P
v_4:	F6P + ATP > G3P + DHAP
v_5:	DHAP = G3P
v_6:	G3P = 3PG
v_7:	3PG = PEP + ATP + NADH
v_8:	PEP > PYR-cyt + ATP
v_9:	G6P > P5P + 2 * NADPH + CO_2
v_{10}:	2 * P5P = S7P + G3P
v_{11}:	P5P + E4P = F6P + G3P
v_{12}:	S7P + G3P = E4P + F6P
v_{13}:	O_2 + 2 * NADH > 2 * PO * ATP
Specialties around G3P and C1-Metabolism	
v_{14}:	3PG > SER + NADH
v_{15}:	SER + NADH > GLY + C_1
v_{16}:	GLY + C_1 > SER + NADH
v_{17}:	C_1 + CO_2 + NADH > GLY
TCA Cycle	
$v_{18:}$	PYR-mit > AcCoA-mit+ NADH + CO_2
v_{18}:	AcCoA-mit + OAA-mit > CIT
v_{20}:	CIT-mit > ICT
v_{21}:	ICT > OGA + CO_2 + NADH
v_{22}:	OGA > SUC + CO_2 + 0.5 * ATP + NADH
v_{23}:	SUC = FUM + NADH
v_{24}:	FUM = MAL
v_{25}:	MAL = OAA-mit + NADH
v_{26}:	MAL > PYR-mit + CO_2 + NADPH
ANAPL Pathways	
v_{27}:	PYR-cyt + CO_2 + ATP > OAA-cyt
v_{28}:	OAA-cyt + ATP > PEP + CO_2
Oxalate Formation	
v_{29}:	OAA-cyt > OA + AC
Formation of AcCoA in the Cytosol	
v_{30}:	AC + ATP > AcCoA-cyt
v_{31}:	CIT-cyt + ATP > OAA-cyt + AcCoA-cyt
Transport Reactions Cytosol-Mitochondria	
v_{32}:	PYR-cyt > PYR-mit
v_{33}:	AcCoA-cyt = AcCoA-mit

v_{34}: CIT-mit > CIT-cyt
v_{35}: OAA-cyt > OAA-mit
v_{36}: OAA-mit > OAA-cyt

Polyole Metabolism

v_{37}: F6P + NADH > MAN-cyt
v_{38}: DHAP + NADH > GLO-cyt
v_{39}: E4P + NADH > EOL-cyt

Secretion to the Medium

v_{40}: Gluconate-cyt > Gluconate-ex
v_{41}: MAN-cyt > MAN-ex
v_{42}: GLO-cyt > GLO-ex
v_{43}: EOL-cyt > EO-Lex
v_{44}: OA-cyt > OA-ex
v_{45}: AC-cyt > AC-ex
v_{46}: CIT-cyt > CIT-ex

Biomass synthesis reactions (mMol/$g_{biomass}$)

1.6 * [G6P] + 0.86 * [F6P] + 0.37 * [P5P] + 0.213 * [MAN] + 0.6 * [GLO] + 0.5 * [EOL] + 0.36 * [E4P] + 0.08 * [G3P] + 0.863 * [GLY] + 0.628 * [SER] + 0.89 * [3PG] + 0.65 * [PEP] + 1.91 * [PYR] + 3.69 * [AcCoA] + 0.15*[AC] + 1.03 * [OAA] + 1.14 * [OGA] + 13.18 * [NADPH] + 0.33 * [O_2] + 2.51 * [NADH] + 61* [ATP] + 0.00281* [CO_2] = 1* [biomass]

Precursor demand for target enzyme fructofuranosidase (Mol/mMol_{FFase})

0.067 * [AcCoA] + 0.258 * [PYR] + 0.126 * [3PG] + 0.338 * [F6P] + 0.018 * [G6P] + 0.065 * [E4P] + 0.115 * [PEP] + 0.134 * [OAA] + 0.116 * [OGA] + 0.025 * [P5P] = 1* [fructofuranosidase]

Amino acids and sugar composition of the target highly glycosylated enzyme fructofuranosidase of *Aspergillus niger*. 50% of the total enzyme mass consists of sugar chains (NetNGlyc, http://www.cbs,dtu.dk/)

The amino acids composition of fructofuranosidase was derived from the corresponding open reading frame-ID An08g110170 (Pel et al. 2007). The sequence length of amino acids is as follows:

(http://www.uniprot.org/uniprot/A2QSK6).MKLQTASVLLGSAAAASPSMQTRASVVIDYNVAPPNLSTLPNGSLFETWRPRAHVLPPNGQIGDPCLHYTDPSTGLFHVGFLHDGSGISSATTDDLATYKDLNQGNQVIVPGGINDPVAVFDGSVIPSGINGLPTLLYTSVSFLPIHWSIPYTRGSETQSLAVSSDGGSNFTKLDQGPVIPGPPFAYNVTAFRDPYVFQNPTLDSLLHSKNNTWYTVISGGLHGKGPAQFLYRQYDPDFQYWEFLGQWWHEPTNSTWGNGTWAGRWAFNFETGNVFSLDEYGYNPHGQIFSTIGTEGSDQPVVPQLTSIHDMLWVSGNVSRNGSVSFTPNMAGFLDWGFSSYAAAGKVLPSTSLPSTKSGAPDRFISYVWLSGDLFEQAEGFPTNQQNWTGTLLLPRELRVLYIPNVVDNALARESGASWQVVSSDSSAGTVELQTLGISIARETKAALLSGTSFTESDRTLNSSGVVPFKRSPSEKFFVLSAQLSFPASARGSGLKSGFQILSSELESTTVYYQFSNESIIVDRSNTSAAARTTDGIDSSAEAGKLRLFDVLNGGEQAIETLDLTLVVDNSVLEIYANGRFALSTWVR.

Amino acids (aa)			(M_{aa}/M_{FFase})	MW pro aa	MW(g_{aa}/M_{FFase})
Serine	SER	(S)	71	105.09	7461.39
Leucine	LEU	(L)	55	131.18	7214.90
Glycine	GLY	(G)	54	075.07	4053.78
Threonine	THR	(T)	45	119.12	5360.40
Alanine	ALA	(A)	42	089.10	3742.20
Valine	VAl	(V)	42	117.15	4803.15
Proline	PRO	(P)	37	115.13	4259.81
Asparagine	ASN	(N)	31	132.10	4095.72
Phenylalanine	PHE	(F)	31	165.19	5120.89
Aspartate	ASP	(D)	30	133.10	3993.00
Glutamine	GLN	(Q)	24	146.15	3507.60
Isoleucine	ILE	(I)	24	131.17	3148.08
Glutamate	GLU	(E)	22	147.13	3236.86
Arginine	ARG	(R)	21	174.20	3658.20
Tyrosine	THR	(Y)	19	181.19	3442.61
Tryptophane	TRP	(W)	15	204.23	3063.45
Lysine	LYS	(K)	12	146.19	1754.28
Histidine	HIS	(H)	10	155.16	1551.60
Methionine	MET	(M)	04	149.21	0596.84
Cysteine	CYS	(C)	01	121.16	0121.16
			589	2738.04	74185.92
Sugar					
Fructose	Fru		06	180.16	1080.96
Glucose	Glc		18	180.16	3242.88
Mannose	Mannose		308	180.16	55489.20
	SUMME		921	3062.52	110095.04

B. Isotopic Steady-State for Flux Analysis

Origin of intermediates in *Aspergillus niger* SKANip8 (wild type) harvested during different time points of exponential phase of ^{13}C-labelled glucose batch cultures.

Time points (h)	^{13}C-labelled glucose	Fraction of total pool (%) (Mean ± SD) 30	32	34
PP pathway				
SER through Glycolysis	1*	27±1	27±1	27±1
R5P from G6P (ld*)	U*	24±2	25±2	22±2
R5P from T3P and S7P (*tkl* reaction)	U	30±3	28±2	32±1
R5P from E4P (*tkl/tal* reaction)	U	47±1	47±1	47±1
E4P from TK	U	67±3	65±1	69±2
C1-Metabolism				
SER from GLY	U	39±1	39±1	38±1
GLY from SER	U	66±1	66±1	66±1
Labeled CO_2	U	49±3	53±1	53±1
Glycolysis, ANAPL and TCA cycle				
PEP-cyt from OAA-cyt (*pepck*)	U	0±0	1±0	0±0
OAA-cyt from PYR-cyt	U	60±1	59±1	61±1
AcCoA-mit from PYR-mit	U	n.d	n.d	n.d
OAA-mt from ANAPL	U	49±1	50±1	50±1
OAA-mit from ANAPL	U	41±1	40±1	41±1
PYR-mit from MAL (*me*, ud*)	U	0±0	1±0	1±0
PYR-mit from MAL (*me,* ld)	U	0±0	1±0	1±0

1: 100% of [1-^{13}C]glucose, U: mixture of [U-^{13}C]glucose and natural glucose, lb: lower bound, up: upper bound, *tkl*: transketolase, *tal*: transaldolase, *pepck:* PEP caboxykinase, *me*: malic enzyme, n. d: not detectable because the fragment needed for tracing this activity is absent, SD: standard deviation). The data were derived from [1-^{13}C] and [U-^{13}C]glucose experiments.

C. Mass Isotopomer Distributions of Metabolite Fragments

Relative mass isotopomer fractions of amino acids of cell protein from *Aspergillus niger* grown on 99% [1-^{13}C] glucose and 50% [U-^{13}C] glucose, respectively. Given data denote experimental GC-MS data. M+0 represents the amount of non-labelled mass isotopomer fraction, M+1 the amount of singly-labelled mass isotopomer fraction and corresponding terms refer to a higher labelling.

A. Mass distributions of metabolite fragments in the fructofuranosidase non-producing strain *A. niger* SKANip8 strain grown on [1-^{13}C] glucose

A

AMINO ACIDS	FL	MASS DISTRIBUTION								
		M+0	M+1	M+2	M+3	M+4	M+5	M+6	M+7	M+8
ALA-57	0.09	0.739	0.257	0.004	-0.001					
ALA-85	0.05	0.890	0.123	-0.014						
ALAf302	0.10	0.790	0.227	-0.018						
ASP-57	0.11	0.616	0.330	0.052	0.001					
ASP-85	0.12	0.681	0.288	0.030	0.002					
GLU-57	0.12	0.527	0.370	0.092	0.009	0.001				
GLU-85	0.12	0.594	0.341	0.063	0.002					
GLUf302	0.01	0.937	0.100	-0.037						
GLY-57	0.02	0.965	0.035	-0.000						
HIS-159	0.05	0.807	0.167	0.007	0.011	0.004	0.003			
HISf302	0.45	0.355	0.386	0.259						
ILE-57	0.02	0.699	0.325	0.073	-0.071	-0.011	-0.005	-0.010		
ILE-85	0.07	0.636	0.301	0.092	-0.010	-0.009	-0.010			
ILEf302	0.20	0.664	0.280	0.056						
LEU-57	0.10	0.537	0.360	0.093	0.009					
LEU-85	0.11	0.539	0.363	0.091	0.006					
LEU-159	0.07	0.723	0.197	0.065	0.013	0.001				
LEUf302	0.26	0.564	0.353	0.082						
LYS-57	0.03	0.852	0.190	0.056	-0.011	-0.037	-0.026	-0.025		
MET-57	0.15	0.834	0.454	0.002	-0.066	-0.094	-0.129			
PHE-57	0.05	0.610	0.322	0.061	0.004	0.001	0.001			
PHEf302	0.09	1.158	-0.134	-0.024						
PRO-57	0.27	0.444	0.203	0.047	0.202	0.087	0.017			
PRO-85	0.05	0.852	0.123	0.015	0.008	0.001				
SER-57	0.05	0.837	0.163	0.000	-0.001					
SER-85	0.07	0.853	0.149	-0.002						
THR-57	0.11	0.615	0.331	0.054						
THR-85	0.03	0.933	0.053	-0.000	0.014					
TYR-85	0.05	0.741	0.365	0.025	-0.018	-0.014	-0.013	-0.029	-0.028	-0.03
TYRf302	0.11	1.184	-0.156	-0.028						
VAL-57	0.07	0.659	0.312	0.042	-0.005	-0.005	-0.004			
VAL-85	0.03	0.877	0.116	0.006	0.003	-0.003				

METABOLIC FLUX RATIOS

SER through glycolysis	0.27+/-0.01
PEP from OAA	0.0+/-0.0

B

AMINO ACIDS	FL	MASS DISTRIBUTION								
		M+0	M+1	M+2	M+3	M+4	M+5	M+6	M+7	M+8
ALA-57	0.09	0.739	0.259	0.004	-0.002					
ALA-85	0.05	0.892	0.121	-0.014						
ALAf302	0.09	0.794	0.229	-0.023						
ASP-57	0.11	0.615	0.331	0.054	0.001					
ASP-85	0.12	0.673	0.294	0.033	0.000					
GLU-57	0.12	0.525	0.372	0.093	0.008					
GLU-85	0.12	0.589	0.340	0.066	0.004					
GLUf302	0.02	0.935	0.098	-0.033						
GLY-57	0.02	0.963	0.037	-0.000						
GLY-85	0.10	1.104	-0.104							
HIS-57	0.00	0.811	0.257	-0.017	-0.022	-0.011	-0.008	-0.009		
HIS-159	0.05	0.806	0.170	0.005	0.011	0.005	0.002			
ILE-57	0.01	0.712	0.329	0.068	-0.081	-0.012	-0.008	-0.008		
ILE-85	0.08	0.625	0.299	0.091	-0.006	-0.004	-0.006			
ILEf302	0.19	0.669	0.279	0.051						
LEU-57	0.10	0.539	0.360	0.090	0.008					
LEU-85	0.11	0.539	0.362	0.092	0.006					
LEU-159	0.07	0.722	0.198	0.065	0.013					
LEUf302	0.26	0.568	0.354	0.078						
LYS-57	0.04	0.880	0.180	0.034	-0.006	-0.026	-0.031	-0.032		
MET-57	0.12	0.779	0.460	0.041	-0.075	-0.094	-0.111			
PHE-57	0.05	0.610	0.323	0.059	0.005	0.001	0.000	0.001	0.001	
PHEf302	0.09	1.159	-0.136	-0.024						
PRO-57	0.27	0.444	0.199	0.047	0.203	0.089	0.016			
PRO-85	0.05	0.851	0.124	0.016	0.008	0.001				
SER-57	0.05	0.840	0.161	-0.001	-0.000					
SER-85	0.08	0.848	0.152	-0.001						
SERf302	0.15	1.271	-0.239	-0.032						
THR-57	0.11	0.613	0.330	0.054	0.002	-0.000				
THR-85	0.03	0.937	0.049	-0.001	0.014					
TYR-85	0.11	0.817	0.410	0.013	-0.028	-0.06	-0.028	-0.03	-0.061	-0.034
TYRf302	0.10	1.180	-0.155	-0.025						
VAL-57	0.07	0.662	0.312	0.041	-0.004	-0.006	-0.005			
VAL-85	0.03	0.871	0.120	0.007	0.003	-0.002				

METABOLIC FLUX RATIOS

SER through glycolysis	0.27+/-0.01
PEP from OAA	0.00+/-0.00

B. Mass distributions of metabolite fragments in the fructofuranosidase non-producing strain *A. niger* SKANip8 strain grown on 50% [U-^{13}C] glucose and 50% unlabeled glucose.

A

AMINO ACIDS	FL	MASS DISTRIBUTION								
		M+0	M+1	M+2	M+3	M+4	M+5	M+6	M+7	M+8
ALA-57	0.50	0.440	0.054	0.059	0.447					
ALA-85	0.32	0.697	-0.035	0.338						
ALAf302	0.21	0.749	0.087	0.164						
ASP-57	0.49	0.195	0.210	0.208	0.210	0.175				
ASP-85	0.49	0.254	0.254	0.251	0.240					
ASPf302	0.34	0.618	0.086	0.295						
GLU-57	0.49	0.117	0.137	0.258	0.251	0.129	0.109			
GLU-85	0.51	0.145	0.176	0.352	0.166	0.161				
GLUf302	0.25	0.625	0.254	0.121						
GLY-57	0.49	0.450	0.112	0.438						
GLY-85	0.27	0.726	0.274							
HIS-57	0.47	0.172	0.231	0.090	0.079	0.107	0.202	0.119		
ILE-57	0.37	0.202	0.149	0.283	0.135	0.120	0.062	0.049		
ILE-85	0.50	0.113	0.128	0.264	0.255	0.137	0.102			
ILE-159	0.44	0.216	0.111	0.236	0.224	0.120	0.094			
ILEf302	0.56	0.330	0.225	0.445						
LEU-57	0.46	0.136	0.052	0.333	0.081	0.278	0.034	0.085		
LEU-85	0.49	0.113	0.143	0.266	0.230	0.142	0.104			
LEU-159	0.45	0.202	0.111	0.236	0.222	0.131	0.097			
LEUf302	0.68	0.273	0.088	0.639						
PHE-57	0.49	0.073	0.049	0.103	0.153	0.144	0.140	0.142	0.092	0.042
PHEf302	0.30	0.703	-0.016	0.313						
PRO-57	0.58	0.058	0.074	0.140	0.464	0.163	0.101			
PRO-85	0.43	0.290	0.127	0.298	0.149	0.136				
SER-57	0.50	0.363	0.134	0.134	0.368					
SER-85	0.50	0.398	0.206	0.396						
SERf302	0.32	0.697	-0.029	0.331						
THR-57	0.49	0.192	0.209	0.207	0.211	0.180				
THR-85	0.40	0.437	0.144	0.206	0.213					
TYRf302	0.32	0.692	-0.020	0.328						
VAL-57	0.50	0.201	0.057	0.243	0.243	0.052	0.203			
VAL-85	0.42	0.370	0.012	0.380	0.050	0.187				

METABOLIC FLUX RATIOS

P5P from G6P (lb)	0.25+/-0.01	PEP from OAA-cyt	0.0+/-0.0
P5P from G3P and S7P	0.28+/-0.03	OAA-mit from ANAPL	0.49+/-0.01
P5P from E4P	0.47+/-0.01	OAA-mit from ANAPL (old)	0.40+/-0.02
E4P through TK	0.65+/-0.03	PYR-mit from MAL (ub)	0.0+/-0.0
SER from GLY	0.39+/-0.01	PYR-mit from MAL (lb)	0.0+/-0.0
GLY from SER	0.66+/-0.01	Labeled CO_2	0.49+/-0.03
OAA-cyt from PYR-cyt	0.59+/-0.01	OAA-mit from rev FUM	0.0+/-0.0
AcCoA-mit from PYR-mit	n.d	cOAA-cyt from rev FUM	0.37+/-0.03

B

AMINO ACIDS	FL	MASS DISTRIBUTION								
		M+0	M+1	M+2	M+3	M+4	M+5	M+6	M+7	M+8
ALA-57	0.50	0.438	0.056	0.062	0.444					
ALA-85	0.32	0.696	-0.034	0.338						
ALAf302	0.20	0.755	0.087	0.159						
ASP-57	0.49	0.195	0.212	0.207	0.209	0.176				
ASP-85	0.49	0.254	0.252	0.252	0.241					
ASPf302	0.34	0.623	0.084	0.293						
GLU-57	0.49	0.117	0.135	0.256	0.251	0.130	0.111			
GLU-85	0.50	0.156	0.172	0.353	0.162	0.157				
GLUf302	0.27	0.609	0.250	0.140						
GLY-57	0.49	0.451	0.113	0.436						
GLY-85	0.27	0.727	0.273							
HIS-57	0.48	0.161	0.219	0.100	0.083	0.108	0.201	0.128		
HIS-159	0.49	0.150	0.209	0.148	0.153	0.204	0.135			
HISf302	0.07	1.021	0.099	-0.120						
ILE-57	0.36	0.208	0.151	0.283	0.127	0.119	0.063	0.048		
ILE-85	0.50	0.115	0.111	0.269	0.264	0.138	0.103			
ILE-159	0.35	0.246	0.122	0.279	0.264	0.144	-0.055			
ILEf302	0.55	0.336	0.225	0.438						
LEU-57	0.46	0.136	0.052	0.331	0.080	0.279	0.034	0.087		
LEU-85	0.49	0.117	0.146	0.270	0.215	0.144	0.107			
LEU-159	0.45	0.207	0.112	0.236	0.220	0.130	0.094			
LEUf302	0.68	0.272	0.089	0.639						
LYS-57	0.44	0.137	0.074	0.278	0.175	0.222	0.058	0.054		
PHE-57	0.49	0.073	0.049	0.101	0.156	0.145	0.136	0.14	0.092	0.043 0.063
PHEf302	0.30	0.702	-0.015	0.312						
PRO-57	0.57	0.064	0.082	0.156	0.419	0.168	0.110			
PRO-85	0.43	0.287	0.127	0.299	0.150	0.137				
SER-57	0.50	0.365	0.134	0.135	0.366					
SER-85	0.50	0.400	0.205	0.395						
SERf302	0.32	0.694	-0.024	0.330						
THR-57	0.49	0.193	0.210	0.207	0.212	0.178				
THR-85	0.40	0.437	0.142	0.207	0.214					
TYR-85	0.42	0.114	0.069	0.199	0.124	0.207	0.101	0.136	0.016	0.033
TYRf302	0.31	0.697	-0.019	0.321						
VAL-57	0.50	0.201	0.056	0.244	0.244	0.052	0.203			
VAL-85	0.42	0.373	0.012	0.380	0.049	0.186				

METABOLIC FLUX RATIOS

P5P from G6P (lb)	0.23+/-0.01	PEP from cOAA	0.0+/-0.0
P5P from G3P and S7P	0.32+/-0.03	OAA-mit from ANAPL	0.50+/-0.01
P5P from E4P	0.47+/-0.01	OAA-mit from ANAPL (old)	0.41+/-0.01
E4P through TK	0.69+/-0.03	PYR-mit from MAL (ub)	0.0+/-0.0
SER from GLY	0.38+/-0.01	PYR-mit from MAL (lb)	0.0+/-0.0
GLY from SER	0.66+/-0.01	Labeled CO_2	0.53+/-0.03
OAA-cyt from PYR-cyt	0.61+/-0.01	OAA-mit from rev FUM	0.0+/-0.0
AcCoA-mit from PYR-mit	n.d	OAA-cyt from rev FUM	0.37+/-0.03

C. Mass distributions of metabolite fragments in *A. niger* recombinant strain SKAn1015 grown on [1-^{13}C] glucose.

A

AMINO ACIDS	FL	MASS DISTRIBUTION								
		M+0	M+1	M+2	M+3	M+4	M+5	M+6	M+7	M+8
ALA-57	0.10	0.710	0.283	0.006	0.001					
ALA-85	0.07	0.859	0.151	-0.010						
ALAf302	0.10	0.779	0.238	-0.017						
ASP-57	0.10	0.641	0.306	0.048	0.003	0.001				
ASP-85	0.11	0.695	0.273	0.030	0.002					
ASPf302	0.02	1.040	-0.033	-0.007						
GLU-57	0.11	0.571	0.336	0.080	0.011	0.001	0.001			
GLU-85	0.11	0.628	0.314	0.053	0.002	0.002				
GLUf302	0.01	0.882	0.218	-0.101						
GLY-57	0.03	0.950	0.046	0.004						
GLY-85	0.10	1.096	-0.096							
HIS-57	0.01	0.806	0.313	-0.056	-0.032	-0.012	-0.007	-0.011		
HIS-159	0.06	0.762	0.200	0.014	0.012	0.008	0.004			
ILE-57	0.03	0.701	0.314	0.072	-0.065	-0.013	-0.006	-0.004		
ILE-85	0.09	0.604	0.312	0.091	0.004	-0.005	-0.005			
ILEf302	0.19	0.672	0.271	0.056						
LEU-57	0.10	0.542	0.357	0.088	0.009	0.002	0.000	0.001		
LEU-85	0.12	0.532	0.368	0.091	0.007	0.001	0.001			
LEU-159	0.08	0.718	0.199	0.068	0.012	0.002	0.001			
LEUf302	0.25	0.572	0.351	0.077						
LYS-57	0.12	1.076	0.118	-0.022	-0.041	-0.043	-0.046	-0.043		
PHEf302	0.09	1.153	-0.132	-0.021						
PRO-57	0.28	0.445	0.180	0.037	0.225	0.094	0.018			
PRO-85	0.04	0.885	0.097	0.008	0.008	0.001				
SER-57	0.06	0.814	0.180	0.003	0.002					
SER-85	0.09	0.827	0.171	0.002						
SERf302	0.12	1.204	-0.177	-0.028						
THR-57	0.10	0.645	0.306	0.046	0.002	0.001				
THR-85	0.02	0.958	0.032	-0.006	0.015					
TYR-85	0.08	0.742	0.414	0.039	-0.022	-0.03	-0.035	-0.02	-0.054	-0.035
TYRf302	0.10	1.183	-0.161	-0.022						

METABOLIC FLUX RATIOS

SER through glycolysis	0.33+/-0.01
PEP from OAA	0.0+/-0.0

B

AMINO ACIDS	FL	MASS DISTRIBUTION								
		M+0	M+1	M+2	M+3	M+4	M+5	M+6	M+7	M+8
ALA-57	0.10	0.709	0.284	0.006	0.001					
ALA-85	0.07	0.859	0.152	-0.011						
ALAf302	0.11	0.766	0.245	-0.011						
ASP-57	0.10	0.647	0.303	0.045	0.003	0.001				
ASP-85	0.11	0.697	0.273	0.028	0.001					
ASPf302	0.02	1.043	-0.037	-0.006						
GLU-57	0.11	0.568	0.343	0.078	0.009	0.002	0.001			
GLU-85	0.11	0.623	0.315	0.056	0.005	0.001				
GLUf302	0.07	0.829	0.209	-0.039						
GLY-57	0.03	0.950	0.046	0.003						
GLY-85	0.10	1.097	-0.097							
HIS-57	0.02	0.817	0.311	-0.054	-0.043	-0.004	-0.010	-0.018		
HIS-159	0.06	0.766	0.196	0.012	0.013	0.007	0.005			
ILE-57	0.02	0.701	0.318	0.068	-0.065	-0.007	-0.010	-0.005		
ILE-85	0.09	0.604	0.321	0.086	-0.003	-0.003	-0.006			
ILEf302	0.19	0.672	0.275	0.052						
LEU-85	0.12	0.531	0.371	0.090	0.006	0.001	0.001			
LEU-159	0.08	0.716	0.201	0.068	0.013	0.002	0.001			
LEUf302	0.25	0.575	0.348	0.078						
LYS-57	0.10	1.031	0.113	-0.003	-0.018	-0.036	-0.040	-0.047		
PHE-57	0.06	0.566	0.340	0.079	0.008	0.002	0.001	0.001	0.001	0.001
PHEf302	0.09	1.153	-0.132		-0.021					
PRO-57	0.28	0.444	0.176	0.036	0.229	0.096	0.019			
PRO-85	0.04	0.884	0.098	0.008	0.009	0.001				
SER-57	0.06	0.813	0.181	0.003	0.003					
SER-85	0.09	0.828	0.170	0.001						
SERf302	0.12	1.201	-0.172	-0.029						
THR-57	0.10	0.645	0.307	0.044	0.002	0.001				
THR-85	0.02	0.958	0.030	-0.004	0.016					
TYR-85	0.09	0.749	0.441	0.032	-0.043	-0.033	-0.035	-0.019	-0.038	-0.054
TYRf302	0.10	1.176	-0.154	-0.022						
VAL-57	0.09	0.602	0.349	0.058	-0.003	-0.004	-0.003			
VAL-85	0.05	0.828	0.149	0.020	0.005	-0.002				

METABOLIC FLUX RATIOS

SER through glycolysis	0.33+/-0.01
PEP from OAA	0.0+/-0.0

D. Mass distributions of metabolite fragments in the recombinant strain *A. niger* SKAn1015 grown on 50% [U-^{13}C] glucose and 50% unlabeled glucose.

A

AMINO ACIDS	FL	MASS DISTRIBUTION								
		M+0	M+1	M+2	M+3	M+4	M+5	M+6	M+7	M+8
ALA-57	0.50	0.439	0.062	0.065	0.433					
ALA-85	0.32	0.702	-0.035	0.333						
ALAf302	0.21	0.743	0.093	0.164						
ASP-57	0.36	0.346	0.221	0.172	0.158	0.103				
ASP-85	0.36	0.408	0.245	0.198	0.150					
ASPf302	0.20	0.783	0.032	0.185						
GLU-57	0.35	0.281	0.184	0.231	0.175	0.073	0.056			
GLU-85	0.34	0.335	0.213	0.278	0.094	0.080				
GLUf302	0.17	0.772	0.123	0.104						
GLY-57	0.48	0.464	0.115	0.421						
GLY-85	0.26	0.741	0.259							
HIS-57	0.48	0.144	0.212	0.112	0.095	0.113	0.206	0.118		
HIS-159	0.47	0.157	0.231	0.171	0.098	0.225	0.117			
HISf302	0.39	0.428	0.372	0.200						
ILE-57	0.28	0.323	0.153	0.266	0.112	0.080	0.043	0.023		
ILE-85	0.40	0.202	0.137	0.312	0.192	0.100	0.057			
ILE-159	0.21	0.425	0.112	0.310	0.183	0.093	-0.123			
ILEf302	0.45	0.450	0.191	0.358						
LEU-57	0.37	0.218	0.065	0.365	0.073	0.223	0.018	0.038		
LEU-85	0.43	0.179	0.105	0.362	0.134	0.172	0.048			
LEU-159	0.38	0.301	0.067	0.307	0.133	0.149	0.043			
LEUf302	0.61	0.346	0.086	0.567						
LYS-57	0.18	0.572	0.067	0.188	0.087	0.069	0.012	0.004		
PHE-57	0.49	0.067	0.050	0.098	0.155	0.141	0.136	0.15	0.091	0.045 0.066
PHEf302	0.31	0.702	-0.022	0.320						
PRO-57	0.26	0.467	0.157	0.118	0.155	0.064	0.040			
PRO-85	0.21	0.608	0.104	0.176	0.068	0.045				
SER-57	0.49	0.364	0.141	0.141	0.354					
SER-85	0.50	0.391	0.226	0.383						
SERf302	0.31	0.707	-0.044	0.336						
THR-57	0.36	0.346	0.222	0.168	0.159	0.104				
THR-85	0.25	0.640	0.092	0.140	0.126					
TYR-85	0.48	0.082	0.056	0.171	0.130	0.186	0.114	0.169	0.04	0.052
TYRf302	0.32	0.692	-0.026	0.334						
VAL-57	0.49	0.209	0.060	0.242	0.241	0.053	0.194			
VAL-85	0.41	0.382	0.012	0.377	0.051	0.179				

METABOLIC FLUX RATIOS

P5P from G6P (lb)	0.09+/-0.01	OAA-cyt from PYR-cyt	0.79+/-0.01
P5P from G3P and S7P	0.35+/-0.01	OAA-mit from ANAPL (old)	0.48+/-0.01
P5P from E4P	0.56+/-0.01	OAA-mit from ANAPL	0.74+/-0.01
E4P through TK	0.67+/-0.01	PYR-mit from MAL (ub)	0.0+/-0.0
SER from GLY	0.40+/-0.01	PYR-mit from MAL (lb)	0.0+/-0.0
GLY from SER	0.67+/-0.01	Labeled CO_2	0.53+/-0.01
PEP from OAA-cyt	0.0+/-0.0	OAA-mit from rev FUM	1.03+/-0.03
AcCoA-mit from PYR-mit	1.04+/-0.01	OAA-cyt from rev FUM	0.76+/-0.01

B

AMINO ACIDS	FL	MASS DISTRIBUTION								
		M+0	M+1	M+2	M+3	M+4	M+5	M+6	M+7	M+8
ALA-57	0.50	0.438	0.062	0.066	0.434					
ALA-85	0.31	0.703	-0.036	0.332						
ALAf302	0.21	0.743	0.093	0.164						
ASP-57	0.36	0.344	0.220	0.172	0.160	0.104				
ASP-85	0.36	0.409	0.243	0.198	0.150					
ASPf302	0.20	0.786	0.033	0.182						
GLU-57	0.35	0.280	0.184	0.233	0.175	0.071	0.056			
GLU-85	0.35	0.333	0.209	0.279	0.099	0.080				
GLUf302	0.18	0.760	0.128	0.111						
GLY-57	0.48	0.464	0.115	0.421						
GLY-85	0.26	0.739	0.260							
HIS-57	0.49	0.140	0.206	0.113	0.096	0.110	0.206	0.127		
HIS-159	0.47	0.155	0.228	0.177	0.104	0.218	0.117			
HISf302	0.29	0.575	0.261	0.164						
ILE-57	0.28	0.318	0.154	0.269	0.113	0.079	0.043	0.024		
ILE-85	0.40	0.200	0.139	0.315	0.190	0.100	0.055			
ILE-159	0.21	0.419	0.113	0.312	0.184	0.094	-0.123			
ILEf302	0.46	0.443	0.194	0.363						
LEU-57	0.37	0.217	0.066	0.365	0.072	0.222	0.019	0.038		
LEU-85	0.43	0.177	0.104	0.363	0.134	0.172	0.049			
LEU-159	0.38	0.303	0.068	0.307	0.131	0.148	0.043			
LEUf302	0.61	0.345	0.088	0.566						
LYS-57	0.18	0.577	0.061	0.185	0.092	0.074	0.008	0.001		
PHE-57	0.49	0.068	0.050	0.097	0.155	0.140	0.139	0.148	0.090	0.048 0.066
PHEf302	0.31	0.705	-0.024	0.319						
PRO-57	0.26	0.466	0.155	0.116	0.160	0.064	0.039			
PRO-85	0.21	0.614	0.103	0.173	0.066	0.044				
SER-57	0.49	0.365	0.142	0.140	0.353					
SER-85	0.49	0.393	0.226	0.381						
SERf302	0.32	0.698	-0.036	0.338						
THR-57	0.36	0.347	0.221	0.171	0.158	0.103				
THR-85	0.25	0.647	0.088	0.140	0.125					
TYR-85	0.48	0.077	0.059	0.169	0.126	0.184	0.124	0.165	0.04	0.056
TYRf302	0.32	0.690	-0.027	0.337						
VAL-57	0.49	0.211	0.059	0.241	0.240	0.054	0.194			
VAL-85	0.41	0.385	0.012	0.375	0.050	0.178				

METABOLIC FLUX RATIOS

P5P from G6P (lb)	0.12+/-0.01	OAA-cyt from PYR-cyt	0.80+/-0.01
P5P from G3P and S7P	0.36+/-0.01	OAA-mit from ANAPL (old)	0.48+/-0.01
P5P from E4P	0.55+/-0.01	OAA-mit from ANAPL	0.74+/-0.01
E4P through TK	0.68+/-0.01	PYR-mit from MAL (ub)	0.0+/-0.0
SER from GLY	0.41+/-0.01	PYR-mit from MAL (lb)	0.0+/-0.0
GLY from SER	0.67+/-0.01	Labeled CO_2	0.53+/-0.01
PEP from OAA-cyt	0.0+/-0.0	OAA-mit from rev FUM	1.04+/-0.03
AcCoA-mit from PYR-mit	1.04+/-0.01	OAA-cyt from rev FUM	0.75+/-0.01

D. Published Metabolic Flux Data in Different *Aspergillus* Species

Reference	Pedersen et al. 1999	Pederson et al. 2000	David et al. 2005	Anderson et al. 2008	Meijer et al. 2009	Panagiotou et al. 2009	This work
Strain	*A. oryzae*	*A. niger*	*A. nidulans*	*A. niger*	*A. niger*	*A. nidulans*	
Enzyme	A1560 /*CF1.1*	BO-1/ Δ *oah 4-1*	A187/*creA*	*wt*/*i*MA871	N402/*icL*	*wt*/*msaS*/*msaS+xpkA*	wt/producer
glucose uptake	100/100	100/100	100/100	100/100	100/100	100/100/100	100/100
***hxk*, hexokinase**	100/100	100/100	100/100	100/100	100/100	100/100/100	68/67
goxC/catR	---/---	---/---	---/---	---/---	---/---	---/---/---	32/33
***g6pdh*, 6-phosphogluconate dehydrogenase**	35/40	58/67	78/61	46/48	95/76	57/46/52	20/27
***pgi*, glucose-6-phosphate isomerise**	48/43	30/20	---/---	39/35	05/20	28/39/36	41/32
***pfk*, 6-phosphofructokinase**	67/63	61/51	56/57	55/53	67/70	39/50/40	42/36
***tk1*, transketolase**	20/23	35/41	26/22	25/27	62/51	15/09/04	10/14
***tk2/tal*, transketolase/ transaldolase**	9/8	16/109	26/22	20/21	62/51	15/09/04	9/13
***man*$_{cycle}$, mannitol cycle**	2/3	---/---	0/0	---/---	0/0	---/---/---	7/8
***glo*$_{ycle}$, glycerol cycle**	1/1	---/---	5/1	---/---	0/0	---/--/---	2/2
***pgk*, phosphoglycerate kinase**	142/140	130/120	122/125	123/118	156/166	110/116/115	78/68
***ser from gly*, c1-Metabolism**	---/---	---/---	3/3	---/---	1/3	---/---/---	32/28
***gly from ser*, c1-Metabolism**	**---/---**	**---/---**	0/0	---/---	0/4	---/---/---	36/30
***pyrk*, pyruvate kinase**	129/119	103/95	111/115	108/106	154/163	110/116/115	71/63
***pyrc*, pyruvate carboxylase**	18/21	27/25	23/22	15/ 12	8/34	23/22/19	19/19
***pepck*, phosphoenolpyruvate carboxykinase**	---/---	---/---	---/---	---/---	---/---	---/---/---	0/0
***oaah*, oxaloacetate hydrolase**	---/---	3/0	---/---	3/0	0/0	---/---/---	12/12
***me*, malic enzyme**	---/---	---/---	---/---	---/---	---/---	---/---/---	0/0
***pyrdh*, pyruvate dehydrogenase**	97/81	103/95	69/79	108/106	146/101	71/77/82	46/38
***cs/ac*, citrate lyase/acetate-CoA ligase**	93/76	82/74	52/58	78/77	200/184	83/75/79	44/36
***ictdh*, isocitrate dehydrogenase**	70/54	64/52	52/58	45/38	153/106	83/75/79	44/36
***ogadh*, α-ketoglutarate dehadrogenase**	52/33	54/39	52/58	45/38	153/106	79/79/94	41/33
***sucdh*, succinate dehadrogenase**	59/43	54/39	39/47	38/31	153/106	79/79/94	41/33
***fum*, fumarase**	59/43	54/39	39/47	38/31	153/106	79/79/94	41/33
***mdh*, malate dehydrogenase**	79/60	54/39	39/47	38/31	153/106	79/79/94	41/33

For abbreviations of enzyme that are written in italics see abbreviations.

E. Influence of the Environmental Process Parameters on Morphology and Productivity

	Organism	Investigated values	System	Morphology	Product	Reference
Inoculum	***A. niger***	spore concentration 10-100 mL^{-1}	shake flasks, pH 4.5, *T*: 25°C, n_{stir}: 150 min^{-1}, *t*: 95 h	pellet: Diameter: 2-10 mm, smooth surface	**Polygalacturonase (homologous):** increases with compactness of pellets	(Hemmers-dorfer et al., 1987b)
		spore concentration 10^4-10^9 mL^{-1}	STR, pH 2.1, *T:* 28°C, n_{stir}: 400 min^{-1}, *t:*150 h *air flow*: 1 $LL^{-1}min^{-1}$,	pellets at concentrations of 10^4–10^5 mL^{-1}, freely dispersed mycelium at concentration of 10^8-10^9 mL^{-1}	**Citric acid (homologous)** yield: > 150g L^{-1} with D-glucose as substrat at 150h of cultivation	(Papagianni and Mattey, 2006)
		spore concentration $5x10^5$-$5x10^6$ mL^{-1} and 10^7 mL^{-1}	Glass beaker and shake flasks, *pH* 5.5, *T*: 30°C, n_{stir}: 240 min^{-1}	increased aggregation velocity with rising spore concentration, maximal aggrgation velocity with a concentration of $3x10^6$ mL^{-1}, > $3x10^6$ mL^{-1} reduced spore germination and hyphal growth	not specified	(Grimm et al., 2004)
		spore concentration 10^3-10^7 mL^{-1}	shake flasks, *T:* 24°C, n_{stir}: 200 min^{-1}, *t*: 6d	Decrease in pellet size with increasing conidia concentration, optimal pellet size of 1.6mm for synthesis, freely dispersed mycelium > 10^7 mL^{-1},	**Glucoamylase-GFP fusion protein (heterologous)** Maximum yield of at spore concentration $4x10^6$ mL^{-1} (pellets of 1.6mm diameter) due to reduction of protease synthesis	(Xu et al., 2000)
	A. terreus	spore concentration in preculture: $1.39x10^9$–$2.56x10^{10}$ L^{-1}	shake flasks, inoculation with 10mL, preculture culture, *T:* 30°C, n_{stir}: 110 min^{-1}, *t:* 168 h	inoculum concentration determines pellet size and growth rate, small pellets and high biomass concentration at $2x10^{10}$ L^{-1}	**Lovastatin and Geodin (homologous),** increased Lovastatin synthesis with small pellets, no correlation of Geodin synthesis and pellet size	(Bizukojc and Leda-kowicz, 2010)
	C. fumago	inoculation with preculture (~10^3 pellet per reactor, 2-3 mm diameter)	airlift reactor, *T*: 22°C, *air flow*: 0.6-1.0 $LL^{-1}min^{-1}$	pellet (small volume of preculture) or amorphous, viscous mycelium (large volume)	**Heme glucoprotein chloroperoxidase (homologous)** no influence of inoculum	(Carmichael and Pickard, 1989)
	P. chrysogenum	spore concentration $5x10^4$-$1x10^6$ mL^{-1}	shake flasks, *T*: 26°C, n_{stir}: 200 min^{-1}, *t:* 75 h	pellets at low concentration, change in morphology between $5x10^4$ and $5x10^5$ mL^{-1} to dispersed mycelium	**Penicillin (homologous)**	(Tucker and Thomas, 1992)
		spore concentration $4x10^7$-$6x10^8$ L^{-1}	STR, *T:* 25°C, n_{stir}: 300 min^{-1} *air flow*: 1 $LL^{-1}min^{-1}$, or controlled to keep a constant dissolved oxygen (DO) saturation of 45%	freely dispersed mycelia, branching frequency linked to total hyphal length, fragmentation correlated to power input	**Penicillin (homologous)**	(Nielsen and Krabben, 1995)
		Spore concentration 10^4-10^6 mL^{-1}	shake flasks and STR	freely dispersed mycelium or aggregates and clumps, reduced aggregation and compactness at higher concentration	**Penicillin (homologous)**	(Tucker and Thomas, 1994)
		spore concentration 2.4-$8.6x10^7$ L^{-1}	STR, *T:* 25°C, n_{stir}: 500 min^{-1} *air flow:* 1 $LL^{-1}min^{-1}$,	small pellets at low concentration, large pellets at intermediate concentrations, mycelial growth at high concentrations	**Penicillin (homologous**) no relation of penicillin production and macroscopic morphology	(Nielsen et al 1995a) (Nielsen et al 1995b)
	R. oryzae	spore concentration $1x10^6$-$3x10^9$ L^{-1}	shake flasks, *T*: 27°C, n_{stir}: 170 min^{-1}, *t*: 48 h	pellet	not specified	(Liu et al. 2008)

	S. tendae	spore concentrations $7.5x10^2$-$2.3x10^8$ L^{-1}	shake flasks, , n_{stir}: $100min^{-1}$ STR, n_{stir}: 400 min^{-1}, air flow: 1 $LL^{-1}min^{-1}$, *pH* 4-8, *T*: 26-30°C, *t*: 6d	concentration < 10^3 L^{-1} large pellets with diameter > 2mm and cellular yield of 0.3-0.6g mL^{-1}, higher conidia concentrations constant biomass yield (1.6 g L^{-1}), pellet size inversely proportional to concentration until a plateau is reached a at high concentrations	not specified	(Vecht-Lifshitz et al., 1990)
	T. reesei	spore concentration in preculture: 10^5-10^7 L^{-1}	shake flasks, inoculation with seeding culture, pH 4.8, *T:* 28°C, n_{stir}: 150 min^{-1}	large pellets at low inoculum levels, small flocs at higher concentration, decrease of pellet size with increase of concentration	**Cellulase (homologous)** Increased synthesis with small flocs due to high inoculum concentration	(Domigues et al., 2000)
pH	***A. niger***	pH 3.5-6.5	CSTR, *D*: $0.07h^{-1}$, 200 mL preculture, addition of 1.6 gL^{-1} Junlon (prop-2-enoic acid, $C_3H_4O_2$), inoculation with, n_{stir}:: 1000 min^{-1} *air flow*: 0.8 $LL^{-1}min^{-1}$,	filamentous growth due to addition of Junlon	**Hen egg white lysozyme (HEWL) (heterologous)** production optimum pH 4.5, specific production rate 0.65 mg g^{-1} h^{-1}	(Mainwaring et al., 1999)
		pH 1.5-4.5	shake flasks, Inoculum *:* $8x10^6$ spores per flask, n_{stir}: $150min^{-1}$, *T*: 27°C	pH < 2.3 free dispersed mycelium, pellet formation under more alkaline conditions, no difference in biomass yield	Not specified	Galbraith and Smith 1969
		pH 4-7	STR, Inoculum *:* $2x10^6$ mL^{-1}, *t*: 12h n_{stir}: 200 min^{-1}, *air flow*: 0.5 $LL^{-1}min^{-1}$, *T*: 30°C	Pellets, First aggregation step of spores only affected by pH, higher number of pellets at pH4 compared to pH7, highest aggregation velocity at pH 4	**Glucoamylase (homologous)** Productivity per biomass lower at pH 7 compared to pH 4	Grimm et al. 2005b
		varying initial pH 3–7 without pH control and constant pH of 5.8-6.0	STR, inoculation with 3d precul-ture, *T*: 30°C, n_{stir}:: 400 min^{-1} *air flow*: $0.5LL^{-1}min^{-1}$	free dispersed mycelium and pellets, high initial pH favoured biomass growth	**Phytase (homologous**) higher activity with lower pH, maximal synthesis with biomass growth at neutral pH with subsequent decline in pH	(Vats et al., 2004)
		pH 3-7 and without pH control	STR, inoculum: $2.5x10^5$ mL^{-1}, *T:* 30°C, n_{stir}: 200 min^{-1} *air flow*: 1L $L^{-1}min^{-1}$,	pellets	**Glucoamylse-GFP fusion protein (heterologous)** optimal pH 6.0 due to reduction of protease activity and increase of product	(O'Donnell et al., 2001)
	A. oryzae	pH 2.5-8.0	STR, inoculum: 3-$6x10^8$ L^{-1}or mycelial preculture, *T*: 32°C, *air flow*: 1 $LL^{-1}min^{-1}$, n_{stir}: 300-800 min^{-1} (DO 70-100%)	pH < 3.5 mycelium, pH 4-5 both morpho-logies, pH > 5 pellets; increasing pellet radius with increasing pH value, no pellet formation with mycelium as inoculum	**α-Amylase (homologous)** production optimum at pH 6, production formation at pH <4 and pH > 7 very low	(Carlsen et al., 1996)
	P. chrysogenum	pH 6.0-7.4	CSTR, , n_{stir}: $1200min^{-1}$, vortex aeration, *T*: 25°C, *D*: 0.05 h^{-h}, *t*: 200-2000h	Decrease of hyphal length of mycelia with rise from pH 6 to pH 7.4, pellet formation and swollen hyphae with increase to pH > 7.0 or 6.7, resp.	**Penicillin (homologous)** Optimal pH of 7.4 for synthesis, two stages cultivation recommended: (1) mycelial growth at low pH-values and (2) production of penicillin due to a shift to pH > 7	(Pirt and Callow, 1959)

	R. oryzae	pH control with or without $CaCO_3$	shake flasks, *T:* 27°C, n_{stir}: 170 min^{-1}, *t:* 48 h	pellets	not specified	(Liu et al., 2008)
	S. tendae	pH 4-8	shake flasks, , n_{stir}: 100min^{-1} STR, n_{stir}: 400 min^{-1}, *air flow*: 1 $LL^{-1}min^{-1}$, Inoculum *:* 7.5x10^2-2.3x10^8 L^{-1}, *T*: 26-32°C, *t*: 6d	Small pellets (0.1-0.2 mm) at pH 7-8 optimal for growth, larger pellets (1.2-1.5 mm) at pH4	not specified	(Vecht-Lifshitz et al., 1990)
	T. reesei	pH 2.2-7.6	STR, inoculum: 2.0x10^8 L^{-1}, *T:* 30°C, n_{stir}: 300, 500 or 600 min^{-1}	freely dispersed mycelium, maximum values of tip extension rate and branching frequencies at pH 4.5, time of spore germination influenced by pH	not specified	(Lejeune et al., 1995a)
Power input due to agitation and aeration	***A. awamori***	DO tension 5-330%	STR, inoculum: 6.3x10^6 L^{-1}, *pH* 4.5, T: 25°C, n_{stir}: 600 min^{-1}, constant *P/V* of 1.07 W kg^{-1}	denser pellets at high DO concentration; weak, fluffly pellets at low DO concentration, DO concentration hardly influence pellet size and hairy length	not specified	(Cui et al., 1998)
	A. niger	Agitation intensity n_{stir}: 100-300 min^{-1} or $(P/V)_{stir}$: 0.014-0.390 W kg^{-1}, resp.	STR, Inoculum *:* 2x10^6 mL^{-1}, *pH* 4.8, *t*: 15h, no aeration, *T*: 30°C	Pellets, no affect of agitation on first aggregation step, second aggregation step of conidia is dependent on agitation	**Glucoamylase (homologous)**	(Grimm et al. 2005b)
		Or Power input due to aeration $(P/V)_{air}$: 0-0.5 m^3 h^{-1}	STR, Inoculum *:* 2x10^6 mL^{-1}, *pH* 4.8, *t*: 15h, *T*: 30°C n_{stir}: 150 min^{-1}	Neglible effect of aeration on spore agitation		
		Agitation intensity n_{stir}: 100-600 min^{-1}	STR, inoculum: 40h-old preculture (initial spore concentration 1x10^7 mL^{-1}), *pH* 2.1, *air flow*: 1 $LL^{-1}min^{-1}$, *T*: 28°C,	clumps, no direct effect of agitation on biomass yield, decrease of clump size with increase of agitation intensity	**Citric acid** Increase of production with raising agitation intensity	(Papagianni et al., 1998)
		power input $(P/V)_{stir}$: 0.05-0.073 W kg^{-1} (n_{stir}: 200-600 min^{-1})	STR, inoculum: 1x10^6 mL^{-1}, *pH* 5.5 *T:* 30°C, *air flow*: 0.5 L L^{-1} min^{-1}	pellets, higher $(P/V)_{stir}$ results in lower biomass concentration, smaller and compacter pellets a high $(P/V)_{stir}$ compared to large and fluffy pellets at low $(P/V)_{stir}$	**Glucoamylase (homologous)**	(Kelly et al., 2006a)
		power input $(P/V)_{stir}$: 0.056-0.099 W kg^{-1} (n_{stir}: 105-190 min^{-1})	STR, inoculum: 1x10^6 mL^{-1}, *pH* 5.5 *T:* 30°C, *air flow*: 0.5 $LL^{-1}min^{-1}$	pellet size and concentration affected by $(P/V)_{stir}$, minimal diameter at $(P/V)_{stir}$ ~ 0.075 W kg^{-1}, decreasing pellet concentration with increasing $(P/V)_{stir}$	**Glucoamylase (homologous)** Maximal synthesis at ~0.065 W kg^{-1}, low production with smaller pellet diameter at power input of 0.075 W kg^{-1}	(Kelly et al., 2004)
		agitation intensity: n_{stir}: 150-300 min^{-1}	shake flasks: *pH* 5.0-5.3, shift in viscosity due to addition of guar gum, *T:* 30°C	small pellets with entangled mycelium at 150 min^{-1}, freely dispersed mycelium at 300 min^{-1}, transition to filamentous growth with increasing viscosity	**Phytase (homologous)** synthesis increased with increasing shaker speeds as well as with gum addition	(Papagianni et al. 2001)

	agitation intensity: n_{stir}: 200 min^{-1} increased to 400 min^{-1} after 13h, raised to 600 min^{-1} after 15h	STR, *pH* 5.5, *T:* 30°C, *air flow*: 1 $LL^{-1}min^{-1}$	pellets, improvement of nutrient availability at the pellet core with decreasing size of dense pellets	**Glucose oxidase (GOD) (recombinant homologous)** higher yields of GOD with smaller pellets with high density	(El-Enshasy et al., 1999)
	agitation intensity: n_{stir}: 200-800 min^{-1} or $(P/V)_{stir}$:0.1-8 W kg^{-1}, resp.	STR, inoculum: 1x10^7 $mL^{-}1$, *pH* 5.5, *T:* 30°C, *air flow*: 1.5 $LL^{-1}min^{-1}$, after initial 5h of 0.75 $LL^{-1}min^{-1}$	range from large pellets at n_{stir}: 200 min^{-1} to a filamentous network with micropellets at n_{stir}: 800 min^{-1}, lower biomass concentration at higher agitation rates	**GOD (recombinant homologous)** GOD increase with shift to mycelial growth at first, intermediate agitation favoured for prolonged cultivation	(El-Enshasy et al., 2006)
	agitation intensity: n_{stir}: 200-500 min^{-1}	STR, inoculation with 3d preculture, no pH control (initial *pH* 5.5–6.0), *T:* 30°C *air flow*: 0.5L L^{-1} min^{-1}	mycelium and pellets, shear thinning with increasing stirring rate leading to short, highly fragmented hyphae compared to long, thin mycelia at lower agitation rates	**Phytase (homologous)** maximum synthesis at n_{stir}: 300 min^{-1}, no significant influence of agitation on extracellular protein	(Vats et al., 2004)
	varying levels of oxygen enrichment within aeration: 0%, 10%, 30% and 50 % O_2 (v/v)	CSTR, inoculation with 1% seeding culture, *pH* 4.0, *T*: 25°C, *air flow*: 1 $LLmin^{-1}$, *D*: 0.06 h^{-1}	under oxygen limitation (0%,10% O_2) long sparsely branched hyphal elements, shorter hyphal elements with high branch frequen-cy with oxygen enrichment (30%, 50% O_2)	**HEWL (heterolog)** and **Glucoamylase (homologous)** increased synthesis with rising oxygen supply	(Wongwicharn et al., 199b)
	constant $(P/V)_{total}$ with varying percentages of aeration (52.5-103.5 W m^{-3}) and agitation (90.5-39.5 W m^{-3})	STR, inoculum: 1x10^6 mL^{-1}, *pH* 5.5, *T:* 30°C, constant $(P/V)_{total}$ of 143 W m^{-3}	pellets, with increasing proportion of aeration of $(P/V)_{total}$ decrease in pellet size and increase of pellet concentration as well as less dense surface structure	**Glucoamylase (GA) (homologous)** increasing formation of GA with raising percentage of aeration and smaller pellets and high pellet concentration	(Lin et al., 2010)
	increase of agitation intensity n_{stir} from 300 min^{-1} to 500 min^{-1} and increase of aeration from 0.5 to 1.2 $LL^{-1}h^{-1}$	STR, no pH control, *T*: 32°C, *t*: 90 -160 h	distinct pellets with long peripheral hyphae, no influence of varied parameters on morphology	**Pectolytic enzymes (homologous)** Growth-associated synthesis of polygalacturonase, pectin esterase, pectinlyase	(Friedrich et al., 1989)
	agitation intensity n_{stir}: 250 min^{-1} and 400 min^{-1}, DO tension: 15% and 35%	STR, inoculum 1x10^6 mL^{-1}, *pH* 6.0, *T:* 32°C, *t:* 90 -160 h	pellets	**Glucoamylse-GFP fusion gene (heterologous)** increase of GFP formation with increased agitation rate, decreased GFP production with raised DO concentration	(Wang et al., 2003b)
A. oryzae	Agitation intensity n_{stir}: 525-825 min^{-1}	STR, fed-batch, *pH* 5.0, *air flow* 1 $LL^{-1}min^{-1}$, gas blending regulated to a constant DO level of 50%, *T*: 32°C	Increase of biomass with increase of agitation rate in batch phase	**Amyloglucosidase (recombinant)** Increase of secretion with increase of agitation rate in batch phase, dependency on hyphal tip activity	(Amanullah et al. 2002b)
A. terreus	agitation rate n_{stir}: 300-800 min^{-1} aeration regimes with air or an oxygen-enriched mixture (80% O_2)	STR, seeding cultures of 250mL, *T:* 28°C, *t:* 7 d *air flow* 1 $LL^{-1}min^{-1}$	pellets, no influence of investigated agitation rates and aeration regimes on biomass formation, but influence on pellet morphology	**Lovastatin (homologous)** high production with large, fluffy pellets at low n_{stir} and with oxygen-enriched aeration	(Casas López et al., 2005)

	P. chrysogenum	agitation intensity: n_{stir}: 800-1200 min^{-1} (10L) or n_{stir}: 350-565 min^{-1} (100L)	STR (10L): 1.5L seed medium,; STR (100L): 10L seed medium, *T:* 26°C, exponential feed rate during the first 20h and than linear	freely dispersed mycelium, 10L cultivations: with higher n_{stir}, mean effective hyphal length decreases faster, similar power inputs in 100L less influence, morphology not affected by aeration	**Penicillin (homologous)** 10L: reduced productivity at higher agitation rates, similar power inputs in 100L higher productivity	(Smith et al., 1990)
		agitation rate controlled by DO concentration (set point 45%)	STR, *T:* 25°C, *air flow*: 1 $LL^{-1}min^{-1}$	reduction of hyphal agglomeration with increasing agitation rate n_{stir}	**Penicillin (homologous)** no relation of penicillin production and macroscopic morphology	(Nielsen et al., 1995)
	R. oryzae	agitation intensity: n_{stir}: 115-350 min^{-1} (orbital shaker)	shake flasks, inoculum:1x10^9 mL^{-1} *T:* 27°C, *t*: 48 h	pellet, low shaking speeds favour pellet formation, pellet size increases with lower shaking speeds	not specified	(Liu et al., 2008)
	T. reeseie	Agitation intensity n_{stir}: 130-400 min^{-1}	STR, inoculum: 72h old preculture, (initial dry weight 0.5 gL^{-1}, initial *pH* > 4.5, no pH control, *air flow*: 0.2 $LL^{-1}min^{-1}$, aeration level regulated to a DO > 30% by changing back pressure, *T*: 30°C, Lactose as carbon source	Pellets, longer lag-phase at n_{stir}: 400 min^{-1}, maximum dry weight not affected by agitation	**Endoglucanase, Xylanase** Decrease of enzyme production with increase of agitation rates	(Lejeune and Baron,. 1995)
Others	***A. japonicus***	effect of immobilization on different carriers	shake flasks, different lignocellu-losic materials as carriers, *T:* 28°C inoculum: 1.8x10^7 mL^{-1}, no pH control, , n_{stir}: 160 min^{-1} *t*: 48 h	corn cobs: material with highest level of microorganism immobilization	**Fructooligosaccharides (FOS) and β-fructofuranosidase (FFase)** with corn cobs as carrier maximal production of FOS and FFase	(Mussatto et al., 2009)
	A. niger	variation of size and concentration of added microparticles	shake flasks, n_{stir}: 120 min^{-1}; STR, , n_{stir}: 200 min^{-1}, *air flow*: 1 $LL^{-1}min^{-1}$ inoculum: 1x10^6 mL^{-1}, *T:* 30°C and 37°C	formation of mycelium even at high pH values due to addition with talc particles, precise adjustment of growth to desired morphology with microparticles	**Fructofuranosidase (FFase), Glucoamylase (GA), GFP** increased formation of GA and FFase with mycelial growth compared to pellets at identical process conditions	(Driouch et al., 2009)
		medium composition	STR, *air flow*: 1 $LL^{-1}min^{-1}$, *pH* 5.5, *T:* 30°C, , n_{stir}: 200 min^{-1} increased to 400 min^{-1} after13 h, raised to 600 min^{-1} after 15 h	pellets, increase in pellet size and decrease in density and number with raising yeast extract concentration	**GOD (recombinant homologous)** higher yields of GOD with smaller pellets of high compactness	(El-Enshasy et al., 1999)
	A. oryzae	temperature (27°C-40°C)	STR, inoculum: 3-6x10^8 L^{-1}or mycelial preculture, *pH* 5.0, *T*: 26°C, *air flow*: 1 $LL^{-1}min^{-1}$, n_{stir}: 300-800 min^{-1} (to maintain DO of 70-100%)	temperature optimum for growth 35°C, active growth layer of pellet about 145 µm	**α-Amylase (homologous)**	(Carlsen et al., 1996)
		cultivation conditions in fed-batch processes	STR, inoculum: 2x10^9 L^{-1}, *pH* 6.0, *T:* 30°C, *air flow*: 1 $LL^{-1}min^{-1}$, n_{stir}: 800 min^{-1}	freely dispersed mycelium, increase of average hyphal length and diameter of tips in exponential batch phase, constant hyphal diameter in fedbatch phase	**Lipase (heterologous)** increase of lipase activity linked to increase of hyphal diameter	(Haak et al., 2006)
	C. fumago	Supplementation and size	shake flasks, , n_{stir}: 180min^{-1}	No effect on morphology of particles	**Chloroperoxidase (homologous)**	(Kaup et al. 2008)

	variation of added microparticles (aluminium oxide and hydrous magnesium silicate)	Inoculum*:* 7d-old preculture, *pH* 6.5 , *t*: 15d, Micorparticle concentration : 0.05-25 gL^{-1}	with diameter of ~500µm, particles ≤ 42 result in freely dispersed mycelium up to dispersion to single hyphae, stimulation of single hyphae formation as result of added microparticels	No effect on protein formation by particles with diameter of ~500µm, maximum specific productivity due to addition of particles with diameter of ≤ 42 µm	
R. oryzae	temperature (22-38°C) carbon source addition of biodegradable polymers	shake flasks, inoculum:1x10^9 mL^{-1}, n_{stir}*:* 170 min^{-1}, *t*: 48 h	pellets, no influence of T on biomass between 22-33°C, biomass yield lower at 38°C, significant influence of polymer concentration on biomass yield	not specified	(Liu et al., 2008)
S. tendae	Temperature 26-32°C	shake flasks, , n_{stir}: 100min^{-1} STR, n_{stir}: 400 min^{-1}, air flow: 1 $LL^{-1}min^{-1}$, Inoculum *:* 7.5x10^2-2.3x10^8 L^{-1}, *pH* 4-8, *t*: 6d	pulpy growth at 31-32°C, pellets at lower temperature of 26-30°C	not specified	(Vecht-Lifshitz et al. 1990)
T. reesei	medium composition	shake flasks, inoculation with seeding culture, *pH* 4.8, *T:* 28°C, n_{stir}*:* 150 min^{-1}	freely dispersed mycelium in presence of Tween 80	**Cellulase (homologous)** enzyme formation significantly influenced by addition of Tween 80	(Domingues et al., 2000)

D – Dilution rate [h^{-1}], DO – Dissolved oxygen [%], GFP – Green fluorescent protein, GOD – Glucose oxidase, HEWL – hen egg white lysozyme, n_{stir} – agitation rate/ shaking intensity [min^{-1}], *(P/V)* – total volumetric power input [W m^{-3}], $(P/V)_{stir}$ – volumetric power input due to agitation [W m^{-3}], $(P/V)_{air}$ – volumetric power input due to aeration [W m^{-3}], *t* – cultivation time [h], *T* – temperature [°C], CSTR – continuous stirred tank reactor, STR – stirred tank reactor. * Table was taken from (Wucherpfennig et al. 2010).

Band 1 **Sunder, Matthias**: Oxidation grundwasserrelevanter Spurenverunreinigungen mit Ozon und Wasserstoffperoxid im Rohrreaktor. 1996. FIT-Verlag. Paderborn, ISBN 3-932252-00-4

Band 2 **Pack, Hubertus**: Schwermetalle in Abwasserströmen: Biosorption und Auswirkung auf eine schadstoffabbauende Bakterienkultur. 1996. FIT-Verlag. Paderborn, ISBN 3-932252-01-2

Band 3 **Brüggenthies, Antje**: Biologische Reinigung EDTA-haltiger Abwässer. 1996. FIT-Verlag. Paderborn, ISBN 3-932252-02-0

Band 4 **Liebelt, Uwe**: Anaerobe Teilstrombehandlung von Restflotten der Reaktivfärberei. 1997. FIT-Verlag. Paderborn, ISBN 3-932252-03-9

Band 5 **Mann, Volker G.**: Optimierung und Scale up eines Suspensionsreaktorverfahrens zur biologischen Reinigung feinkörniger, kontaminierter Böden. 1997. FIT-Verlag. Paderborn, ISBN 3-932252-04-7

Band 6 **Boll Marco**: Einsatz von Fuzzy-Control zur Regelung verfahrenstechnischer Prozesse. 1997. FIT-Verlag. Paderborn, ISBN 3-932252-06-3

Band 7 **Büscher, Klaus**: Bestimmung von mechanischen Beanspruchungen in Zweiphasenreaktoren. 1997. FIT-Verlag. Paderborn, ISBN 3-932252-07-1

Band 8 **Burghardt, Rudolf**: Alkalische Hydrolyse – Charakterisierung und Anwendung einer Aufschlußmethode für industrielle Belebtschlämme. 1998. FIT-Verlag. Paderborn, ISBN 3-932252-13-6

Band 9 **Hemmi, Martin**: Biologisch-chemische Behandlung von Färbereiabwässern in einem Sequencing Batch Process. 1999. FIT-Verlag. Paderborn, ISBN 3-932252-14-4

Band 10 **Dziallas, Holger**: Lokale Phasengehalte in zwei- und dreiphasig betriebenen Blasensäulenreaktoren. 2000. FIT-Verlag. Paderborn, ISBN 3-932252-15-2

Band 11 **Scheminski, Anke**: Teiloxidation von Faulschlämmen mit Ozon. 2001. FIT-Verlag. Paderborn, ISBN 3-932252-16-0

Band 12 **Mahnke, Eike Ulf**: Fluiddynamisch induzierte Partikelbeanspruchung in pneumatisch gerührten Mehrphasenreaktoren. 2002. FIT-Verlag. Paderborn, ISBN 3-932252-17-9

Band 13 **Michele, Volker**: CDF modeling and measurement of liquid flow structure and phase holdup in two- and three-phase bubble columns. 2002. FIT-Verlag. Paderborn, ISBN 3-932252-18-7

Band 14 **Wäsche, Stefan**: Einfluss der Wachstumsbedingungen auf Stoffübergang und Struktur von Biofilmsystemen. 2003. FIT-Verlag · Paderborn, ISBN 3-932252-19-5

Band 15 **Krull Rainer**: Produktionsintegrierte Behandlung industrieller Abwässer zur Schließung von Stoffkreisläuren. 2003. FIT-Verlag. Paderborn, ISBN 3-932252-20-9

Band 16 **Otto, Peter**: Entwicklung eines chemisch-biologischen Verfahrens zur Reinigung EDTA enthaltender Abwässer. 2003. FIT-Verlag. Paderborn, ISBN 3-932252-21-7

Band 17 **Horn, Harald**: Modellierung von Stoffumsatz und Stofftransport in Biofilmsystemen. 2003. FIT-Verlag. Paderborn, ISBN 3-932252-22-5

Band 18 **Mora Naranjo, Nelson**: Analyse und Modellierung anaerober Abbauprozesse in Deponien. 2004. FIT-Verlag. Paderborn, ISBN 3-932252-23-3

Band 19 **Döpkens, Eckart**: Abwasserbehandlung und Prozesswasserrecycling in der Textilindustrie. 2004. FIT-Verlag. Paderborn, ISBN 3-932252-24-1

Band 20 **Haarstrick, Andreas**: Modellierung millieugesteuerter biologischer Abbauprozesse in heterogenen problembelasteten Systemen. 2005. FIT-Verlag. Paderborn, ISBN 3-932252-27-6

Band 21 **Baaß, Anne-Christina**: Mikrobieller Abbau der Polyaminopolycarbonsäuren Propylendiamintetraacetat (PDTA) und Diethylentriaminpentaacetat (DTPA). 2004. FIT-Verlag · Paderborn, ISBN 3-932252-26-8

Band 22 **Staudt, Christian**: Entwicklung der Struktur von Biofilmen. 2006. FIT-Verlag. Paderborn, ISBN 3-932252-28-4

Band 23 **Pilz, Roman Daniel**: Partikelbeanspruchung in mehrphasig betriebenen Airlift-Reaktoren. 2006. FIT-Verlag. Paderborn, ISBN 3-932252-29-2

Band 24 **Schallenberg, Jörg**: Modellierung von zwei- und dreiphasigen Strömungen in Blasensäulenreaktoren. 2006. FIT-Verlag. Paderborn, ISBN 3-932252-30-6

Band 25 **Enß, Jan Hendrik**: Einfluss der Viskosität auf Blasensäulenströmungen. 2006. FIT-Verlag. Paderborn, ISBN 3-932252-31-4

Band 26 **Kelly, Sven**: Fluiddynamischer Einfluss auf die Morphogenese von Biopellets filamentöser Pilze. 2006. FIT-Verlag. Paderborn, ISBN 3-932252-32-2

Band 27 **Grimm, Luis Hermann**: Sporenaggregationsmodell für die submerse Kultivierung koagulativer Myzelbildner. 2006. FIT-Verlag. Paderborn, ISBN 3-932252-33-0

Band 28 **León Ohl, Andrés**: Wechselwirkungen von Stofftransport und Wachstum in Biofilsystemen. 2007. FIT-Verlag. Paderborn, ISBN 3-932252-34-9

Band 29 **Emmler, Markus**: Freisetzung von Glucoamylase in Kultivierungen mit *Aspergillus niger*. 2007. FIT-Verlag. Paderborn, ISBN 3-932252-35-7

Band 30 **Leonhäuser, Johannes**: Biotechnologische Verfahren zur Reinigung von quecksilberhaltigem Abwasser. 2007. FIT-Verlag. Paderborn, ISBN 3-932252-36-5

Band 31 **Jungebloud, Anke**: Untersuchung der Genexpression in *Aspergillus niger* mittels Echtzeit-PCR. 1996. FIT-Verlag. Paderborn, ISBN 978-3-932252-37-2

Band 32 **Hille, Andrea**: Stofftransport und Stoffumsatz in filamentösen Pilzpellets. 2008. FIT-Verlag. Paderborn, ISBN 978-3-932252-38-9

Band 33 **Fürch, Tobias**: Metabolic characterization of recombinant protein production in *Bacillus megaterium*. 2008. FIT-Verlag. Paderborn, ISBN 978-3-932252-39-6

Band 34 **Grote, Andreas Georg**: Datenbanksysteme und bioinformatische Werkzeuge zur Optimierung biotechnologischer Prozesse mit Pilzen. 2008. FIT-Verlag. Paderborn, ISBN 978-3-932252-40-120

Band 35 **Möhle, Roland Bernhard**: An Analytic-Synthetic Approach Combining Mathematical Modeling and Experiments – Towards an Understanding of Biofilm Systems. 2008. FIT-Verlag. Paderborn, ISBN 978-3-932252-41-9

Band 36 **Reichel, Thomas**: Modelle für die Beschreibung das Emissionsverhaltens von Siedlungsabfällen. 2008. FIT-Verlag. Paderborn, ISBN 978-3-932252-42-6

Band 37 **Schultheiss, Ellen**: Charakterisierung des Exopolysaccharids PS-EDIV von *Sphingomonas pituitosa*. 2008. FIT-Verlag. Paderborn, ISBN 978-3-932252-43-3

Band 38 **Dreger, Michael Andreas**: Produktion und Aufarbeitung des Exopolysaccharids PS-EDIV aus *Sphingomonas pituitosa*. 1996. FIT-Verlag. Paderborn, ISBN 978-3-932252-44-0

Band 39 **Wiebels, Cornelia**: A Novel Bubble Size Measuring Technique for High Bubble Density Flows. 2009. FIT-Verlag. Paderborn, ISBN 978-3-932252-45-7

Band 40 **Bohle, Kathrin**: Morphologie- und produktionsrelevante Gen- und Proteinexpression in submersen Kultivierungen von *Aspergillus niger*. 2009. FIT-Verlag. Paderborn, ISBN 978-3-932252-46-2

Band 41 **Fallet, Claas**: Reaktionstechnische Untersuchungen der mikrobiellen Stressantwort und ihrer biotechnologischen Anwendungen. 2009. FIT-Verlag. Paderborn, ISBN 978-3-932252-47-1

Band 42 **Vetter, Andreas**: Sequential Co-simulation as Method to Couple CFD and Biological Growth in a Yeast. 2009. FIT-Verlag. Paderborn, ISBN 978-3-932252-48-8

Band 43 **Jung, Thomas**: Einsatz chemischer Oxidationsverfahren zur Behandlung industrieller Abwässer. 2010. FIT-Verlag · Paderborn, ISBN 978-3-932252-49-5

Band 45 **Herrmann, Tim**: Transport von Proteinen in Partikeln der Hydrophoben Interaktions Chromatographie. 2010. FIT-Verlag. Paderborn, ISBN 978-3-932252-51-8

Band 46 **Becker, Judith**: Systems Metabolic Engineering of *Corynebacterium glutamicum* towards improved Lysine Production. 2010. Cuvillier-Verlag. Göttingen, ISBN-10: 3869554266, ISBN-13: 9783869554266

Band 47 **Melzer, Guido**. 2010. Metabolic Network Analysis of the Cell Factory *Aspergillus niger* Cuvillier-Verlag. Göttingen, ISBN: 978-3-86955-456-3, ISSN: 1431-7230*5*

Band 48 **Bolten, Christoph J**. 2010. Bio-based Production of L-Methionine in *Corynebacterium glutamicum.* Cuvillier-Verlag. Göttingen, ISBN: 978-3-86955-486-0, ISSN: 1431-7230

Band 49 **Lüders, Svenja**. 2010. Prozess-und Proteomanalyse gestresster Mikroorganismen
Cuvillier-Verlag. Göttingen, ISBN: 978-3-86955-435-8, ISSN: 1431-7230

Band 50 **Wittmann, Christoph**. 2010. Entwicklung und Einsatz neuer Tools zur metabolischen Netzwerkanalyse des industriellen Aminosäure-Produzenten *Corynebacterium glutamicum.* Cuvillier-Verlag. Göttingen, ISBN: 978-3-86955-445-7, ISSN: 1431-7230

Band 51 **Edlich, Astrid**. 2010. Entwicklung eines Mikroreaktorsystems als Screening-Instrument für biologische Prozesse. Cuvillier-Verlag. Göttingen, ISBN-10: 3869554703, ISBN-13: 9783869554709

Band 52 **Hage, Kerstin**. 2010: Bioprozessoptimierung und Metabolomanalyse zur Proteinproduktion in *Bacillus licheniformis*. 2010. Cuvillier-Verlag. Göttingen, ISBN-10: 3869555785, ISBN-13: 9783869555782

Band 53 **Kiep, Katina***.* 2010. Einfluss von Kultivierungsparametern auf die Morphologie und Produktbildung von *Aspergillus niger*. Cuvillier-Verlag. Göttingen, ISBN-10: 3869556323, ISBN-13: 9783869556321

Band 54 **Fischer, Nicole***.* 2011. Experimental investigations on the influence of physico-chemical parameters on anaerobic degradation in MBT residual waste. Cuvillier-Verlag. Göttingen, ISBN-10: 386955679X, ISBN-13: 97838695

Band 56 **Wichter, Johannes**. 2011. Untersuchung der L-Cystein-Biosynthese in *Escherichia coli* mit Techniken der Metabolom und ^{13}C-Stoffflussanalyse. Cuvillier-Verlag. Göttingen, ISBN: 978-3-86955-750-2, ISSN: 1431-7230

Band 57 **Knappik, Irena Isabell**. 2011. Charakterisierung der biologischen und chemischen Reaktionsprozesse in Siedlungsabfällen. Cuvillier-Verlag. Göttingen, ISBN-10: 3869557605**,** ISBN-13: 9783869557601